IAEA-TECDOC-1595

Nuclear and Isotopic Techniques for the Characterization of Submarine Groundwater Discharge in Coastal Zones

Results of a coordinated research project 2001–2006

IAEA
International Atomic Energy Agency

July 2007

IAEA-TECDOC-1595

Nuclear and Isotopic Techniques for the Characterization of Submarine Groundwater Discharge in Coastal Zones

Results of a coordinated research project 2001–2006

IAEA
International Atomic Energy Agency

July 2007

The originating Section of this publication in the IAEA was:

Isotope Hydrology Section
International Atomic Energy Agency
Wagramer Strasse 5
P.O. Box 100
A-1400 Vienna, Austria

NUCLEAR AND ISOTOPIC TECHNIQUES FOR THE CHARACTERIZATION OF SUBMARINE GROUNDWATER DISCHARGE IN COASTAL ZONES
IAEA, VIENNA, 2008
IAEA-TECDOC-1595
ISBN 978–92–0–106408–0
ISSN 1011–4289

Printed by the IAEA in Austria
July2008

FOREWORD

Submarine groundwater discharge (SGD) is now recognized as an important pathway between land and sea. As such, this flow may contribute to the biogeochemical and other marine budgets of near-shore waters. These discharges typically display significant spatial and temporal variability, making direct assessments difficult. Groundwater seepage is patchy, diffuse, temporally variable, and may involve multiple aquifers. Thus, the measurement of its magnitude and associated chemical fluxes is a challenging enterprise.

An initiative on SGD characterization was developed by the IAEA and UNESCO in 2000 as a 5-year plan to assess methodologies and importance of SGD for coastal zone management. The IAEA component included a Coordinated Research Project (CRP) on Nuclear and Isotopic Techniques for the Characterization of Submarine Groundwater Discharge (SGD) in Coastal Zones, carried out jointly by the IAEA's Isotope Hydrology Section in Vienna and the Marine Environment Laboratory in Monaco, together with 9 laboratories from 8 countries. In addition to the IAEA, the Intergovernmental Oceanographic Commission (IOC) and the International Hydrological Programme (IHP) have provided support. This overall effort originally grew from a project sponsored by the Scientific Committee on Ocean Research (SCOR) who established a Working Group (112) on SGD.

The activities included joint meetings (Vienna 2000, 2002, and 2005; Syracuse, Italy, 2001; and Monaco 2004), sampling expeditions (Australia 2000; Sicily 2001 and 2002; New York 2002; Brazil 2003; and Mauritius 2005), joint analytical work, data evaluation, and preparation of joint publications. The objectives of the CRP included the improvement of capabilities for water resources and environmental management of coastal zones; application of recently developed nuclear and isotopic techniques suitable for quantitative estimation of various components of SGD; understanding of the influence of SGD on coastal processes and on groundwater regimes; a better management of groundwater resources in coastal areas; and development of numerical models of SGD.

This report examines several methodologies of SGD assessment, which were carried out during a series of five intercomparison experiments in different hydrogeological environments (coastal plains, karst, glacial till, fractured crystalline rocks and volcanic terrains). This report reviews the scientific and management significance of SGD, measurement approaches, and the results of the intercomparison experiments. We conclude that while SGD is essentially ubiquitous in coastal areas, the assessment of its magnitude at any one location is subject to enough variability that measurements should be made by a variety of techniques and over large enough spatial and temporal scales to capture the majority of these variable conditions.

The IAEA officers in charge of designing and coordinating all of the related work in this CRP were K.M. Kulkarni of the Division of Physical and Chemical Sciences, Vienna, and P.P. Povinec and J. Scholten of the Marine Environment Laboratory, Monaco. W.S. Moore assisted in technical editing of the contributions. The IAEA officer responsible for this publication was K.M. Kulkarni of the Division of Physical and Chemical Sciences.

EDITORIAL NOTE

The papers in these proceedings are reproduced as submitted by the authors and have not undergone rigorous editorial review by the IAEA.

The views expressed do not necessarily reflect those of the IAEA, the governments of the nominating Member States or the nominating organizations.

The use of particular designations of countries or territories does not imply any judgement by the publisher, the IAEA, as to the legal status of such countries or territories, of their authorities and institutions or of the delimitation of their boundaries.

The mention of names of specific companies or products (whether or not indicated as registered) does not imply any intention to infringe proprietary rights, nor should it be construed as an endorsement or recommendation on the part of the IAEA.

The authors are responsible for having obtained the necessary permission for the IAEA to reproduce, translate or use material from sources already protected by copyrights.

CONTENTS

SUMMARY

1. BACKGROUND

Subsurface discharge of water from coastal aquifers, called submarine groundwater discharge (SGD), has been recognized as an important component of the hydrological cycle. This discharge includes meteoric water from land drainage as well as seawater that has entered coastal aquifers. We follow Burnett et al. [1] in defining submarine groundwater discharge as any and all flow of water on continental margins from the seabed to the coastal ocean, regardless of fluid composition or driving force.

Coastal aquifers may consist of complicated arrays of confined, semi-confined, and unconfined systems. Simple hydrologic models do not consider the anisotropic nature of coastal sediments, dispersion, and tidal pumping. Moreover, cycling of seawater through the coastal aquifer may be driven by the flow of freshwater from coastal uplands [2,3]. As freshwater flows through an aquifer driven by an inland hydraulic head, it can entrain seawater diffusing and dispersing up from the salty aquifer that underlies it. Superimposed upon this terrestrially-driven circulation are a variety of marine-induced forces that result in flow into and out of the seabed even in the absence of a hydraulic head. Such 'subterranean estuaries' [4] are characterized by biogeochemical reactions that influence the transfer of nutrients to the coastal zone in a manner similar to that of surface estuaries [5–7].

SGD is increasingly being recognized as an important factor in the understanding and sustainable management of coastal fresh aquifers in many highly populated areas of the world. In addition, SGD is a significant pathway for transfer of matter between the land and the sea [4,6]. SGD is known to supply essential nutrients and trace metals to coastal oceans [8–20]. In some cases SGD may result in contamination of the near-shore marine environment from land-based activities [21–23]. Additionally, SGD may remove certain components (e.g. uranium) from seawater during circulation through coastal aquifers. As we learn more about SGD and subterranean aquifers, we recognize how significant these processes are to the coastal ocean and environment.

Estimation of SGD is complicated due to the fact that direct measurement over large temporal and spatial scales is not possible by conventional means. Measurement of a range of isotopic tracers at the aquifer–marine interface and in the coastal ocean provides the possibility to produce integrated flux estimates of discharge not possible by non-nuclear methods [4]. Many researchers have applied a variety of methods to estimate submarine groundwater discharge (see [24] for review). A large spread of estimates for SGD values illustrates the high degree of variability and uncertainty of present estimates. It should be noted that estimates based on water balance considerations usually include only the freshwater fraction of the total hydrological flow. Recirculated seawater and saline groundwater fluxes are often volumetrically important and may increase these flows.

In cases of freshwater fluxes chemical anomalies such as salinity are useful for estimation of SGD. However, in cases of brackish and saline SGD fluxes, which in many cases have more impact on the coastal environment, isotopes have distinct advantages over chemical techniques. Investigations using the combination of stable, long-lived, and short-lived radioisotopes along with other complementary techniques allow various aspects of coastal hydrology to be studied.

Several natural radioactive (^{3}H, ^{14}C, U isotopes, etc.) and stable (^{2}H, ^{3}He, ^{4}He, ^{13}C, ^{15}N, ^{18}O, $^{87/86}Sr$, etc.) isotopes and some anthropogenic atmospheric gases (e.g. CFCs) have been used for conducting SGD investigations, tracing water masses, and calculating the age of groundwater. Stable isotope data can help to evaluate groundwater–seawater mixing ratios, important for the estimation of the SGD in coastal areas. Seawater and the fresh groundwater end members often have specific signatures due to different tracers/isotopes. Under good circumstances, such differences between end members would allow calculation of the percent groundwater contribution. This may be especially useful when mixing

is occurring between more than two end members including saline groundwater. Besides the mixing ratio calculations, each tracer can be used for interpretation of various groundwater characteristics. In mixed waters, the selection of the related fresh groundwater end member is an important issue that may be addressed via use of stable isotopes. For example, oxygen and hydrogen isotopes generally carry valuable information about recharge conditions. Such information may include recharge elevation, temperature, and degree of evaporation.

Other variables that change the characteristics of the groundwater component in the mixture are the hydrodynamic properties of the aquifer because of change in length of flowpaths, groundwater velocity, and flow conditions (e.g. diffuse or conduit flow). Such hydrodynamic characteristics of the aquifer are important for the chemically reactive (e.g. ^{13}C) and radioactive (e.g. ^{3}H) isotopes. Such processes have to be taken into account for interpretation of water mixture calculations.

The isotopic measurements such as ^{222}Rn, ^{226}Ra, ^{228}Ra, ^{224}Ra, ^{223}Ra, ^{87}Sr, ^{3}He, ^{4}He, ^{3}H, ^{14}C and ^{234}U among others can serve as key indicators of fluxes across the groundwater/marine interface. Of these ^{222}Rn, ^{226}Ra, ^{228}Ra, ^{224}Ra, and ^{223}Ra have been used extensively [6, 16–20, 24–47]. These isotope techniques enable large-scale estimates of various components of SGD, allowing detail studies on processes involved. Such knowledge is essential in improving the possibilities for better management of coastal water resources. Most of the presently applied isotope techniques are of potential use in a variety of SGD investigations. Additionally, new isotope techniques for *in situ* monitoring are under development [48]. These techniques also could be tested for identification and estimation of SGD. The development of framework and methodology under which nuclear and isotope techniques could be applied to SGD investigations was investigated in the CRP. It also integrated approaches adopted by researchers from different scientific disciplines, e.g. hydrogeology, geophysics, and coastal oceanography.

2. OBJECTIVES OF THE CRP

The overall objective of the CRP was to improve the capability of the Member States for water resources and environmental management of coastal areas.

The specific objectives were:

(a) To identify and integrate the application of isotope methods with conventional methods appropriate for detection, characterization, and quantification of submarine groundwater discharge in coastal areas.

(b) To explore application of recently developed nuclear and isotopic techniques suitable for quantitative estimation of various components of SGD. The results could provide valuable inputs for development of numerical models.

(c) To develop a better understanding of the influence of SGD on coastal oceanographic processes and on groundwater regimes for better management of groundwater resources and environmental concerns in coastal areas.

3. ACHIEVEMENTS AND RESULTS

The Isotope Hydrology Section of Division of Physical and Chemical Sciences (NAPC) and the Radiometrics Laboratory of Marine Environmental Laboratory (NAML) jointly implemented the CRP. In the frame of the CRP the participants have applied their techniques to detect, characterize, and quantify SGD in three reference sites: Italy, Brazil, and Mauritius. A state-of-the-art review of these efforts at above mentioned sites and at other complementary sites appears in this TECDOC as a contribution of the CRP team following this summary.

Upon reviewing the results from the intercomparison experiments conducted thus far, it is clear that SGD is fairly ubiquitous in the coastal zone. Rates of discharge above 100 cm/day are considered

high, while values below 5 cm/day are considered low (or even marginally detectable). In unconfined aquifers measurement strategies should be designed to search for patterns of decreasing SGD with distance from the shore and temporal patterns modulated by waves and tides; not only the diurnal tidal variations but also the spring-neap lunar cycle. Superimposed on these predictable patterns are the effects of storms and other events that may cause large SGD fluxes in a short time. Semi-confined aquifers may discharge many km offshore without a clear pattern. Regardless of location, however, both spatial and temporal variations are to be expected. Preferential flow paths (sometimes revealed as submarine springs) are commonly found not only in karst environments but also in situations that appear reasonably homogeneous and isotropic. Tidal variations generally appear as higher SGD rates at low tide levels and lower rates at high tides. However, the modulation is not necessarily linear and the relationships are not completely understood. In some situations, the rate of SGD seems to change abruptly without an obvious cause. The composition of SGD is often a mixture of fresh and saline groundwater with recirculating seawater accounting for 90% or more of the discharge in some locations or less than 10% in the case of some offshore springs. While each study site must be approached individually, a few generalizations to assist planning could be made. Different measurement techniques applied in the CRP are valid although they each have their own advantages and disadvantages. It is recommended that multiple approaches be applied whenever possible. In addition, a continuing effort is required in order to capture long-period tidal fluctuations, storm-induced effects, and seasonal variations.

The choice of technique will depend, of course, not only on what is perceived to be the 'best' approach, but by practical considerations (cost, availability of equipment, etc.) as well. For many situations, it is found that in calm seas not affected by significant waves or strong currents, seepage meters appear to work very well. These meters provide a flux at a specific time and location from a limited amount of seabed (generally ~0.25 m^2). Seepage meters range in cost from almost nothing for a simple bag-operated meter to several thousands of dollars for those equipped with more sophisticated measurement devices. However, labour costs to install and maintain seepage meters over a large area for more than a few days are substantial. Seepage meters are subject to artefacts but can provide useful information if one is aware of the potential problems and if the devices are used in the proper manner. This seems to be especially true in environments where seepage flux rates are relatively rapid (>5 cm/day).

Use of natural geochemical tracers, especially isotopes, involves the use of costly equipment and requires personnel with special training and experience. One of the main advantages of the tracer approach is the integration of the SGD signal through the water column so smaller-scale variations, which may be unimportant for larger-scale studies, are smoothed out. The approach may thus be optimal in environments where especially large spatial variation is expected (e.g., fractured rock aquifers). In addition to the spatial integration, tracers integrate the water flux over the time-scale of the isotope and the water residence time of the study area. Depending upon what one wants to know, this can often be a great advantage. Finally, different components of SGD can be recognized and quantified using isotopic tracers. This allows discharge from surficial and semi-confined aquifers to be separated. In all cases conclusions based on isotopic tracers depend on the validity of the models and their assumptions used to interpret the distributions. Mixing and atmospheric exchanges in the case of radon must be evaluated and care must be exercised in defining the end members. Multiple tracers are recommended when possible.

Simple water balance calculations have been shown to be useful in some situations as an estimate of the fresh groundwater discharge. Hydrogeological, variable density, groundwater modelling can also be conducted as simple steady state (annual average flux) or non-steady state (requires real time boundary conditions) methods. Unfortunately, at present neither approach generally compares well with seepage meter and tracer measurements, often because of differences in scaling in both time and space. Particular problems can be encountered in the proper scaling and parameterizing dispersion

processes. Apparent inconsistencies between modelling and direct measurement approaches often arise because different components of SGD (fresh and salt water) are being evaluated or the models do not include transient terrestrial (e.g., recharge cycles) or marine processes (tidal pumping, wave set up, storms, etc.) that drive part of all of the SGD. Isotopic and geochemical tracers as well as seepage meters measure total flow, very often a combination of fresh groundwater and seawater. Water balance calculations and most models evaluate just the fresh groundwater flow.

Although the techniques described here are well developed, there is no 'standard' methodology. If one plans to work in karstic or fractured bedrock environments, heterogeneity must be expected. In this case, it would be best to plan on multiple approaches. Rates are likely to be controlled by the presence or absence of buried fracture systems where flow is focused, or dispersed, by the topography of the buried rock surface. In such situations, integrated SGD might be assessed with dispersed tracers or described statistically from many, randomly situated, seepage measurements. In volcanic aquifers, especially young basalts, the radium signal may be low. This was found to be the case in the Mauritius and in other studies in Hawaii. Such a situation might hamper the application of radium (Ra) and radon (Rn) tracers in these settings. It is suggested in such an environment that one should also confirm the spatial heterogeneity with some preliminary seepage meter deployments and geophysical techniques; and use traditional modelling approaches with caution as good results will likely require more complex models and a significant amount of data.

If one plans to work in a coastal plain setting without an underlying semi-confined aquifer, it is likely that the results will be more homogeneous. Seepage meters often work well in such environments where conditions are calm. These can provide good estimates that can be checked by looking for a distinctive pattern in the results. Such a pattern might, for example, consist of a systematic drop off in seepage rates as a function of distance offshore in unconfined aquifers. Simple modelling approaches (e.g., hydraulic gradients, tidal propagation, thermal gradients) can often be valuable in this type of environment. Tracers also will work very well in coastal plain environments.

Based on experiences during this project, the following suggestions are made to improve the performance of future SGD assessments:

- Some geophysical surveying (e.g., resistivity profiling, infrared imaging) should be performed prior to the actual assessments so areas prone to high and low SGD can be mapped out in advance.
- Point discharge measurements are best recorded in units of cm/day. It is often most useful to design measurements to allow for integrated assessments of groundwater flow per unit width of shoreline, the best way to make comparisons and to extrapolate results. For example, seepage meter transects normal to the shoreline that cover the entire seepage face (which can be mapped with the resistivity probes) would fit this requirement.
- The experimental design should attempt to incorporate at least two independent techniques.
- Coordination among groups should ensure that method-to-method intercomparisons can be made. For example, in some experiments data sets from different devices overlapped only for short periods. Extending these overlapping periods would benefit the evaluation process.

4. IMPACT AND RELEVANCE OF THE CRP

This CRP brought together investigators from diverse scientific backgrounds to assess submarine groundwater discharge (SGD) in different hydrogeological regimes. A combination of geochemical, geophysical, and hydrological techniques and models revealed substantial SGD at each site. The CRP compared different techniques and arrived at a consensus protocol for future SGD studies. As a result of this CRP as well as the SCOR, IHP, and IOC support, several scientific papers have been published

or are in press. We anticipate that this list will continue to grow over the next few years. The list of publications is given in the Appendix.

SGD has been shown to be an important factor in the supply of nutrients and carbon to coastal waters. The natural supply of nutrients by SGD may be necessary to sustain biological productivity in some environments. There is also awareness that in some cases, SGD may be involved in harmful algal blooms and other negative effects. As coastal development continues, changes in the flux and composition of SGD are expected to occur. To evaluate the effects of SGD on coastal waters, it is necessary to know the current flux of SGD and its composition. This CRP provided the opportunity to test various techniques of estimating SGD in the same location and to synthesize the results into a comprehensive paper. We expect that the products of this CRP will serve as standard reference materials in ongoing and future studies of SGD.

5. SUGGESTIONS FOR FUTURE ACTION

As more scientists and coastal managers recognize the importance of SGD, it is likely that studies similar to ones supported by this CRP will be initiated. To guide these studies, the IAEA should provide a fact sheet that summarizes the application of isotopic techniques to SGD studies. This information should also be included on the IAEA web site for quicker and wider dissemination. Training sessions, including practical training in the field, laboratory training for the measurements, and training in the interpretation and modeling of the data, on the isotopic techniques would be beneficial for the researchers. Additionally, efforts to improve the isotopic measurements should be supported. These efforts should include workshops on the different methods and the establishment of reference materials for calibration.

REFERENCES

[1] BURNETT, W.C., BOKUNIEWICZ, H., HUETTEL, M., MOORE, W.S., Taniguchi, M., Groundwater and porewater inputs to the coastal zone, Biogeochemistry **66** (2003) 3–33.

[2] COOPER, H.H., JR., A hypothesis concerning the dynamic balance of fresh water and salt water in a coastal aquifer, J. Geophys. Res. **64** (1959) 461–467.

[3] DESTOUNI, G., PRIETO, C., On the possibility for generic modeling of submarine groundwater discharge, Biogeochemistry **66** (2003) 171–186.

[4] MOORE, W.S., The subterranean estuary: a reaction zone of ground water and sea water, Mar.ne Chem. **65** (1999) 111–125.

[5] NIXON, S.W., AMMERMAN, J.W., ATKINSON, L.P., BEROUNSKY, V.M., BILLEN, G., BOICOURT, W.C., BOYNTON, W.R., CHURCH, T.M., DITORO, D.M., ELMGREN, R., GARBER, J.H., GIBLIN, A.E., JAHNKE, R.A., OWENS, N.J.P., PILSON, M.E.Q., SEITZINGER, S.P., The fate of nitrogen and phosphorus at the land–sea margin of the North Atlantic Ocean, Biogeochemistry **35** (1996) 141–180.

[6] CHARETTE, M.A., SHOLKOVITZ, E.R., Oxidative precipitation of groundwater-derived ferrous iron in the subterranean estuary of a coastal bay, Geophys. Res. Lett. **29** (2002) 1444.

[7] TALBOT, J.M., KROEGER, K.D., RAGO, A., ALLEN, M.C., CHARETTE, M.A., Nitrogen flux and speciation through the subterranean estuary of Waquoit Bay, Massachusetts, Biol. Bull. **205** (2003) 244–245.

[8] VALIELA, I., TEAL, J.M., VOLKMAN, S., SHAFER, D., CARPENTER, E.J., Nutrient and particulate fluxes in a salt marsh ecosystem: tidal exchanges and inputs by precipitation and groundwater, Limnol. Oceanogr. **23** (1978) 798–812.

[9] VALIELA, I., D'ELIA, C., Groundwater inputs to coastal waters, Biogeochemistry **10** (1990) 328.

[10] VALIELA, I., FOREMAN, K., LAMONTAGNE, M., HERSH, D., COSTA, J., PECKOL, P., DEMEO-ANDERSON, B., D'AVANZO, C., BABIONE, M., SHAM, C., BRAWLEY, J., LAJTHA, K., Couplings of watersheds and coastal waters: sources and consequences of nutrient enrichment in Waquoit Bay, Massachusetts, Estuaries **15** (1992) 443–457.

[11] VALIELA, I., BOWEN, J.L., KROEGER, K.D., Assessment of models for estimation of land-derived nitrogen loads to shallow estuaries, Appl. Geochem. **17** (2002) 935–953.
[12] JOHANNES, R.E., The ecological significance of the submarine discharge of groundwater, Mar. Ecol. Pro. Ser. **3** (1980) 365–373.
[13] D'ELIA, C.F., WEBB, D.K.L., PORTER, J.W., Nitrate-rich groundwater inputs to Discovery Bay, Jamaica: A significant source of N to local coral reefs?, Bull. Mar. Sci. **31** (1981) 903–910.
[14] CAPONE, D.G., BAUTISTA, M.F., A groundwater source of nitrate in nearshore marine sediments, Nature **313** (1985) 214–216.
[15] CAPONE, D.G., SLATER, J.M., Interannual patterns of water table height and groundwater derived nitrate in nearshore sediments, Biogeochemistry **10** (1990) 277–288.
[16] CORBETT D.R., CHANTON, J.P., BURNETT, W.C., DILLON, K., RUTKOWSKI, C., FOURQUREAN, J., Patterns of groundwater discharge into Florida Bay, Limnol. Oceanogr. **44** (1999) 1045–1055.
[17] CORBETT, D.R., DILLON, K., BURNETT, W.C., CHANTON, J.P., Estimating the groundwater contribution into Florida Bay via natural tracers ^{222}Rn and CH_4, Limnol. Oceanogr. **45** (2000) 1546–1557.
[18] KREST, J.M., MOORE, W.S., GARDNER,L.R., Marsh nutrient export supplied by groundwater discharge: evidence from radium measurements, Global Biogeochemical Cycles **14** (2000) 167–176.
[19] CROTWELL, A.M., MOORE, W.S., Nutrient and Radium Fluxes from Submarine Groundwater Discharge to Port Royal Sound, South Carolina, Aquat. Geochem. **9** (2003) 191–208.
[20] MOORE, W.S., Radium Isotopes as tracers of submarine groundwater discharge in Sicily, Cont. Shelf Res. **26** (2006) 852–861.
[21] OBERDORFER, J.A., VALENTINO, M.A., SMITH, S.V., Groundwater contribution to the nutrient budget of Tomales Bay, California, Biogeochemistry **10** (1990) 199–216.
[22] LAPOINTE, B., O'CONNELL, J.D., GARRETT, G.S., Nutrient coupling between on-site sewage disposal systems, groundwaters, and nearshore surface waters of the Florida Keys, Biogeochemistry **10** (1990) 289–307.
[23] LAROCHE, J., NUZZI, R., WATERS, R., WYMAN, K., FALKOWSKI, P.G., WALLACE, D.W.R., Brown tide blooms in Long Island's coastal waters linked to interannual variability in groundwater flow, Glob. Change Biol. **3** (1997) 397–410.
[24] BURNETT, W.C., CHANTON, J., CHRISTOFF, J., KONTAR, E., KRUPA, S., LAMBERT,M., MOORE, W.S., O'ROURKE, D., PAULSEN, R., SMITH, C., SMITH, L., TANIGUCHI, M., Assessing methodologies for measuring groundwater discharge to the ocean, EOS **83** (2002) 117–123.
[25] BURNETT, W.C., COWART, J.B., DEETAE, S., Radium in the Suwannee River and estuary: spring and river input to the Gulf of Mexico, Biogeochemistry **10** (1990) 237–255.
[26] BURNETT, W.C., CABLE, J.E., CORBETT, D.R., CHANTON, J.P., Tracing groundwater flow into surface waters using natural ^{222}Rn, Proc. Int. Symp. Groundwater Discharge in the Coastal Zone, Land–Ocean Interactions in the Coastal Zone (LOICZ), Moscow (1996) 22–28.
[27] ELLINS, K.K., ROMAN-MAS, A., LEE, R., Using Rn-222 to examine ground water/surface discharge interaction in the Rio Grande de Manati, Puerto Rico, J. Hydrol. **115** (1990) 319–341.
[28] MOORE, W.S., 1996. Large groundwater inputs to coastal waters revealed by ^{226}Ra enrichments. Nature **380** (1996) 612–614.
[29] RAMA, MOORE, W.S., Using the radium quartet for evaluating groundwater input and water exchange in salt marshes, Geochim. Cosmochim. Acta **60** (1996) 4245–4252.
[30] CABLE, J.E., BUGNA, G., BURNETT, W.C., CHANTON, J.P., Application of ^{222}Rn and CH_4 for assessment of groundwater discharge to the coastal ocean, Limnol. Oceanogr. **41** (1996a) 1347–1353.
[31] CABLE, J.E., BURNETT, W.C., CHANTON, J.P., WEATHERLY, G.L., Estimating groundwater discharge into the northeastern Gulf of Mexico using radon-222, Earth Planet. Sci. Lett. **144** (1996b) 591–604.
[32] MOORE, W.S., High fluxes of radium and barium from the mouth of the Ganges–Brahmaputra River during low river discharge suggest a large groundwater source, Earth Planet. Sci. Lett., **150** (1997) 141–150.

[33] MOORE, W. S., SHAW, T.J., Chemical signals from submarine fluid advection onto the continental shelf, J. Geophys. Res. **103** (1998) 21543–21552.
[34] HUSSAIN, N., CHURCH, T.M., KIM, G., Use of ^{222}Rn and ^{226}Ra to trace submarine groundwater discharge into the Chesapeak Bay, Mar. Chem. **65** (1999) 127–134.
[35] MOORE, W.S., Determining coastal mixing rates using radium isotopes, Cont. Shelf Res. **20** (2000) 1995–2007.
[36] KREST, J.M., HARVEY, J.W., Using natural distributions of short-lived radium isotopes to quantify groundwater discharge and recharge, Limnol. Oceanogr. **48** (2003) 290–298.
[37] CHARETTE, M.A., BUESSELER, K.O., ANDREWS, J.E., Utility of radium isotopes for evaluating the input and transport of groundwater-derived nitrogen to a Cape Cod estuary, Limnol. Oceanogr. **46** (2001) 465–470.
[38] KIM, G., HWANG, D.W., Tidal pumping of groundwater into the coastal ocean revealed from submarine Rn-222 and CH_4 monitoring, Geophys. Res. Lett. **29** (2002) doi:10.1029/ 2002GL015093.
[39] KELLY, R.P., MORAN,S.B., Seasonal changes in groundwater input to a well–mixed estuary estimated using radium isotopes and implications for coastal nutrient budgets, Limnol. Oceanogr. **47** (2002) 1796–1807.
[40] BURNETT, W.C., DULAIOVA, H., Estimating the dynamics of groundwater input into the coastal zone via continuous radon-222 measurements, J. Environ. Radioact. **69** (2003) 21–35.
[41] GARRISON, G.H., GLENN, C.R., MCMURTRY, G.M., Measurement of submarine groundwater discharge in Kahana Bay, Oahu, Hawaii. Limnol. Oceangr. **48** (2003) 920–928.
[42] KIM, G., LEE, K.K., PARK, K.S., HWANG, D.W., YANG, H.S., Large submarine groundwater discharge (SGD) from a volcanic island, Geophys. Res. Lett. **30** (2003) doi:10.1029/ 2003GL018378.
[43] BURNETT, W.C., DULAIOVA, H., Radon as a tracer of submarine groundwater discharge into a boat basin in Donnalucata, Sicily, Cont. Shelf Res. **26** 7 (2006) 862–873.
[44] DULAIOVA, H., PETERSON, R., BURNETT, W.C., SMITH, D.-L., A multi-detector continuous monitor for assessment of ^{222}Rn in the coastal ocean, J. Radioanal. Nucl. Chem. **263** 2 (2005) 361–365.
[45] HWANG, D.W., KIM, G., LEE, Y.-W., YANG, H.-S., Estimating submarine inputs of groundwater and nutrients to a coastal bay using radium isotopes, Mar. Chem. **96** (2005) 61–71.
[46] MOORE, W.S., WILSON, A.M., Advective flow through the upper continental shelf driven by storms, buoyancy, and submarine groundwater discharge, Earth Planet. Sci. Lett. **235** (2005) 564–576.
[47] MOORE, W.S., BLANTON, J.O., JOYE, S., Estimates of Flushing Times, Submarine Groundwater Discharge, and Nutrient Fluxes to Okatee River, South Carolina, J. Geophys. Res., **111** (2006) C09006 doi:10.1029/2005JC003041.
[48] POVINEC, P.P., LA ROSA, J., LEE, S.-H., MULSOW, S., OSVATH, I., WYSE, E., Recent developments in radiometric and mass spectrometry methods for marine radioactivity measurements, J. Radioanal. Nucl. Chem. **248** (2001) 713–718.

QUANTIFYING SUBMARINE GROUNDWATER DISCHARGE IN THE COASTAL ZONE VIA MULTIPLE METHODS*

W.C. Burnett[1], P.K. Aggarwal[2], A. Aureli[3], H. Bokuniewicz[4], J.E. Cable[5], M.A. Charette[6], E. Kontar[7], S. Krupa[8], K.M. Kulkarni[2], A. Loveless[9], W.S. Moore[10], J.A. Oberdorfer[11], J. Oliveira[12], N. Ozyurt[13], P. Povinec[14†], A.M.G. Privitera[15], R. Rajar[16], R.T. Ramessur[17], J. Scholten[14], T. Stieglitz[18, 19], M. Taniguchi[20], J.V. Turner[21]

[1]Department of Oceanography, Florida State University, Tallahassee, FL, United States of America
[2]Isotope Hydrology Section, International Atomic Energy Agency, Vienna
[3]Department of Water Resources Management, University of Palermo, Catania, Italy
[4]Marine Science Research Center, Stony Brook University, United States of America
[5]Department of Oceanography, Louisiana State University, United States of America
[6]Department of Marine Chemistry, Woods Hole Oceanographic Institution, United States of America
[7]P.P. Shirshov Institute of Oceanology, Russian Federation
[8]South Florida Water Management District, United States of America
[9]University of Western Australia, Australia
[10]Department of Geological Sciences, University of South Carolina, United States of America
[11]Department of Geology, San Jose State University, United States of America
[12]Instituto de Pesquisas Energéticas e Nucleares, Brazil
[13]Department of Geological Engineering, Hacettepe University, Turkey
[14]Marine Environment Laboratory, International Atomic Energy Agency, Monaco
[15]U.O. 4.17 of the G.N.D.C.I., National Research Council, Italy
[16]Faculty of Civil and Geodetic Engineering, University of Ljubljana, Slovenia
[17]Department of Chemistry, University of Mauritius, Mauritius
[18]Mathematical & Physical Sciences, James Cook University, Australia
[19]Australian Institute of Marine Sciences, Townsville, Australia
[20]Research Institute for Humanity and Nature, Japan
[21]CSIRO, Land and Water, Perth, Australia

Abstract. Submarine groundwater discharge (SGD) is now recognized as an important pathway between land and sea. As such, this flow may contribute to the biogeochemical and other marine budgets of near-shore waters. These discharges typically display significant spatial and temporal variability making assessments difficult. Groundwater seepage is patchy, diffuse, temporally variable, and may involve multiple aquifers. Thus, the measurement of its magnitude and associated chemical fluxes is a challenging enterprise. A joint project of the UNESCO and the International Atomic Energy Agency (IAEA) has examined several methods of SGD assessment and carried out a series of five intercomparison experiments in different hydrogeologic environments (coastal plain, karst, glacial till, fractured crystalline rock, and volcanic terrains). This report reviews the scientific and management significance of SGD, measurement approaches, and the results of the intercomparison experiments. We conclude that while the process is essentially ubiquitous in coastal areas, the assessment of its magnitude at any one location is subject to enough variability that measurements should be made by a variety of techniques and over large enough spatial and temporal scales to capture the majority of these changing conditions. We feel that all the measurement techniques described here are valid although they each have their own advantages and disadvantages. It is recommended that multiple approaches be applied whenever possible. In addition, a continuing effort is required in order to capture long-period tidal fluctuations, storm effects, and seasonal variations.

* This article was published in Science of the Total Environment, vol. 367, Burnett et al., Quantifying submarine groundwater discharge in the coastal zone via multiple methods, 498–543 © 2006 Elsevier B. V. Reprinted with permission from Elsevier. http://www.sciencedirect.com/science/journal/00489697
† Present Address: Comenius University, Bratislava, Slovakia.

1. Introduction

1.1. Background

Submarine groundwater discharge (SGD) has been recognized as an important pathway for material transport to the marine environment. It is important for the marine geochemical cycles of elements and can lead to environmental deterioration of coastal zones. While inputs from major rivers are gauged and well analyzed, thus allowing relatively precise estimates of fresh water and contaminant inputs to the ocean, assessing groundwater fluxes and their impacts on the near-shore marine environment is much more difficult, as there is no simple means to gauge these fluxes to the sea. In addition, there are cultural and disciplinary differences between hydrogeologists and coastal oceanographers which have inhibited interactions.

The direct discharge of groundwater into the near-shore marine environment may have significant environmental consequences because groundwater in many areas has become contaminated with a variety of substances like nutrients, heavy metals, radionuclides and organic compounds. As almost all coastal zones are subject to flow of groundwater either as submarine springs or disseminated seepage, coastal areas are likely to experience environmental degradation. Transport of nutrients to coastal waters may trigger algae blooms, including harmful algae blooms, having negative impacts on the economy of coastal zones [1].

We present here a review of the subject and the results of a recently completed project initiated as a concerted effort to improve the measurement situation by development of an expert group to: (1) assess the importance of SGD in different environments; and (2) to organize a series of 'intercomparison experiments' involving both hydrological and oceanographic personnel and techniques.

1.2. Significance of SGD

It is now recognized that subterranean non-point pathways of material transport may be very important in some coastal areas [2,3]. Because the slow, yet persistent seepage of groundwater through sediments will occur anywhere that an aquifer with a positive head relative to sea level is hydraulically connected to a surface water body, almost all coastal zones are subject to such flow [4–11]. Groundwater seepage is patchy, diffuse, temporally variable, and may involve multiple aquifers. Reliable methods to measure these fluxes need to be refined and the relative importance of the processes driving the flow needs clarification and quantification.

Specific examples of the ecological impact of groundwater flow into coastal zones have been given by Valiela et al. [12–14], who showed that groundwater inputs of nitrogen are critical to the overall nutrient economy of salt marshes. Corbett et al. [15,16] estimated that groundwater nutrient inputs are approximately equal to nutrient inputs via surface freshwater runoff in eastern Florida Bay. Krest et al. [17] estimated that SGD to salt marshes on the South Carolina coast supplies a higher flux of nutrients than that derived from all South Carolina rivers. Bokuniewicz [18] and Bokuniewicz and Pavlik [19] showed that subsurface discharge accounts for greater than 20% of the freshwater input into the Great South Bay, New York. Follow-up studies by Capone and Bautista [20] and Capone and Slater [21] showed that groundwater is a significant source (~50%) of nitrate to the bay. Lapointe et al. [22] found significant groundwater inputs of nitrogen and dissolved organic phosphorus to canals and surface waters in the Florida Keys and suggested this may be a key factor for initiating the phytoplankton blooms observed in that area. Nitrogen-rich groundwater is also suspected of nourishing *Cladophora* algal mats in Harrington Sound, Bermuda [23]. One possible hypothesis for the triggering mechanism of Harmful Algal Blooms (HABs) is increased nutrient supply via SGD [1,24] In many of the cases cited above, shallow groundwaters were enriched in nitrogen because of contamination from septic systems. In a more pristine environment, submarine springs were shown to cause measurable dilution of salinity and enrichment of nitrogen in Discovery Bay, Jamaica [25]. Groundwater was also shown

to be a significant component of terrestrial nutrient and freshwater loading to Tomales Bay, California [26]. Johannes [4] investigating coastal waters in Western Australia, stated that "it is ... clear that submarine groundwater discharge is widespread and, in some areas, of greater ecological significance than surface runoff."

1.3. Definition of submarine groundwater discharge

We have noted confusion in the literature concerning use of the term 'groundwater discharge' (e.g. see comment to Moore [7] by Younger [27] and subsequent reply on whether groundwater‡ is meteorically derived or 'any water in the ground'). The most general and frequently cited definition of groundwater is water within the saturated zone of geologic material (e.g. [28, 29]; in other words, water in the pores of submerged sediments ('pore water') is synonymous with 'groundwater'. We thus consider 'submarine groundwater discharge' to be any flow of water out across the sea floor. We define SGD without regard to its composition (e.g. salinity), its origin, or the mechanism(s) driving the flow [30]. Although our broad definition of SGD would technically allow inclusion of such processes as deep sea hydrothermal circulation, fluid expulsion at convergent margins, and density driven cold seeps on continental slopes, we restrict the term here (and thus focus our attention) to fluid circulation through continental shelf sediments with emphasis on the coastal zone (Fig.1).

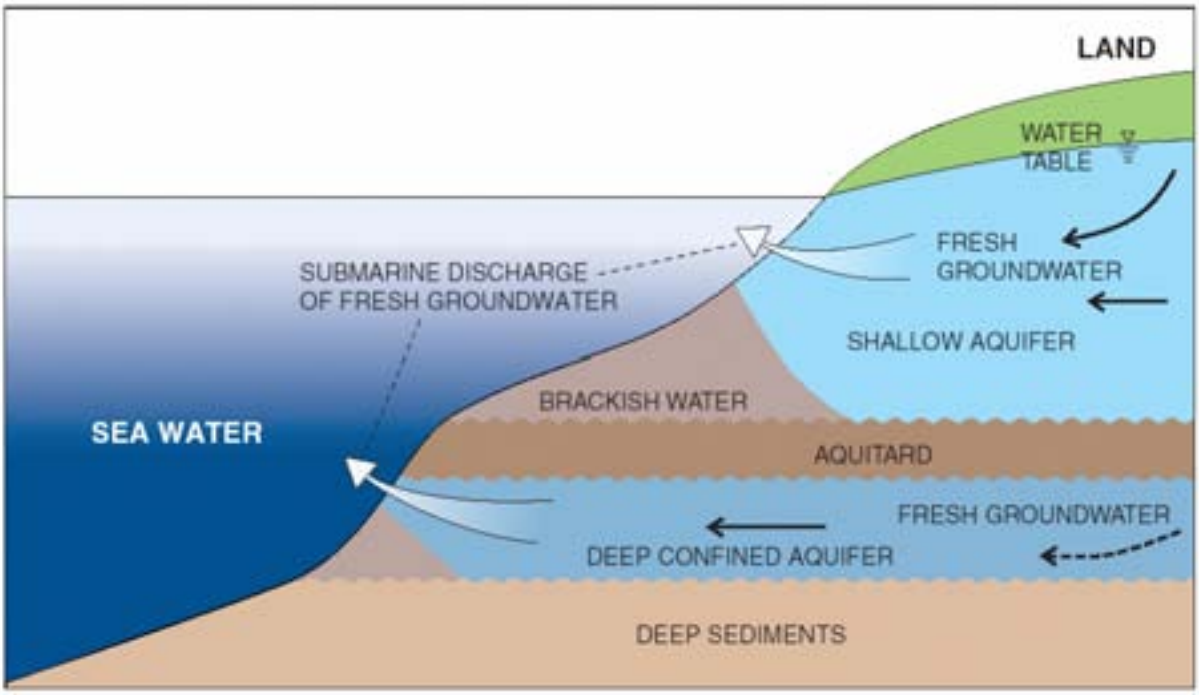

FIG.1. Schematic depiction (no scale) of processes associated with SGD. Arrows indicate fluid movement.

Traditional hydrology, however, has been concerned with terrestrial fresh water. As a result, some definitions identify groundwater as rainwater that has infiltrated and percolated to the water table, or put on some similar qualifications, consistent with the applications to freshwater, terrestrial systems (e.g. [31, 32]). Such qualifications on the definition of groundwater are too restrictive and lead to conceptual problems when dealing with submarine discharges. In our view, SGD does not have to be terrestrially derived, although it can be and is in many important situations. It may be legitimate to

‡ The modern convention is to write 'groundwater' as one word. The early practice was to write it as two words and hyphenated (or compounded) when used as an adjective. This usage is becoming more rare, although it is still the convention of the U.S. Geological Survey and the journal Ground Water. Writing it as one word may be done to emphasize "the fact that it is a technical term with a particular meaning" [33].

require water classified as 'groundwater' to move, when it does move, according to Darcy's Law§, but even that is too restrictive in some highly channelized (e.g. karst) situations. At least one definition of groundwater specifically excludes underground streams [34] while another specifically includes underground streams [35, 29]. Since karst is such an important setting for SGD, we think it best to include 'underground streams.'

So we have a system of terminology as follows. The flow of water across the sea floor can be divided into SGD, a discharging flow out across the sea floor, or submarine groundwater recharge (SGR), a recharging flow in across the sea floor. The two terms do not have to balance, however, because SGD can, and often will, include a component of terrestrially recharged water. Alternatively, some or all of the SGR can penetrate the subaerial aquifer, raising the water table or discharging as terrestrial surface waters (e.g., saline springs) rather than discharging out across the sea floor. The net discharge is the difference between these two components.

Coastal aquifers may consist of complicated arrays of confined, semi-confined, and unconfined systems. Simple hydrologic models do not consider the anisotropic nature of coastal sediments, dispersion, and tidal pumping. Moreover, cycling of seawater through the coastal aquifer may be driven by the flow of freshwater from coastal uplands [36]. As freshwater flows through an aquifer driven by an inland hydraulic head, it can entrain seawater that is diffusing and dispersing up from the salty aquifer that underlies it. Superimposed upon this terrestrially driven circulation are a variety of marine-induced forces that result in flow into and out of the seabed even in the absence of a hydraulic head. Such 'subterranean estuaries' [2] will be characterized by biogeochemical reactions that influence the transfer of nutrients to the coastal zone in a manner similar to that of surface estuaries [3, 37,38].

1.4. Drivers of SGD

SGD forcing has both terrestrial and marine components. The following drivers of fluid flow through shelf sediments may be considered: (1) the terrestrial hydraulic gradient (gravity) that results in water flowing downhill; (2) water level differences across a permeable barrier; (3) tide, wave, storm, or current-induced pressure gradients in the near-shore zone; (4) convection (salt-fingering) induced by salty water overlying fresh groundwater in some near-shore environments; (5) seasonal inflow and outflow of seawater into the aquifer resulting from the movement of the freshwater-seawater interface in response to annual recharge cycles; and (6) geothermal heating.

Hydrologists have traditionally applied Darcy's Law to describe the fresh water flow resulting from measured hydraulic gradients. However, when comparisons have been made, the modeled outflow is often much less than what is actually measured (e.g., [39]. Differences in water levels across permeable narrow reefs such as the Florida Keys [40,41] or barrier islands such as Fire Island, New York [19] are also known to induce subterranean flow. Such differences in sea level could be the result of tidal fluctuations, wave set-up, or wind forcing. Pressure gradients due to wave set-up at the shore [8], tidal pumping at the shore [42,43], large storms [44], or current-induced gradients over topographic expressions such as sand ripples also result in SGD [45,46]; If the density of the ocean water increases above that of the pore water for any reason, pore water can float out of the sediment by gravitational convection in an exchange with denser seawater without a net discharge [47]. Moore and

§ Whose law is it anyway? Darcy's? D'Arcy's? d'Arcy's? D'Arcys'? Darcys'? DArcys? Darcys? Or even, Darcies? You'll find them all in the literature or on the WEB. The correct version is "Darcy's" [48]. Although the man was born d'Arcy, his Jacobin tutor compelled him to change it to Darcy at an early age, a convention he permanently adopted (Darcy, 1957 as cited in Brown et al. [48]). 'Darcy' is the name on his tombstone, although we have it on good authority that Elvis Presley's name is misspelled on his tombstone so perhaps the grave marker is not necessarily definitive. (But, then again, maybe Elvis's not really dead either). We are indebted to Glenn Brown for his scholarship in sorting this all out. There might be a slim case made for 'Darcys' based on the convention in geography to drop the possessive apostrophe (e.g. 'Gardiners Island' not 'Gardiner's Island'). However, this is not the convention in physics and chemistry (e.g. Newton's Laws or Henry's Law). You, and Henry Darcy, apparently can possess a law.

Wilson [44] documented the exchange of pore water to a depth of 1.5 m following an intrusion of cold water onto the shelf.

An annual recharge cycle causing a seasonal inflow and outflow of seawater within an unconfined coastal aquifer is a new concept introduced by a team at MIT [49]. This group had shown earlier via a seepage meter survey of Waquoit Bay that the groundwater discharge was largely saline [50]. To explain the source and timing of the high flux of salty water (highest discharge in early summer), these investigators proposed a seasonal shift in the freshwater–seawater interface in response to the annual recharge cycle (highest recharge in the early spring). As the water table rises in response to enhanced recharge, more fresh water is drawn from further inland displacing salty groundwater and causing it to be discharged offshore (Fig.2). The opposite pattern occurs during the period of maximum evapotranspiration in the summer and salt water flows into the aquifer. A numerical model predicted that there would be a time lag of up to 3 months for the interface to move through the aquifer. So the observed maximum discharge in the early summer is thought to have been generated by the maximum water table thickness that occurred following greatest recharge in the early spring.

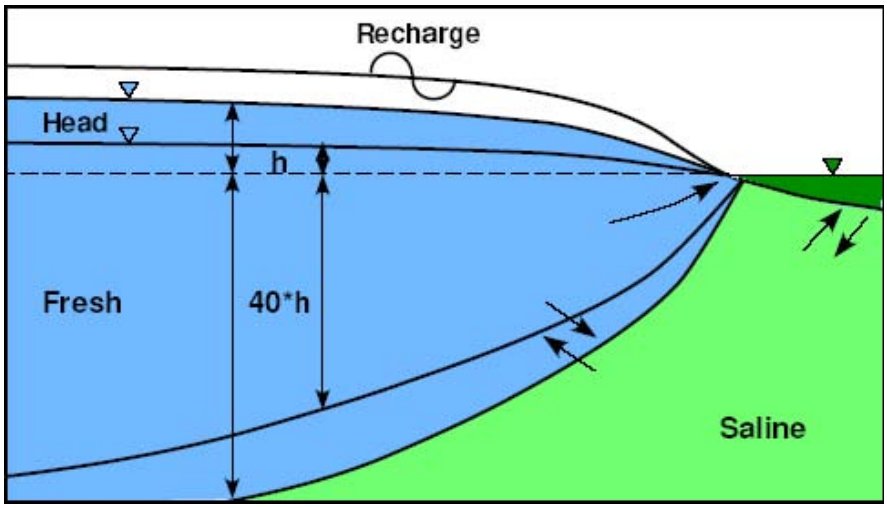

FIG.2. Schematic showing how interface position may shift within an unconsolidated aquifer in response to aquifer head level according to Ghyben–Herzberg relation. Because of differences in density between fresh water and seawater, seasonal changes in recharge will generate corresponding changes in the interface that would be magnified by ~40× (density of fresh water divided by the difference in densities). Diagram from Michael et al. [49].

From an oceanographic point of view, the total (fresh + seawater) SGD flux is important because all flow enhances biogeochemical inputs. Hydrologists have typically been concerned with the fresh water flow and seawater intrusion along the coast. The terrestrial and oceanic forces overlap in space and time; thus, measured fluid flow through coastal sediments is a result of composite forcing.

Seepage meter records that display temporal trends in near-shore regions typically show variations that correspond to the tidal period in that area. For example, Lee [51] showed that seepage rates were distinctly higher at low tide. While some correspondence between tides and seepage flux is typical for near-shore environments, the timing of the seepage maximum relative to the tidal stage varies depending upon the hydrologic setting at each location. Some areas show a direct inverse correlation between seepage rate and tidal stage, probably reflecting a modulation of a terrestrially driven flow by changing hydrostatic pressure. In other situations, tidal pumping or wave set-up recharges the coastal aquifer with seawater on the flood tide that discharges seaward at a later time, complicating this simple picture [43].

Recent investigations have reported longer-term (weeks to months) tidally modulated cycles in seepage based on continuous measurements of the groundwater tracers radon and methane [11] and automated seepage meter observations. Taniguchi [52] continuously recorded seepage flux rates in Osaka Bay, Japan, from May to August 2001 and analyzed these data via the Fast Fourier Transfer (FFT) method to discern the dominant periods of variation (Fig.3). Both studies showed that there is not only a semi-diurnal to diurnal tidal relationship to SGD but also a semi-monthly variation in flow reflecting the neap-spring lunar cycle. Superimposed on this predictable behaviour in tidally driven response, are variations in terrestrial hydrologic parameters (water table height, etc.). This terrestrial influence showed up in tracer data from Korea, where Kim and Hwang [11] noted that groundwater discharge was more limited in the dry season when the aquifer was not recharging. These results demonstrate the overlapping nature between terrestrial and marine SGD forcing components.

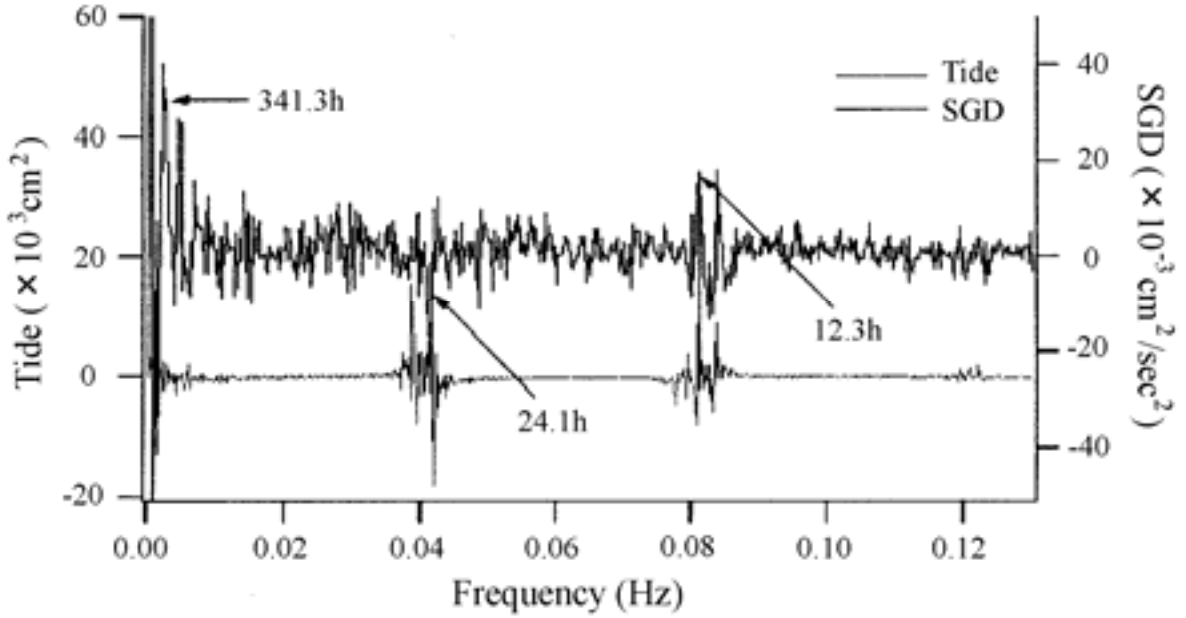

FIG.3. Time series analysis (FFT method) of long-term SGD measurements and tides in Osaka Bay, Japan, from May 29 to August 23, 2001. The main SGD frequencies correspond to semi-diurnal (12.3 h), diurnal (24.1 h), and bi-weekly (341.3 h) lunar cycles [52].

In the coastal zone, discharges influenced by terrestrial and marine forces are typically coincident in time and space but may differ significantly in magnitude. Since the hydraulic gradient of a coastal aquifer, tidal range, and position of the freshwater–seawater interface change over time; it is possible that the situation in any one area could shift (e.g., seasonally) between terrestrially governed and marine dominated systems.

2. A Short History of SGD Research

2.1. Overview

Knowledge concerning the undersea discharge of fresh groundwater has existed for many centuries. According to Kohout [53], the Roman geographer, Strabo, who lived from 63 B.C. to 21 A.D., mentioned a submarine spring 2.5 miles offshore from Latakia, Syria, near the island of Aradus in the Mediterranean. Water from this spring was collected from a boat, utilizing a lead funnel and leather tube, and transported to the city as a source of fresh water. Other historical accounts tell of water vendors in Bahrain collecting potable water from offshore submarine springs for shipboard and land use [54], Etruscan citizens using coastal springs for ‘hot baths’ (Pausanius, ca. 2nd century A.D.), and

submarine ‘springs bubbling fresh water as if from pipes’ along the Black Sea (Pliny the Elder, ca. 1st century A.D.).

The offshore discharge of fresh water has been investigated and used in a number of cases for water resource purposes. One particularly spectacular example of such use involved the construction of dams in the sea near the southeastern coast of Greece. The resulting ‘fence’ allowed the formation of a freshwater lake in the sea that was then used for irrigation on the adjacent coastal lands [55]. Thus, while the existence of the direct discharge of groundwater into the sea has been realized for many years, the impetus was largely from water resource considerations and much of the information was anecdotal.

Groundwater hydrologists have traditionally been primarily concerned with identifying and maintaining potable groundwater reserves. At the shoreline, their interest is naturally directed landward and attention has been focused only on the identification of the saltwater/freshwater ‘interface’ in coastal aquifers. The classic Ghyben–Herzberg relationship sufficed in many practical applications in unconfined aquifers (Baydon-Ghyben [56]; Herzberg [57] both as cited in Bear et al., [58]) even though it represented an unrealistic, hydrostatic situation. The gravitational balance between the fresh groundwater and the underlying salty groundwater cannot predict the geometry of the freshwater lens but only estimate the depth of the saltwater/freshwater interface if the elevation of the water table is measured. A truly stable, hydrostatic distribution, however, would find saline groundwater everywhere below sea level. Maintaining a freshwater lens requires a dynamic equilibrium supported by freshwater recharge. The Dupuit approximation (Dupuit, 1888, as cited in [28]) was incorporated to account for this equilibrium. The assumption is essentially that the flow of groundwater is entirely horizontal. In that treatment, the saltwater/freshwater interface is a sharp boundary across which there is no flow and which intersects the shoreline; the salty groundwater is stationary. None of this is strictly true and the Dupuit–Ghyben–Herzberg relationship leads to the awkward, but not debilitating, result that all the freshwater recharge had to escape exactly at the shoreline. Hubbert [59] removed this awkwardness by introducing the concept of an outflow gap. The saltwater/freshwater interface was still sharp and was considered a boundary of no flow. The saline groundwater was still stationary, but the interface did not intersect the shoreline. Rather it intersected the sea floor at some distance from shore leaving, a band or gap through which the fresh groundwater could escape into the sea. If the depth of the saltwater/freshwater interface at the shoreline is measured, the Dupuit–Ghyben–Herzberg methodology can be used, with this as a boundary condition, to calculate the width of the outflow gap [60]. Potential theory [61] and the Glover solution [62] provided independent means to calculate the size of this gap and the position of the saltwater/freshwater interface. These representations, simplified for calculational necessity, unfortunately could lead one to the mistaken impression that SGD is entirely fresh water derived from land. Hubbert [59] had also pointed out that the interface was not necessarily sharp and that the cyclic flow of salty groundwater needed to maintain a transition zone must be driven by the presence of hydraulic gradients in the saline groundwater. It thus became recognized that the saline groundwater is not necessarily stationary.

With the development of numerical models, it became possible to calculate more realistic hydrodynamics. One early numerical model calculated the groundwater seepage into lakes [63]. While this lacustrine seepage had nothing to do with the saltwater/freshwater interface, it is noteworthy because it was the first use of the notion of an exponential decrease to approximate the distribution of seepage rates offshore.

The next generations of models allowed the saline groundwater to circulate in response to hydraulic gradients but still prohibited flow across the ‘interface’ although the interface itself might move. Modern, two-phase models recognize that water can cross isohalines and can track both salt and water in the continuum, and they allow density driven circulation as well as flows driven by other hydraulic

gradients onshore. Bear et al. [58] provide a review of the complex array of modern models. There is, however, a serious lack of data to calibrate and verify such models. In addition, dispersion is usually incorporated in a single parameter although it is recognized that numerous processes can cause salt dispersion on a wide range of time and space scales.

It is important to recognize that the Ghyben–Herzberg relationship cannot be used to estimate the width of the fresh–salt interface for semi-confined artesian aquifers. Such aquifers can leak freshwater or salt–fresh water mixtures for considerable distances from shore.

SGD was neglected scientifically for many years because of the difficulty in assessment and the perception that the process was unimportant. This perception is changing. Within the last several years there has emerged recognition that in some cases, groundwater discharge into the sea may be both volumetrically and chemically important [4]. A decade after Johannes' benchmark paper, Valiela and D'Elia [64] published a compilation on the subject and stated, "We are very much in the exploratory stage of this field." The exploration has continued and there is now growing agreement that groundwater inputs can be chemically and ecologically important to coastal waters.

As a result of this increased interest, the Scientific Committee on Oceanic Research (SCOR) formed two working groups (WG) to examine this emerging field more closely. SCOR WG-112 (Magnitude of Submarine Groundwater Discharge and its Influence on Coastal Oceanographic Processes) was established in 1997 to 'define more accurately and completely how submarine groundwater discharge influences chemical and biological processes in the coastal ocean' [65]. This group published a special issue of Biogeochemistry on SGD in 2003 as their final product [66]. WG-114 (Transport and Reaction in Permeable Marine Sediments) was established in 1999 to investigate the importance of fluid flow through permeable sediments to local and global biogeochemical cycling and its influence on surrounding environments [67]. That group completed its work in 2003 with the introduction of a continuing conference on the subject, the 'Gordon Research Conference on Permeable Sediments'.

2.2. Worldwide studies

Taniguchi et al. [68] presented a review of all available studies that have attempted to estimate the magnitude of SGD or indicated that SGD in the area studied was significant. This compilation was limited to literature citations of discharge estimates using seepage meters, piezometers, and/or geochemical/geophysical tracers.

Locations of specific SGD estimates showed that many independent studies have been performed on the east coast of the United States, Europe, Japan, and Oceania (Fig.4). Fewer studies have been done on the west coast of the US, South America, and Hawaii. They were unable to find any quantitative data from Africa, India, or China, though indications of groundwater discharge have been reported for Bangladesh [69] and Kenya [70].

2.3. The IAEA/UNESCO SGD initiative

An initiative on SGD was developed by the International Atomic Energy Agency (IAEA) and UNESCO in 2000 as a 5-year plan to assess methodologies and importance of SGD for coastal zone management. The IAEA component included a Coordinated Research Project (CRP) on 'Nuclear and Isotopic Techniques for the Characterization of Submarine Groundwater Discharge in Coastal Zones' carried out jointly by IAEA's Isotope Hydrology Section in Vienna and the Marine Environment Laboratory in Monaco, together with nine laboratories from eight countries. The activities have included joint meetings (Vienna 2000, 2002, and 2005; Syracuse, Sicily 2001; and Monaco 2004), sampling expeditions (Australia 2000; Sicily 2001 and 2002; New York 2002; Brazil 2003; and Mauritius 2005), joint analytical work, data evaluation and preparation of joint publications. The objectives of the CRP included the improvement of capabilities for water resources and environmental management of coastal zones; application of recently developed nuclear and isotopic techniques

suitable for quantitative estimation of various components of SGD; understanding of the influence of SGD on coastal processes and on groundwater regimes; a better management of groundwater resources in coastal areas; and development of numerical models of SGD.

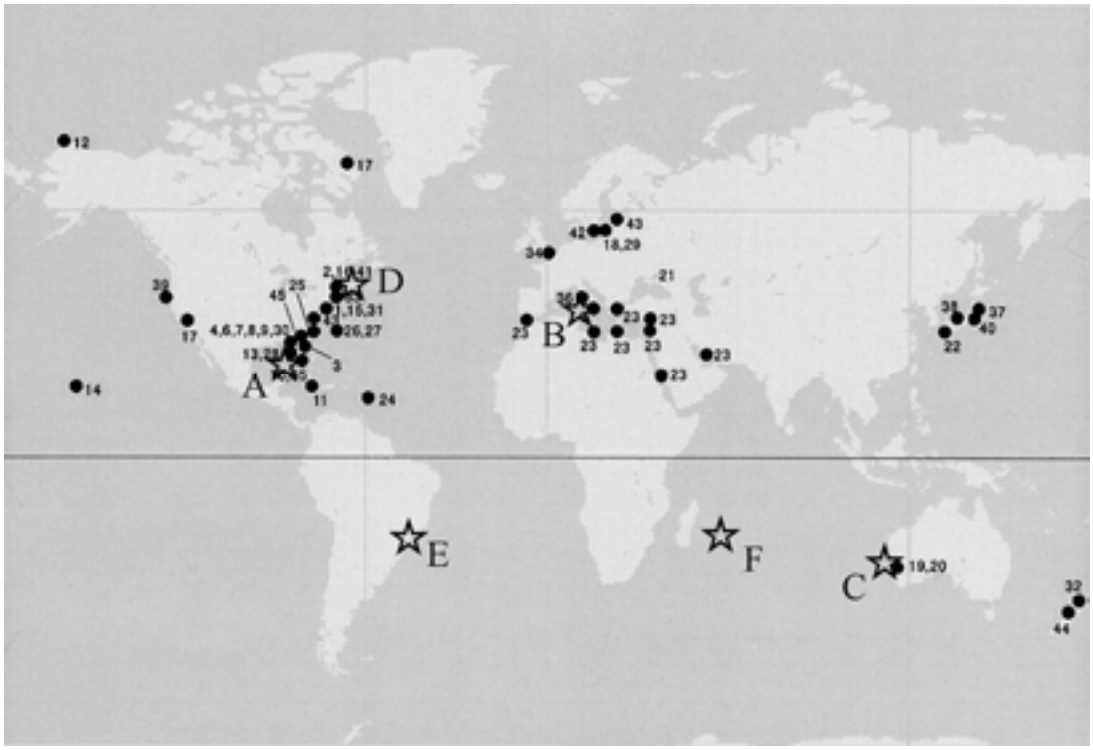

FIG.4. Location of published investigations of submarine groundwater discharge (SGD). All studies used provided SGD estimations using seepage meters, piezometers, or geochemical/ geophysical (temperature) tracers. Sites labeled 'A' through 'F' are locations where SGD assessment intercomparisons have been carried out. Site 'A' was an initial experiment in Florida [71] and 'B' through 'F' represent the five experiments reported in this paper. The numbers refer to 45 sites where SGD evaluations were identified by Taniguchi et al. [68].

The UNESCO component included sponsorship from the Intergovernmental Oceanographic Commission (IOC) and the International Hydrological Program (IHP). The main objective of this aspect of the project was to provide both the scientific and coastal zone management communities with the tools and skills necessary to evaluate the influence of SGD in the coastal zone. A central part of this program was to define and test the most appropriate SGD assessment techniques via carefully designed intercomparison experiments. The plan was to run one experiment per year over approximately five years. The sites were selected based on a variety of criteria including logistics, background information, amount of SGD expected, hydrological and geological characteristics, etc. The intention was to include as many different hydrogeologic environments as possible (e.g., karst, coastal plain, volcanic, crystalline bedrock, glacial, etc.). Each systematic intercomparison exercise involved as many methodologies as possible including modeling approaches, 'direct' measurements (e.g., seepage meters of varying design, piezometers), and natural tracer studies (e.g., radium isotopes, radon, methane, artificial tracers, etc.).

Because of differences in the nature and scale of each of these approaches, the final experimental design necessarily varied from site to site. The general experimental plan consisted of transects of piezometers (to measure the hydraulic gradients and conductivities), transects of bulk ground conductivity measurements, manual and automated seepage meters (to measure flow directly), with specialized experiments and water sampling at appropriate points within the study area. Various seepage meter designs were evaluated during the field experiments. Water sampling for tracer studies

was conducted while the hydrological measurements were in progress with most analyses being performed at the field site. Samples for geochemical tracers were collected from both the water column as well as from the aquifer itself. The specific sampling plan for tracer samples was determined by the spatial and temporal variations expected at each site.

The IAEA/UNESCO group developed the following list of desirable characteristics for 'flagship' site(s) to perform such intercomparisons. These were not intended to be representative sites of SGD, but rather sites where the processes could be evaluated and methods compared with minor complications.

(1) *General Characteristics*: Known occurrence of SGD at the site, and preferably, some prior assessments including some understanding of the temporal and spatial variability. In addition, the study site should have a significant amount of SGD and a large ratio of groundwater discharge to other inputs (streams, precipitation).

(2) *Geology/Hydrogeology*: A reasonable understanding of the local hydrogeology. Good access to historical and current records (potentiometric levels, hydraulic conductivity, rainfall, etc.). Uniform geology and bottom type (sandy or silt, but not rocky is best for seepage meters).

(3) *Climate*: Good local/regional ancillary data such as climate, coastal oceanography, water budget, hydrologic cycle, etc.

(4) *Site geometry/oceanography*: A sheltered enclosed or semi-enclosed basin with a small adjacent drainage basin would be easier to handle in many ways than an open shelf environment with tidal currents, and other complicating factors.

(5) *Logistics*: Good access to the site, both local and long distance; local logistical support (vans, support personnel, housing, etc.), proximity to laboratory facilities (perhaps a marine laboratory), easy access to electric power for such things as data loggers, etc., local sponsor or coordinator.

3. Methods Used to Measure SGD

3.1. Seepage meters

Measurements of groundwater seepage rates into surface water bodies are often made using manual 'seepage meters'. Israelsen and Reeve [72] first developed this device to measure the water loss from irrigation canals. Lee [51] designed a seepage meter consisting of one end of a 55-gal (208 L) steel drum that is fitted with a sample port and a plastic collection bag (Fig.5). The drum forms a chamber that is inserted open end down into the sediment. Water seeping through the sediment will displace water trapped in the chamber forcing it up through the port into the plastic bag. The change in volume of water in the bag over a measured time interval provides the flux measurement.

Studies involving seepage meters have reached the following general conclusions: (1) many seepage meters are needed because of the natural spatial and temporal variability of seepage flow rates [73,74]; (2) the resistance of the tube [75] and bag [76,77] should be minimized to the degree possible to prevent artifacts; (3) use of a cover for the collection bag may reduce the effects of surface water movements due to wave, current or stream flow activity [78]; (4) the bag should initially contain a measured volume of water; thus, positive and negative seepage may be determined; (5) caution should be applied when operating near the seepage meter detection limit, i.e., a few cm^3/cm^2 day [79,80]; and (6) artifacts occasionally exist from pressure gradients developed by uni-directional currents passing over the meter [81]. In a recent rebuttal to the criticism concerning pressure-induced flow, Corbett and Cable [82] question whether sufficient evidence was presented to support the conclusion that seepage meters are not a practical instrument to use in coastal environments.

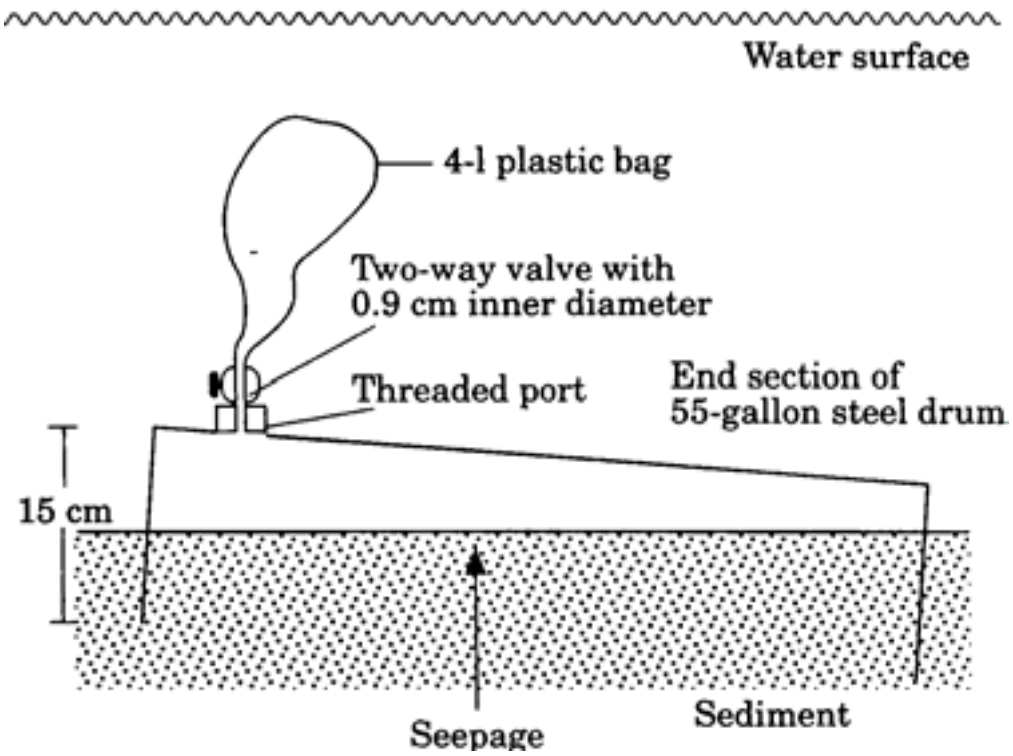

FIG.5. Sketch of a simple 'Lee-type' manual seepage meter [51].

Perhaps the most serious disadvantage for coastal zone studies is that manual seepage meters are very labour intensive. In order to obtain the groundwater discharge rate automatically and continuously, various types of automated seepage meters have been developed. Fukuo [83], Cherkauer and McBride [84], and Boyle [85] describe remote installations of seepage meters from the surface of various water bodies. Sayles and Dickinson [86] constructed a seepage meter that was a benthic chamber for the sampling and analysis of seepage through sediments associated with hydrothermal vents. Another example of an automated approach for measurement of SGD seepage is the heat-pulse device described by Taniguchi and Fukuo [87] and a similar meter constructed by Krupa et al. [88]. The 'Taniguchi-type (heat-pulse type)' automated seepage meter is based on the travel time of a heat pulse down a narrow tube. The device uses a string of thermistors in a column positioned above an inverted funnel covering a known area of sediment (Fig.6 [87]). The method involves measuring the travel time of a heat pulse generated within the column by a nichrome wire induction heater. Since heat is a conservative property, the travel time is a function of the advective velocity of the water flowing through the column. Thus, once the system is calibrated in the laboratory, measurements of seepage flow at a field site can be made automatically on a near-continuous basis. The Taniguchi meter has successfully measured seepage up to several days at a rate of about one measurement every five minutes [89].

Taniguchi and Iwakawa [10] more recently developed a 'continuous-heat type automated seepage meter' (Fig.7). This design makes it possible to measure the temperature gradient of the water flowing between the downstream (sensor A) and upstream (sensor B) positions in a flow tube with a diameter of 1.3 cm. The temperature gradient is caused by the heat continuously generated within the column, the so-called 'Granier method' [90]. When there is no water flow, the temperature difference between sensors A and B in the column is the maximum, and it decreases with increasing the water flow velocity [91].

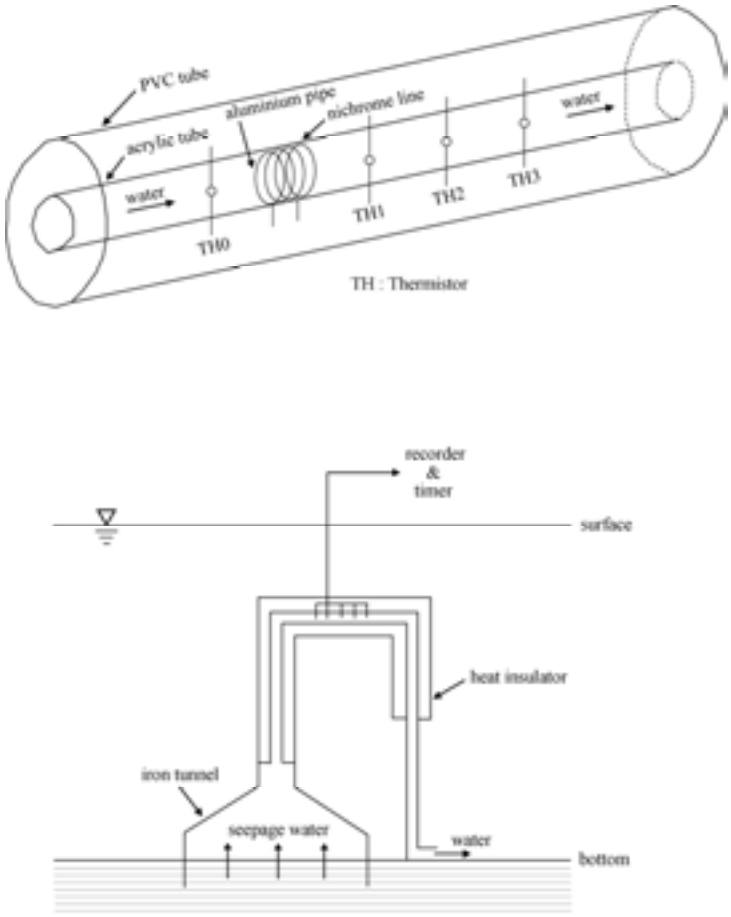

FIG.6. Taniguchi-type (heat pulse) automated seepage meter [87].

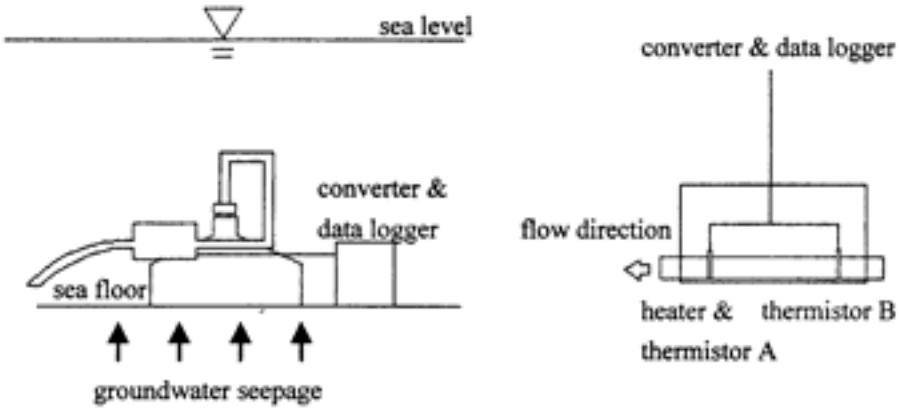

FIG.7. Continuous heat-type automated seepage meter [10].

The 'dye-dilution seepage meter', developed at Woods Hole Oceanographic Institution, involves the injection of a colored dye into a mixing chamber attached to a seepage meter and the subsequent measurement of the dye absorbance in the mixing chamber over time. Typically, dye is injected every hour into a mixing chamber of known volume (usually 0.5 L), and the absorbance is recorded every five minutes. The rate at which the dye is diluted by the inflowing seepage water is used to calculate the flow-rate. In order to avoid the cost and complexity of a dedicated spectrophotometer, a nitrate analyzer is used to inject the dye and make the absorbance measurements [92].

Flow meters based on ultrasonic measurements are also used to evaluate seepage flow [93]. The benthic chamber uses a commercially-available, acoustic flow meter to monitor the SGD. Since the speed of sound depends on salinity, the same sensor output can be used to continuously calculate the salinity of SGD as well as the flow rates.

A serious limitation of seepage meters is the requirement that they be deployed in a relatively calm environment. Breaking waves dislodge seepage meters and strong currents induce flow through the seabed when passing over and around large objects [46].

3.2. Piezometers

Another method for assessing groundwater seepage rates is the use of multi-level piezometer nests. With this approach, the groundwater potential in the sediments can be measured at several depths [28]. Using observations or estimates of the aquifer hydraulic conductivity (here assumed constant), one can then easily calculate the groundwater discharge rate into the ocean by use of a one-dimensional form of Darcy's Law:

$$q = -K\, dh/dL \quad (1)$$

where q is Darcian flux (groundwater discharge volume per unit area per unit time), K is hydraulic conductivity, and dh/dL is the hydraulic gradient in which h is hydraulic head and L is distance.

Piezometer nests suffer from the natural variability in seepage rates due to heterogeneity in the local geology. Typically, it is difficult to obtain representative values of hydraulic conductivity, which often varies over several orders of magnitude within an aquifer. Therefore, accurate evaluations of SGD using piezometers depend largely on the estimate of the aquifer's hydraulic conductivity. Therefore, piezometer nests are often used in conjunction with seepage meters to estimate the hydraulic conductivity from observed seepage rates and the hydraulic gradient [94,95].

3.3. Natural tracers

One approach for local to regional-scale estimation of groundwater inputs into the ocean uses naturally occurring geochemical tracers. An advantage of groundwater tracers is that they present an integrated signal as they enter the marine water column via various pathways in the aquifer. Although small-scale variability is a serious drawback for the use of seepage meters or piezometers, such small spatial scale variations tend to be smoothed out over time and space in the case of tracer methods [96]. On the other hand, natural tracers require that all other tracer sources and sinks except groundwater be evaluated, an often difficult exercise.

Natural geochemical tracers have been applied in two ways to evaluate groundwater discharge rates into the ocean. First is the use of enriched geochemical tracers in the groundwater relative to the seawater. In other words, the concentration of a solute in the receiving water body is attributed to inputs of that component derived only from groundwater [7, 97–99]. A second approach is the use of vertical profiles of the geochemical compositions in sediment pore waters under the assumption that its distribution can be described by a vertical, one-dimensional advection-diffusion model (e.g., [100,101]. However, this is usually limited to the case of homogeneous media.

Over the past few years, several studies used natural radium isotopes and ^{222}Rn to assess groundwater discharge into the ocean [7,9,11,15–17,44,71,97,98,102–114]. Ideally, in order to provide a detectable signal, a groundwater tracer should be greatly enriched in the discharging groundwater relative to coastal marine waters, conservative, and easy to measure. Radium isotopes and radon have been shown to meet these criteria fairly well and other natural tracer possibilities exist which may be exploited for groundwater discharge studies. In applying geochemical tracing techniques, several criteria must be assessed or defined, including boundary conditions (i.e., area, volume), water and constituent sources and sinks, residence times of the surface water body, and concentrations of the

tracer. Sources may include ocean water, river water, groundwater, precipitation, in situ production, horizontal water column transport, sediment resuspension, or sediment diffusion. Sinks may include in situ decay or consumption, horizontal water column transport, horizontal or vertical eddy diffusivity, and atmospheric evasion. Through simple mass balances or box models incorporating both sediment advection and water column transport, the geochemical approach can be quite useful in assessing SGD.

Radium isotopes are enriched in groundwater relative to surface waters, especially where salt water is coming into contact with surfaces formally bathed only in fresh waters. Moore [7] showed that waters over the continental shelf off the coast of the southeastern USA were enriched in ^{226}Ra with respect to open ocean values. The radium concentrations also showed a distinct gradient being highest in the near-shore waters. By using an estimate of the residence time of these waters on the shelf and assuming steady-state conditions, one can calculate the offshore flux of the excess ^{226}Ra (Fig.8). If this flux is supported by SGD along the coast, then the SGD can be estimated by dividing the radium flux by the estimated ^{226}Ra activity of the groundwater. A convenient enhancement to this approach is that one may use the short-lived radium isotopes, ^{223}Ra and ^{224}Ra, to assess the water residence time [108].

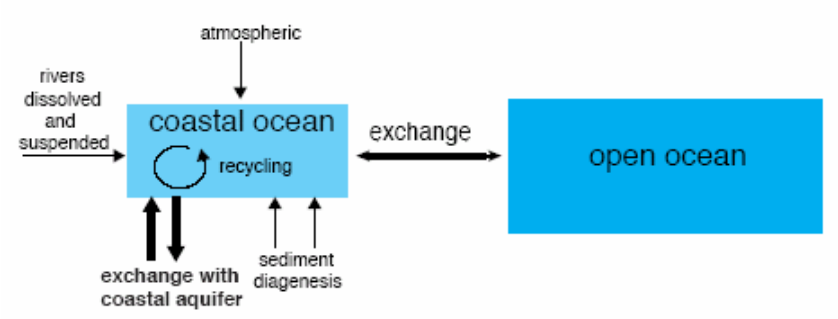

FIG.8. Box model showing how radium isotopes can be used to investigate exchange between the coastal and open ocean.

Moore ([7] and elsewhere) has suggested the following general strategy to determine the importance of oceanic exchange with coastal aquifers: (1) Identify tracers derived from coastal aquifers that are not recycled in the coastal ocean; map their distribution and evaluate other sources. (2) Determine the exchange rate of the coastal ocean with the open ocean. (3) Calculate the tracer flux from the coastal ocean to the open ocean, hence the tracer flux from the aquifer to the coastal ocean. (4) Measure the average tracer concentration in the coastal aquifer to calculate fluid flux. (5) Use the concentrations of other components (nutrients, carbon, metals) in the aquifer or their ratios to the tracer to estimate their fluxes.

Hwang et al. [24] developed a geochemical model for local-scale estimation of SGD. If the system under study is steady state, than radium additions are balanced by losses. Additions include radium fluxes from sediment, river, and groundwater; losses are due to mixing and, in the case of ^{223}Ra and ^{224}Ra, radioactive decay. Using a mass balance approach on a larger scale with the long-lived isotopes ^{226}Ra and ^{228}Ra, Kim et al. [115] determined that SGD-derived silicate fluxes to the Yellow Sea were on the same order of magnitude as the Si flux from the Yangtze River, the fifth largest river in the world.

A steady-state mass balance approach may also be used for ^{222}Rn with the exception that atmospheric evasion must also be taken into account [116]. The main principle of using continuous time-series radon measurements to decipher rates of groundwater seepage is that if we can monitor the inventory of ^{222}Rn over time, making allowances for losses due to atmospheric evasion and mixing with lower concentration waters offshore, any changes observed can be converted to fluxes by a mass balance approach (Fig.9). Although changing radon concentrations in coastal waters could be in response to a

number of processes (sediment resuspension, long-shore currents, etc.), advective transport of groundwater (pore water) through sediment of Rn-rich solutions is often the dominant process. Thus, if one can measure or estimate the radon concentration in the advecting fluids, the ^{222}Rn fluxes may be easily converted to water fluxes.

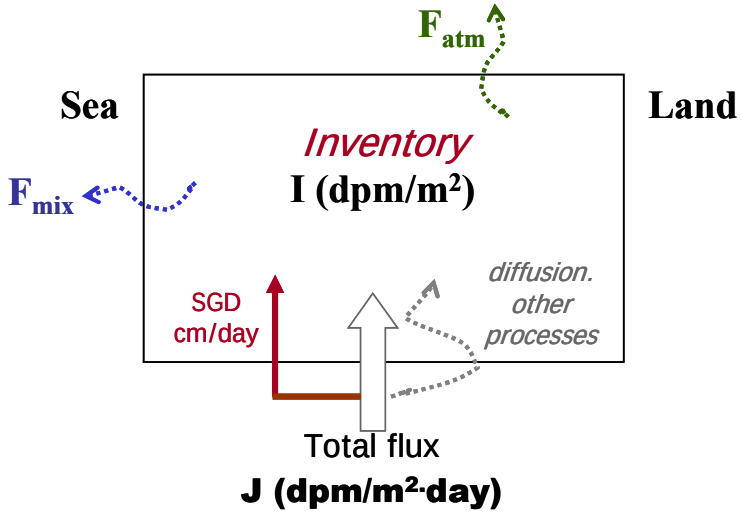

FIG.9. Conceptual model of use of continuous radon measurements for estimating SGD in a coastal zone. The inventory refers to the total amount of excess ^{222}Rn per unit area. Losses considered include atmospheric evasion and mixing with offshore waters. Decay is not considered because the fluxes are evaluated on a very short time scale relative to the half-life of ^{222}Rn [111].

Although radon and radium isotopes have proven very useful for assessment of groundwater discharges, they both clearly have some limitations. Radium isotopes, for example, may not be enriched in fresh water discharges such as from submarine springs. Radon is subject to exchange with the atmosphere which may be difficult to model under some circumstances (e.g., sudden large changes in wind speeds, waves breaking along a shoreline). The best solution may be to use a combination of tracers to avoid these pitfalls.

New and improved technologies have assisted the development of approaches based on radium isotopes and radon. The measurement of the short-lived radium isotopes ^{223}Ra and ^{224}Ra, for example, used to be very tedious and time-consuming until the development of the Mn-fiber and delayed coincidence counter approach [117]. Now it is routine to process a sample (often 100–200 L because of very low environmental activities) through an Mn-fiber adsorber, measure the short-lived isotopes the same day by the delayed coincidence approach, and then measure the long-lived isotopes (^{226}Ra and ^{228}Ra) at a later date by gamma spectrometry. Burnett et al. [96] developed a continuous radon monitor that allows much easier and unattended analysis of radon in coastal ocean waters. The system analyses ^{222}Rn from a constant stream of water delivered by a submersible pump to an air–water exchanger where radon in the water phase equilibrates with radon in a closed air loop. The air stream is fed to a commercial radon-in-air monitor to determine the activity of ^{222}Rn. More recently, an automated multi-detector system has been developed that can be used in a continuous survey mode to map radon activities in the coastal zone [118]. By running as many as six detectors in parallel, one may obtain as many as 12 readings per hour for typical coastal ocean waters with a precision of better than 10–15%.

Another approach consists of application of in situ gamma-ray spectrometry techniques that have been recognized as a powerful tool for analysis of gamma-ray emitters in sea-bed sediments, as well as for continuous analysis of gamma-ray emitters (e.g., ^{137}Cs, ^{40}K, ^{238}U and ^{232}Th decay products) in seawater (e.g., Povinec et al. [119]). In situ gamma-ray spectrometers have been applied for continuous

stationary and spatial monitoring of radon (as well as thoron, i.e., ^{220}Rn) decay products in seawater, together with salinity, temperature and tide measurements, as possible indicators of SGD in coastal waters of SE Sicily and at the Ubatuba area of Brazil [120].

Methane (CH_4) is another useful geochemical tracer that can be used to detect SGD. Both ^{222}Rn and CH_4 were measured along the Juan de Fuca Ridge as a means of estimating heat and chemical fluxes from the hydrothermal vents of that area [121]. Both ^{222}Rn and CH_4 were used to evaluate SGD in studies performed in a coastal area of the northeastern Gulf of Mexico [97]. Tracer (^{222}Rn and CH_4) inventories in the water column and seepage rates measured using a transect of seepage meters were evaluated over several months within a shallow water location. The linear relationships between tracer inventories and measured seepage fluxes were statistically significant (Fig.10). These investigators found that inventories of ^{222}Rn and CH_4 in the coastal waters varied directly with groundwater seepage rates and had a positive relationship (95% C.L.). In addition, water samples collected near a submarine spring in the same area displayed radon and methane concentrations inversely related to salinity and considerably greater than those found in surrounding waters. In a related study, Bugna et al. [122] demonstrated that groundwater discharge was an important source for CH_4 budgets on the inner continental shelf of the same region. In another example, Tsunogai et al. [123] found methane-rich plumes in the Suruga Trough (Japan) and postulated that the plume was supplied from continuous cold fluid seepage in that area. Another technological advance, the 'METS' sensor (Capsum Technologies GmbH, Trittau, Germany), can now automatically and continuously measure methane at environmental levels in natural waters [11].

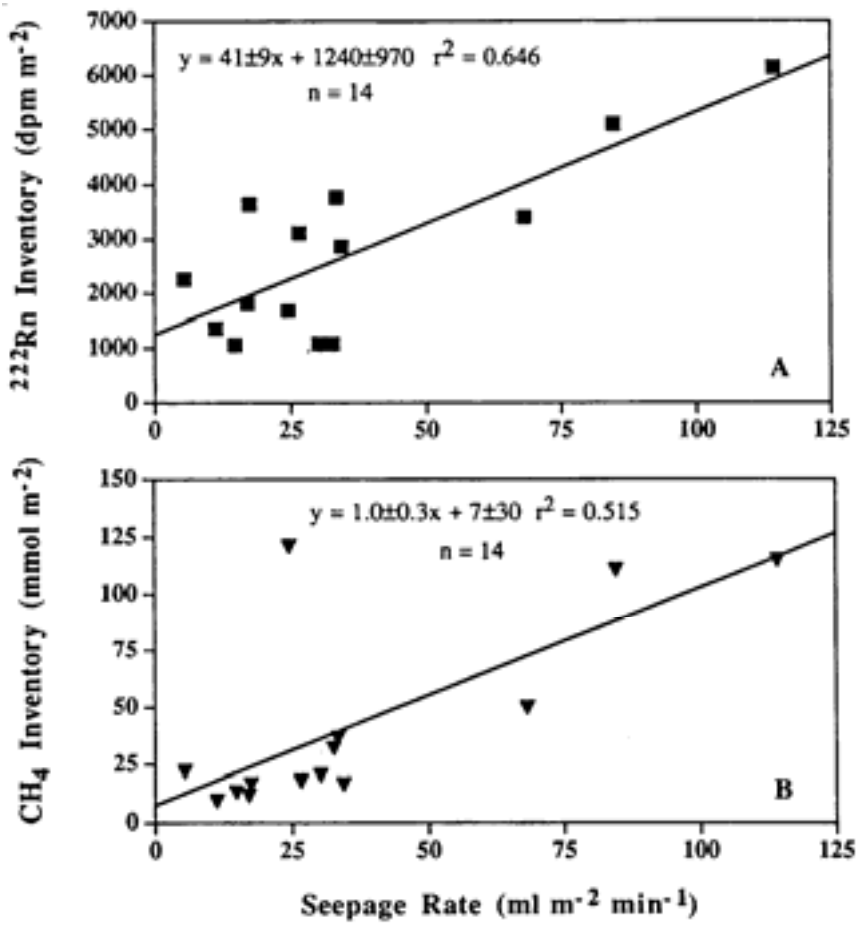

FIG.10. Relationship between (A) ^{222}Rn and (B) CH_4 inventories in the overlying water column and groundwater fluxes measured at one station by seepage meters in the coastal Gulf of Mexico[97].

Several other natural radioactive (^{3}H, ^{14}C, U isotopes, etc.) and stable (^{2}H, ^{3}He, ^{4}He, ^{13}C, ^{15}N, ^{18}O, $^{87/86}Sr$, etc.) isotopes and some anthropogenic atmospheric gases (e.g., CFCs) have been used for conducting SGD investigations, tracing water masses, and calculating the age of groundwater. Uranium may be removed to anoxic sediments during submarine groundwater recharge (SGR). Moore and Shaw [124] used deficiencies of uranium concentration (relative to expected concentrations based on the U/salinity ratio in sea water) to estimate SGR in several southeast US estuaries. Stable isotope data can help to evaluate groundwater–seawater mixing ratios, important for the estimation of the SGD in coastal areas [125]. Seawater and the fresh groundwater end members often have specific signatures due to different tracers/isotopes. Under good circumstances, such differences between end members would allow calculation of the percent groundwater contribution. This may be especially useful when mixing is occurring between more than two end members including saline groundwater.

Besides the mixing ratio calculations, each tracer can be used for interpretation of various groundwater characteristics. In mixed waters, the selection of the related fresh groundwater end member is an important issue that may be addressed via use of stable isotopes. For example, oxygen and hydrogen isotopes generally carry valuable information about recharge conditions. Such information may include recharge elevation, temperature, and degree of evaporation.

Other variables that change the characteristics of the groundwater component in the mixture are the hydrodynamic properties of the aquifer because of change in length of flow paths, groundwater velocity, and flow conditions (e.g., diffuse or conduit flow). Such hydrodynamic characteristics of the aquifer are important for the chemically reactive (e.g. ^{13}C) and radioactive (e.g. ^{3}H) tracers/isotopes. Such processes have to be taken into account in the interpretation of water mixture calculations [126].

For evaluating freshwater fluxes, salinity anomalies are useful for estimation of SGD. However, to assess brackish and saline fluxes, which in many cases have more impact on the coastal environment; isotopes have an added advantage over chemical techniques. Various aspects of coastal hydrology could be addressed by investigations using a combination of stable, long-lived, and short-lived isotopes along with other complementary techniques.

In addition to geochemical tracers, geophysical tracers such as groundwater temperature can be used to estimate groundwater discharge rates. Two basic methods are used when using temperature as a tracer: (1) temperature–depth profiles under the assumption of conservative heat conduction–advection transport; and (2) temperature differences in the groundwater – surface water system as a qualitative signal of groundwater seepage using techniques such as infrared sensors or other remote sensing methods.

Temperature–depth profiles in boreholes have been widely used to estimate groundwater fluxes because heat in the subsurface is transported not only by heat conduction but also by heat advection due to groundwater flow [127]. Bredhoeft and Papadopulos [128] developed the type curves method for estimating one-dimensional groundwater fluxes based on a steady state heat conduction-advection equation derived from Stallman [129]. This method has been widely used to estimate one dimensional vertical groundwater fluxes [130,131], one-dimensional horizontal groundwater fluxes [132], and one-dimensional vertical groundwater fluxes with the effect of horizontal groundwater fluxes [133]. Simultaneous movement of one-dimensional transient heat and steady water flow were analyzed observationally [134,135], numerically [136], and theoretically [137–140]. The relationship between two-dimensional subsurface temperature and groundwater flux was theoretically analyzed by Domenico and Palciauskas [141], and Smith and Chapman [142]. More recently, surface warming caused by global warming and urbanization [143] or deforestation [144] was used as a tracer to detect groundwater fluxes (Fig.11). Fisher et al. [145] analyzed thermal data from the upper 150 m of sediment below the seafloor, which were collected during ODP (Ocean Drilling Program) Leg 150. They suggested that the observed thermal data indicated recent warming of the shallow slope bottom water off New Jersey. Borehole temperature data near the coast was also used for estimations of SGD

into Tokyo Bay, Japan [146] and a saltwater–freshwater interface in Toyama Bay, Japan [147]. In a recent application of borehole temperature data, Martin et al. [148] estimated the magnitude of the saline SGR/SGD component exchanging within the sediments using heat flux calculations to aid in evaluating the fresh component of groundwater discharge. Moore et al. [149] reported cyclic temperature variations 4 m below the seabed that were in phase with the tidal signal during the summer. They used this relationship to estimate SGD fluxes. All of these studies suggest that groundwater temperature–depth profiles in the coastal zone can be used as a valuable tracer to evaluate SGD.

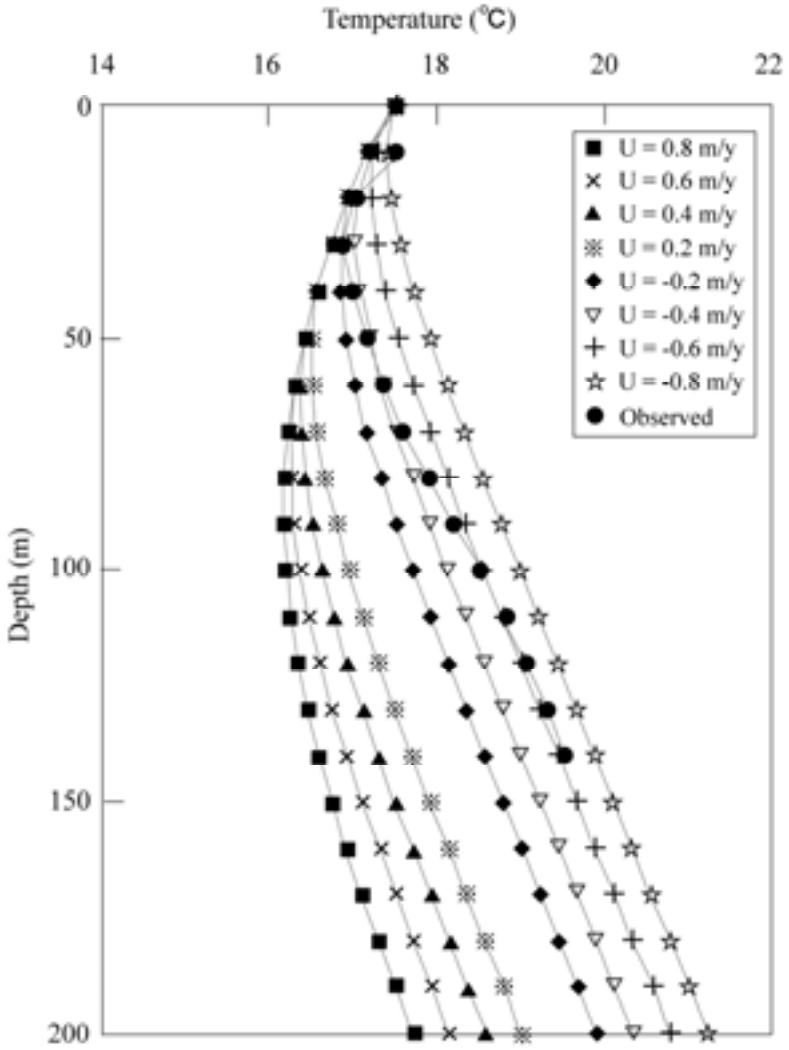

FIG.11. Observed and calculated temperature-depth profiles using a heat conduction-convection equation to estimate upward groundwater fluxes (groundwater discharge rates) near Tokyo Bay [143].

In order to evaluate regional-scale influence of SGD by using surface temperature as a tracer, infrared sensors have been used in many areas [150–153]. However, SGD values were not evaluated quantitatively though the locations of SGD influence were documented. These detectable locations are attributed to the spatial and temporal variation of both seawater and groundwater temperatures, which requires intensive field calibration. The use of remote sensing technologies to identify and quantify SGD is clearly an area for future research exploitation.

Another geophysical tracer, the bulk ground conductivity of seafloor and beach sediments can be employed to investigate the spatial distribution of saline and fresh porewater. Using these methods,

preferential flowpaths of fresh, terrestrially-derived groundwater such as submarine paleochannels can be readily identified from their conductivity signature [154, 155].

3.4. Water balance approaches

The water balance equation for a basin has also been used to estimate fresh SGD and may be described as follows:

$$P = E_T + D_S + D_G + dS \quad (2)$$

where P is precipitation, E_T is evapotranspiration, D_S is surface discharge, D_G is fresh groundwater discharge, and dS is the change in water storage. Over extended periods (i.e., years), dS is usually assumed to be negligible. Therefore, one needs to know precisely the precipitation, evapotranspiration and surface runoff for an accurate estimation of DG by this approach.

Basin-scale estimations of fresh SGD via a water balance method have been performed in many places, e.g., Perth, Australia (1.0×10^8 m^3/year [156]), Santa Barbara (1.2×10^5 m^3/year [157]), Long Island, New York (2.5×10^7 m^3/year [158]), and in the Adriatic Sea (1.7×10^{11} m^3/year [159]). When both the area and volume of SGD are known, one can calculate the fresh SGD flux. For example in the case of the Adriatic Sea [159], the mean fresh SGD flux of 0.68 m/year is calculated from the estimated fresh SGD volume and the discharge area. More typically, the area over which SGD occurs is unknown. Therefore, the SGD volume or sometimes 'volume of SGD per unit length of shoreline' [160,161] is used for water balance studies, making it difficult to compare with the observed (local) SGD estimates shown as Darcy's flux (e.g., $cm^3/cm^2 \cdot s$, cm/s, m/year).

Water budget calculations, while relatively simple, are typically imprecise for fresh groundwater discharge estimations because uncertainties associated with values used in the calculations are often of the same magnitude as the discharge being evaluated. For instance in the global water budget constructed by Garrels and MacKenzie [162], the estimated fresh SGD is about 6% of estimated evaporation from the land, which is about the same order as the uncertainty of the evaporation rate. Moreover, these estimates do not include the salt water that mixes into the aquifer and often comprises a significant fraction of total SGD.

In a study designed to test the effects of climate change on groundwater discharge, Oberdorfer [163] concluded that use of a water budget is an adequate first approach for assessing expected changes in simple groundwater basins. On the other hand, numerical modeling provides a better quantitative estimate of climate change perturbations when dealing with basins characterized by multiple sources and sinks. Another water balance approach using a budget based on the change in soil moisture has been performed for Tomales Bay, California [26]. Their result was comparable to the result obtained by more traditional water balance estimations.

3.5. Hydrograph separation techniques

The hydrograph separation technique is based on the assumption that the amount of fresh groundwater entering streams can be obtained via a hydrograph separation and this estimate may be extrapolated to the coastal zone. This technique was used by Zektser and Dzhamalov [164] for the Pacific Ocean rim, by Boldovski [165] in eastern Russia, by Williams and Pinder [166] in the local coastal plain stream in South Carolina, and by Zektser et al. [167] for global-scale estimation of fresh SGD. Two approaches were used to separate the hydrograph for estimating the fresh groundwater flow component. The first method is simply to assign a base flow due to the shape of the hydrograph. This technique can be performed several ways including the unit graph method [167,168]. However, a problem with this simple approach is evaluating baseline conditions; often the baseline changes depending on time, space, and prevailing hydrological conditions. The hydrograph separation technique for large-scale SGD estimates applies only to coastal areas with well-developed stream networks and to zones of relatively shallow, mainly freshwater aquifers.

As with the water balance method, the uncertainties in the hydrograph separation terms are often on the same order of magnitude as the discharge being evaluated. For instance, the estimation of groundwater discharge in central and eastern European countries showed the average of estimated fresh groundwater discharge (6% of total water flow) is about 12% of the estimated evaporation [169]. This estimate is close to the uncertainty usually assigned to evaporation estimates.

The second method of hydrograph separation is the use of geochemical end member concentrations. Usually, water and geochemical mass balances in a river are shown as follows:

$$D_T = D_S + D_G \quad (3)$$

$$C_T D_T = C_S D_S + C_G D_G \quad (4)$$

where D and C are the discharge rate and geochemical concentrations, respectively, and subscripts T, S and G represent the total, surface water and groundwater components. From those two equations, measured D_T, C_T, C_S, and C_G, we can solve for the two unknown values, D_S and D_G.

Recently, not only surface water–groundwater separation [170], but also the separation of three water components, namely groundwater, surface water and soil water, has been studied by using three different compositions of these end-members [171]. This method may also be applicable for separation of SGD into the fresh, mixing, and seawater components of SGD if one can identify tracers with sufficient sensitivity and resolution.

Another problem of the hydrograph separation for estimating direct groundwater discharge into the ocean is that gauging stations for measuring the discharge rate in rivers are always located some finite distance upstream from the coast to avoid tidal effects. Therefore, the groundwater discharge downstream of the gauging station is excluded [172].

3.6. Theoretical analysis and numerical simulations

Offshore seepage rates were described by an exponentially decreasing function, as explained by McBride and Pfannkuch [63], who investigated the distribution of groundwater seepage rate through lakebeds using numerical models. Bokuniewicz [173] questioned the use of such an exponentially decreasing function and developed an analytical solution for SGD as follows:

$$q = (Ki/\pi k) \ln[\coth(\pi x k/4l)] \quad (5)$$

where q is vertical groundwater seepage flux, K is vertical hydraulic conductivity (assumed constant), i is hydraulic gradient, k is the square root of the ratio of the vertical to the horizontal hydraulic conductivity, l is aquifer thickness and x is the distance from the shoreline. The author concluded that a single exponential function underestimated the analytical solution of SGD both near-shore and far from shore, and overestimated the SGD at intermediate distances. Further details concerning the derivation and use of this equation may be found in Bokuniewicz [173]. This relationship between an exponential approximation and analytical solution is similar to the contrast between an exponential representation and the numerical examples calculated by McBride and Pfannkuch [63].

Fukuo and Kaihotsu [174] made a theoretical analysis of groundwater seepage rates for areas with a gentle slope into surface water bodies by use of conformal mapping techniques. They used the x-axis along with the slope (the x axis in Bokuniewicz [173] is horizontal), and found that in an unconfined aquifer most of the groundwater flows through a nearshore interface between surface water and groundwater. Equipotential and streamlines in the near-shore vicinity of the aquifer and the distribution of specific discharge through the sediment with different slopes demonstrate this point (Fig.12a [174]). Analytical solutions indicate that SGD decreases exponentially with distance from the coast and that the rate of decrease is greater when a gentler slope is present (Fig.12b). Interactions between surface waters and groundwaters also have been studied numerically by Winter [175–177], Anderson and Chen [178] and Nield et al. [179]. Linderfelt and Turner [180]) numerically evaluated

the net advected groundwater discharge to a saline estuary while Smith and Turner [181] numerically evaluated the role of the density-driven recirculation component in the overall groundwater discharge to the same saline estuary.

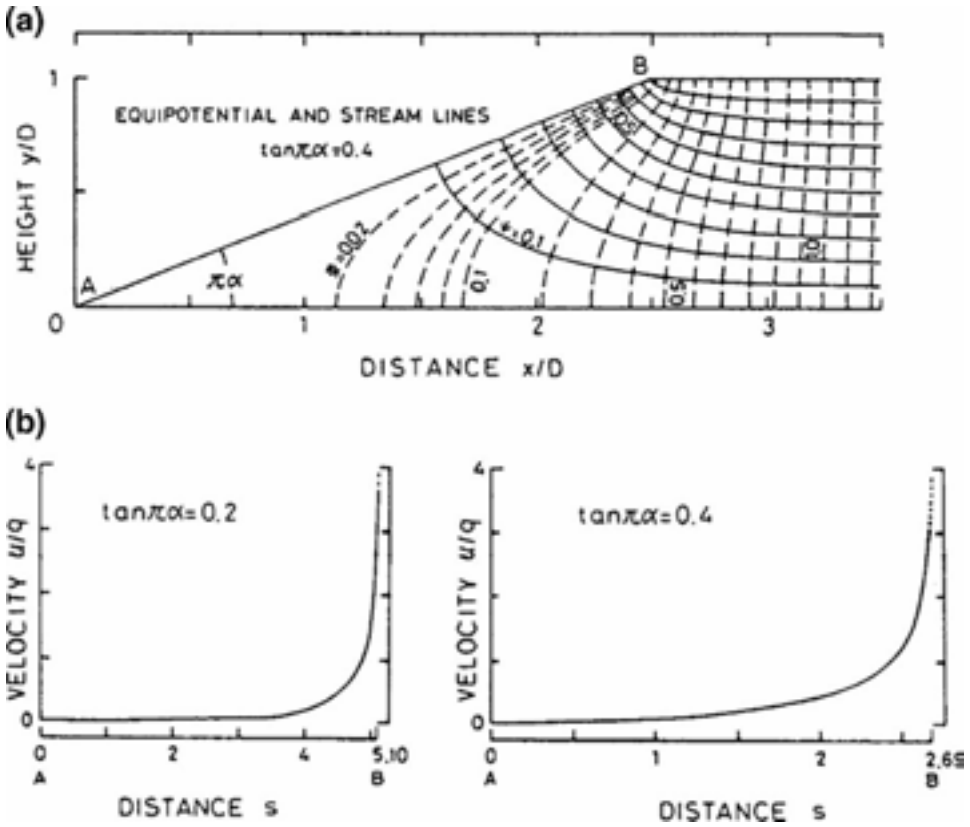

FIG.12. (a) Equipotential and streamlines near the sediment surface; and (b) distribution of specific discharge on the sediment surface with a gentle slope [174].

Although modeling approaches using packages such as MODFLOW [182] are widely used for the analysis of basin-scale groundwater hydrology, all of these techniques have certain limitations. For example, aquifer systems are usually heterogeneous, and it is difficult to obtain sufficient representative values such as hydraulic conductivity and porosity to adequately characterize this heterogeneity. Hydraulic conductivity often varies over several orders of magnitude within short distances. Spatial and temporal variations for boundary conditions are also required for hydrological modeling, but this information is often hampered by our ability to acquire adequate field data within the time frame of a typical study.

When estimating nutrient transport by groundwater, it is important to evaluate the groundwater capture zone at near-shore zones. Taniguchi et al. [183] analyzed the groundwater seepage rate into Lake Biwa, Japan, to evaluate the capture zone of groundwater entering a surface water body. Transient numerical simulations were made using a two-dimensional (2-D) unsaturated–saturated model with three-layered sediments. They concluded that calculated values agreed well with observed groundwater seepage rates when the thickness of the aquifer was estimated to be 110 m. This model also agreed with the capture zone results estimated by stable isotope data ($\delta^{18}O$ and deuterium). It is clear that aquifer thickness and hydraulic conductivity values are the most important factors for reliable estimates of groundwater seepage rates by theoretical and numerical analysis.

All the above described numerical models simulate groundwater flow. A complementary numerical approach is proposed in which the salinity distribution in the surface water body is simulated by a three-dimensional (3-D) numerical model to determine the location and strength of SGD.

Measurements of the salinity field (or another typical parameter) are needed in the region of the SGD source. One example of such a model is PCFLOW3D, a 3-D, non-linear baroclinic numerical model originally developed to simulate the hydrodynamic circulation and transport and dispersion of different contaminants such as mercury [184] or radionuclides [185]. The basic idea is to assume a location and strength of the SGD, simulate the salinity distribution, and compare it with the measured distribution. The final information on SGD is obtained by a trial and error procedure. The possibility of the model application was shown with the SGD measurements in Sicily (see section 5.2).

4. Coastal Zone Management Implications of SGD

Groundwater seepage into the coastal zone may be important for coastal area management for at least three reasons: (1) dissolved solutes that result in chemical and ecological effects in the receiving waters; (2) saltwater intrusion and associated hydrologic aspects involving water resources; and (3) geotechnical aspects (as sediment stability) of the shoreline. SGD may have significant environmental consequences as groundwaters in many areas have become contaminated with a variety of substances (e.g., nutrients, metals, organics). Because the slow, yet persistent seepage of groundwater through sediments will occur almost anywhere, almost all coastal zones are subject to flow of terrestrially driven groundwater either as submarine springs or disseminated seepage [4,6,7]. In addition, significant amounts of recirculated seawater pass through permeable sediments as a result of tidal pumping, topographically induced flow, and other marine processes (see Section 1.4. 'Drivers of SGD'). The potential for discharging groundwaters to have a significant impact on surface waters is greatest in regions where fluids may seep into a body of water having limited circulation.

Because groundwaters typically have higher concentrations of dissolved solids than most terrestrial surface waters, SGD often makes a disproportionately large contribution to the flux of dissolved constituents, including nutrients and pollutants. In addition, discharging groundwater interacts with and influences the recirculation of seawater, which can affect coastal water quality and nutrient supplies to nearshore benthic habitats, coastal wetlands, breeding and nesting grounds. Thus, one of the more important implications for coastal zone managers concerns nutrient (or other solute) loading to near-shore waters. Impacts in the coastal zone from these inputs could be the basis for land-use planning and may place limits on development.

Hwang et al. [24] estimated SGD using a variety of tracers including ^{222}Rn and radium isotopes into Bangdu Bay, a semi-enclosed embayment on the Korean volcanic island, Jeju. Their estimated SGD inputs of 120–180 $m^3 \cdot m^{-2} \cdot yr^{-1}$ are much higher than those reported from typical continental margins. The nutrient fluxes from SGD were about 90%, 20%, and 80% of the total input (excluding inputs from open ocean water) for dissolved inorganic nitrogen, phosphorus, and silica, respectively. The authors concluded that these excess nutrient inputs from SGD are the major sources of 'new nutrients' to this bay and could contribute to eutrophication.

From a management standpoint, a key issue will be the determination of whether SGD is of actual or probable importance in an area of interest. Furthermore, managers must consider the relative importance of SGD among the multiple factors considered in management activities. In this respect, coastal managers face the following problems: (1) they may not be aware of the growing realization of the importance of SGD; (2) if they are aware, they may not know how to decide whether or not SGD is relevant to their situation; and (3) if they do decide this is important, they may not know how to quantify it.

Since SGD is essentially 'invisible', the problem that arises, from both a management and scientific standpoint, is determining how to avoid the error of ignoring an important process on the one hand, and wasting valuable resources on an unimportant issue on the other. Where terrestrially driven SGD is a significant factor in maintaining or altering coastal ecosystems, coastal zone managers will need to consider management of water levels and fluxes through controls on withdrawal or alterations in

recharge patterns, as well as groundwater quality management (e.g., through controls on land use, waste disposal, etc.). Such major interventions in the coastal zone management system require a sound scientific justification and technical understanding that does not currently exist.

How can a manager tell if SGD may be important in a particular area? Several potential, indirect indicators of freshwater submarine discharge have been suggested but not yet widely applied. Its color, temperature, salinity, or some other geochemical fingerprint might distinguish the water itself. Escaping groundwater, for example, might be stained red by the oxidation of iron or colored by tiny gas bubbles. Because groundwater tends to exist at the average annual temperature, cold water anomalies in the open water during the summer and warm water anomalies during the winter, as might be detected by infrared aerial photography, or a person walking barefoot on the beach, can be an indicator of SGD. Salinity anomalies have also long been used to identify subsea freshwater seeps, and can also be used at a variety of scales from regional water budgets to vertical profiles at specific locations.

Particular site conditions may also provide clues to the occurrence of SGD. The presence of coastal ponds or unconsolidated coastal bluffs, which may maintain a high hydraulic head near shore, may be other indicators. Growths of freshwater coastal vegetation may indicate regions of high SGD offshore. It has also been suggested that the presence of barite, oxidized shells, or beach rock may indicate the occurrence of groundwater discharges. In Great South Bay (New York, USA), there occurs a phenomenon known as ‘anchor ice’, in which the bay floor freezes while the saline open waters of the bay are still ice-free. This is attributed to the presence of fresh water in the sediments maintained by SGD. It is also reported to occur in the Baltic. Alternatively, in coastal areas that are covered with ice in the water, like the Schlei estuary in northern Germany, ice-free spots, called ‘wind-spots’, are found above the SGD of relatively warm freshwater. In Eckernforde Bay (southeast Baltic Sea) pockmarks in the fine-grained sediments of the sea floor have been identified as bathymetric expressions of groundwater seeps [186]. If the SGD is great enough, the water itself can be domed and ‘boiling’ such at Crescent Beach Spring off Florida [187].

Managers must consider the relative relationships and priorities of SGD among the multiple factors considered in management activities. This presents at least two ways that current approaches to the study of groundwater discharge will need to be modified for such studies to be useful to managers: (1) The scale of emphasis would be that of management areas — probably tens to hundreds of kilometres. By contrast, scientists are typically performing investigations at the lower end of this scale (although some tracer investigations work at scales of 10–100 km). (2) Scientists may study one area for years, often reflecting the typical 2–3 year grant cycle. Managers, on the other hand, will need relatively simple and rapid diagnostic and assessment tools to evaluate the local importance and management issues related to SGD in specific settings. The concerns could be either natural processes or human impacts (which may be extreme in some cases).

5. The UNESCO/IAEA Joint SGD Intercomparison Activities

Five SGD assessment intercomparison exercises were organized over the course of the UNESCO/IAEA project (Table 1). The results of each of these experiments are summarized below. Measured seepage rates are provided in a series of tables for each site with the values given as integrated flow rates ($m^3/m \cdot day$) in all cases except for the measurements at the Brazilian site (given as $cm^3/cm^2 \cdot day$ or cm/day) where there was so much variability that the width of the seepage face could not be reliably estimated.

TABLE 1. LOCATIONS, DATES, AND VARIOUS CHARACTERISTICS OF THE FIVE SITES USED FOR SGD ASSESSMENT INTERCOMPARISON EXPERIMENTS. FURTHER DETAILS ARE PROVIDED IN THE FOLLOWING SECTIONS.

Number, site	Dates of assessment intercomparison	Geologic/oceano-graphic settings	Tidal characteristics, climate	SGD assessment methods
(1) Cockburn Sound, Western Australia	25 November – 6 December 2006	Coastal plain; marine embayment	Diurnal (~1 m) Temperate, semi-arid; occasional high on-shore winds	Seepage meters; Ra isotopes; Rn; hydrologic modelling
(2) Donnalucata, southeastern Sicily	18–24 March 2002	Volcanic with limestone veneer; small boat basin and up to a few km offshore	Semidiurnal (~0.2 m); semi-arid; winds calm to strong (>10 m/s) during experiment	Seepage meters; Ra isotopes; Rn; numerical modelling
(3) Shelter Island, Long Island, New York	18–24 May 2002	Glacial moraine; Protected embayment (West Neck Bay)	Semidiurnal (~1.2 m); temperate wet	Seepage meters; Ra isotopes; Rn; previous hydrogeologic modelling
(4) Ubatuba, Sao Paulo State, Brazil	16–22 November 2003	Fractured crystalline rocks; marine embayment	Semidiurnal (~1 m), subtropical, wet (rain ~1,800 mm/year)	Seepage meters; Ra isotopes; Rn; artificial tracers
(5) Mauritius Islands (Indian Ocean)	19–26 March 2005	Volcanic island; partially enclosed (barrier reef) lagoon	Semidiurnal (~0.5 m); tropical, very wet (rain up to 4000 mm/year)	Seepage meters; Ra isotopes; Rn; water balance

5.1. Cockburn Sound, Australia

5.1.1. Introduction

We performed our first intercomparison experiment (25 November – 6 December 2000) within the Northern Harbour area (Jervoise Bay) of Cockburn Sound, located in the southwest margin of continental Australia, near metropolitan Perth and Fremantle (Fig.13). Cockburn Sound is a marine embayment protected from the open Indian Ocean by reefs, a chain of islands, and a man-made causeway. Recently, the area has been the subject of extensive environmental assessment in order to address strategic environmental concerns and the management of waste discharges into Perth's coastal waters.

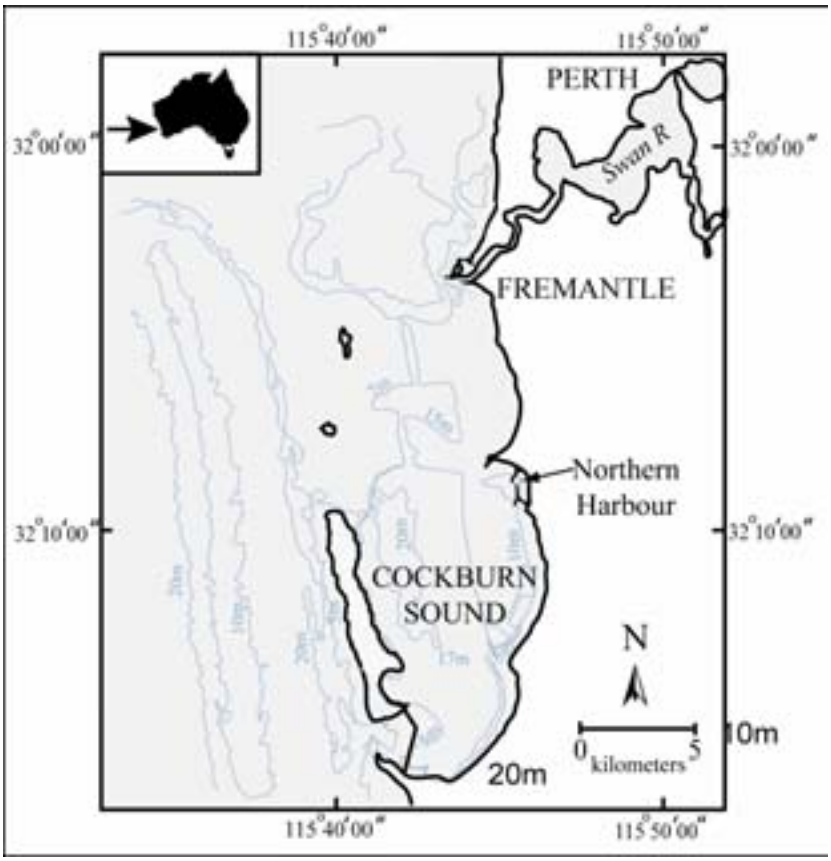

FIG.13. Location map of Cockburn Sound, Western Australia. The SGD assessment intercomparison was run mainly off the beach in the Northern Harbour area.

Cockburn Sound itself is flanked on its eastern margin by a low-lying sandy coastal plain. Much of Perth's commercial and industrial activity is focused along the southern metropolitan coastline and includes the shoreline of Cockburn Sound. Influx of pollutants to the near-shore marine environment from these activities has been a point of major concern in recent years, and SGD has been recognized as an important pathway for contaminants. Accordingly, a significant amount of baseline environmental information has been gathered over the past 20 years. The primary site for the SGD assessment intercomparison was along an open beach in the Northern Harbour area.

Over 20 scientists from Australia, USA, Japan, Sweden, and Russia participated in this experiment. Several types of SGD assessment approaches, including hydrogeologic measurements, manual and automated seepage meter readings, and tracer measurements were collected during the 10-day intensive experiment.

5.1.2. Seepage meters

Several manual seepage meter measurements were made each day of the experiment for each of eight 'Lee-type' meters deployed along two transects (4 m on each transect) set up normal to shore and extended out to a distance of ~100 m. Each day, after several measurements were taken, the results were pooled as a 'daily average' and integrated by distance offshore to obtain estimates of total seepage per day per metre of shoreline (Fig.14).

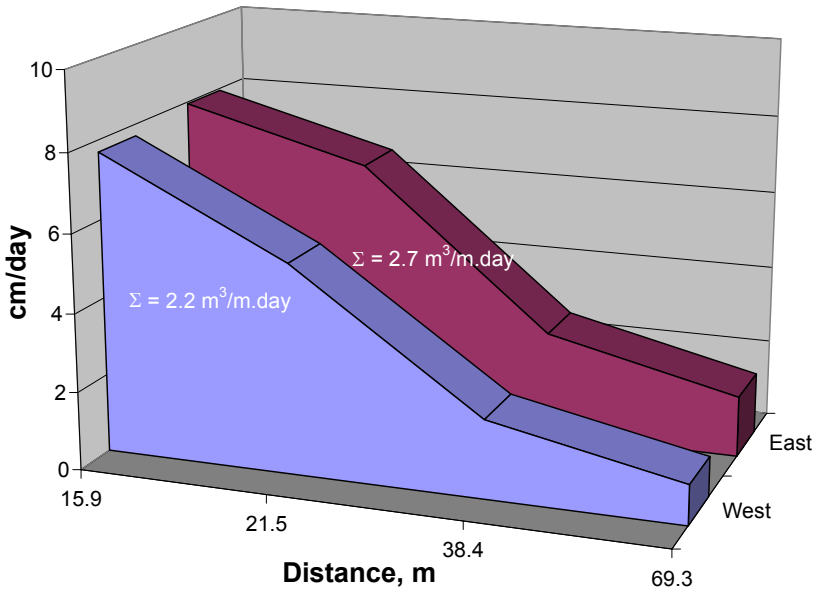

FIG.14. Manual seepage meter results for 28 November 2000, Cockburn Sound. The two trends correspond to the west (integrated flux = 2.2 $m^3/m \cdot d$) and east (2.7 $m^3/m \cdot d$) transects, respectively.

5.1.3. Radium isotopes

The Ra isotope data in Cockburn Sound does not follow a predictable pattern of steadily decreasing activities with distance from shore. Instead there are regions of higher activity occurring at considerable distances from shore. We conclude that SGD fluxes occur throughout the Sound, not just at the shoreline. Because of the irregular pattern of enrichments, a simple one-dimensional model cannot be used to interpret the data.

Loveless [188] used a ^{226}Ra mass-balance approach based on a model of Charette et al. [109] to determine the quantity of groundwater input into Cockburn Sound. The residence time of the waters in the system were estimated based on the ^{224}Ra/^{226}Ra activity ratios in the harbour compared to pre-discharge groundwaters. The derived estimate of 3.3 days is comparable with a summer value of 2.8–3 days, determined using a Lagrangian water particle tracking model [189]. Using the calculated residence time to account for dilution of ^{226}Ra, the activity in excess of the benthic sediment and ocean end-member sources is attributed to the groundwater source. Oceanic values were taken from Parmelia Bank sampling stations. A reported literature value of 0.044 dpm/m^2·day was used to account for the contribution of ^{226}Ra from benthic sediment particles [109]. Normalized to the area of the harbour, this is a benthic sediment flux of 3.4×10^4 dpm/day. It must be recognized that the value given in Charette et al. [109] was a maximum value intended to demonstrate that little ^{226}Ra was entering their study area from sediments. However, when extrapolated to the area of Cockburn Sound, this flux is a considerable component of the ^{226}Ra input to the Sound.

Seepage water concentrations of ^{224}Ra and ^{226}Ra were used to represent the SGD activities following procedures outlined earlier in this paper and in Moore [7,108] and Charette et al. [109]. To support the ^{226}Ra in the surface waters required an 'excess' of 2.51×10^7 dpm/day of ^{226}Ra over that activity calculated to be supported from marine and local sediment sources. Using a pre-discharge ^{226}Ra activity 0.46 dpm/L, this excess represents a total SGD input of 50×10^3 m^3/day. It is expected that during the period of the intercomparison (December), the groundwater aquifer displayed a higher recharge condition (peak recharge normally occurs at the end of winter: September–October). Extrapolating to the total shoreline length (16 km) provides an estimated discharge of 3 $m^3/m \cdot$day into Cockburn Sound. This estimate of SGD based on radium isotopes falls nicely in the middle of the reported upper and lower recharge estimate determined by flow net analysis [190]. However, it must

be recognized that the flow net analysis estimates only fresh SGD, while ^{226}Ra estimates total SGD. Since the seepage water was near seawater salinity, total SGD must be considerably greater than fresh SGD. It is likely that the ^{226}Ra model underestimated total SGD because the value taken for the sedimentary input was too large.

5.1.4. Radon

One of the stations in a central portion of the experimental area was equipped with a continuous radon monitor [191]. Grab samples of seawater were also collected from the same location at various times and analyzed by conventional radon emanation techniques with results very close to those provided by the continuous monitor. The radon data showed a pattern generally similar to that of an automated seepage meter deployed by Taniguchi with higher radon concentrations and higher seepage rates during the lowest tides, a feature that has been observed elsewhere. Both the radon record and the seepage meter results are suggestive of a strong tidal influence on the transient magnitude of the SGD flux. The estimated flow based on modeling the radon record as described in Burnett and Dulaiova [111] ranged from 2.0 to 2.7 $m^3/m \cdot day$.

5.1.5. Summary

A summary of all the seepage flux estimates from the intercomparison shows that there was good agreement at this site (Table 2). Both the radium isotopes and radon models fall within the range of the seepage meter estimates and the hydrological modeling. This was not the case in a preliminary intercomparison experiment in Florida, where the radiotracers and seepage meters agreed closely, but the modeling showed much lower values [71]. The somewhat higher estimate seen by the radium isotopic approach than radon may be a consequence of differences in scale. The radium samples were collected over distances of several kilometers, from the nearshore out to the mouth of Cockburn Sound. In addition, the radium data suggests that SGD is occurring throughout the Sound, not just along the shoreline where the radon monitor and seepage meters were deployed. The radon estimates were based on continuous measurements at one location near the beach. The seepage meter estimates may be expected to be somewhat higher because the measurements were all made during the day, which happened to coincide with the low tide (higher seepage) intervals.

TABLE 2. ESTIMATED INTEGRATED SGD RANGES (DAILY AVERAGES) VIA FOUR DIFFERENT APPROACHES FOR COCKBURN SOUND, AUSTRALIA (25 NOVEMBER –6 DECEMBER 2000). THE SEEPAGE METER, RADIUM ISOTOPES, AND RADON MEASUREMENTS WERE ALL MADE DURING THE SAME PERIOD. THE MODELLING WAS PERFORMED LATER FOR AVERAGE CONDITIONS.

Estimated groundwater discharge ($m^3/m \cdot day$)			
Seepage meters	Radium isotopes	Radon	Modelling*
2.5 – 3.7	3.2	2.0 –2.7	2.5 – 4.8

*Spatially averaged SGD via a distributed groundwater flow model [192].

5.2. Donnalucata, Sicily

5.2.1. Introduction

Two expeditions were carried out (June 2001 and March 2002) in collaboration with the University of Palermo, Italy, to sample groundwater, seawater, and sediment along the southeastern Sicilian coast. The studied area (Fig.15) belongs to a structure, noted in the literature as the Hyblean Plateau that represents one of the principal structural elements of eastern Sicily, which is considered geologically

as part of the African continental crust (thickness over 30 km). The western sector, where Donnalucata is found, has an aquifer in the calcarenite sands of Pleistocene origin (an average depth from 50–100 m). The second aquifer is in the Ragusa Formation, confined by the marls of the Tellaro Formation. Along the coast, the carbonate aquifers directly discharge their waters into the sea producing numerous springs observed on beaches. The groundwater also flows through the faults directly to the sea forming submarine springs, locally called 'bugli' [193]. Well-known submarine springs are located in the port of Donnalucata (where our intercomparison study was done), in the inlet of Ognina and in the mouth of the River Cassibile called 'Balatone'. Further to the east, near Syracuse city, the Aretusa spring has been well known from mythology.

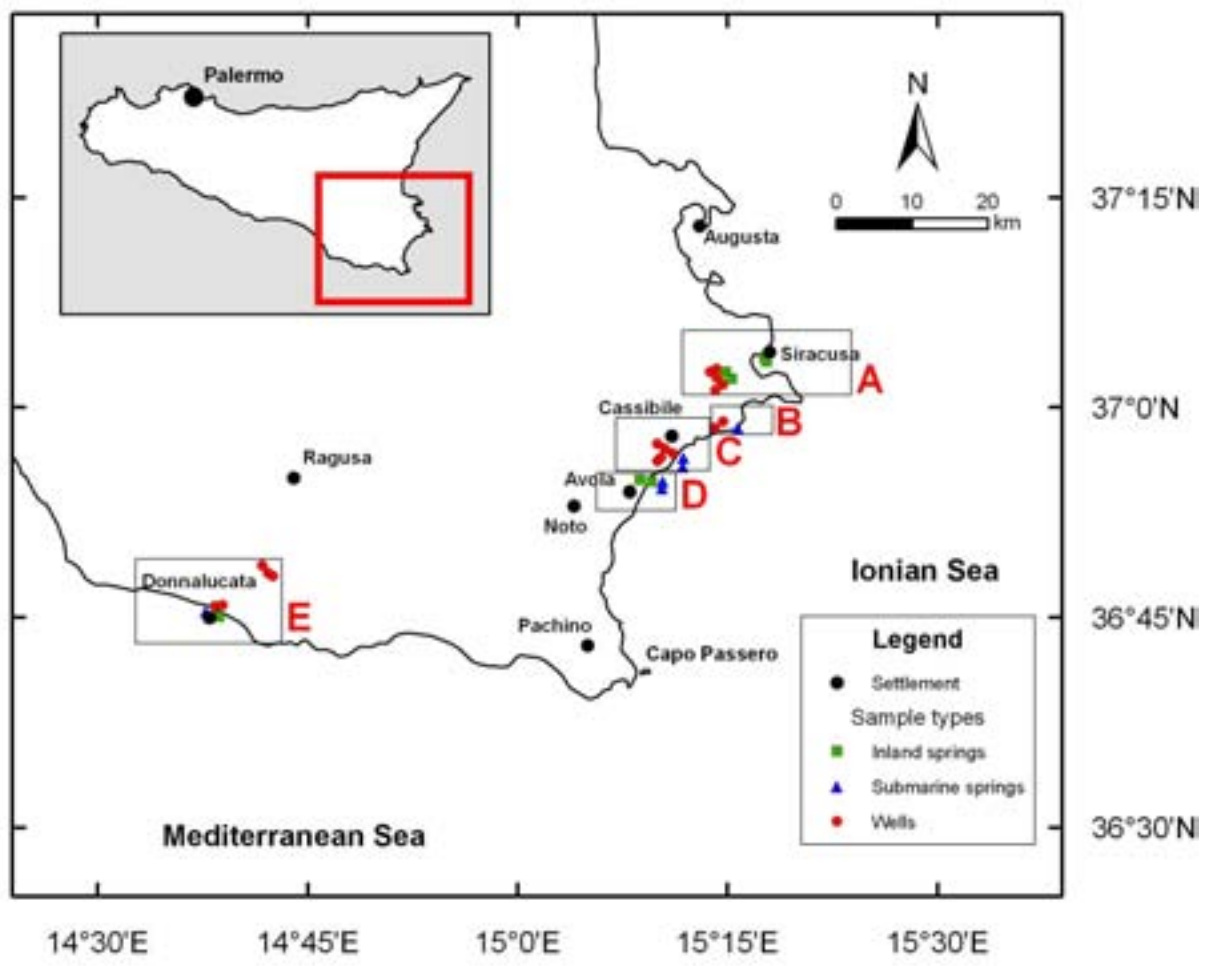

FIG.15. Areas in southeastern Sicily where SGD studies have been undertaken as part of the IAEA–UNESCO project on SGD. The area around Donnalucata (E) was where the detailed intercomparison studies were performed.

5.2.2. Study area and geophysical characterization

The study area for the intercomparison was in the small town of Donnalucata in the province of Ragusa along the southeastern coast of Sicily. Many springs are known to occur in this area, both on-shore and offshore. Our original main goal was to assess SGD along a several kilometer stretch of coastline in this area. Unfortunately, high wind and surf conditions prevented us from making many measurements along the open coastline. However, a protected boat basin (Fig.16) allowed us to conduct a series of measurements for assessing SGD.

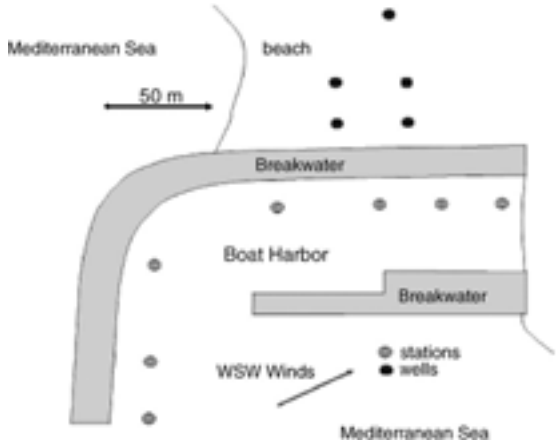

FIG.16. Sketch diagram of the Donnalucata boat basin.

A portable, geoelectric instrument based on time domain electromagnetic sounding technology was used during the 2002 experiment in Donnalucata to obtain subsurface information. The analysis of 3D structures of geoelectrical data shows the presence of several layers with different formation resistivities. The top 50 m represents a freshwater saturated zone (formation resistivity above 50 Ω·m) with water flowing towards the sea. However, closer to the pier (Fig.16) a saltwater intrusion can be observed. The pier acts as a barrier for the transport of fresh water to the sea; i.e., it has blocked a superficial drain. The saltwater horizon is located at the depth between about 50 and 80 m, at the east corner of the pier with a formation resistivity between 3 and 30 Ω·m. Below the 80 m layer a fresh water horizon is seen again, which may represent a deeper freshwater aquifer.

5.2.3. Isotopic analyses

Stable isotope data shows that the fresh groundwater and some springs discharging groundwater lie close to the Mediterranean meteoric water line, and are depleted in $\delta^{18}O$ (from about –4.5 to –6 ‰) with respect to Vienna Standard Mean Ocean Water (Fig.17). In contrast, the seawater samples are highly enriched in $\delta^{18}O$ (from about 0 to 2 ‰). The SGD waters have $\delta^{18}O$ values from about –2 to –3 ‰, and fall on a mixing line between groundwater and seawater. These samples may consist of about 40 to 50% fresh groundwater, implying high SGD fluxes into the coastal waters off Sicily [125]. The seawater samples have $\delta^{18}O$ values from about 1.5 to 0‰, and fall on the right end of the curve. The tritium content of collected seawater and groundwater samples varied from 1.5 to 4.1 TU. The residence time of groundwater in the limestone formations of southeastern Sicily, estimated using the $^{3}H/^{3}He$ method and CFC measurements ranges from 2 to 30 years.

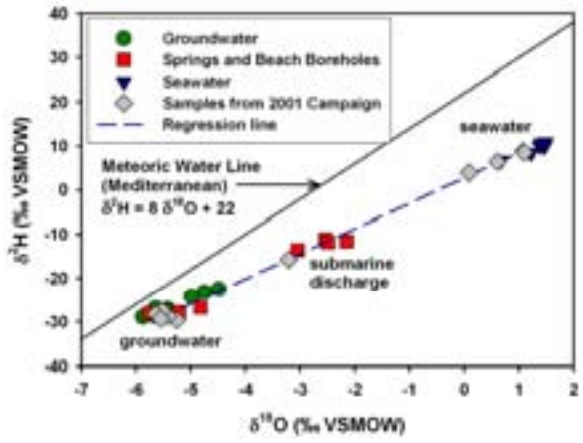

FIG.17. Isotopic composition (δ^2H and $\delta^{18}O$) of groundwater and seawater samples from southeastern Sicily [125].

5.2.4. SGD evaluations

Quantitative assessments of SGD made by seepage meters, radon, and radium isotopes are given in Table 3. The seepage meter and radon estimates were only made within the boat basin while the radium isotope evaluation of groundwater discharge was based on measurements made within a few kilometers offshore of the boat harbour. The SGD estimate per unit shoreline made by radium isotopes, thought to be conservative, is much higher than either the radon or seepage meter measurements [194]. The lower shoreline flux inside the harbour may be because the presence of springs was lower inside the boat basin. Alternatively, it may be that the offshore data was responding more to SGD created by wave set up (e.g., Li et al. [8]) on the beach and this effect was damped in the protected environment of the boat basin.

The proposed numerical method (PCFLOW3D) was applied using parameters measured in the Donnalucata boat basin. For the purpose of numerical simulations measured SGD inflow velocity was assumed to be constant in each region A to E (Fig.18) using seepage rates determined via seepage meters with the values of: 2.2; 35.7; 2.8; 2.0; and 15.1 cm/day respectively [195]. The initial value for salinity was 38.2 and the salinity of the inflow SGD sources was assumed to be 1. Wind from WSW, with the velocity of 6 m/s was taken into account. The hydrodynamic and salinity fields were simulated with these data. Tidal elevation changes were below 20 cm and were not taken into account in this case. Simulated and measured salinity distribution is presented in Fig.18. Generally, the simulation results confirmed the observations and suggest possible future applications of numerical modeling in SGD studies.

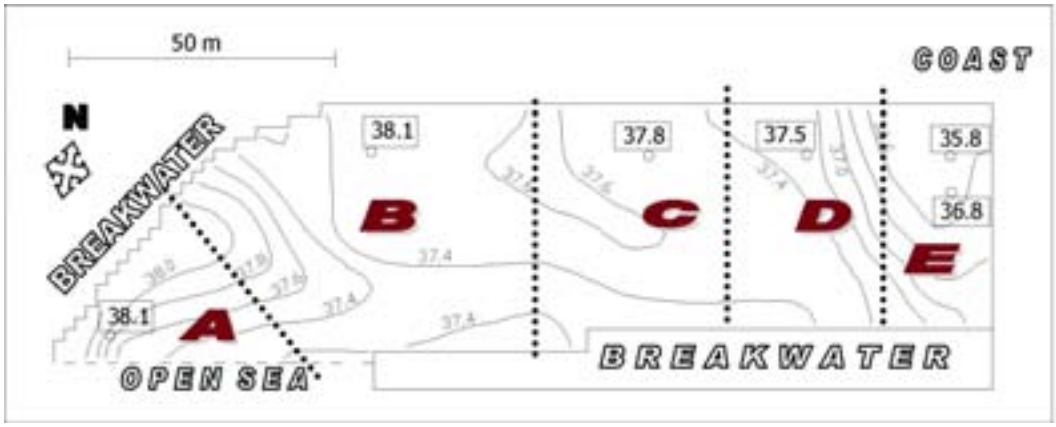

FIG.18. A comparison of simulated salinity distributions (isolines) with measured salinity (numbers in rectangles) on 22 March 2002.

TABLE 3. ESTIMATED SGD DISCHARGE RATES INTO THE BOAT BASIN AT DONNALUCATA, SICILY VIA SEEPAGE METERS, AND RADON. THE SHORELINE FLUXES WERE DETERMINED FROM OFFSHORE SAMPLING OF RADIUM ISOTOPES AND BY NORMALIZING THE SEEPAGE METER AND RADON ESTIMATES TO THE WIDTH OF THE BOAT BASIN.

	Seepage meters	**Radon**	**Radium**
Boat basin (m^3/day)	300–1000	1200–7400	–
Shoreline flux ($m^3/m^2 \cdot$day)	10–30	30–200	1000

Seepage meter data from [195]; radon estimates from [196] and radium results from [194].

5.3. Shelter Island, New York

5.3.1. Introduction

Shelter Island is located in Peconic Bay between the north and south forks of Long Island, New York (Fig.19). The island is composed of upper Pleistocene glaciofluvial deposits consisting of outwash sands (fine, medium, and coarse) and gravel, cobbles, boulders, clay, and silt (drift/till). There are no major streams or creeks on the island and, therefore, groundwater that enters the aquifer primarily discharges through the coastline into the surrounding coastal waters. Freshwater on Shelter Island is restricted to the unconfined Upper Glacial aquifer. Two clay units lie below the Upper Glacial. Water sampled from these lower units was previously determined to be salt water. The clay layers overlie two deeper, unconsolidated aquifers. The deepest aquifers rest on Precambrian crystalline bedrock.

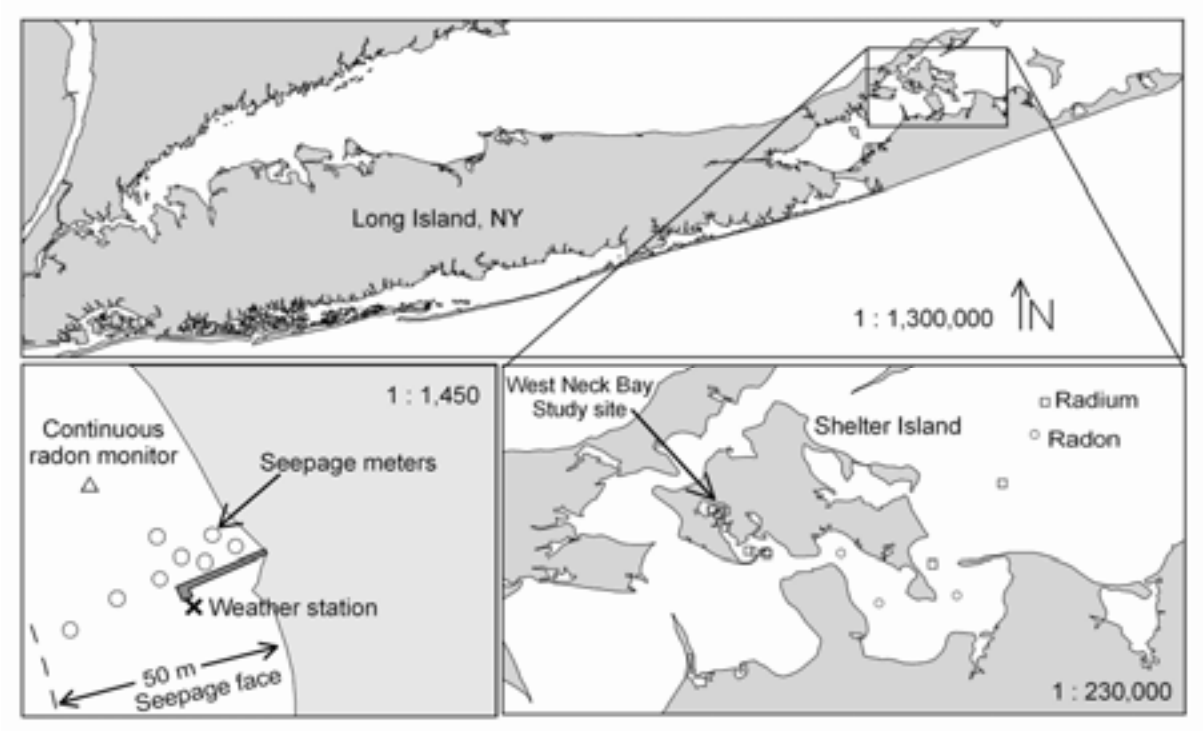

FIG.19. Location map of West Neck Bay, the study site located at the eastern end of Long Island, New York. The numbers refer to station locations for collection of water samples for geochemical tracers.

The intercomparison experiment was conducted 18–24 May 2002, in West Neck Bay, located in the southwestern portion of Shelter Island. The bay and its associated creek comprise a total area of approximately 1.6 km^2, with a mean tidal volume of 3.7 Mm^3. The tidal range is approximately 1.2 m and water depths are generally less than 6 m. With the exception of sheet runoff, no surface waters discharge into the bay. The average salinity of the bay is approximately 26. Since 1985, West Neck Bay has been affected by nuisance algal blooms of *Aureococcus anophagefferens*, referred to as 'brown tide'.

5.3.2. Seepage meters

Various types of seepage devices including manual or 'Lee-type' meters [51], constant heat [10], ultrasonic [93], and a dye-dilution meter [92] were deployed at distances up to ~50 m from the shoreline. Although SGD is expected to decrease offshore, this pattern is not always found. A pattern of SGD decreasing uniformly offshore was not found at this site. In fact, seepage devices measured rates ranging from less than 10 cm/day to almost 200 cm/day at a similar distance off shore (Fig.20). This variation was attributed to the influence of a pier that ran perpendicular to the shoreline past the

seepage devices. As corroborated by conductivity measurements, the pilings of the pier had apparently pierced a shallow aquitard, allowing local (artesian) discharge of groundwater. Estimated integrated seepage rates for different types of seepage meters show a total range from 2–16 $m^3/m \cdot day$ (Table 4). The ultrasonic and Lee-type meters produced generally higher values than the other types due to the influence of locally high seepage rates near the pier where they were located.

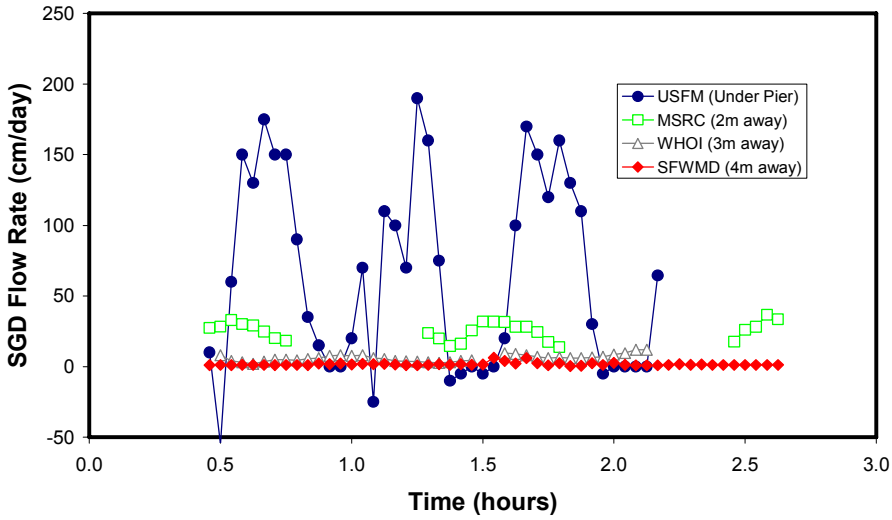

FIG.20. Variation of SGD at approximately the same distance from shore but at increasing distance from a pier, Shelter Island, New York. The apparent differences in seepage rates were caused by the influence of pilings from the nearby pier that intercepted an aquitard and artificially enhanced seepage.

TABLE 4. ESTIMATED INTEGRATED SGD (DAILY AVERAGES WHEN RANGES ARE SHOWN) VIA SEVERAL DIFFERENT TYPES OF SEEPAGE METERS DEPLOYED AT THE SHELTER ISLAND INTERCOMPARISON (18–24 MAY 2002).

Seepage meters estimated groundwater discharge ($m^3/m \cdot day$)				
Manual (Lee-Type)	**Heat pulse (KrupaSeep)**	**Continuous heat (Taniguchi)**	**Dye-dilution (WHOI)**	**Ultrasonic (Paulsen)**
11.5[a]	0.4–0.8	2.5	3.4	17.5
n = 3[b]	n = 2	n = 1	n = 2	n = 6

[a]Using an average flux of 23.2 cm/day.

[b]The 'n' in the last row refers to the number of positions each type of meter occupied during the intercomparison.

5.3.3. Radon and radium isotopes

The radiotracers produced results (Table 5) that were overlapping but generally higher than the seepage meter results. The radon model shows two ranges based on how the mixing term is evaluated. One way involves inspecting the calculated radon fluxes after corrections for atmospheric evasion and tidal changes. We assumed that the maximum negative fluxes, representing a loss of radon from the system, would be a lower estimate of the mixing loss because greater losses could be masked by concurrently higher inputs. A second approach involves estimating the mixing via inspection of both short-lived radium isotopes and ^{222}Rn along a transect away from the study site. Multiplying the derived horizontal mixing coefficient (Kh; [108]) by the linear gradient of the ^{222}Rn and the average depth produces an offshore flux. This result can then be converted to a seabed flux that is equivalent to

how the fluxes are expressed in the radon model. The two mixing loss estimates agreed very well at 670 dpm/m^2·h and 730 dpm/m^2·h via inspection of the Rn fluxes and use of radium isotopes, respectively. The integrated seepage rate based solely on radium isotopes overlaps the radon model and the results from the ultrasonic seepage meter.

TABLE 5. ESTIMATED INTEGRATED SGD RANGES (DAILY AVERAGES) VIA FOUR DIFFERENT APPROACHES FOR THE SHELTER ISLAND INTERCOMPARISON. THE SEEPAGE METER AND ISOTOPIC MEASUREMENTS WERE MADE DURING THE SAME PERIOD. THE MODELING WAS PERFORMED BY OTHER INVESTIGATORS FOR AVERAGE AND EXTREME CONDITIONS.

Estimated groundwater discharge (m^3/m·day)			
Seepage meters (all types)	**Radon**	**Radium isotopes**	**Modelling**
0.4 – 17.5	8 – 16[a]	16 – 26	0.23 – 1.4[c]
	18 – 20[b]		0.5[d]
			10[e]

[a]Mixing losses of Rn based on inspection of calculated Rn fluxes.

[b]Mixing losses of Rn based on short-lived radium isotopes.

[c]Based on estimate of mean fresh water discharge into West Neck Harbour [197].

[d]Based on a water budget estimate of Shelter Island [198].

[e]Based on a MODFLOW model of West Neck Bay [199].

The integrated discharge calculated from the geochemical techniques was near the upper range of the measurements made with the seepage devices. One possible reason that the radiotracer estimates may tend to be higher than the seepage meter results is that the tracers, measured in the water column, integrate a larger area than the seepage meters. For example, the gradient for ^{223}Ra, which was used to calculate the mixing and the residence time in West Neck Bay, was based on a transect from the study site in the interior of the bay out to the bay's mouth, over 4 km from the seepage meter site. In addition, results from the WHOI dye-dilution seepage meter, which continuously records the salinity of the seepage fluid, and resistivity profiling both indicate that a significant portion of the nearshore SGD was as freshwater. Therefore, because of the limited scale of the seepage meter study, the seepage meters may have missed a key component of the total SGD flux at this site; i.e., the seepage meters were responding mostly to near-shore fresh water flow while the radiotracers reflected total (fresh + saline) flow. This suggests that, regionally, there are other areas of high seepage (in addition to the high seepage under the pier) that were not sampled by the meters, but contributed to the SGD measured with geochemical tracers.

There were no modeling estimates made of SGD during the Shelter Island intercomparison. However, a consultant's report concerning the flushing time of West Neck Harbour [197]) included an estimate of 'freshwater inflow' that we assume would be all via groundwater discharges. That report estimated the long-term mean inflow at 1.07 cfs (0.03 m^3/s) and the maximum inflow at 6.56 cfs (0.19 m^3/s). We estimated the shoreline length of the bay at 11.3 km. That results in an estimated mean freshwater seepage rate of only 0.23 m^3/m·day and 1.4 m^3/m·day as a maximum inflow. A later USGS study [198] estimated fresh water inflow into West Neck Bay at 198,000 cfd (0.065 m^3/s) via a water balance approach. Again normalizing to our estimated shoreline length of 11.3 km, we derive an integrated seepage rate of 0.5 m^3/m·day. All these estimates are lower than the direct measurement approaches. These differences may be attributed to one or more of the following: (1) the models

underestimate the groundwater discharge; (2) the seepage meters and tracers are recording higher flows due to large amounts of recirculated seawater; or (3) the intercomparison exercise was conducted during an atypical period relative to the long term averages that the model-derived fluxes are based upon.

5.3.4. Geophysical studies

Concurrent to the direct measurements of seepage rates, the bulk ground conductivity of seafloor sediments were mapped near a pier at the study site. A shallow sediment layer was identified to provide confinement for lower aquifer units. The conductivity and seepage rate data indicate that pilings of the pier apparently pierce this shallow sediment layer, producing a comparatively high seepage rate driven by the hydraulic head of the (semi)confined aquifer, resulting in a substantial increase in SGD in the immediate vicinity of the pier.

5.3.5. Summary

While there is obviously some uncertainty about the 'best' integrated seepage values to apply at the Shelter Island site, some of the comparisons produced some very encouraging results. For example, a comparison of calculated radon fluxes with measured seepage rates via the WHOI dye-dilution seepage meter, and water levels (Fig.21) shows a great deal of similarity in the derived patterns. During the period (17–20 May) when both devices were operating at the same time, there is a clear and reproducible pattern of higher fluxes during the low tides. There is also a suggestion that the seepage spikes slightly led the radon fluxes, which is consistent with the notion that the groundwater seepage is the source of the radon. The excellent agreement in patterns and overlapping calculated advection rates (seepage meter = 2–37 cm/day; radon model = 0–34 cm/day, average = 12 ± 7 cm/day) by these two completely independent assessment tools is reassuring. An important lesson from this site was the significance, even dominance, of anthropogenic influences as seen in the elevated SGD at the pier pilings.

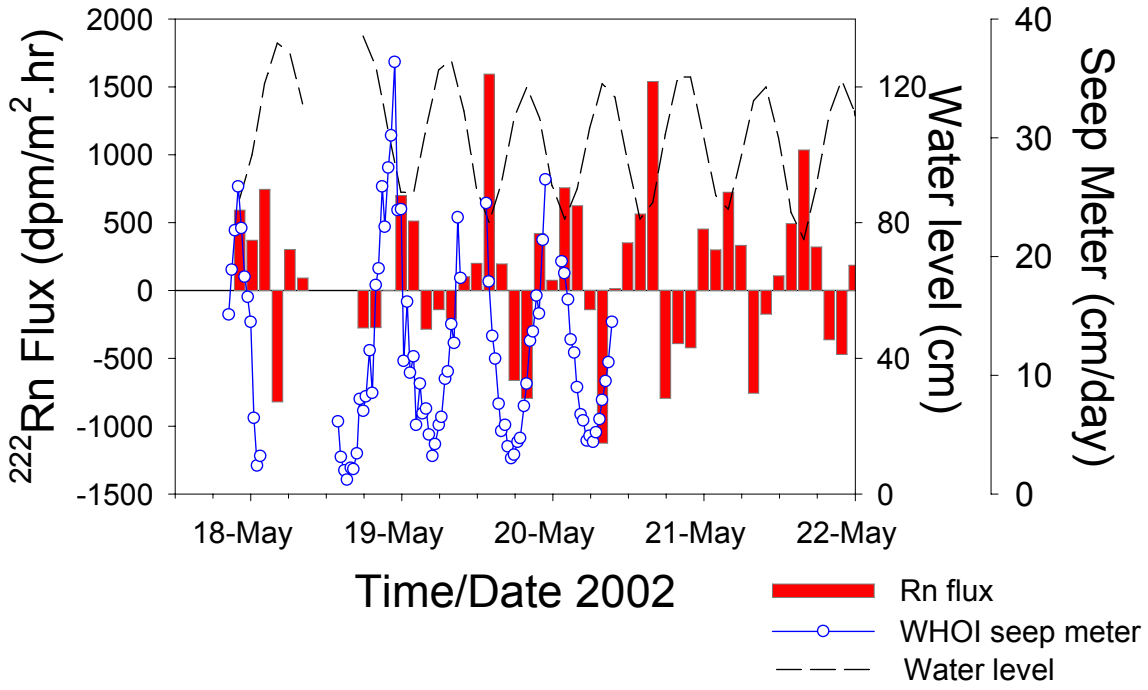

FIG.21. Plot comparing variations in seepage based on a dye-dilution seepage meter developed at Woods Hole Oceanographic Institution [92], radon fluxes, and water level. Negative Rn fluxes interpreted as being due to mixing losses.

5.4. Ubatuba, Brazil

5.4.1. Introduction

The intercomparison in Brazil (16–22 November 2003) was carried out mainly in Flamengo Bay, one in a series of small embayments near the city of Ubatuba, São Paulo State (Fig.22). Besides Flamengo Bay (where there is a marine laboratory of the University of São Paulo that served as a base of operations), these embayments included Fortaleza Bay, Mar Virado Bay and Ubatuba Bay. The study area also included the northernmost part of São Paulo Bight, southeastern Brazil, a tropical coastal area. The geological/geomorphologic/hydrogeological characteristics of the area are strongly controlled by the presence of fractured crystalline rocks, especially the granites and migmatites of a mountain chain locally called Serra do Mar (altitudes up to 1000 m), which reaches the shore in almost all of the study area, and limits the extension of the drainage systems and of the Quaternary coastal plains [200]. The mean annual rainfall is about 1800 mm, the maximum rainfall rates usually occurring in February. Sea level varies from 0.5 to 1.5 m, the highest values occurring in months August/September due to greater volume of warm waters of Brazil Current [201]. Despite the small drainage basins between the mountain range and the shore, freshwater discharge is sufficient to reduce the salinity of coastal waters.

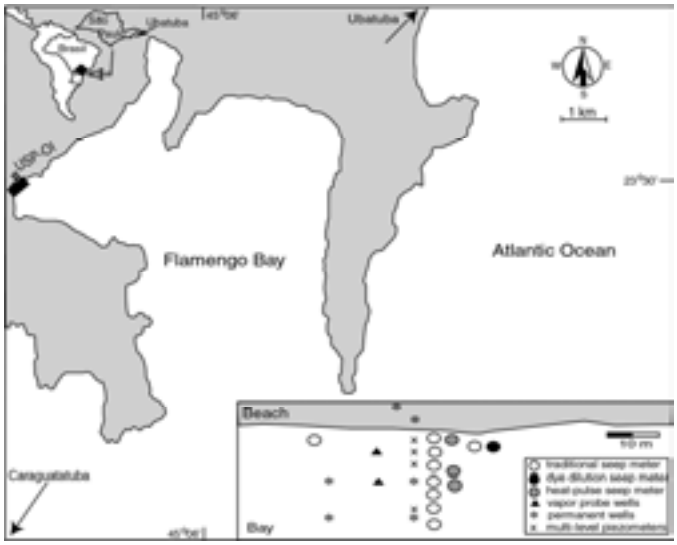

FIG.22. Field intercomparison of nearshore techniques were performed at the University of Sao Paulo Oceanography Institute (USPOI), near Ubatuba, Brazil. Transects were set up normal to the shoreline for Lee-type seepage meters (open circles), heat-pulse seepage meters (gray circles), and one dye-dilution seepage meter (black circle). In addition, multi-level piezometers (small x's) were installed along a pre-existing transect of wells (stars) or parallel (black triangles) to this well transect.

5.4.2. Geophysical Studies

Preliminary subsurface conductivity/resistivity investigations were run to reveal the structure of the flow field of the freshwater component of SGD. Such measurements allow for predictions of entry points of fresh SGD. While it is not possible to derive absolute SGD fluxes from such geoelectric measurements, the relative distribution of SGD can be investigated in great detail, especially where seepage or discharge follows preferential flow paths [154].

Both conductivity and resistivity were measured with electrode arrays, either directly by deploying an electrode array in the ground, or by inverse modeling of remotely sensed resistivity measured on electrodes deployed only on the surface (Fig.23). The high-resolution transect (Fig.24a) was interpolated from 130 single-point measurements recorded on electrodes inserted into the ground at different locations along a transect. The significantly reduced ground conductivity close to the

sediment surface at around 23–25 m distance suggests a greater influence of fresh SGD at this location than along other parts of the transect. A manual seepage meter, which was deployed at this location subsequent to the conductivity investigations, confirmed both the highest flow rate and lowest salinity discharge along the transect. Without the conductivity investigations, only the seepage meters at 20 m and 31 m distance would have been deployed, and thus the total flow rate would have been significantly underestimated [155].

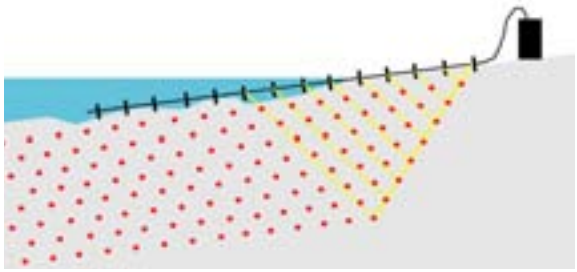

FIG.23. Schematic diagram showing principle of remote sensing of resistivity (conductivity). The system shown portrays the case where electrodes are only mounted on the surface. Depth of penetration and resolution are dependent upon spacing between these electrodes.

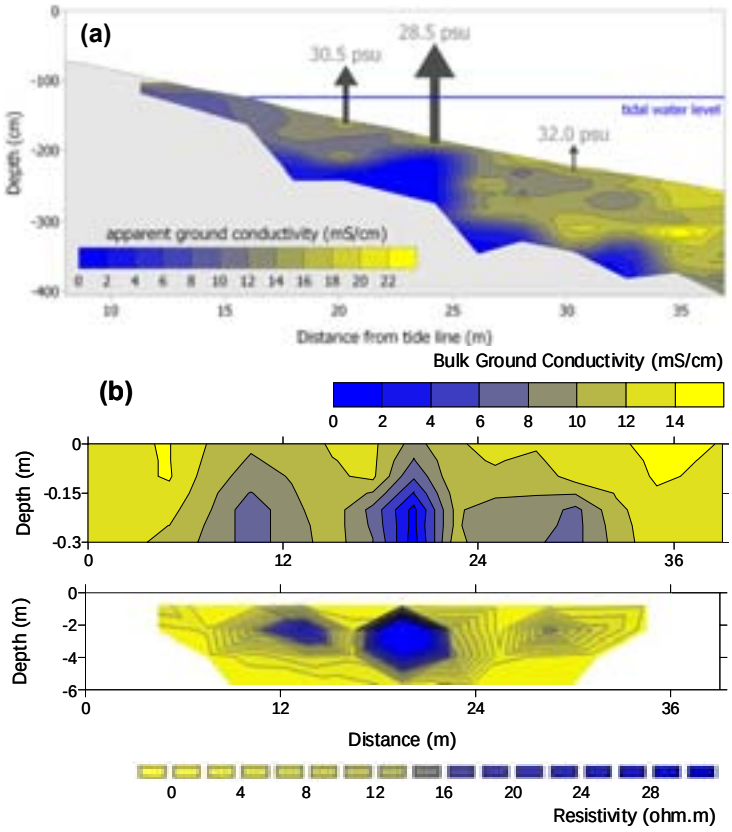

FIG.24. (a) Ground conductivity shore-normal transect of Flamingo Bay Beach. The arrows at 20 m, 24 m and 31 m distance mark the locations of manual seepage meters deployed along the transect. The length of the arrows is proportional to the average flux of SGD at these sites together with the average salinity. (b) Shore-parallel transects of ground conductivity and resistivity at Fazenda Beach. (top) apparent ground conductivity in the top 30 cm of beach sediment across a shallow creek (center of transect); (bottom) resistivity in the top 5.6 m of beach sediment.

Simultaneously recorded conductivity and resistivity transects at Fazenda Beach reveal similar features of the subsurface distribution of seawater and freshwater (Fig.24b). Despite the very different

spatial scales of operation of the methods (cm vs. m scale), both methods detected the general features of three low conductivity/high resistivity regions along the beach-parallel profile. The good agreement between the two methods suggests that the results do not suffer from significant artifacts. The transect was recorded across a dry creek on the beach. The low conductivity/high resistivity central region of the transect likely represents the alluvial aquifer of the creek.

5.4.3. Seepage meters

Seven manual seepage meters were deployed along a transect perpendicular from shore at a small beach at the marine laboratory. The shoreward device was exposed at low tide. The other six devices were placed at distances out to 44 m from the low-tide shoreline. Two other devices were placed at the low tide shoreline 19 m east and 14 m west of the transect.

The highest rates of SGD were found at the low tide shoreline, but they were not uniform. The device to the east recorded flow rates as high as 268 cm/day, and collection bags with a capacity of about 6 liters had to be replaced every 10 min, whereas at other locations flow rates were often sufficiently low that collections every hour or two were adequate. A tidal modulation was not detected in the results of the manual seepage meters, but this lack of evidence of tidal influence seems to be an artifact of the sampling interval; continuously recording devices did resolve tidal changes.

The dye-dilution seepage meter was deployed for three days (hourly resolution for seepage) at a nearshore location along the beachfront of the marine lab. The meter recorded a pattern of flow that was closely correlated with tidal stage (Fig.25). Seepage rates ranged from a minimum of 2 cm/day for the high tide on the morning of Nov. 18th to 110 cm/day for the low tide on the morning of 20 November. The average seepage rate for the three-day deployment was 15 cm/day. The salinity inside the seepage chamber ranged from ~26 to 31. Given an ambient bay water salinity of ~31, the lower salinities suggest that a portion of the SGD included freshwater. The pattern of gradual freshening of the water inside the seepage housing is likely explained by the replacement of bay water (which is trapped inside the housing upon installation of the meter) with fresh/brackish groundwater. The rate at which this bay water is replaced is a function of the seepage rate and the headspace volume inside the seepage chamber. If we assume a headspace volume of ~5 L, a flow rate of ~16 cm/day would be required to explain the gradual freshening inside the seepage chamber from 18–20 November, which is in excellent agreement with the average flow rate of our dye-dilution method.

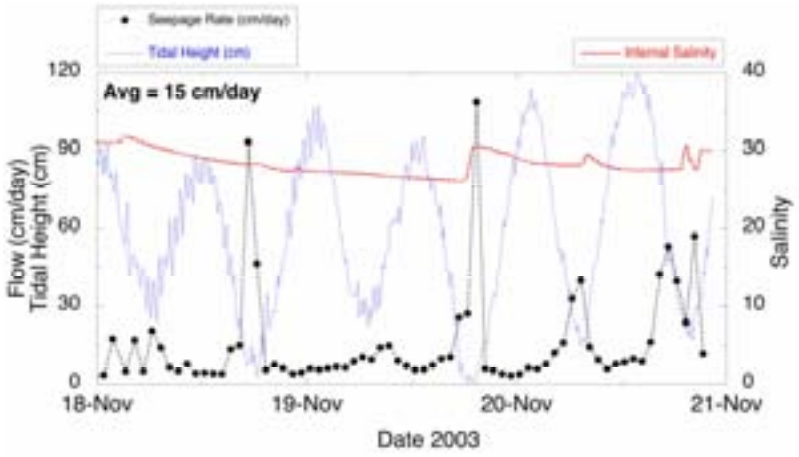

FIG.25. Water level, seepage rate, and salinity as measured by a dye-dilution seepage meter in a near-shore area off the beach at the marine laboratory, Ubatuba, Brazil (18–21 November 2003).

SGD was continuously recorded with continuous heat automatic seepage meters every 10 minutes at three locations along a transect line. The averaged SGD rates were 260 cm/day, 4.2 cm/day, and 356 cm/day at these stations. The averaged conductivities at these same sites were 48.7, 48.9 and 39.9

mS/cm. Semi-diurnal variations of SGD using these automated seepage meters were observed at two of the three stations.

5.4.4. Artificial tracer approach

Multi-level pore water samplers ('multisamplers') were installed from 2 m below low tide range to about 50 m offshore in the same area as the seepage devices above. Artificial tracers (fluorescien dye saturated with SF_6) were injected into one of the deeper subsurface ports of the multisamplers and the other ports were sampled at a later time in order to estimate vertical advective velocities. Based on tracer arrivals at shallower ports than where the tracer was injected, the calculated flow rates ranged from 28 to 184 cm/day.

5.4.5. Radon and radium isotopes

Continuous radon measurements of coastal waters (~2–3 m water depth) were made at a fixed location from a float about 300 m off the marine lab from the afternoon of 15 November to about noon on 20 November. There was a short period on 16 November when the system was down for maintenance. The record of radon concentrations showed that they generally range from about 2–6 dpm/L and show the highest activities at the lowest tidal stages. Furthermore, the radon maxima tend to have a period of 24-h corresponding to the lowest low tide each day in this semidiurnal, mixed tidal environment. There is one exception to this observation in the early morning of 17 November, when an 'extra' peak occurred at about the highest tide that day.

We estimated SGD rates from the continuous ^{222}Rn measurements as described in detail in [111]. These rates (Fig.26a) had a somewhat similar pattern as seen by some of the manual and automated seepage meters deployed at the same time. Over a 109-h period, the estimated SGD based on the radon measurements ranged from 1 to 29 cm/day with an average of 13±6 cm/day. The average seepage rate is very close to the average calculated from the dye-dilution seepage meter of 15 cm/day although that device indicated a much broader range — from about 2 up to over 100 cm/day for short periods during the lowest tides. Most of the seepage spikes that were observed occurred during the lowest tides, with the exception of that one peak around noon on 17 November. Inspection of the rainfall record shows that this was also a period when there was a significant amount of rain (Fig.26b).

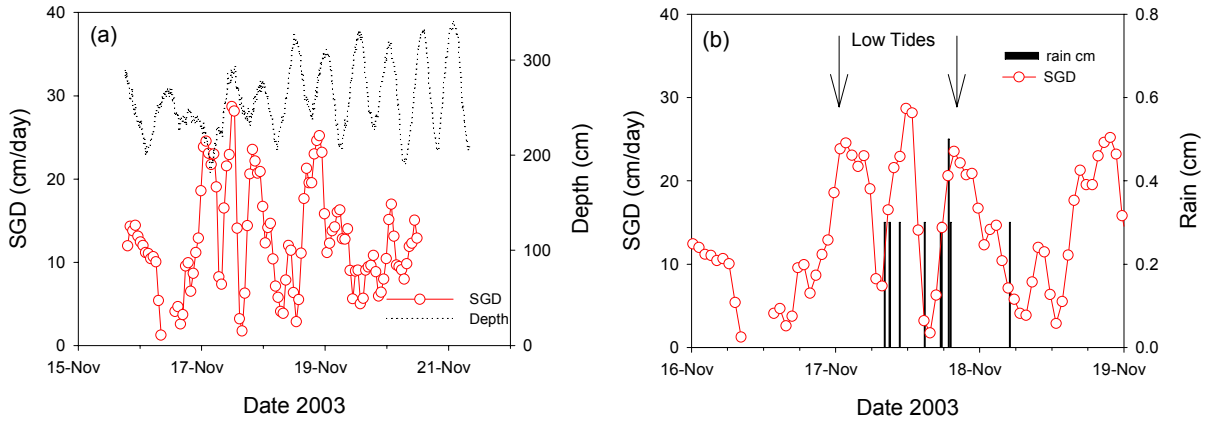

FIG.26. (a) Calculated SGD rates based on continuous radon measurements at a fixed location about 300 m off the marine laboratory together with water level fluctuations. (b) A portion of the same record showing that the SGD peak that did not correspond to a low tide may have been related to a rain event at that time. Hourly rainfall amounts are shown by the vertical lines [202].

A direct comparison of continuous ^{222}Rn measurements and advection rates measured by the dye-dilution seepage meter shows some interesting patterns (Fig.27). It is important to note that these

observations showed that the tidal modulation of SGD can be strongly non-linear. While the two instruments only overlapped about 2.5 days during the weeklong experiment, there are clear indications that both measurements were responding to either tidally induced or modulated forcing. The main peaks in both data sets have a 24-h period and correspond to the lowest low tide each day. The seepage peaks led the peaks in the radon by an hour or two as was also seen in the data from Shelter Island. There are also indications in both records of secondary peaks occurring at the higher low tide. This is more obvious in the seepage meter record, but the radon does show a clear shoulder during the evening low tide on 19 November. It is encouraging that these two completely independent tools respond in such a similar manner to the same process. The seepage meter measured flow directly from a small portion of seabed close to shore while the radon was measured in the overlying water a few hundred meters away and presumably with a much larger sphere of influence.

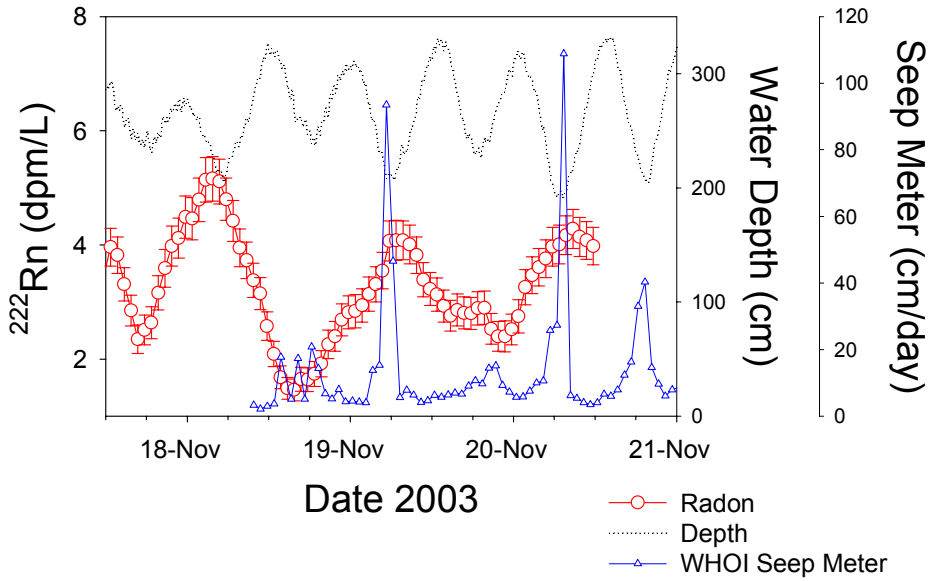

FIG.27. Combined data sets from the dye-dilution seepage meter (triangles), radon concentration (circles), for the time period when both instruments were running. The water level record (dots) is also shown.

The Ra isotope studies at Ubatuba revealed inputs of radium occurring in Flamengo Bay at considerable distances from shore. Moore and de Oliveira [203] calculated apparent ages of water within Flamengo Bay and used an age vs. distance plot to estimate a water residence time of the order of 10 days. They then developed a mass balance of ^{228}Ra based on measured values in then seepage bags, Flamengo Bay waters, and offshore waters. They concluded that nearshore SGD as measured by seepage meters can support only 10% of the total SGD to these coastal waters. Most of the SGD must be originating from fracture systems that discharge offshore.

5.4.6 Summary

A summary of the shoreline groundwater discharge estimates, expressed as specific discharge, is given in Table 6. We postulate that the irregular distribution of SGD seen at Ubatuba is a characteristic of fractured rock aquifers. The bay floor sediments were sandy and not noticeably different from place to place in the study area. However, bedrock is exposed at the shoreline and an irregular rock surface was encountered at shallow depths offshore. For example, investigators could drive probes to a depth of a few meters in some places but less than half a meter at adjacent locations. The water feeding the SGD is supplied to the bottom of the thin blanket of unconsolidated sediment through a fractured system and concentrated (or dispersed) along the irregular surface of the buried rock. Presumably, this is fresh groundwater working its way seaward through the fractured rock (Fig.28). The relatively high salinity

in the pore water of the sediment blanket, despite high discharge rates, must be due to some efficient mixing process in the surficial sediments themselves, perhaps a combination of gravitational, free convection, and wave pumping [204].

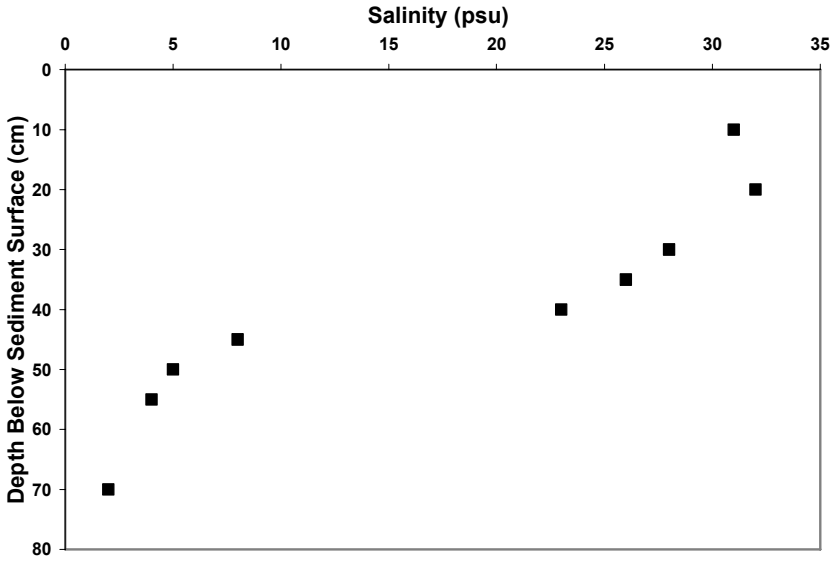

FIG.28. Porewater salinity profile, located 2 m offshore from the high tide line and measured at high tide. A hard, fine-grained layer was encountered around 42 cm.

It is clear from all these results that the advection of pore water fluids across the seabed in Flamengo Bay is not steady state but episodic with a period that suggests non-linear tidal forcing. This is very similar to observations reported from other environments [68,71,92].

TABLE 6. RANGES AND MEAN VALUES OF SPECIFIC DISCHARGE MEASUREMENTS MADE DURING THE BRAZIL INTERCOMPARISON (16–22 NOVEMBER 2003) BY DIFFERENT APPROACHES.

	Seepage meters			**Other**	
	Manual meters	**Continuous heat**	**Dye-dilution**	**Continuous radon**	**MLS SF_6**
Range (cm/day)	5–270	0–360	2–109	1–29	28–184*
Mean (cm/day)		1A: 260 3A: 3.1 4A: 190	15±19	13±6	88±84

All values are given as units of cm/day (cm^3/cm^2 day) from various locations in the near-shore zone off the marine laboratory in Flamengo Bay. Note that the standard deviations reported reflect the actual variation of the measured seepage and do not reflect an uncertainty of the reported value.
*SF_6 tracer-derived seepage rates are minimums.

5.5. Mauritius

5.5.1. Introduction

One setting was not investigated in a previous intercomparison: volcanic terrain. Volcanic areas, especially islands, may be of particular interest in terms of SGD. The total groundwater discharge to the world oceans estimated by the 'combined hydrological and hydrogeological method' [205] is 2400 km^3/year (river flow ~35,000–40,000 km^3/year, so this global SGD estimate represents 6–7% of the world's river discharge). Of this total flow, Zektser estimates that 1485 km^3/year is derived from continents and 915 km^3/year from 'major islands'. Thus, the flow from large islands is estimated to be more than one-third of the total global SGD. Recent studies by Kim et al. [206] and Hwang et al. [24] on the volcanic island of Jeju, off Korea, have also shown much higher SGD rates than typically observed on continental areas.

The observation that oceanic islands apparently account for such a disproportionately high amount of SGD is likely a combination of several factors. The largest islands (New Guinea, Java, Sumatra, Madagascar, West Indies, etc.) are located in humid tropical regions with high rainfall. In addition, large islands are often characterized by high relief, high permeability of fractured volcanic rocks, and an 'immature' landscape with poorly developed river drainage systems. All of these factors contribute to the potential for high groundwater discharges.

We thus decided to investigate a volcanic area for the final intercomparison exercise. While data specifically on SGD in Mauritius (Fig.29) was not available, reports suggested that substantial groundwater discharges in the lagoons from the volcanic aquifers. In addition to the reports of considerable seepage and large submarine springs, the lagoons are experiencing enhanced nutrient loading and eutrophication. While not documented, SGD likely plays an important role here. The rainfall is high (up to 4000 mm in the mountains), and it has all the other characteristics of areas that have elevated SGD.

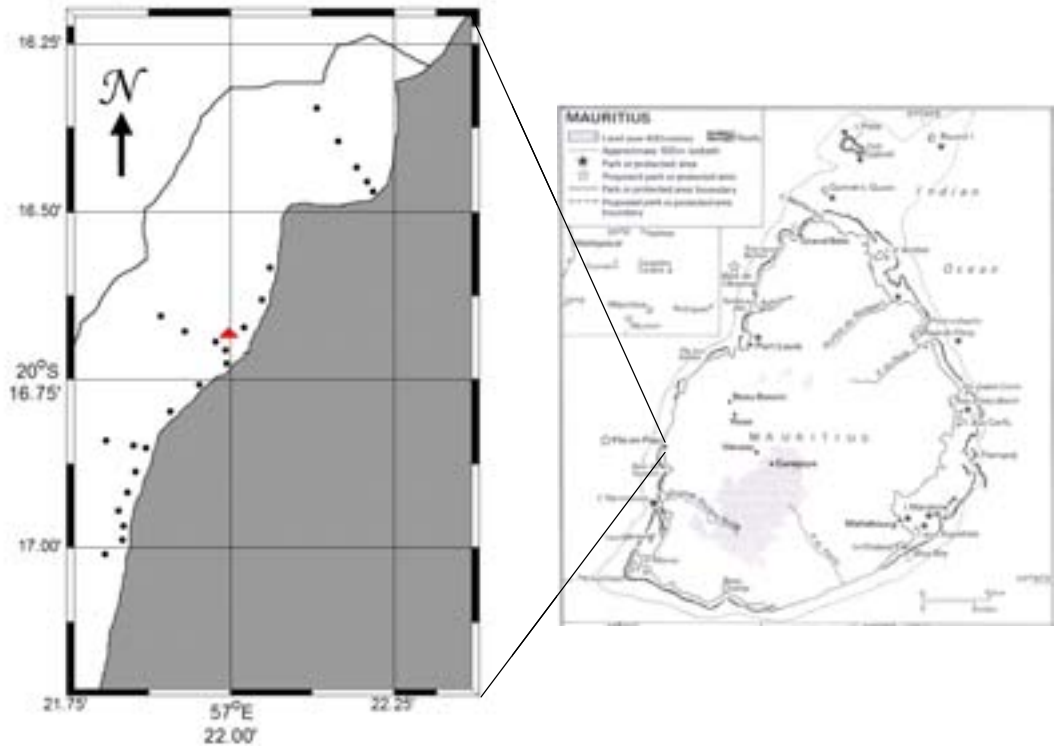

FIG.29. Map of the island of Mauritius together with a detailed view of the locations of the intercomparison experiments near the town of Flic-en-Flac on the southwest coast. The circles show the locations of manual seepage devices. The triangle denotes the location of a submarine spring.

5.5.2. Water Balance Estimate

Mauritius relies heavily upon groundwater to meet both potable water demand (about 56% of that demand is satisfied by groundwater; Ministry of Public Works [207]) and agricultural demand, primarily for the sugarcane industry. Because of this, a network of monitoring wells, stream gauging stations, and meteorological stations has been established on the island to collect a variety of data related to both groundwater and surface water. These data provide the basis for an estimate of freshwater SGD.

The Curepipe Aquifer extends from the high plateau in the center of the island to the western shoreline, approximately 15 km to the west. The total area is approximately 95 km^2. It consists of highly permeable, Recent (1.5 Ma to 25 ka) lava flows with a saturated thickness of 10 to 20 m [208] and a range of transmissivity of 10^{-5} to 10^{-2} m^2/s.

Seasonal rainfall on Mauritius varies from an average maximum of 310 mm/month during the rainy season (December to April) to an average minimum of 75 mm/month during the dry season. For the Curepipe Aquifer, rainfall is about 4000 mm/year near the groundwater divide on the central plateau and decreases with topography to about 800 mm/year near Flic-en-Flac [208]. Surplus rainfall (rainfall in excess of evapotranspiration) is about 70 mm/year along the coast (Medine meteorological station), 840 mm/year halfway inland (Vacoas meteorological station), and 2160 mm/year on the central plateau (Union Park meteorological station) [209]. This excess rainfall would go either to surface runoff or groundwater recharge.

The Curepipe aquifer is covered with highly permeable Recent flows and consequently has almost no surface runoff. The majority of the water infiltrates through the permeable geologic materials, and there are no streams large enough to gauge within the groundwater basin. Because of this, surface runoff can be neglected from the water budget calculation, and the excess rainfall described above is considered to go entirely to groundwater recharge.

The rate of groundwater extraction is known with the least certainty. The Mauritius Water Resources Unit provided data on groundwater pumping for five of the major water supply wells within the basin. The extraction rate for these five wells for 2004 was 2.4×10^6 m^3/year (Zeadally, personal communication). An additional 36 wells are identified as being in use in the basin [207]. Assuming similar pumping rates for these additional wells, a total of 2.0×10^7 m^3/year is pumped from the aquifer.

Subtracting the groundwater pumping from the estimated recharge leaves an estimated freshwater discharge at the shoreline of 7.5×107 m^3/year. Dividing this discharge rate by the 8 km of shoreline yields an estimated discharge rate of 9400 m^3/year per metre of shoreline or 26 m^3/day per metre of shoreline. Assuming the discharge takes place over a 40 m zone perpendicular to the coast, an average seepage rate of 64 cm/day is calculated.

5.5.3. Seepage meters

The rate and distribution of SGD was measured using vented, benthic chambers on the floor of a shallow lagoon on the west coast of Mauritius Island (Flic-en-Flac). Discharge rates were found as high as 490 cm^3 of pore water per cm^2 of sea floor per day (490 cm/day). High SGD rates were associated with low pore water conductivity in the region of a freshwater spring. Large variations in SGD rates were seen over distances of a few metres. We attribute variations to the geomorphologic features of the fractured rock aquifer underlying a thin blanket of coral sands as well as the presence of lava tubes leading to sites of high discharge. Clustering of fractures and the topography of the rock–sediment interface might be focusing or dispersing the discharge of groundwater.

Nine seepage meters were placed at a total of 28 locations. Devices were deployed in three shore normal transects (one adjacent to a large submarine spring, one in a cove 1000 m north of the spring,

and one about 500 m south of the spring), as well as in a 1500 m shore parallel transect, corresponding to areas of low bulk ground conductivity that was measured previously.

The shore parallel transect consisted of measurements taken at various times from devices all located within 15 m of the low tide line. This transect consisted of 18 devices that were in place for a period of 10 h to 5 days. Not all measurements along this transect were made simultaneously; however, at least six devices along this transect were measuring SGD throughout the sampling period.

The average flow rate along this shore parallel transect was 54.5 cm/day. If integrated over the entire length of the transect, we estimate a total discharge of 2.2 × 105 L/m of shoreline per day (220 m^3/m·day). These measurements probably overestimate SGD because of the very high values near the spring. If the calculation is revised using only the measurements from the offshore transect by the north cove, the integrated SGD would be 3.5 × 104 L/m of shoreline per day (35 m^3/m·day). Any evidence of tidal modulation was very weak, but seepage rates at particular sites were seen to abruptly increase (or decrease), and to persist at the new levels, for no obvious reason. Such behavior had also been observed at Ubatuba and, anecdotally, at other sites.

Water collected from the benthic chambers showed fresh water dilution only in the vicinity of the spring. Ambient salinities were about 35, but water samples with salinities as low as 5 were accumulated in the benthic chambers, where an inverse correlation was seen between salinity and SGD rates (Fig.30).

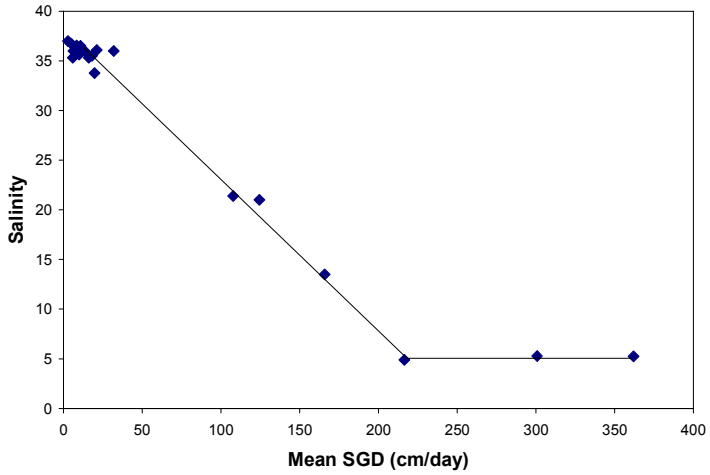

FIG.30. Mean SGD as measured from each of the 28 locations versus the mean salinity measurements of the water that was discharged through the drum. Below a flow rate of 40 cm/day the seepage device water had virtually the same salinity as ambient seawater. At intermediate salinities between 10 and 20, we find fairly high flow rates (between 100 and 170 cm/day). Above 210 cm/day the salinity of the discharged water was constant at 5. This is the same salinity as measured directly at the spring.

5.5.4. Radon

In the case of the Mauritius experiment, it was not possible to deploy the equipment for a complete tidal cycle at any of the stations investigated. We thus modified our normal approach in the following manner. Time-series plots were constructed of ^{222}Rn inventories (concentration multiplied by water depth, assuming a well-mixed layer in these shallow coastal waters) against deployment time. Periods when there were systematic increases in radon inventories were then regressed to estimate radon fluxes (slope of the inventory versus time plot). Assuming that these fluxes were due largely to advection of radon-rich pore waters (groundwater), we then estimated flow by dividing the fluxes by measured groundwater concentrations. Samples collected from piezometers and shallow wells showed radon concentrations between 310–535 dpm/L.

An example is shown for a deployment near the large submarine spring in the lagoon (Fig.31). Based on the slopes of the regressions (labeled 'a', 'b', and 'c') and whether the upper (535 dpm/L) or lower (310 dpm/L) groundwater radon concentration estimate is applied, we estimate that seepage rates through the sandy sediments near the spring range from 65 to 140 cm/day. A comparison to the 3 manual seepage meters that were closest to our deployment site (M2, M15, and M6) shows that M2 was lower with an average of 15 cm/day, M15 was much higher at an average of 360 cm/day, and M6 was also higher at about 300 cm/day (Table 7). This high variability was thus observed by both the radon system and seepage meters in this dynamic environment around the submarine spring. The high variability in the radon record is thought to be a consequence of sampling too close to the groundwater source, resulting in incomplete mixing between high-radon groundwater and low-radon seawater.

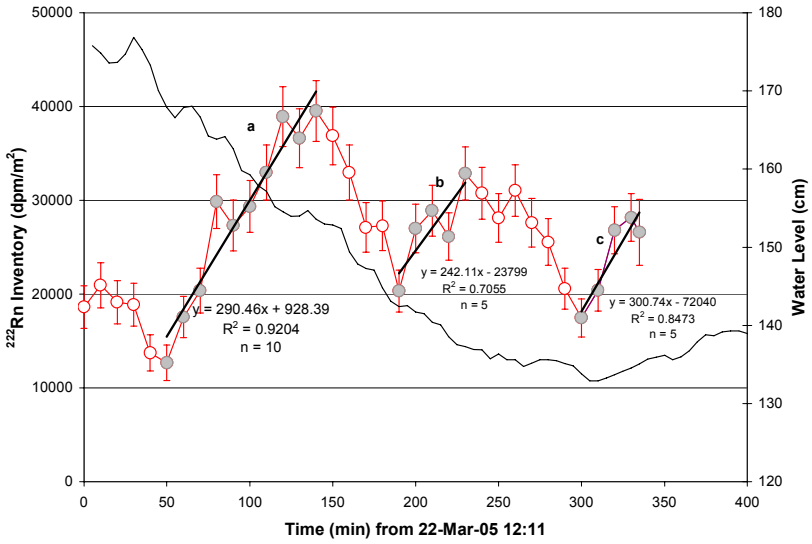

FIG.31. Time-series radon measurements reported as inventories (^{222}Rn activity multiplied by the water depth; circles) just north of the spring on 22 March 2005. The solid line indicates the water level during the same period. Filled circles indicate the points used for regressions (see text for discussion).

Using the same radon approach, we estimated a seepage rate through the sediments at 13–23 cm/day at the south beach site. This compares reasonably well to the manual seepage meter closest to this deployment (M9) that had a range of 2.5–22 cm/day and an average of 8.3 cm/day during the same period. Our final deployment was in a small cove immediately behind the Klondike Hotel. While this was one of the longest deployments, it had to be cut shorter than desired because of a tropical storm that approached the island that day. We calculated a range in seepage of 14–25 cm/day based on the slope of the inventory versus time regression and the radon concentrations in the shallow groundwater. There were no manual seepage meters deployed at this site but the dye-dilution seepage meter was operating nearby at the same time. Their results (5–28 cm/day; average = 10 cm/day; Table 7) closely match the radon rates. That was especially true for the last 3 dye-dilution data points (average = 20 cm/day) that were the closest in timing to the radon measurements.

Measured specific seepage rates (cm/day or $cm^3/cm^2 \cdot day$) can be converted to average shoreline fluxes if one knows or can assume a width of the seepage face. Based on the seepage meter measurements, we estimate that the width of the seepage area in the lagoon is about 40 m. Using this value, we have calculated the shoreline fluxes for the same three sites as in Table 7 as well as the water balance estimate for the entire lagoon (~8 km; Table 8). We note that the water balance estimate (26 $m^3/m \cdot day$) is quite close to the seepage meter value (35 $m^3/m \cdot day$), derived by using the northern meters distant from the large spring.

TABLE 7. ESTIMATES OF SGD FROM 3 SITES IN THE LAGOON OF MAURITIUS ESTIMATED BY EXAMINATION OF THE TRENDS IN ^{222}Rn INVENTORIES COMPARED TO DISCRETE SEEPAGE METER MEASUREMENTS.

Site	Approx. time interval for Rn	^{222}Rn estimate cm/day*	Seepage meters		
			Type#	n	cm/day
Spring	22 March 2005 13:00–14:30	a) 78–130 b) 65–110 c) 81–140	M2 M15 M6	18 2 21	1–28; av = 15 360±5 110–490; av = 300
South Beach	23 March 2005 15:00–16:15	13–23	M9	12	2.5–22 av = 8.3
Klondike Hotel	24 March 2005 15:00–16:20	14–24	WHOI	41	5–28 av = 10 last 3 pts = 20

*The reported range in SGD estimates via this approach is based on upper (535 dpm/L) and lower (310 dpm/L) estimates for the radon concentration in the seepage waters.
#The 'M' meters are standard manually operated flux chambers [51]; the WHOI device is an automatic dye-dilution seepage meter [92].

TABLE 8. ESTIMATES OF SGD ON A PER UNIT WIDTH OF SHORELINE BASIS FROM 3 SITES IN THE MAURITIUS LAGOON.

Area	Radon estimates $m^3/m \cdot day$	Seepage meter estimates $m^3/m \cdot day$
Spring	26–56	0.4–120
South Beach	5.2–9.2	1–8.8
Klondike Hotel	5.6–9.6	2–11
Large area unit shoreline flux estimates		
Water balance estimate = 26 $m^3/m \cdot day$ (Curepipe Aquifer; [210])		
Shore parallel seepage meter transect = 220 $m^3/m \cdot day$ (includes spring; [211].		
Shore parallel transect, north area = 35 $m^3/m \cdot day$ (without spring; [211].		

These estimates are based on the specific seepage measurements (Table 7) and assume a 40 m wide seepage face. Also shown are three wide area estimates.

5.5.5. Summary

Our measurements show significant discharge of groundwater into the Flic-en-Flac Lagoon, Mauritius. This discharge shows large spatial and temporal heterogeneity likely caused by the presence of specialized conduits of groundwater flow created by the coralline basement of the lagoon and occasional lava tubes. Most of the samples collected show no significant difference between SGD salinity and ambient lagoon salinity, likely due to seawater recirculation and mixing. In the region of a submarine spring, however, SGD was measured to be as high as 490 cm/day and the salinity of SGD was reduced accordingly. The high variability at the spring site was observed by both seepage meters and the radon measurements.

6. Overall Findings and Recommendations

Upon reviewing the results from all the intercomparison experiments, we have come to expect SGD to be fairly ubiquitous in the coastal zone. Rates above 100 cm/day should be considered high while values below 5 cm/day are low (or even marginally detectable). Regardless of location, however, both spatial and temporal variation is to be expected. Measurement strategies should be designed to search for patterns of decreasing SGD with distance from the shore, elevated SGD at submerged springs, and temporal patterns modulated by the tides; not only the diurnal tidal variations but also variations over the spring-neap lunar cycle. Preferential flow paths (the most obvious being submarine springs) are commonly found not only in karstic environments but also in situations that appear more-or-less homogeneous and isotropic. Tidal variations generally appear as higher SGD rates at low tide levels (and lower rates at high tides). However, the modulation is not necessarily linear and the hydrodynamic driving forces are not completely understood. In some situations, the rate of SGD seems to change abruptly without an obvious cause. The composition of SGD will be a mixture of fresh and saline groundwater; recirculated seawater could account for 90% of the discharge or more in some locations.

While each study site must be approached individually, we can make a few generalizations for planning purposes. We have reason to believe that all the measurement techniques described here are valid although they each have their own advantages and disadvantages. We recommend that multiple approaches be applied whenever possible. In addition, a continuing effort is required in order to capture long-period tidal fluctuations, storm effects, and seasonal variations.

The choice of technique will depend not only on what is perceived to be the 'best' approach, but also by practical considerations (cost, availability of equipment, etc.). For many situations, we think that seepage meters, the only device that measures seepage directly, appear to work very well. These devices provide a flux at a specific time and location from a limited amount of seabed (generally ~0.25 m^2). Seepage meters range in cost from almost nothing for a simple bag-operated meter to several thousands of dollars for those equipped with more sophisticated measurement devices. They are subject to some artifacts but can provide useful information if one is aware of the potential problems and if the devices are used in the proper manner. This seems to be especially true in environments where seepage flux rates are relatively rapid (>5 cm/day) and ambient open-water currents due to waves and tides are negligible.

Use of natural geochemical tracers involves the use of more costly equipment and requires personnel with special training and experience. One of the main advantages of the tracer approach is that the water column tends to integrate the signal. As a result, smaller-scale variations, which may be unimportant for larger-scale studies, are smoothed out. The approach may thus be optimal in environments where especially large spatial variation is expected (e.g., fractured rock aquifers). In addition to the spatial integration, tracers integrate the water flux over the time-scale of the isotope and the water residence time of the study area. Depending upon what one wants to know, this can often be a great advantage. Mixing and atmospheric exchanges (radon) must be evaluated as described earlier and care must be exercised in defining the end members. The use of multiple tracers is recommended when possible. As described earlier, the simultaneous measurement of ^{222}Rn and Ra isotopes can be used to constrain the mixing loss of radon.

Simple water balance calculations have been shown to be useful as a first estimate of the fresh groundwater discharge. Hydrogeologic, dual-density, groundwater modeling can also be done either as simple steady-state (annual average flux) or non-steady state (requires real-time boundary conditions) methods. Unfortunately, at present, model results usually do not compare well with seepage meter and tracer measurements. Particular problems can be encountered in the proper scaling, both in time and space, and in parameterizing dispersion processes. Apparent inconsistencies between modeling and direct measurement approaches often arise because different components of SGD (fresh and salt

water) are being evaluated or because the models do not include transient terrestrial (e.g., recharge cycles) or marine processes (tidal pumping, wave set up, etc.) that drive part of all of the SGD. Geochemical tracers and seepage meters measure total flow, very often a combination of fresh groundwater and seawater and driven by a combination of oceanic and terrestrial forces. Water balance calculations and most models evaluate just the fresh groundwater flow driven by terrestrial hydraulic heads.

It is important to remember that, although the techniques described here are well-developed, there is as yet no widely accepted 'standard' methodology. We can certainly say that if one plans to work in karstic or fractured bedrock environments, heterogeneity must be expected and it would be best to plan on multiple approaches. Rates are likely to be controlled by the presence or absence of buried fracture systems and focused, or dispersed, by the topography of the buried rock surface. In such a situation, integrated SGD might be assessed with dispersed geochemical tracers or described statistically from many, randomly situated, spot measurements. Since the radiometric tracers integrate over time and space, it seems best to avoid making such measurements too close to strong, submarine springs where gradients may be sharp and mixing incomplete. This was a concern, for example, in interpreting the ^{222}Rn data from near the large spring in the Mauritius. In volcanic aquifers, especially young basalts, the radium signal may be low. This was found to be the case in the Mauritius and in Hawaii. This situation might hamper the application of Ra and Rn tracers in these settings. We suggest in such an environment that one should also confirm the spatial heterogeneity with some preliminary seepage meter deployments and geophysical techniques; and use traditional modeling with caution, as good results will likely have to use more complex models and would require a significant amount of data.

If one plans to work in a coastal plain setting, there likely will be more homogeneous results. These settings can still exhibit pseudo-karstic characteristics, especially where anthropogenic influences modify SGD. Deep pilings at the Shelter Island site artificially created enhanced SGD. Bulk-headed shorelines, dredged channels that intercept shallow confined aquifers or channelized drainage done to roads or other infrastructure can also introduce karst-like characteristics to otherwise homogeneous aquifers. Seepage meters often work well in such environments and can provide good estimates, especially when there is a distinctive pattern in the results. Such a pattern might, for example, consist of a systematic drop in seepage rates as a function of distance offshore and a correlation between tidal stage and flow. Simple modeling approaches (e.g., hydraulic gradients, tidal propagation, thermal gradients) can often be valuable in this type of environment. Tracers also will work very well in coastal plain environments.

In summary, we make the following suggestions to improve the performance of future SGD assessments:

Some geophysical surveying (e.g., resistivity profiling) should be performed prior to the actual assessments so areas prone to high and low SGD can be mapped out in advance.

Point discharge measurements are best recorded in units of cm/day. It is often most useful to design measurements to allow for integrated assessments of groundwater flow per unit width of shoreline (e.g., $m^3/m \cdot day$), the best way to make comparisons and to extrapolate results. For example, seepage meter transects normal to the shoreline that cover the entire seepage face (which can be mapped with the resistivity probes) would fit this requirement.

The experimental design should put on a spatial and temporal scale that is appropriate for the methodologies being used.

Coordination among groups would ensure that method-to-method intercomparisons could be made. For example, we occasionally had data sets from different devices that only overlap for short periods. Extending these overlapping periods would benefit the evaluation process.

Because of the expected complexity and importance of SGD, a continuing effort is strongly recommended; that is, one that can provide measurements of SGD over time periods encompassing the semidiurnal tidal period to seasonal climatic variations.

ACKNOWLEDGEMENTS

The authors of this report are grateful for the assistance received from the UNESCO's Intergovernmental Oceanographic Commission (IOC) and the International Hydrologic Program (IHP), through their project 'Assessment and Management Implications of Submarine Groundwater Discharge into the Coastal Zone.' We also acknowledge support from the International Atomic Energy Agency (IAEA), which financed this activity through their Coordinated Research Project (CRP) entitled Nuclear and Isotopic Techniques for the Characterization of Submarine Groundwater Discharge in Coastal Zones. The IAEA is grateful to the government of the Principality of Monaco for the support provided to the Marine Environment Laboratory in Monaco. Lastly, we wish to thank the many local organizers of the various intercomparison experiments in Australia, Sicily, New York, Brazil, and Mauritius for all their hard work and patience. Without their cooperation, these experiments could not have been conducted.

REFERENCES

[1] LAROCHE, J., NUZZI, R., WATERS, R., WYMAN, K., FALKOWSKI, P.G., WALLACE, D.W.R., Brown tide blooms in Long Island's coastal waters linked to interannual variability in groundwater flow, Glob. Change Biol. **3** (1997) 397–410.

[2] MOORE, W.S., The subterranean estuary: a reaction zone of ground water and sea water, Mar. Chem. **65** (1999) 111–125.

[3] CHARETTE, M.A., SHOLKOVITZ, E.R., Oxidative precipitation of groundwater-derived ferrous iron in the subterranean estuary of a coastal bay, Geophys. Res. Lett. **29** (2002) 1444.

[4] JOHANNES, R.E., The ecological significance of the submarine discharge of groundwater, Mar. Ecol. Pro. Ser. **3** (1980) 365–373.

[5] FANNING, K.A., BYRNE, R.H., BRELAND, J.A., BETZER, P.R., MOORE, W.S., ELSINGER R.J., PYLE, T.E., Geothermal springs of the west Florida continental shelf: Evidence for dolomitization and radionuclide enrichment, Earth Planet. Sci. Lett. **52** (1981) 345–354.

[6] CHURCH, T.M., An underground route for the water cycle, Nature **380** (1996) 579–580.

[7] MOORE, W.S., Large groundwater inputs to coastal waters revealed by ^{226}Ra enrichments, Nature **380** (1996) 612–614.

[8] LI, L., BARRY, D.A., STAGNITTI, F., PARLANGE, J.U., Submarine groundwater discharge and associated chemical input into a coastal sea, Water Resour. Res. **35** (1999) 3253–3259.

[9] HUSSAIN, N., CHURCH, T.M., KIM, G., Use of ^{222}Rn and ^{226}Ra to trace submarine groundwater discharge into the Chesapeak Bay, Mar. Chem. **65** (1999) 127–134.

[10] TANIGUCHI, M., IWAKAWA, H., Measurements of submarine groundwater discharge rates by a continuous heat-type automated seepage meter in Osaka Bay, Japan, J. Groundw. Hydrol. **43** (2001) 271–277.

[11] KIM, G., HWANG, D.W., Tidal pumping of groundwater into the coastal ocean revealed from submarine Rn-222 and CH_4 monitoring, Geophys Res. Lett. **29** (2002) 10.1029/2002 GL015093.

[12] VALIELA, I., TEAL, J.M., VOLKMAN, S., SHAFER, D., CARPENTER, E.J., Nutrient and particulate fluxes in a salt marsh ecosystem: tidal exchanges and inputs by precipitation and groundwater, Limnol. Oceanogr. **23** (1978) 798–812.

[13] VALIELA, I., FOREMAN, K., LAMONTAGNE, M., HERSH, D., COSTA, J., PECKOL, P., DEMEO–ANDERSON, B., D'AVANZO, C., BABIONE, M., SHAM, C., BRAWLEY, J., LAJTHA, K., Couplings of watersheds and coastal waters: sources and consequences of nutrient enrichment in Waquoit Bay, Massachusetts, Estuaries **15** (1992) 443–457.

[14] VALIELA, I., BOWEN, J.L., KROEGER, K.D., Assessment of models for estimation of land-derived nitrogen loads to shallow estuaries, Appl.Geochem. **17** (2002) 935–953.

[15] CORBETT, D.R., CHANTON, J., BURNETT, W., DILLON, K., RUTKOWSKI, C., FOURQUREAN, J., Patterns of groundwater discharge into Florida Bay, Limnol. Oceanogr. **44** (1999) 1045–1055.
[16] CORBETT, D.R., DILLON, K., BURNETT, W., CHANTON, J., Estimating the groundwater contribution into Florida Bay via natural tracers ^{222}Rn and CH_4, Limnol. Oceanogr. **45** (2000) 1546–1557.
[17] KREST, J.M., MOORE, W.S., GARDNER, L.R., Marsh, nutrient export supplied by groundwater discharge: evidence from radium measurements, Glob. Biogeochem. Cycles **14** (2000) 167–176.
[18] BOKUNIEWICZ, H., Groundwater seepage into Great South Bay, New York, Estuar. Coast. Mar. Sci. **10** (1980) 437–444.
[19] BOKUNIEWICZ, H., PAVLIK, B., Groundwater seepage along a barrier island, Biogeochemistry **10** (1990) 257–276.
[20] CAPONE, D.G., BAUTISTA, M.F., A groundwater source of nitrate in nearshore marine sediments, Nature **313** (1985) 214–216.
[21] CAPONE, D.G., SLATER, J.M., Interannual patterns of water table height and groundwater derived nitrate in nearshore sediments, Biogeochemistry **10** (1990) 277–288.
[22] LAPOINTE, B., O'CONNELL, J.D., GARRETT, G.S., Nutrient coupling between on-site sewage disposal systems, groundwaters, and nearshore surface waters of the Florida Keys, Biogeochemistry **10** (1990) 289–307.
[23] LAPOINTE, B.E., O'CONNELL, J., Nutrient-enhanced growth of Cladophora prolifera in Harrington Sound, Bermuda: eutrophication of a confined, phosphorus-limited marine ecosystem, Estuar. Coast. Shelf Sci. **28** (1989) 347–360.
[24] HWANG, D.W., KIM, G., LEE, Y.-W., YANG, H.-S., Estimating submarine inputs of groundwater and nutrients to a coastal bay using radium isotopes, Mar. Chem. **96** (2005) 61–71.
[25] D'ELIA, C.F., WEBB, D.K.L., PORTER, J.W., Nitrate-rich groundwater inputs to Discovery Bay, Jamaica: A significant source of N to local coral reefs? Bull. Mar. Sci. **31** (1981) 903–910.
[26] OBERDORFER, J.A., VALENTINO, M.A., SMITH, S.V., Groundwater contribution to the nutrient budget of Tomales Bay, California, Biogeochemistry **10** (1990) 199–216.
[27] YOUNGER, P.L., Submarine groundwater discharge, Nature **382** (1996) 121–122.
[28] FREEZE, R.A., CHERRY, J.A., Groundwater, Prentice-Hall Inc., Englewood Cliffs, N.J. (1979) 604p.
[29] JACKSON, J.A., (Ed.). Glossary of Geology, 4th edition, American Geological Institute, Alexandria, Va. (1977).
[30] BURNETT, W.C., BOKUNIEWICZ, H., HUETTEL, M., MOORE, W.S., TANIGUCHI, M., Groundwater and porewater inputs to the coastal zone, Biogeochemistry **66** (2003) 3–33.
[31] CONSIDINE, D.M., (Ed.), Van Nostrand's Scientific Encyc., 8th edition, Van Nostrand, Reinhold, NY. (1995).
[32] STIEGELER, S.E., A Dictionary of Earth Science, PICA Press, NY. (1977).
[33] TODD, D.K., Groundwater Hydrology, 2nd edition, John Wiley and Sons, NY. (1980) 535p.
[34] WYATT, A., Challinor's Dictionary of Geology, 6th edition, University of Wales Press, Cardiff, (1986) 374p.
[35] BATES, R.L., JACKSON, J.A., Dictionary of Geological Terms, American Geological Institute, NY. (1984).
[36] DESTOUNI, G., PRIETO, C., On the possibility for generic modeling of submarine groundwater discharge, Biogeochemistry **66** (2003) 171–186.
[37] NIXON, S.W., AMMERMAN, J.W., ATKINSON, L.P., BEROUNSKY, V.M., BILLEN, G., BOICOURT, W.C., BOYNTON, W.R., CHURCH, T.M., DITORO, D.M., ELMGREN, R., GARBER, J.H., GIBLIN, A.E., JAHNKE, R.A., OWENS, N.J.P., PILSON, M.E.Q., SEITZINGER, S.P., The fate of nitrogen and phosphorus at the land-sea margin of the North Atlantic Ocean, Biogeochemistry **35** (1996) 141–180.
[38] TALBOT, J.M., KROEGER, K.D., RAGO, A., ALLEN, M.C., CHARETTE, M.A., Nitrogen flux and speciation through the subterranean estuary of Waquoit Bay, Massachusetts, Biol. Bull. **205** (2003) 244–245.
[39] SMITH, L., ZAWADZKI, W., A hydrogeologic model of submarine groundwater discharge: Florida intercomparison experiment, Biogeochemistry **66** (2003) 95–110.

[40] REICH, C.D., SHINN, E.A., HICKEY, T.D., TIHANSKY, A.B., Tidal and meteorological influences on shallow marine groundwater flow in the upper Florida Keys, In: The Everglades, Florida Bay, and Coral Reefs of the Florida Keys (Eds J.W. Porter and K.G. Porter), CRC Press, Boca Raton, (2002) 659–676.
[41] CHANTON, J.P., BURNETT, W.C., TANIGUCHI, M., DULAIOVA, H., CORBETT, D.R., Seepage rate variability derived by Atlantic tidal height, Biogeochemistry **66** (2003) 187–202.
[42] RIEDL, R., HUANG, N., MACHAN, R., The subtidal pump: a mechanism of interstitial water exchange by wave action, Mar. Biol. **13** (1972) 210–221.
[43] NIELSEN, P., Tidal dynamics in the water table in a beach, Water Resour. Res. **26** (1990) 2127–2134.
[44] MOORE, W.S., WILSON, A.M., Advective flow through the upper continental shelf driven by storms, buoyancy, and submarine groundwater discharge, Earth Planet Sci. Lett. **235** (2005) 564–576.
[45] HUETTEL, M., GUST, G., Solute release mechanisms from confined sediment cores in stirred benthic chambers and flume flows, Mar. Ecol. Pro. Ser. **82** (1992) 187–197.
[46] HUETTEL, M., ZIEBIS, W., FORESTER, S., Flow-induced uptake of particulate matter in permeable sediments, Limnol. Oceanogr. **41** (1996) 309–322.
[47] WEBSTER, I.T., NORQUAY, S.J., ROSS, F.C., WOODING, R.A., Solute exchange by convection within estuarine sediments, Estuar. Coast. Shelf Sci. **42** (1996) 171–183.
[48] BROWN, G., ROGERS, J., GARBRECHT, J., Task Committee Planning: Darcy Memorial Symposium on the History of Hydraulics, J. Hydraul. Eng. **126** (2000) 799–801.
[49] MICHAEL, H.A., MULLIGAN, A.E., HARVEY, C.F., Seasonal oscillations in water exchange between aquifers and the coastal ocean, Nature **436** (2005) 1145–1148.
[50] MICHAEL, H.A., LUBETSKY, J.S., HARVEY, C.F., Characterizing submarine groundwater discharge: a seepage meter study in Waquoit Bay, Massachusetts, Geophys. Res. Lett. **30** 6 (2003) 10.1029/GL016000.
[51] LEE, D.R., A device for measuring seepage flux in lakes and estuaries, Limnol. Oceanogr. **22** (1977) 140–147.
[52] TANIGUCHI, M., Tidal effects on submarine groundwater discharge into the ocean, Geophys. Res. Lett. **29** (2002) 10.1029/2002GL014987.
[53] KOHOUT, F.A., Submarine springs: A neglected phenomenon of coastal hydrology, Hydrology **26** (1966) 391–413.
[54] WILLIAMS, M.O., Bahrain: port of pearls and petroleum, Natl. Geogr. **89** (1946) 194–210.
[55] ZEKTSER, I.S., Groundwater discharge into the seas and oceans: state of the art. In: Buddemeier RW (Ed.) Groundwater discharge in the coastal zone (pp 122–123), LOICZ IGBP, LOICZ, Texel, Netherlands, Russian Academy of Sciences, Moscow (1996) 179 p.
[56] BAYDON–GHYBEN, W., 'Nota in verband met de voorgenomen putboring nabij Amsterdam,' Koninklyk Instituut Ingenieurs Tijdschrift (The Hague), (1888-1889) 8–22.
[57] HERZBERG, A., Die wasserversorgung einiger Nordseebader. Journal Gasbeleuchtung und Wasserversorgung (Munich) **44** (1901) 815–819, 842–844.
[58] BEAR, J.A., CHENG, H.D., SOREK, S., OUUZAR, D., HERRERA, I., (Eds), Seawater intrusion in coastal aquifers – concepts, methods and practices, Kluwer Academic Publishers, Dordrecht, The Netherlands (1999) 625p.
[59] HUBBERT, M.K., The theory of ground-water motion, J. Geol. **48** (1940) 785–944.
[60] VACHER, H.L., Dupuit–Ghyben–Herzberg analysis of strip-island lenses, Geol. Soc. Am. Bull. **100** (1988) 580–591.
[61] HENRY, H.R., Interface between salt water and fresh water in a coastal aquifer, In: Cooper, H.H. Jr., Kohout, F.A., Henry, H.R., Glover, R.E. (Eds), Sea water in coastal aquifers (p. C35–C70), U.S. Geological Survey Water Supply Paper (1964) p.1613–C.
[62] GLOVER, R.E., The patterns of fresh-water flow in a coastal aquifer, In: Cooper H.H. Jr., Kohout, F.A., Henry, H.R., Glover, R.E. (Eds), Sea water in coastal aquifers (p. C32–C35), U.S. Geological Survey Water Supply Paper (1964) p.1613–C.
[63] MCBRIDE, M.S., PFANNKUCH, H.O., The distribution of seepage within lakebed, J. Res. US Geol. Surv. **3** (1975) 505–512.
[64] VALIELA, I., D'ELIA, C., Groundwater inputs to coastal waters, Special Issue, Biogeochemistry **10** (1990) 328p.

[65] BURNETT, W.C., Offshore springs and seeps are focus of working group, EOS **80** (1999) 13–15.
[66] BURNETT, W.C., CHANTON, J.P., KONTAR, E. (Eds), Submarine Groundwater Discharge, Special Issue, Biogeochemistry **66** 1–2 (2003) 202p.
[67] BOUDREAU, B.P., HUETTEL, M., FROSTER, S., JAHNKE, R.A., MCLACHLAN, A., MIDDELBURG, J.J., NIELSEN, P., SANSONE, F., TAGHON, G., Van, RAAPHORST, W., WEBSTER, I., WESLAWSKI, J.M., WIBERG, P., SUNDBY, B., Permeable marine sediments: overturning an old paradigm, EOS **82** (2001) 133–136.
[68] TANIGUCHI, M., BURNETT, W.C., CABLE, J.E., TURNER, J.V., Investigations of submarine groundwater discharge, Hydrol. Process. **16** (2002) 2115–2129.
[69] MOORE, W.S., High fluxes of radium and barium from the mouth of the Ganges–Brahmaputra River during low river discharge suggest a large groundwater source, Earth Planet. Sci. Lett. **150** (1997) 141–150.
[70] KITHEKA, J.U., Groundwater outflow and its linkage to coastal circulation in a Mangrove-fringed Creek in Kenya, Estuar. Coast. Shelf Sci. **47** (1988) 63–75.
[71] BURNETT, W.C., CHANTON, J., CHRISTOFF, J., KONTAR, E., KRUPA, S., LAMBERT, M., MOORE, W., O'ROURKE, D., PAULSEN, R., SMITH, C., SMITH, L., TANIGUCHI, M., Assessing methodologies for measuring groundwater discharge to the ocean, EOS **83** (2002) 117–123.
[72] ISRAELSEN, O.W., REEVE, R.C., Canal lining experiments in the delta area, Utah, Utah Agr. Exp. Sta. Tech. Bull. **313** (1944) 52p.
[73] SHAW, R.D., PREPAS, E.E., Groundwater–lake interactions: I, Accuracy of seepage meter estimations of lake seepage, J. Hydrol. **119** (1990) 105–120.
[74] SHAW, R.D., PREPAS, E.E., Groundwater–lake interactions: II, Nearshore seepage patterns and the contribution of ground water to lakes in central Alberta, J. Hydrol. **119** (1990) 121–136.
[75] FELLOWS, C.R., BREZONIK, P.L., Seepage flow into Florida lakes, Water Resour. Bull. **16** (1980) 635–641.
[76] SHAW, R.D., PREPAS, E.E., Anomalous, short-term influx of water into seepage meters, Limnol. Oceanogr. **34** (1989) 1343–1351.
[77] BELANGER, T.V., MONTGOMERY, M.E., Seepage meter errors, Limnol. Oceanogr. **37** (1992) 1787–1795.
[78] LIBELO, E.L., MACINTYRE, W.G., Effects of surface-water movement on seepage-meter measurements of flow through the sediment-water interface, Hydrogeol. J. **2** (1994) 49–54.
[79] CABLE, J.E., BURNETT, W.C., CHANTON, J.P., CORBETT, D.R., CABLE, P.H., Field evaluation of seepage meters in the coastal marine environment, Estuar. Coast. Shelf Sci. **45** (1997) 367–375.
[80] CABLE, J.E., BURNETT, W.C., CHANTON, J.P., Magnitudes and variations of groundwater seepage into shallow waters of the Gulf of Mexico, Biogeochemistry 38 (1997) 189–205.
[81] SHINN, E.A., REICH, C.D., HICKEY, T.D., Seepage meters and Bernoulli's revenge, Estuaries **25** (2002) 126–132.
[82] CORBETT, D.R., CABLE, J.E., Seepage meters and advective transport in coastal environments: Comments on "Seepage Meters and Bernoulli's Revenge by E.A. Shinn, C.D. Reich, and T.D. Hickey, Estuaries **25** (2002) 126–132", Estuaries **26** (2003) 1383–1389.
[83] FUKUO, Y., Studies on groundwater seepage in the bottom of Lake Biwa, Report for Environmental Sciences by the Ministry of Education, Science and Culture, Japan, B289-R-12-2 (1986) 1–23.
[84] CHERKAUER, D.S., MCBRIDE, J.M., A remotely operated seepage meter for use in large lakes and rivers, Ground Water **26** (1988) 165–171.
[85] BOYLE, D.R., Design of a seepage meter for measuring groundwater fluxes in the nonlittoral zones of lakes – evaluation in a boreal forest lake, Limnol. Oceanogr. **39** (1994) 670–681.
[86] SAYLES, F.L., DICKINSON, W.H., The seep meter: a benthic chamber for the sampling and analysis of low velocity hydrothermal vents, Deep-Sea Res. **88** (1990) 1–13.
[87] TANIGUCHI, M., FUKUO, Y., Continuous measurements of ground-water seepage using an automatic seepage meter, Ground Water **31** (1993) 675–679.
[88] KRUPA, S.L., BELANGER, T.V., HECK, H.H., BROK, J.T., JONES, B.J., KRUPASEEP, – the next generation seepage meter, J. Coast. Res. **25** (1998) 210–213.

[89] TANIGUCHI, M., FUKUO, Y., An effect of seiche on groundwater seepage rate into Lake Biwa, Japan, Water Resour. Res. **32** (1996) 333–338.
[90] GRANIER, A., Une nouvelle methode pour la measure du flux de seve brute dans tronc desarbres, Ann. Sci. For. **42** (1985) 81–88.
[91] TANIGUCHI, M., TURNER, J.V., SMITH, A., Evaluations of groundwater discharge rates from subsurface temperature in Cockburn Sound, Western Australia, Biogeochemistry **66** (2003) 111–124.
[92] SHOLKOVITZ, E.R., HERBOLD, C., CHARETTE, M.A., An automated dye-dilution based seepage meter for the time-series measurement of submarine groundwater discharge, Limnol. Oceanogr. Methods **1** (2003) 17–29.
[93] PAULSEN, R.J., SMITH, C.F., O'ROURKE, D., WONG, T., Development and evaluation of an ultrasonic ground water seepage meter, Ground Water **39** (2001) 904–911.
[94] BARWELL, V.K., LEE, D.R., Determination of horizontal-to-vertical hydraulic conductivity ratios from seepage measurements on lake beds, Water Resour. Res. **17** (1981) 565–570.
[95] TANIGUCHI, M., Change in groundwater seepage rate into Lake Biwa, Japan, Jpn. J. Limnol. **56** (1995) 261–267.
[96] BURNETT, W.C, TANIGUCHI, M., OBERDORFER, J., Measurement and significance of the direct discharge of groundwater into the coastal zone, J. Sea Res. **46** 2 (2001) 109–116.
[97] CABLE, J., BUGNA, G.C., BURNETT, W.C., CHANTON, J.P., Application of ^{222}Rn and CH_4 for assessment of groundwater discharge to the coastal ocean, Limnol. Oceanog. **41** (1996) 1347–1353.
[98] CABLE, J.E., BURNETT, W.C., CHANTON, J.P., WEATHERLY, G.L., Estimating groundwater discharge into the northeastern Gulf of Mexico using radon-222, Earth Planet. Sci. Lett. **144** (1996) 591–604.
[99] PORCELLI, D., SWARZENSKI, P.W., The behaviour of U and Th series nuclides in groundwater and the tracing of groundwater, Rev. Mineral.Geochem. **52** (2003) 317–361.
[100] CORNETT, R.J, RISTO, B.A., LEE, D.R., Measuring groundwater transport through lake sediments by advection and diffusion, Water Resour. Res. **25** (1989) 1815–1823.
[101] VANEK,V., Groundwater regime of a tidally influenced coastal pond, J. Hydrol. **151** (1993) 317–342.
[102] BURNETT, W.C., COWART, J.B., DEETAE, S., Radium in the Suwannee River and estuary: spring and river input to the Gulf of Mexico, Biogeochemistry **10** (1990) 237–255.
[103] BURNETT, W.C., CABLE., J.E., CORBETT, D.R., CHANTON, J.P., Tracing groundwater flow into surface waters using natural ^{222}Rn, Proc. Int. Symp. Groundwater Discharge in the Coastal Zone, Land–Ocean Interactions in the Coastal Zone (LOICZ), Moscow (1996) 22–28.
[104] ELLINS, K.K., ROMAN–MAS, A., LEE, R., Using Rn-222 to examine groundwater/surface discharge interaction in the Rio Grande de Manati, Puerto Rico, J. Hydrol. **115** (1990) 319–341.
[105] RAMA, MOORE, W.S., Using the radium quartet for evaluating groundwater input and water exchange in salt marshes, Geochim. Cosmochim. Acta **60** (1996) 4245–4252.
[106] CABLE, J.E., MARTIN, J., SWARZENSKI, P., LINDENBURG, M., STEWARD, J., Advection within shallow pore waters of a coastal lagoon, Ground Water **42** (2004) 1011–1020.
[107] MOORE, W.S., SHAW T.J., Chemical signals from submarine fluid advection onto the continental shelf, J Geophys Res – Oceans **103** (1998) 21543–21552.
[108] MOORE, W.S., Determining coastal mixing rates using radium isotopes, Cont. Shelf Res. **20** (2000) 1995–2007.
[109] CHARETTE, M.A., BUESSELER, K.O., ANDREWS, J.E., Utility of radium isotopes for evaluating the input and transport of groundwater-derived nitrogen to a Cape Cod estuary, Limnol. Oceanogr. **46** (2001) 465–470.
[110] KELLY, R.P., MORAN, S.B., Seasonal changes in groundwater input to a well-mixed estuary estimated using radium isotopes and implications for coastal nutrient budgets, Limnol. Oceanogr. **47** (2002) 1796–1807.
[111] BURNETT, W.C., DULAIOVA, H., Estimating the dynamics of groundwater input into the coastal zone via continuous radon-222 measurements, J. Environ. Radioact. **69** (2003) 21–35.
[112] GARRISON, G.H., GLENN, C.R., MCMURTRY, G.M., Measurement of submarine groundwater discharge in Kahana Bay, Oahu, Hawaii, Limnol. Oceangr. **48** (2003) 920–928.

[113] KREST, J.M., HARVEY, J.W., Using natural distributions of short-lived radium isotopes to quantify groundwater discharge and recharge, Limnol. Oceanogr. **48** (2003) 290–298.
[114] CROTWELL, A.M., MOORE, W.S., Nutrient and radium fluxes from submarine groundwater discharge to Port Royal Sound, South Carolina, Aqua. Geochem. **9** (2003) 191–208.
[115] KIM, G., RYU, J.W., YANG, H.S., YUN, S.T., Submarine groundwater discharge (SGD) into the Yellow Sea revealed by Ra-228 and Ra-226 isotopes: Implications for global silicate fluxes, Earth Planet. Sci. Lett. **237** 1-2 (2005) 156–166.
[116] BURNETT, W.C., CABLE, J.E., CORBETT, D.R., Radon tracing of submarine groundwater discharge in coastal environments, In: Land and Marine Hydrogeology (Eds: M. Taniguchi, K. Wang, T. Gamo), Elsevier, Amsterdam (2003) 25–43.
[117] MOORE, W.S,, ARNOLD, R., Measurement of ^{223}Ra and ^{224}Ra in coastal waters using a delayed coincidence counter, J. Geophys. Res. **101** (1996) 1321–1329.
[118] DULAIOVA, H., PETERSON, R., BURNETT, W.C., A multi-detector continuous monitor for assessment of 222Rn in the coastal ocean, J. Radioanal. Nucl. Chem. **263** 2 (2005) 361–365.
[119] POVINEC, P.P., LA ROSA, J., LEE, S.-H., MULSOW, S., OSVATH, I., WYSE, E., Recent developments in radiometric and mass spectrometry methods for marine radioactivity measurements, J. Radioanal. Nucl. Chem. **248** (2001) 713–718.
[120] LEVY–PALOMO, I., COMANDUCCI, J.F., POVINEC, P.P., Investigation of submarine groundwater discharge in Sicilian and Brazilian coastal waters using underwater gamma spectrometer, Book of Extended Synopses, International Atomic Energy Agency, Vienna (2004) 228–229.
[121] ROSENBERG, N.D., LUPTON, J.E., KADKO, D., COLLIER, R., LILLY, M.D., PAK, H., Estimation of heat and chemical fluxes from a seafloor hydrothermal vent field using radon measurements, Nature **334** (1988) 604–608.
[122] BUGNA, G.C., CHANTON, J.P., YOUNG, J.E., BURNETT, W.C., CABLE, P.H., The importance of groundwater discharge to the methane budget of nearshore and continental shelf waters of the NE Gulf of Mexico, Geochim. Cosmochim. Acta **60** (1996) 4735–4746.
[123] TSUNOGAI, U., ISHIBASHI, J., WAKITA, H., GAMO, T., Methane-rich plumes in the Suruga Trough (Japan) and their carbon isotopic characterization, Earth Planet. Sci. Lett. **160** (1999) 97–105.
[124] MOORE, W.S., SHAW, T.J., Fluxes and behaviour of radium isotopes, barium, and uranium in seven Southeastern US rivers and estuaries, Mar. Chem. Submitted for publication.
[125] AGGARWAL, P.K., KULKARNI, K.M., POVINEC, P.P., HAN, L.-F., GROENING, M., Environmental isotope investigation of submarine groundwater discharge in Sicily, Italy, Book of Extended Synopses, IAEA, Vienna (2004) 222–223.
[126] AGGARWAL, P.K., GAT, J.R., FROEHLICH, K.F.O., Isotopes in the Water Cycle: Past, Present and Future of a Developing Science, Springer, Dordrecht (2005) 381p.
[127] TANIGUCHI, M., BURNETT, W.C., SMITH, C.F., PAULSEN, R.J., O'ROURKE, D., KRUPA, S., CHRISTOFF, J.L., Spatial and temporal distributions of submarine groundwater discharge rates obtained from various types of seepage meters at a site in the northeastern Gulf of Mexico, Biogeochemistry **66** (2003) 35–53.
[128] BREDEHOEFT, J.D., PAPADOPULOS, I.S., Rates of vertical groundwater movement estimated from the Earth's thermal profile, Water Resour. Res. **1** (1965) 325–328.
[129] STALLMAN, R.W., Computation of groundwater velocity from temperature data. US Geol. Surv. Water Supply Paper **1544-H** (1963) 36–46.
[130] CARTWRIGHT, K., Measurement of fluid velocity using temperature profiles: Experimental verification, J. Hydrol. **43** (1979) 185–194.
[131] BOYLE, J.M., SALEEM, Z.A., Determination of recharge rate using temperature depth profiles in wells, Water Resour. Res. **15** (1979) 1616–1622.
[132] SAKURA, Y., The method for estimations of the groundwater velocity from temperature distributions: On the groundwater around Sapporo, Japan, Stud. Water Temp. **21** (1977) 2–14.
[133] LU, N., GE, S., Effect of horizontal heat and fluid flow on the vertical temperature distribution in a semiconfining layer, Water Resour. Res. **32** (1996) 1449–1453.
[134] SILLMAN, S.E., BOOTH, D.F., Analysis of time-series measurements of sediment temperature for identification of gaining vs. losing portions of Juday Creek, Indiana, J. Hydrol.**146** (1993) 131–148.

[135] CONSTANTZ, J., THOMAS, C.L., ZELLWEGER, G., Influence of diurnal variations in stream temperature on streamflow loss and groundwater recharge, Water Resour. Res. **30** (1994) 3253–3264.
[136] LAPHAM, W.W., Use of temperature profiles beneath streams to determine rates of vertical ground-water flow and vertical hydraulic conductivity, U S Geol. Surv. Water Supply Paper **2337** (1989) 35p.
[137] SUZUKI, S., Percolation measurements based on heat flow through soil with special reference to paddy fields, J. Geophys. Res. **65** (1960) 2883–2885.
[138] STALLMAN, R.W., Steady one-dimensional fluid flow in a semi-infinite porous medium with sinusoidal surface temperature, J. Geophys. Res. **70** (1965) 2821–2827.
[139] TANIGUCHI, M., Evaluation of vertical groundwater fluxes and thermal properties of aquifers based on transient temperature–depth profiles, Water Resour. Res. **29** (1993) 2021–2026.
[140] TANIGUCHI, M., Estimated recharge rates from groundwater temperatures in Nara basin, Japan, Appl. Hydrogeol. **2** (1994) 7–13.
[141] DOMENICO, P.A., PALCIAUSKAS, V.V., Theoretical analysis of forced convective heat transfer in regional ground-water flow, Geol. Soc. Am. Bull. **84** (1973) 3803–3813.
[142] SMITH, L., CHAPMAN, D.S., On the thermal effects of groundwater flow: 1. Regional scale system, J. Geophys. Res. **88** (1983) 593–608.
[143] TANIGUCHI, M., SHIMADA, J., TANAKA, T., KAYANE, I., SAKURA, Y., SHIMANO, Y., DAPAAH–SIAKWAN, S., KAWASHIMA, S., Disturbances of temperature–depth profiles due to surface climate change and subsurface water flow: 1. An effect of linear increase in surface temperature caused by global warming and urbanization in the Tokyo metropolitan area, Japan, Water Resour. Res. **35** (1999) 1507–1517.
[144] TANIGUCHI, M., WILLIAMSON, D.R., PECK, A.J., Disturbances of temperature–depth profiles due to surface climate change and subsurface water flow: 2. An effect of step increase in surface temperature caused by forest clearing in southwest Western Australia, Water Resour. Res. **35** (1999) 1519–1529.
[145] FISHER, A.T., Von, HERZEN, R.P., BLUM, P., HOPPIE, B., WANG, K., Evidence may indicate recent warming of shallow slope bottom water off New Jersey shore, EOS **80** (1999) 171–173.
[146] TANIGUCHI, M., SAKURA, Y., ISHII, T., Estimations of saltwater–fresh water interfaces and groundwater discharge rates in coastal zones from borehole temperature data, Proc. Japanese Association of Groundwater Hydrology Meeting, Tokyo (1998) 86–89.
[147] TANIGUCHI, M., Evaluation of the saltwater–groundwater interface from borehole temperature in a coastal region, Geophys. Res. Lett. **27** (2000) 713–716.
[148] MARTIN, J.B., CABLE, J.E., JAEGER, J., HARTL, K., SMITH, C.G., Thermal and chemical evidence for rapid water exchange in the Indian River Lagoon, Florida, Limnol. Oceanogr. **51** (2006) 1332–341.
[149] MOORE, W.S., KREST, J., TAYLOR, G., ROGGENSTEIN, E., JOYE, S., LEE, R., Thermal evidence of water exchange through a coastal aquifer: Implications for nutrient fluxes, Geophys. Res. Lett. **29** (2002) 10.1029/2002GL014923.
[150] FISCHER, W.A., MOXHAM, R.M., POLCYN, F., LANDIS, G.H., Infrared surveys of Hawaiian volcanoes, Science **146** (1964) 733–742.
[151] ROXBURGH, I.S., Thermal infrared detection of submarine spring associated with the Plymouth Limestone, Hydrol. Sci. J. **30** (1985) 185–196.
[152] BANKS, W., PAYLOR, R., HUGHES, W., Using thermal infrared imagery to delineate groundwater discharge, Ground Water **34** (1996) 434–444.
[153] BOGLE, F.R., LOY, K., The application of thermal infrared thermography in the identification of submerged spring in Chickamaura Reservoir, Hamilton County, Tennessee, Karst Geohzards: Proc. fifth multidisciplinary conference on sinkholes and the engineering and environmental impacts of Karst (1995) 415–424.
[154] STIEGLITZ, T., Submarine groundwater discharge into the near-shore zone of the Great Barrier Reef, Australia, Mar. Pollut. Bull. **51** (2005) 51–59.
[155] STIEGLITZ, T., TANIGUCHI, M., NEYLON, S., Spatial variability of submarine groundwater discharge, Ubatuba, Brazil, Estuar. Coast. Shelf Sci. **76** (2008) 493–500.

[156] ALLEN, A.D., Outline of the hydrogeology of the superficial formations of the Swan Coastal Plain, Western Australia Geol. Surv. Ann. Rep. (1976) 31–42.
[157] PLUHOWSKI, E.J., KANTROWITZ, I.H., Hydrology of the Babylon – Islip Area, Suffolk County, Long Island, New York, US Geol. Surv. Water Supply Paper **1768** (1964) 128p.
[158] MUIR, K.S., Groundwater reconnaissance of the Santa Barbara – Montecito Area, Santa Barbara County, California, US Geol. Surv. Water Supply Paper **1859-A** (1968) 28p.
[159] SEKULIC, B., VERTACNIK, A., Balance of average annual fresh water inflow into the Adriatic Sea, Water Resour. Dev. **12** (1996) 89–97.
[160] ROBINSON, M.A., A finite Element Model of Submarine Ground Water Discharge to Tidal Estuarine Waters, PhD dissertation, Virginia Polytechnic Institute (1996).
[161] SELLINGER, Groundwater flux into a portion of eastern Lake Michigan, J. Great Lakes Res. **21** (1995) 53–63.
[162] GARRELS, R.M., MACKENZIE, F.T., Evolution of sedimentary rocks, Norton & Co., New York (1971) 397p.
[163] OBERDORFER, J.A., Numerical modeling of coastal discharge: predicting the effects of climate change, In: Groundwater discharge in the coastal zone (edited by R.W. Buddemeier, pp.179), LOICZ, Texel, Netherlands, Russian Academy of Sciences, Moscow (1996) 69–75.
[164] ZEKTSER, I.S., DZHAMALOV, R.G., Groundwater discharge to the Pacific Ocean, Hydrol. Sci. Bull. **26** (1981) 271–279.
[165] BOLDOVSKI, N.V., Groundwater flow in the coastal zone of the east Sikhote-Alin' volcanogenic belt, Proc. Int. Symp. Groundwater Discharge in the Coastal Zone, Land-Ocean Interactions in the Coastal Zone (LOICZ), Moscow (1996) 8–15.
[166] WILLIAMS, J.B., PINDER, III., J.E., Ground water flow and runoff in a coastal plain stream, Water Resour. Bull. **26** (1990) 343–352.
[167] ZEKTZER, I.S., IVANOV, V.A., MESKHETELI, A.V., The problem of direct groundwater discharge to the seas, J. Hydrol. **20** (1973) 1–36.
[168] BOUWER, H., Groundwater Hydrology, McGraw-Hill, New York (1978) 480p.
[169] ZEKTSER, I.S., LOAICIGA, H.A., Groundwater fluxes in the global hydrologic cycle: past, present and future, J. Hydrol**. 144** (1993) 405–427.
[170] FRITZ, P., CHERRY, J.A., WEYER, K.U., SKLASH, M., Storm runoff analyses using environmental isotopes and major ions, In: Interpretation of Environmental Isotope and Hydrochemical Data in Groundwater Hydrology, International Atomic Energy Agency, Vienna (1976) 111-130.
[171] TANAKA, T., ONO, T., Contribution of soil water and its flow path to stormflow generation in a forested headwater catchment in central Japan, IAHS Publ. **248** (1998) 181–188.
[172] BUDDEMEIER, R.W., (Ed.), Groundwater Discharge in the Coastal Zone, Proc.Int. Sym., Texel, The Netherlands, (1996) LOICZ/R&S/96-8, iv+179 p.
[173] BOKUNIEWICZ, H.J., Analytical descriptions of subaqueous groundwater seepage, Estuaries **15** (1992) 458–464.
[174] FUKUO, Y., KAIHOTSU, I., A theoretical analysis of seepage flow of the confined groundwater into the lake bottom with a gentle slope, Water Resour. Res. **24** (1988) 1949–1953.
[175] WINTER, T.C., The interaction of lakes with variably saturated porous media, Water Resour. Res. **19** (1983) 1203–1218.
[176] WINTER, T.C., Effect of ground-water recharge on configuration of the water table beneath sand dunes and on seepage in lakes in the sand hills of Nebraska, U.S.A., J. Hydrol. **86** (1986) 221–237.
[177] WINTER, T.C., Numerical simulation analysis of the interaction of lakes and groundwater, US Geol. Survey Prof. Paper **1001** (1996) 45p.
[178] ANDERSON, M.P., CHEN, X., Long and short term transience in a groundwater/lake system in Wisconsin, U.S.A., J. Hydrol. **145** (1993) 1–18.
[179] NIELD, S.P., TOWNLEY, L.R., BARR, A.D., A framework for quantitative analysis of surface water – groundwater interaction: Flow geometry in a vertical section, Water Resour. Res. **30** (1994) 2461–2475.

[180] LINDERFELT, W.R., TURNER, J.V., Interaction between shallow groundwater, saline surface water and nutrient discharge in a seasonal estuary: The Swan-Canning River and estuary system, Western Australia, In: Integrating Research and Management for an Urban Estuarine System: The Swan-Canning Estuary, Western Australia, Hydrol. Process. Special Issue **15** (2001) 2631–2653.
[181] SMITH, A.J., TURNER, J.V., Density-dependent surface water-groundwater interaction and nutrient discharge: The Swan-Canning River and estuary system, Western Australia, In: Integrating Research and Management for an Urban Estuarine System: The Swan-Canning Estuary, Western Australia, Hydrol. Process. Special Issue **15** (2001) 2595–2616.
[182] MCDONALD, M.G., HARBAUGH, A.W., A modular three-dimensional finite-difference groundwater flow model, US Geol. Surv. Open File Report **83-875** (1984) 528p.
[183] TANIGUCHI, M., INOUCHI, K., TASE, N., SHIMADA, J., Combination of tracer and numerical simulations to evaluate the groundwater capture zone, IAHS Publ. **258** (1999) 207–213.
[184] RAJAR, R., ŽAGAR, D., ŠIRCA, A., HORVAT, M., Three-dimensional modeling of mercury cycling in the Gulf of Trieste, Sci. Total. Environ. **260** (2000) 109–123.
[185] ČETINA, M., RAJAR, R., POVINEC, P.P., Modelling of circulation and dispersion of radioactive pollutants in the Japan Sea, Oceanol. Acta **23** (2000) 819–836.
[186] SCHLUTER, M., SUESS, E., LINKE, P., SAUTER, E., SUBGATE–coordination: Submarine groundwater fluxes and transport processes from methane-rich coastal environments, In: Suess, E. (Ed.), GEOMAR report 97, Kiel, Germany (2000) 119–120.
[187] SWARZENSKI, P.W., REICH, C.D., SPECHLER, R.M., MOORE, W.S., Using multiple geochemical tracers to characterize the hydrogeology of the submarine spring off Crescent Beach, Florida, Chem. Geol. **179** (2002) 187–202.
[188] LOVELESS, A.M., Biogeochemical, spatial and temporal dynamics of submarine groundwater discharge in an oligotrophic semi-enclosed coastal embayment, PhD Thesis, University of Western Australia, Perth, Australia (2006).
[189] WRIGHT, M.D., The flushing and circulation patterns of Jervoise Bay, Northern Harbour, B.Eng. Honours Thesis, University of Western Australia, Perth (2000).
[190] SMITH, A.J., TURNER, J.V., HERNE, D.E., HICK, W.P., Quantifying Submarine Groundwater Discharge and Nutrient Discharge into Cockburn Sound Western Australia, CSIRO Land and Water, Perth (2003) 185p.
[191] BURNETT, W.C., KIM, G., LANE–SMITH, D., A continuous radon monitor for assessment of radon in coastal ocean waters, J. Radioanal. Nucl. Chem. **249** (2001) 167–172.
[192] SMITH, A.J., NIELD, S.P., Groundwater discharge from the superficial aquifer into Cockburn Sound, Western Australia: estimation by inshore water balance, Biogeochemistry **66** (2003) 125–144.
[193] AURELI, A., Esperienze e. programmidi intervento in materia di ricarica delle falde, per contrastare l'intrusione marina in un acquifero carbonatico sovrasfruttato. IV Congr. di Geoingegneria"Difesa e valorizzazione del suolo e degli acquiferi", Ass. Mineraria Subalpina, Torino, vol. 3 (1994) 813–818.
[194] MOORE, W.S., Radium Isotopes as tracers of submarine groundwater discharge in Sicily, Cont. Shelf Res. **26** (2006) 852–861.
[195] TANIGUCHI, M., BURNETT, W.C., DULAIOVA, H., KONTAR, E.A.,POVINEC, P.P., MOORE, W.S., Submarine groundwater discharge measured by seepage meters in Sicilian coastal waters, Cont. Shelf Res. **26** (2006) 835–842.
[196] BURNETT, W.C., DULAIOVA, H., Radon as a tracer of submarine groundwater discharge into a boat basin in Donnalucata, Sicily, Cont. Shelf Res. **26** (2006) 862–873.
[197] DILORENZO, J.L., RAM, R.V., Flushing-time estimates for West Neck Harbour: a small tidal embayment of the Peconic Bays, New York, Report – Najarian Associates, L.P. Eatontown, New Jersey (1991) 44p.
[198] SCHUBERT, E., Areas contributing ground water to the Peconic estuary, and ground-water budgets for the North and South forks and Shelter Island, Eastern Suffolk County, New York. U.S. Geological Survey, Water Resources Investigations Report **97-4136** (1998).

[199] O'ROURKE, D., Quantifying specific discharge into West Neck Bay, Shelter Island, New York using a three-dimensional finite-difference groundwater flow model and continuous measurements with an ultrasonic seepage meter, Master's Thesis, State University of New York at Stony Brook, (2000).
[200] MAHIQUES, M.M., Sedimentary dynamics of the bays off Ubatuba, State of São Paulo, Boletim do Instituto Oceanográfico, São Paulo, **43** 2 (1995) 111–122.
[201] MESQUITA, A.R., MARÉS, circulação e nível do mar na Costa Sudeste do Brasil, Relatório Fundespa, São Paulo (1997).
[202] BURNETT, W.C., PETERSON, R., MOORE, W.S., DE OLIVEIRA, J., Radon and radium isotopes as tracers of submarine groundwater discharge – results from the Ubatuba, Brazil SGD assessment intercomparison, Estuar. Coast. Shelf Sci. **76** (2008) 501–511.
[203] MOORE, W.S., DE OLIVEIRA, J., Determination of residence time and mixing process of Ubatuba, Brazil, inner shelf waters using natural Ra isotopes, Estuar. Coast. Shelf Sci. **76** (2008) 512–521.
[204] BOKUNIEWICZ, H., POLLOCK, M., BLUM, J., WILSON, R., Submarine ground water discharge and salt penetration across the sea floor, Ground Water-Oceans Special Issue **42** (2004) 983–989.
[205] ZEKTSER, I.S., Groundwater and the Environment: Applications for the Global Community, Lewis Publishers, Boca Raton (2000) 175p.
[206] KIM, G., LEE, K.K., PARK, K.S., HWANG, D.W., YANG, H.S., Large submarine groundwater discharge (SGD) from a volcanic island, Geophys. Res. Lett. **30** (2003) 10.1029/2003GL018378.
[207] MINISTRY OF PUBLIC WORKS, Hydrology data book (1995–1999), Mauritius, Water Resource Unit (2003).
[208] GIORGI, L., BORCHEILLINI, S., DELUCCHI, L., ile, Maurice., Carte Geologique au 1:50 000, Schema hydrogeologique, Geolab July (1999).
[209] PROAG, V., The Geology and Water Resource of Mauritius, Mahatma Gandhi Institute, Mauritius (1995).
[210] OBERDORFER, J., Fresh groundwater discharge to the coastline of the Curepipe Aquifer, Mauritius, Submarine Groundwater Discharge Assessment Intercomparison Experiment, Mauritius, Report to UNESCO (2005).
[211] RAPAGLIA, J., BECK, A., STIEGLITZ, T., BOKUNIEWICZ, H., KONTAR, E., Submarine groundwater discharge patterns through volcanic fractured rock, Submarine Groundwater Discharge Assessment Intercomparison Experiment, Mauritius, Report to UNESCO (2006).

CHARACTERIZATION OF SUBMARINE GROUNDWATER DISCHARGE ALONG THE SOUTHEASTERN COAST OF SICILY (ITALY)

A. Aureli[1], G. Cusimano[2], D. Fidelibus[3], L. Gatto[2], S. Hauser[4], A.M.G. Privitera[1], M.A. Schiavo[4], G.M. Zuppi[5]

[1]Member of the U.O. 4.17 of the G.N.D.C.I. of the National Research Council of Italy
[2]Department of Geology and Geodesy, Palermo University, Italy
[3]Department of Civil and Environmental Engineering, Technical University of Bari, Italy
[4]Department of Chemistry and Physics of the Earth, Palermo University, Italy
[5]Department of Environmental Sciences, 'Ca' Foscari' University of Venice, Italy

Abstract. In research and management of groundwaters, an important role is played by coastal aquifers. Pollution due to salinization and human activities poses serious concerns to the economy of the related territories. Under the project, established through collaboration between the Italian Universities of Palermo, Bari, Venice and the IAEA and the UNESCO, study of coastal aquifers from Syracuse to Donnalucata on the southeastern coast of Sicily was carried out. The study area, known as Hyblean Plateau, is characterized by carbonate and vulcanite outcrops, connected to the tectonic activity during the Cretaceous and the Pliocene period. The aquifers are subjected to overexploitation due to the high water demand for intensive agricultural practices. Thus, the equilibrium between fresh groundwaters and seawater is getting disturbed with consequent salinization. The research project involved the geochemical and isotopic study of well waters, springs and submarine discharges in order to understand the relationships existing among these waters, to identify the best tracers of the natural and human–related phenomena occurring in the area as well as to estimate the presence of possible environmental effects of them on the coastal ecosystem. Hydrogeochemical surveys were carried out, every three months, from 2002 to 2004 on a net of wells, sub-aerial and submarine springs. The present report synthesizes the main results of the research.

1. Introduction

Carbonate groundwater systems hosted in coastal areas are of particular concern, for multi-fold reasons. Firstly, in Sicily, as in many other islands, coastal areas are the most densely populated areas: the increase of anthropogenic pressure considerably raises the potential risk of groundwater contamination. This is even more dangerous considering that groundwater is often the main source of potable water for the coastal communities. Secondly, coastal areas are the sites of potential interactions between fresh groundwater and seawater, the morphology and location of the interface between them being a complex function of groundwater discharge rate, permeability of the host rocks and hydrodynamic features. As the groundwater/seawater interface results from a complex dynamic equilibrium of several contemporaneously acting forces, it turns out that diffuse and uncontrolled overexploitation of coastal aquifers, along with structural and climatic circumstances, may increase the possibility of seawater intrusion, as encountered all over the world.

The outcropping successions hosting the aquifers consist of thick carbonate formations that derive from northern sector of African foreland. The upper part of this carbonate succession is made up by the Ragusa deposits (glauconitic calcarenites), strongly karstified and fractured, and the Tellaro deposits (marls and marl limestone) of middle–upper Miocene. The Plio–Pleistocene tectonic phase produced NE–SW and NW–SE faults that represent preferential drainage for groundwater and surface waters.

2. Sampling and Methodology

The complete study comprised the chemical analysis of a total of 362 water samples, collected in five zones (named Ciane, Avola, Ognina, Donnalucata, Cassibile) during periodical surveys throughout 2002–2004. The analysed samples are clustered in three groups, namely wells (222), subaerial springs

(48) and submarine springs (SGD) (92). A number of selected samples have been also analysed for stable (^{18}O, ^{2}H, ^{13}C) and radioactive (^{14}C) isotopes.

Temperature, pH, Eh and EC were measured directly in the field. Collected samples were analysed for cations, anions and nutrients (NO_3^{1-}, NO_2^{1-}, NH_4^{1+}, PO_3^{4-}) both at the laboratory of Department of Chemistry and Physics of the Earth of Palermo University and Hydrogeology Laboratory of Department of Civil and Environmental Engineering of Technical University of Bari.

Trace metals were also analysed by ICP–MS in some selected water samples. Filtered and acidified with ultrapure HNO_3, samples for trace element determination were stored in HDPE (Nalgene) bottles at 4°C.

The stable (^{18}O, ^{2}H) isotope measurements of water samples were carried out by mass spectrometry at INGV–Section of Palermo. ^{14}C analyses were performed at Hydroisotop GmbH, Germany, by conventional β–counting or by AMS, depending on sample availability. The results are reported in percent Modern Carbon (pMC) along with the analytical error.

3. Results and Discussion

The mineralogical and chemical composition or carbonate formations making up the aquifer play a decisive role in determining the chemical composition of groundwaters. This statement is consistent with the thermodynamic model indicating that the studied fluids are at thermodynamic equilibrium with calcite at the prevailing pH and pCO_2 conditions, such equilibrium conditions being the result of prolonged interaction with fast congruently-dissolving carbonate minerals.

An outline of the main chemical processes affecting the studied groundwater and SGD can be derived by inspection of $Ca^{2+}/(Ca^{2+} + Mg^{2+})$ vs. $SO_4^{2-}/(SO_4^{2-} + HCO_3^{1-})$ diagram (Fig. 1), which shows that most samples fall inside the calcite–anhydrite–dolomite field (CAD). The composition of the samples inside the CAD triangle is essentially governed by dissolution of calcite, dolomite and gypsum, which are the main minerals of the carbonate rocks hosting the aquifers: the low $SO_4^{2-}/(SO_4^{2-} + HCO_3^{1-})$ values suggest that interaction with sulphate minerals is minor. The diagram evidences as well that the other main additional process governing water composition is the mixing between fresh (carbonate) waters and seawater. Mixing with a seawater component is, in fact, the second main source of groundwater mineralization. The importance of this process is made clear by the widespread occurrence of Na–Cl-rich saline groundwater, which, also according to ^{18}O and ^{2}H enrichment, claims for non-negligible seawater contribution (exceptionally up to 50%).

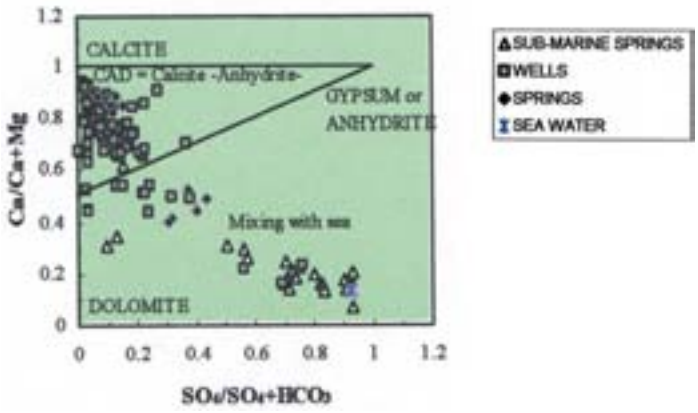

FIG.1. $Ca^{2+}/(Ca^{2+}+Mg^{2+})$ vs. $SO_4^{2-}/(SO_4^{2-}+HCO_3^{2-})$ for the sampled waters.

These findings reveal that the indiscriminate proliferation of private and public wells during the last decades is by now altering the delicate hydraulic equilibrium typical of the coastal aquifers.

Coastal and submarine springs' chemical characteristics indicate that a renewing of karstification occurs within the mixing zone, i.e. the zone where fresh waters and salt waters coexist: the non-linearity of mineral solubility with respect to variation in ion strength, partial pressure of carbon dioxide and temperature, causes the brackish waters to be undersaturated with respect to most carbonate minerals in a large range of salinity.

As to pollutants, the abundance of nitrogen species in studied groundwaters (nitrate and its reduced form precursors nitrite and ammonia) is too high to be explained as derived from the N–poor carbonates: nitrate concentrations in unpolluted carbonate aquifers from the nearby carbonate massif rarely exceed 10 mg/L, which is 4 to 20 times lower than the typical content in groundwaters from southeastern Sicily. The same is true for ammonia: concentrations in the range 5–20 mg/L should be typical of unpolluted carbonate groundwater, whereas significant enrichments are observed in the concerned aquifers (Fig.2).

The Nitrogen is of anthropogenic origin and most specifically derives from the leaching of N–bearing fertilizer by infiltrating water in the intensely cultivated coastal areas. This is also consistent with the very high concentrations of many toxic metals, some of them (Cd, Pb and Zn) being at concentration levels higher than those compatible with an exclusive crustal derivation.

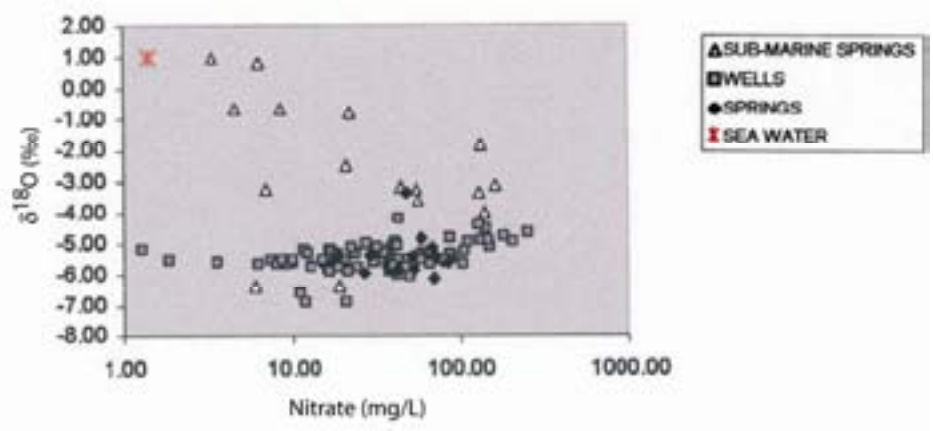

FIG.2. $\delta^{18}O$ vs. NO_3^{1-} concentration for the sampled waters.

Further information about pollution state comes from the interpretation of Cl^{1-}/Br^{1-} weight ratio. The Cl^{1-}/Br^{1-} weight ratio has been used to distinguish between marine and nonmarine origin of salinity [1]. Since Cl^{1-} and Br^{1-} are relatively conservative in hydrogeological systems, the Cl^{1-}/Br^{1-} ratio of fresh waters is primarily controlled by the initial ratio in precipitation. As sea salt spray is the primary source of these ions in precipitation in coastal areas, precipitation should have a Cl^{1-}/Br^{1-} weight ratio similar to that of seawater (288–292): thus, in absence of anthropogenic contamination, the Cl^{1-}/Br^{1-} ratio should be constant when salinization of fresh water occurs by simple mixing with seawater. On the bivariate plot of Cl^{1-}/Br^{1-} ratio vs. Cl^{1-} (Fig.3), the Cl^{1-}/Br^{1-} ratio of ground waters with high Cl^{1-} concentration maintains in the normal seawater range (288–292) with a mean value of 291, indicating that the salinization of the related groundwaters results mainly from mixing with seawater. However, Cl^{1-}/Br^{1-} ratios greater than 300 can generally be related directly to sources of Cl^{1-} other than seawater or atmospheric deposition [2]: these sources may be related to human activity, such as waste water supplied by the urban pollution, the use of salt for industrial processes, and agricultural fertilizers. In contrast, a slight decrease of the Cl^{1-}/Br^{1-} weight ratio in low–Cl samples is observed. This probably results from some pesticides and runoff supply carrying Br^{1-} from the oxidation of ethylene di-bromide, used as soil fumigant in greenhouse growing.

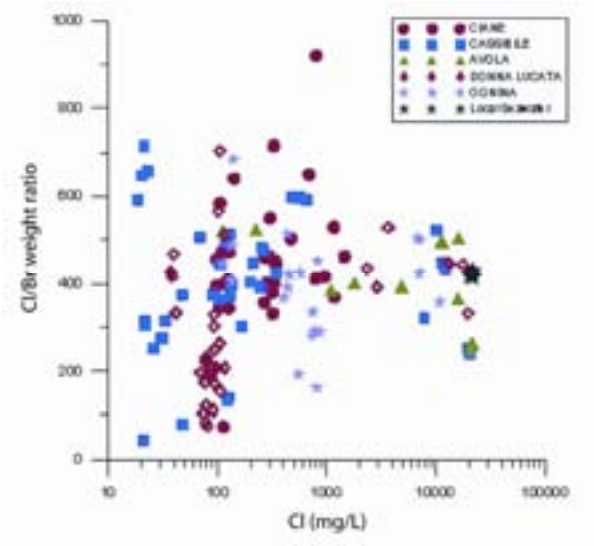

FIG.3. Cl^{1-}/Br^{1-} ratios vs. Cl^{1-} concentrations for sampled waters grouped according to their belonging to the five studied zones.

The stable isotope ratios $\delta^{18}O$ and $\delta^{2}H$ provide information on rainfall sources, the mode of recharge of the groundwater and help further to solve overall questions relating to mixing processes. Results for the analysed water samples are shown in Fig.4 in comparison with the Global Meteoric Water Line (GMWL, d = +10, [3]) and the East Mediterranean Meteoric Water Line (d = +22, [4]). The weighted mean values for $\delta^{18}O$ and $\delta^{2}H$ of modern rainfall [5–8] are equal respectively to –5.0‰ and to –26‰, respectively. The mean modern rainfall has a deuterium excess of +15‰, which is in agreement with the trend observed elsewhere for the central Mediterranean [9,10].

Sampled groundwaters lie as a group on a local meteoric water line; isotope analyses reveal a contrasting isotope composition between the samples collected inland (sub-aerial springs and wells) and the submarine discharges. Sub-aerial springs and wells have hydrogen isotope compositions in the range –39 to –24‰ vs. VSMOW, while oxygen compositions are between –6.9 and –4.2‰ vs. VSMOW; the evolution of $\delta^{18}O$ and $\delta^{2}H$ (according to $\delta^{2}H = 5.6\ \delta^{18}O + 0.7$) during mixing processes is also clear.

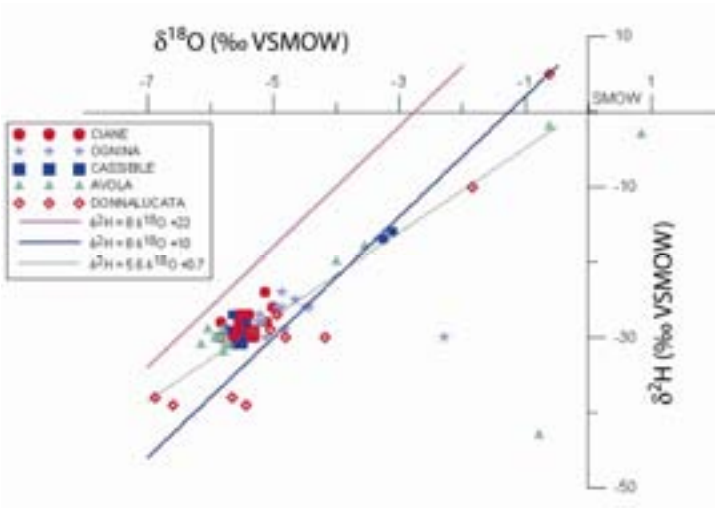

FIG.4. $\delta^{2}H$ vs. $\delta^{18}O$ plot of water samples from Sicily. Water samples are reported in relation to the Global Meteoric Water Line (GMWL d = +10, [3]) and East Mediterranean Meteoric Water Line (d = +22 [4]).

Samples from Donnalucata show a wide scatter and a wide range of $\delta^{18}O$ variation (displacement below the meteoric water line). The deviation of the Donnalucata wells from the GMWL indicates that either the waters experienced some extent of evaporation relatively to the local precipitation, or that they contain some isotopically enriched water from surface systems. The contributions from reservoirs and irrigation water supplies could be considered as the primary reason for isotopic enrichment, as suggested by the positive relation between NO_3^{1-} and $\delta^{18}O$ (Fig.2). Low nitrate concentrations and depleted $\delta^{18}O$ values are representative of groundwater from more continental areas on the Hyblean plateau; on the contrary, the high-nitrate and enriched $\delta^{18}O$ values correspond to groundwater circulating in coastal plains where agriculture is well developed.

The relationship between dissolved inorganic carbon (DIC) and $\delta^{13}C$ for a few groundwaters and spring waters is shown in Fig.5.

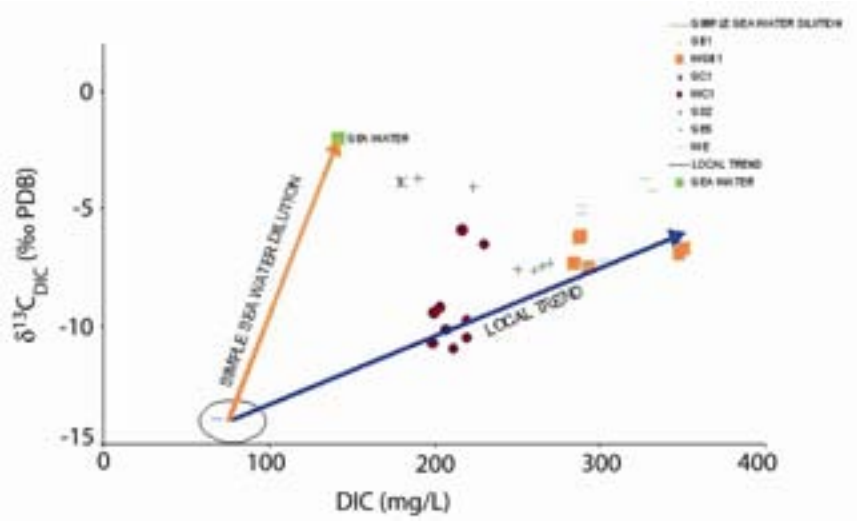

FIG.5. $\delta^{13}C$ vs DIC for part of the sampled waters.

The $\delta^{13}C$ varies between –14‰ (fresh groundwater) and –2 ‰ (seawater); the first pole corresponds to a system where the soil derived CO_2 mixes with a dead dissolved carbon from the aquifer matrix [11]. In the submarine springs, the input signal is masked by isotopic equilibration with limestone and atmospheric CO_2 due to the longer residence time of water. The isotopic composition of total DIC in local seawater, around –2.0 ‰, reflects exchange–fractionation processes between the atmosphere $\delta^{13}C$ (atm) CO_2 = –8.0‰ [12] and, at some degree, biological processes. Unfortunately, in the case of coastal and submarine discharges, the $\delta^{13}C$ cannot distinguish between seawater intrusion and water–rock interactions processes. Certainly, the relation between the continental and the marine poles describe the dilution, taking place along the flow pathway during mixing and water salinisation processes. Nevertheless, water samples (Ciane and Ognina), displaying lower $\delta^{13}C$, require another more depleted carbon source to be considered. It corresponds to the degradation of organic matter present in the aquifer. Indeed, organic matter participates as pollutant due to wastewater contribution, as indicated also by the high nitrate content. On the contrary, the loss of alkalinity via $CaCO_3$ precipitation in some samples from Donnalucata, Avola and Cassibile is enough to offset the isotopically heavy carbon in the submarine and coastal discharges. Seasonally, groundwater in discharge zones have heavier $\delta^{13}C$ values in the summer than in the fall and winter, a consequence of preferential ^{12}C consumption by photosynthetic plants in the unsaturated zone during the growth season. In the downstream portion, influx of isotopically light carbon causes progressive $\delta^{13}C$ depletion.

Residence times have been calculated using the models described by Olive [13]. The following values have been used in age calculation: the activity of soil CO_2 equal to 100 pMC, $\delta^{13}C$ = –25‰, the

activity of inorganic carbonates within the aquifer matrix equal to 0 pMC and $\delta^{13}C = 0‰$. Water age indicates that recharge is current or recent less than 200 years.

The continuous mixing of different hydraulic components and the generalized human perturbation homogenize tracers and do not allow evaluating the transit time. Groundwater flows essentially following a mixing model, as indicated in Fig.6, by the radiometric decay of ^{14}C and by the variables values of $\delta^{13}C$ around –14‰ in recharge areas and –2‰ in submarine springs. Moreover, from recharge to discharge areas, the water velocity cannot be easily evaluated due to the variable aquifer sections, consequence of the intense tectonics.

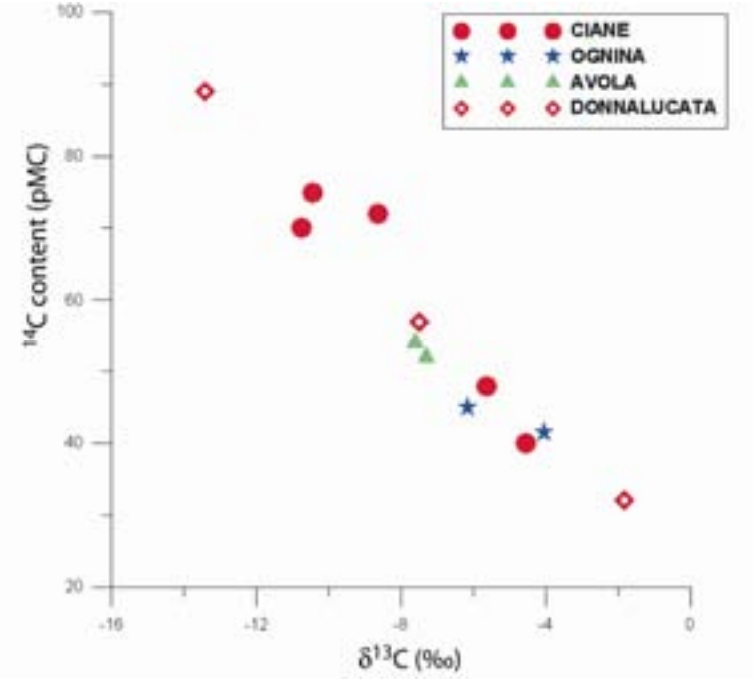

FIG.6. Relation between ^{14}C and $\delta^{13}C$.

4. Conclusions

Due to the high porosity of the limestone, the upstream aquifers accumulate high water volumes and rapidly discharge. The porous reservoirs seem to have the same effect as the limestone aquifer on the concentration of proximal groundwater. It means that both systems, containing high water volumes, can dilute the alluvial and coastal groundwater. In turn, the alluvial groundwater, which flows through the less permeable argillaceous materials rich in soluble minerals, such as gypsum, contains high ion concentration (Avola and Donnalucata).

Some of the analysed parameters are potential indicators of the influence of pumping on groundwater quality. It can be degraded by depressurization of the production zone through pumping, which can cause upconing of (highly) mineralized and/or saline water. Chloride is only one of the parameters that change following increasing pumping and consequent saltwater upconing: anyway, other significant sources of chloride within the Sicilian aquifers at a certain location may be constituted by local contamination from wastewater disposal areas, landfills, or other contaminant point sources, in areas where the confinement to the aquifers is thin, breached or absent.

The $\delta^{18}O$ and $\delta^{2}H$ values close to precipitations indicate rapid comeback to the recharge processes, also on the light of the $\delta^{13}C$ (DIC) values due to soil signals and of the modern ^{14}C due to the short residence time of groundwater.

REFERENCES

[1] ANDREASEN, D.C., FLECK, W.B., Use of bromide/chloride ratios to differentiate potential sources of chloride in a shallow, unconfined aquifer affected by brackish water intrusion, Hydrogeol. J. **5** (1997) 17–26.

[2] DAVIS, S.N., WHITTEMORE, D.O., FABRYKA-MARTIN, J., Uses of Cl^-/bromide ratios in studies of potable water, Ground Water **36** (1998) 338–350.

[3] CRAIG, H., Isotope variations in meteoric waters, Science **133** (1961) 1702–1703.

[4] GAT, J.R., DANSGAARD, W., Stable isotope survey of the fresh water occurrences in Israel and the Northern Jordan Rift Valley, J. Hydrol. **16** 3 (1972) 177–211.

[5] INTERNATIONAL ATOMIC ENERGY AGENCY, Statistical treatment of data on environmental isotopes in precipitation, IAEA, Vienna, Technical Reports Series **206** (1981) 690p.

[6] INTERNATIONAL ATOMIC ENERGY AGENCY, Statistical treatment of data on environmental isotopes in precipitation, IAEA, Vienna, Technical Reports Series **331** (1992) 720p.

[7] ROZANSKI, K., ARAGUAS ARAGUAS, L., GONFIANTINI, R., Relation between long-term trends of oxygen-18 isotope composition of precipitation and climate, Science **258** (1992) 981–985.

[8] LONGINELLI, A., SELMO, E., Isotopic composition of precipitation in Italy: a first overall map, J Hydrol. **270** 1–2 (2003) 75–88.

[9] CELLE-JEANTON, H., GONFIANTINI, R., TRAVI, Y., SOL, B., Oxygen-18 variations of rainwater during precipitation: application of the Rayleigh model to selected rainfalls in Southern France, J. Hydrol. **289** (2004) 165–177.

[10] GOURCY, L., ARAGUAS, L.J., ARGIRIOU, A.A., BONO, P., DIAZ-TEIJEIRO, M.F., DIRICAN, A., EL-ASRAG, A.M., GAT, J.R., GONFIANTINI, R., HORVATINCIC, N., OUDA, B., PAQUETE, P., RANK, D., TRAVI, Y., VRECA, P., Isotopic composition of precipitation in relation to air circulation patterns in the Mediterranean basin. (in preparation).

[11] CLARK, I., FRITZ, P., Environmental Isotopes in Hydrogeology, Lewis Publishers, New York, (1997) 328p.

[12] MOOK, W.G., BOMMERSON, J.C., STAVERMAN, W.H., Carbon isotopic fractionation between bicarbonatic and gaseous carbon dioxide, Earth Planet. Sci. Lett. **22** (1974) 169–172.

[13] OLIVE, PH., La datation des eaux souterraines à long temps de résidence par le radiocarbone, Mode d'emploi. Hydrogéologie **1** (1999) 3–19.

ISOTOPIC AND CHEMICAL CHARACTERIZATION OF COASTAL AND SUBMARINE KARSTIC GROUNDWATER DISCHARGES IN SOUTHERN TURKEY

C.S. Bayari, N.N. Ozyurt

Department of Geological Engineering, Hydrogeological Engineering Section
& International Research & Application Center for Karst Water Resources,
Hacettepe University Beytepe, Ankara,Turkey

Abstract. This study aims to determine the sites of SGD and their physical, chemical and isotopic properties along a 100 km long coastal zone in southwestern Turkey. The aquifer feeding coastal and submarine SGDs comprises of well karstified Mesozoic carbonate massifs that extends from coast to more than 100 km inland. The carbonate massif forms a rugged topography stretching from sea level to over 3000 m. Systematic search dives for every metre of coastal zone down to 30 m below sea level were carried out for precise determination of SGDs. Majority of karstic SGDs were found to be point wise outflows through cracks and submarine caves rather than being spatially dispersed discharges. Comparison of SGD locations detected by means of search dives with those inferred from thermal/infrared satellite images and lineament analyses revealed that systematic screening of coastal zone by divers is essential to determine all existing SGDs. Visual disturbance caused by halocline and temperature gradient felt by diver's skin were the most effective tools to locate SGDs. Stable isotope (^{18}O and ^{2}H) and specific electrical conductivity (SEC) data gathered from SGDs in summer and autumn revealed a freshwater contribution rate ranging from 20% to 80%. Autumn samples which had more depleted stable isotopic signal were found to have relatively high freshwater contribution based on SEC. This suggests apparently higher SGD rate in autumn while precipitation to meet such increase has not occurred. Samples from fresh groundwater indicated a local deuterium excess value of +14 which is typical of research area and neighboring coastal zone. SGDs are located fairly well along a freshwater–seawater mixing line that intersects meteoric line around –6 ‰ and –30 ‰ for O-18 and H-2, respectively. Tritium composition of SGDs ranges between 0 TU and 4.5 TU and is not correlated with mixing ratio. This implies that freshwater components of different SGDs have different residence times. High frequency (10 minutes) SEC and temperature observations carried out in two submarine caves at depths around 20 m bgl for a period of 9 months revealed different discharge dynamics. While one observation site showed SGD pattern that was in line with seasonal recharge, the SGD rate in the other site had an oscillating behaviour that is independent of recharge dynamics.

1. Introduction

This report presents the results obtained within the scope of Research Contract 12570/R0 "Isotopic and chemical characterization of coastal and submarine karstic groundwater discharges in southern Turkey"

The aim of the study is:

- to determine the coastal and submarine groundwater discharge locations,
- to determine physical, chemical and isotopic characteristics of water at these spots,
- to determine factors affecting the seawater contribution rate in selected karstic SGDs.

The study has been carried out in a 100 km long coastal zone in southwestern Turkey. The study area is bounded by well karstified geologic units that form steep mountain flanks next to coastline. Karstic SGDs, first determined from satellite images, have been explored by search dives carried out for every metre along the coastline. During these activities, SCUBA-carried datalogging was carried out in penetrable submarine karstic caves, 217 specific electrical conductivity (SEC) measurements were taken and samples for chemical (179), stable isotopic (84) and tritium (41) analyses were collected. Two SGDs were monitored for EC and temperature for a period of 10 months.

2. Study Area

The study area, comprising of a 100 km long coastline, is located in southwestern Turkey. The area is a part of the Turkish Riviera and is subject to intense tourist activities that cause enormous increase in

population between early spring and late autumn. Both the surface and groundwater supplies are scarce due to extreme karstic nature of geology. Potable water demand is met by a pipeline system that is fed from inland karstic springs. The area is abound with historical sites dating back to 1000 BC and hosts endangered species such as, Mediterranean Monk Seal and sea turtles (Caretta caretta).

The morphology is represented by steep mountain flanks that rise right after the coast line up to elevations over 1000 m. Further inland, mountains rise above 2500 m and over 3000 m. Parts of the coast line has been shaped by block faulting which created a number of islands and bays. Typical Mediterranean climate prevails in the area where mean annual precipitation ranges between 700 mm and over 1000 mm.

Mesozoic and Tertiary carbonates make up the geologic structure. Extensive karstification is widespread all over the area. Faults extending parallel, sub-parallel and perpendicular to coastline are the major elements that have given the morphology to its present shape. Intramountain karst plains are common in the inland part while dolines and sinkholes constitute the characteristic landforms in the coastal zone. Surface drainage is almost absent except small temporary streams that are fed by karstic baseflow.

FIG.1. Location map of the study area.

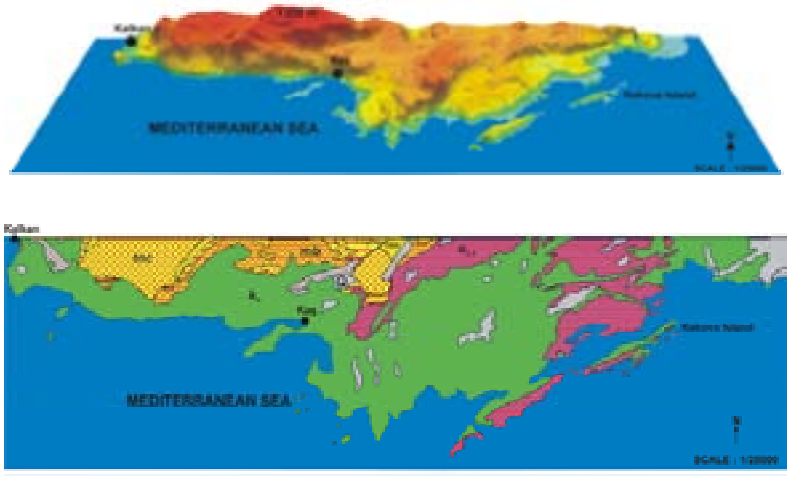

FIG.2. Digital elevation model (top) and lithologic units (bottom) in the area (k2: Mesozoic carbonates, mc, mb: Miocene carbonates and clastics, e: Eocene carbonates, q: Quaternary alluvium).

3. Conceptual Model of SGD Development in Coastal Karst Aquifers

A conceptual model of SGD development in a typical coastal Alpine karst aquifer is outlined below to ease understanding the preliminary results of this study.

In an aquifer groundwater flux (q, LT^{-1}) is governed by the Darcy's equation ($q = k \cdot x \cdot i$) that relates the head (i, LL^{-1}; the force driving groundwater) and the conductance of fluid and medium (k, LT^{-1}) to flux.

For a given hydraulic head, the flux rate is linearly dependent on the hydraulic conductivity of the aquifer. In porous (non-karstic) aquifer spatial variability of hydraulic conductivity is usually limited when compared to karstic systems. Carbonate rocks are subject to continuous dissolution, which is driven by the dissolved carbon dioxide in groundwater. Continuing dissolution of karstic unit leads the much wider spatial variability of hydraulic conductivity compared to non-karstic aquifer. Hydraulic conductivity development in the karstic aquifer is time–continuous unless the dissolution ceases. In addition to conduit development by dissolution, carbonate rocks may also include tiny and large fractures and faults which are a result of tectonic activity.

Figure 3 (a and b) shows the hydraulic conductivity development in vertical section. Any fracture in carbonate rock creates a high conductivity zone (dissolution/flow conduit) through which groundwater flow is favored against rock matrix. Continuing flow causes continuing dissolution in conduit and increases its hydraulic conductivity in time. Thus, a competition among fractures and karstic conduits is always dominant on the groundwater flux through a karstic aquifer. Larger conduits act as major drains that tend to collect water from narrow conduits and fractures. Prevailing conduit development leads to formation of underground stream(s) that are connected to karstic springs. A common feature of karst development is the interplay of surface and underground drainage systems. Valleys and gorges, as perennial and temporary course of surface flow, are formed when well-developed conduit systems collapse. These topographically low-lying features with low-hydraulic heads may also control the direction of groundwater flow and the direction of further conduit development.

Figure 3 (c) shows the possible hydraulic conductivity types of a carbonate rock in plan view. The matrix of a carbonate rock may be homogeneous and isotropic with respect to spatial distribution of initial hydraulic conductivity. In such a system, groundwater flux is said to be diffuse as the flow occurs through voids in rock matrix. When fractures develop in a diffuse flow system, the flux is attracted and conduit development starts. At this stage, the system has both diffuse and fracture flows. Enlargement of fractures by dissolution causes most of the flux be concentrated in conduits (conduit flow) in the later stages of karst development. In conclusion, most probable sites where karstic SGDs with appreciable discharge rates can be found are conduits leading to coastline or sea bottom. On the other hand, karstic groundwater outflow toward sea via diffuse flow should exist every place where the aquifer is in contact with sea. Because fractures and conduits that develop over them are related to tectonic features, tracing lineaments along coastline seems to be an efficient way to detect SGDs.

Determination of the spots where conduit flow toward sea occurs is difficult. Detecting temperature anomalies in seawater and visual inspection of coastline–sea bottom appear to be most practical ways to determine such spots. Under favourable climatic conditions, temperatures of seawater and karstic groundwater may be sufficiently different to enable satellite thermal imagery techniques to be used. An alternative technique could be systematic spatio–temporal measurement of seawater temperature either via an appropriate device or by "skin–probing" (i.e. swimmer's sense of temperature). The difference between the temperatures of seawater (e.g. 25 °C) and of fresh groundwater (e.g. 16°C) along the Aegean and Mediterranean coastline of Turkey during the summer makes the 'skin-probing' an effective tool in detecting SGDs.

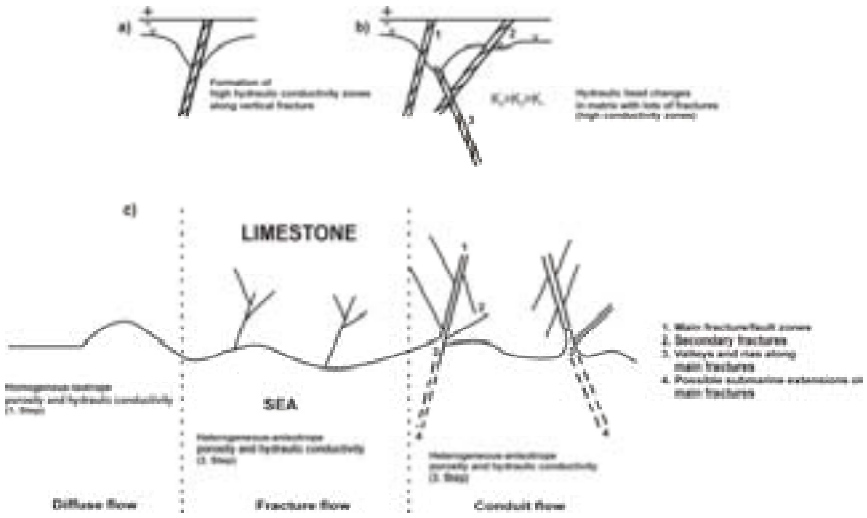

FIG.3. Development of hydraulic conductivity in a karstic aquifer.

4. Lineaments and SGD Locations

Several Landsat TM images have been used to determine the major tectonic lineaments in the study area (Fig. 4 top). This information was further extended from lineament data collected from available geologic maps and field observations. Figure 3 (bottom) shows a combined view of lineament data and positions of SGDs determined in this study. As can be inferred, to the contrary of common belief, many of the freshwater discharge spots seem to unrelated to major lineaments. It appears that, though the major lineaments may be effective in collecting groundwater in the land side, ground waters final arrival spot at the sea should be associated with local lineaments which are not visible on satellite and geologic map data. Field observations revealed that most of the SGDs in the study area are located along fault lines that are parallel to coastline and intersected by local fractures/faults of limited extension.

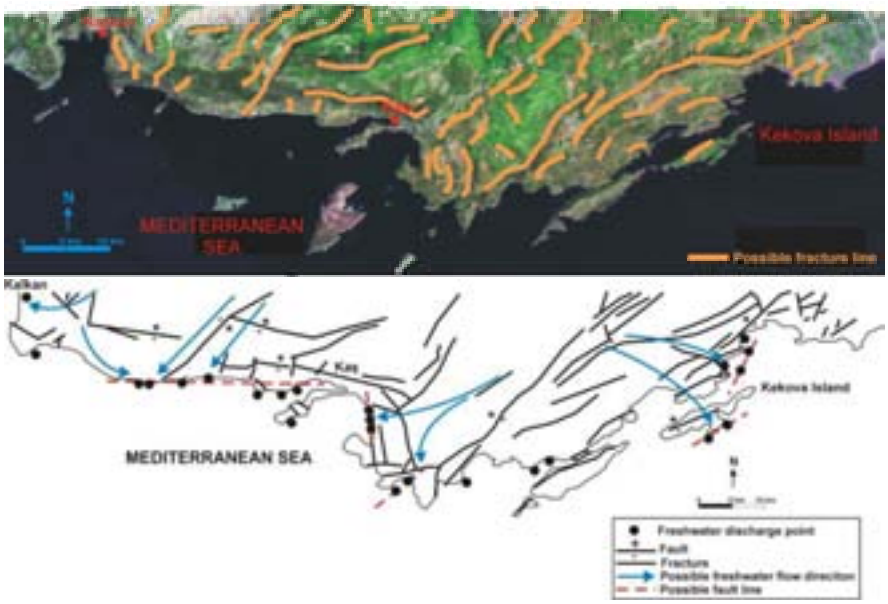

FIG.4. Lineaments determined on Landsat TM image (top) and their relation to SGDs in the study area (bottom).

5. Satellite Based Freshwater Discharge Spots

The thermal band of Landsat TM images taken on 26th August 1987 and 1st August 1990 have been used to determine the spatial distribution of thermal anomaly spots along the coastline. Satellite images in the form of digital numbers have been radiometrically calibrated and contrast enhanced. The period August has been chosen as the time of maximum temperature gradient and minimum cloud cover. Black and white circles in Fig. 5 show the all spots that were determined from the images as the potential groundwater discharge sites. While the black-dot spots were proven to have apparent freshwater discharges, those with white-dot either have no or negligible freshwater contribution. It seems that the rate of groundwater outflow is the major control that makes it visible on the satellite image. Moreover, some of the freshwater spots on satellite image seem to be related to false radiance that is caused by evaporative cooling and/or sea currents. Cool zones on the lee side of islands suggest that east–west trending offshore currents could have dominated the sea surface temperature distribution.

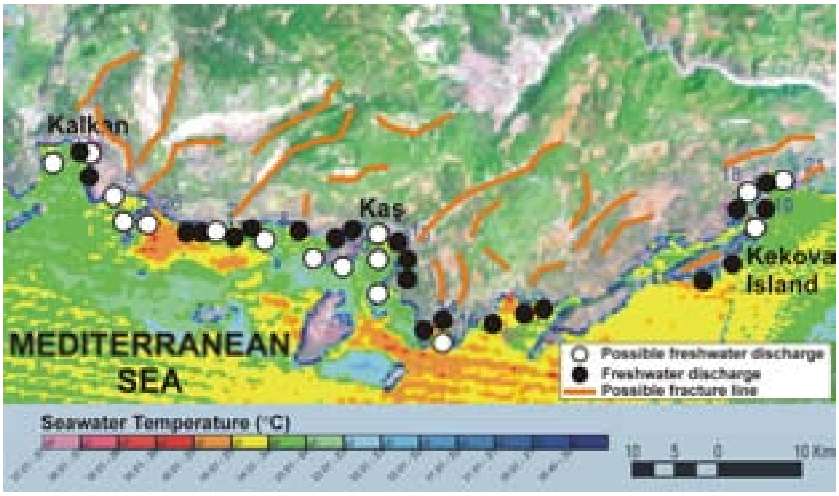

FIG.5. Thermal anomaly spots as determined from Landsat TM image (red: warmer, blue: cooler).

6. SGDs Proven by Search Dives

To prove the existence of freshwater spots determined by lineament and thermal anomaly analyses, a systematic search dive survey has been carried out. Depth ranges of surface to –10 m, –10 m to –20 m and –20 m to –30 m have been surveyed by snorkeling and SCUBA diving for the 70 km range of coastline. Spots suggested by lineament and thermal anomaly analyses have been carefully inspected. Figure 6 shows the spatial distribution of freshwater discharge sites in the study area. Among the 26 sites, 14 were found to be associated with solution conduits whereas 12 spots are related to flow through fracture zones.

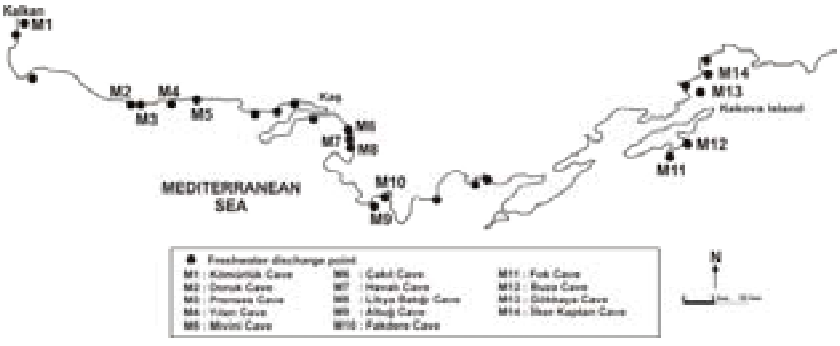

FIG.6. Proven sites of freshwater discharge.

During the search dives, water samples were also collected. In addition, a Hydrolab Data Sonde 3 water quality instrument that is capable of collecting data at pre-programmed time intervals, have been used in SGD caves. With this instrument, temperature, electrical conductivity and depth have been logged.

7. Examples of SGDs Studied

The SGD caves studied revealed that four different types of evolutionary conduit development models exist in the study area: a) bathy–phreatic, b) epikarstic, c) water table, d) freshwater/salt water interface (Fig. 7 a, b, c, d).

The 'Bathy–phreatic' conduits are those developed by dissolution in the saturated zone because of the 'mixing corrosion' effect.

Epikarstic conduits are formed in the unsaturated zone when the system was above present sea level. Water table caves exist at present sea level and extend horizontally. Freshwater/salt water interface caves are developed due to mixing corrosion along the interface.

Details of SGDs in some of these caves are presented in the following paragraphs.

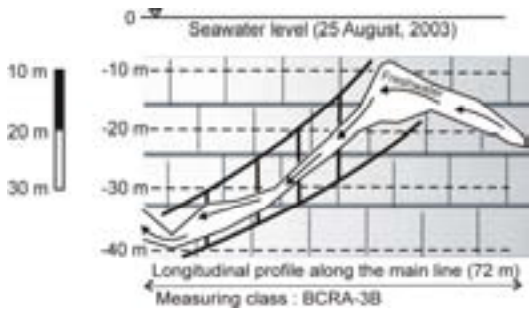

FIG.7a. Bathy–phreatic cave.

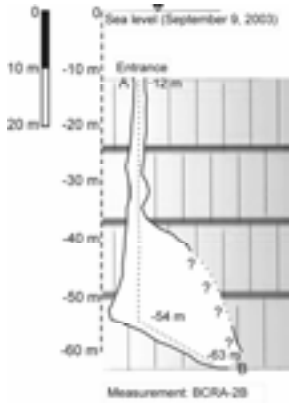

FIG.7b. Epikarstic cave.

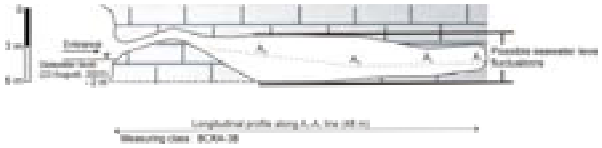

FIG.7c. Water table cave.

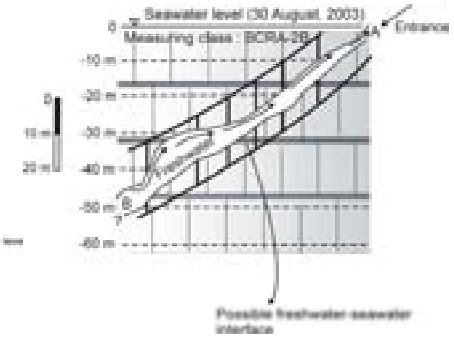

FIG.7d. Freshwater/salt water interface cave.

7.1. Prenses cave

The entrance of the cave is located ca. –40 m below sea level. The conduit extends upwards to – 10 m depth then continues down to –20 m. Total penetrable projected length is ca. 90 m. Its morphology is typical example of a bathy–phreatic conduit development that might have been subject to aerial condition during its formation (Fig. 8a).

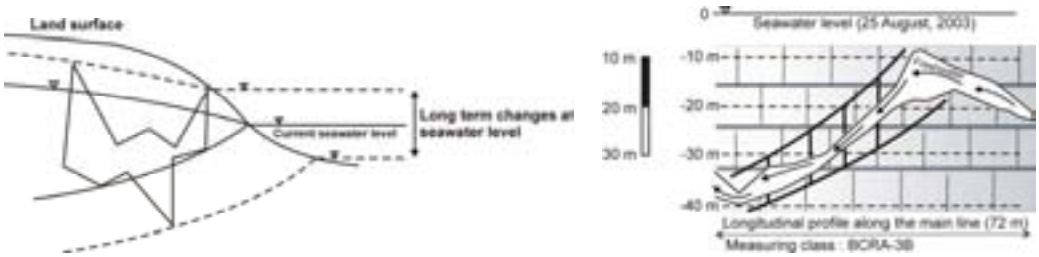

FIG.8a. Prenses Cave (left: development model, right: extended elevation).

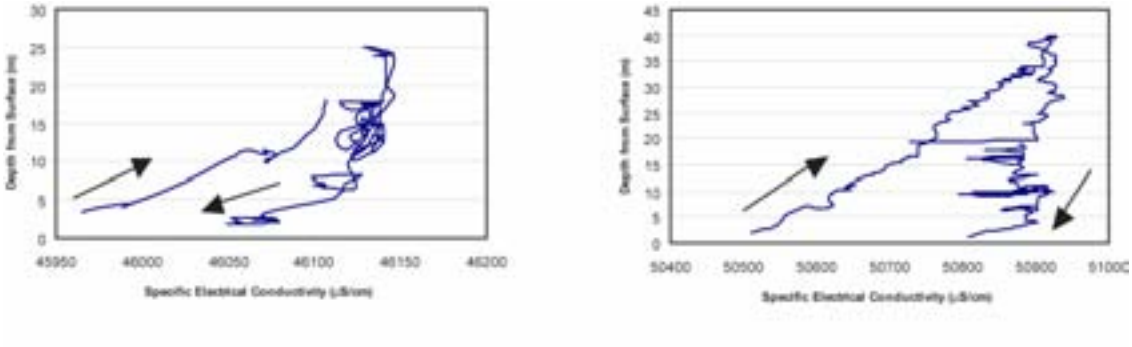

FIG.8b. Prenses Cave electrical conductivity vs. depth (left: August 2003, right: November 2003, arrows indicate start and end of dive/data collection)

Measured electrical conductivity (EC) vs. depth profiles indicates out flowing groundwater in August and in November (Fig. 8b). The difference between the magnitudes of observed EC values is due to increase in seawater conductivity from August to November. It is not known whether this increase is due to large-scale high EC November currents or due to decrease in large-scale fresh water contribution rate to seawater.

7.2. Mivini cave

The entrance of Mivini cave is reached at 3.5 m below sea level. The conduit gently extends downwards to –53 m depth and beyond. Searching the rest of conduit requires technical diving equipment. Total penetrated projected length is ca. 60 m. Its morphology suggests a freshwater/salt water interface dissolution model though development through bathy–phreatic conduits sounds also possible (Fig. 9a).

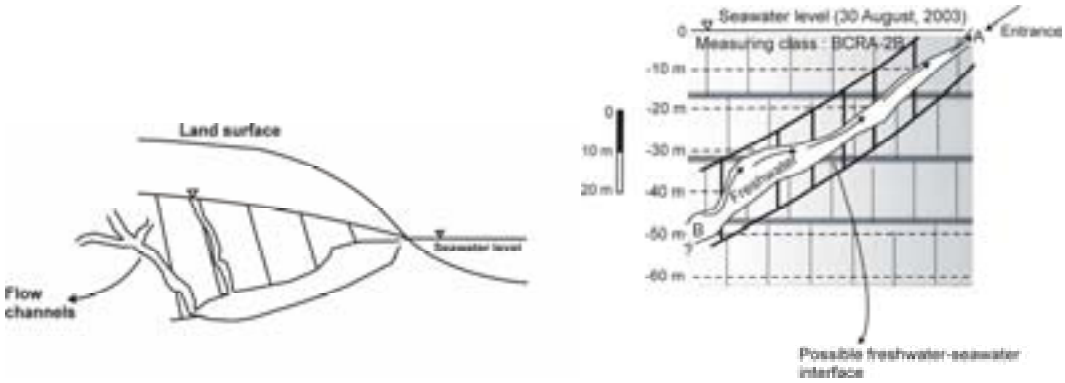

FIG.9a. Mivini Cave (left: development model, right: extended elevation).

Measured electrical conductivity (EC) vs. depth profiles of August and November indicate groundwater outflow originating from the deepest point (Fig. 9b). November profile is uniform due to

diver's fast descent and ascent. It sounds like the upwelling water has already been well mixed with seawater at depths deeper than accessible by diving.

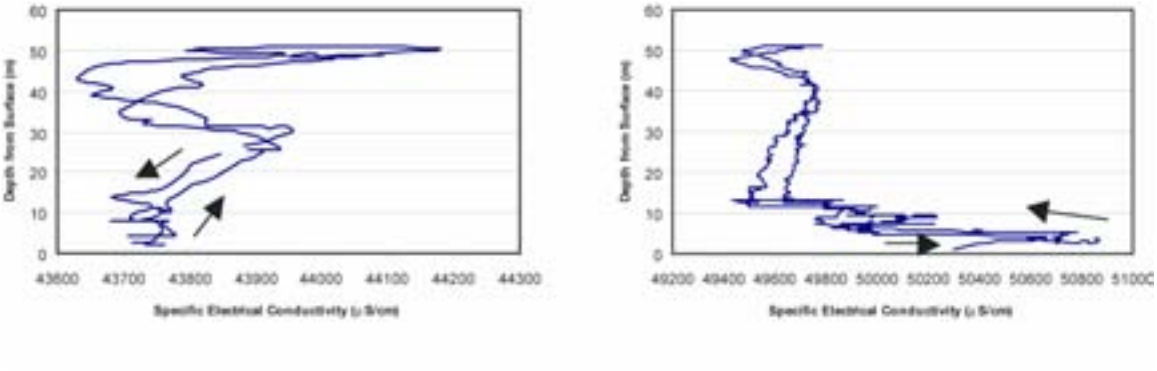

FIG.9b. Mivini Cave electrical conductivity vs. depth (left: August 2003, right November 2003, arrows indicate start and end of dive/data collection).

7.3. Altuğ cave

Altuğ cave comprises of a 20 long vertical shaft connected to a large chamber extending 20 m further down. The entrance is located at 12 m below sea and has a diameter of ca. 1.5 m. Total explorable projected length is ca. 60 m. The conduit continues beyond this depth and further exploration requires technical diving equipment. Its morphology suggests a conduit development due to epikarstic dissolution (Fig.10a).

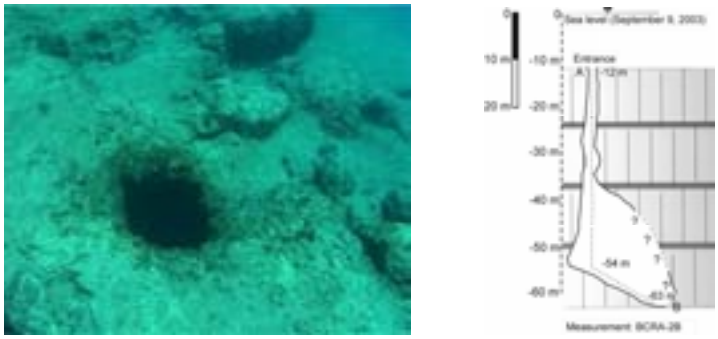

FIG.10a. Altuğ Cave (left: looking down to 1.5 m wide entrance, right: extended elevation).

Measured electrical conductivity (EC) vs. depth profiles of August and November indicate groundwater outflow originating somewhere at – 40 m (Fig.10b). August outflow seems stronger than that of November though *in situ* datalogging is required to verify this observation.

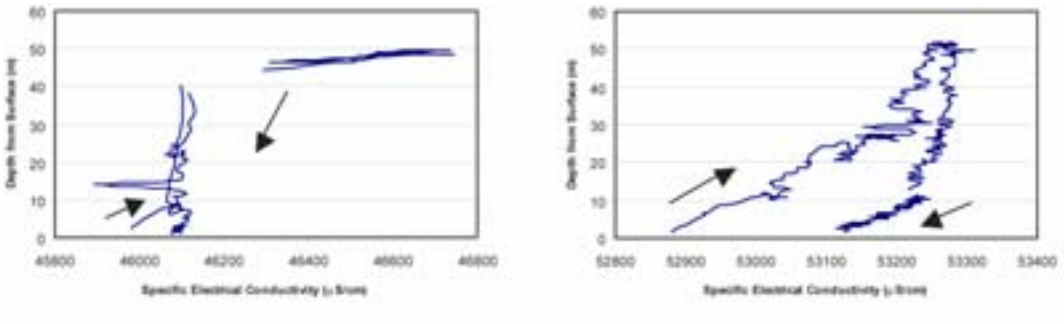

FIG.10b. Altuğ Cave electrical conductivity vs. depth (left: August 2003, right: November 2003, arrows indicate start and end of dive/data collection).

8. Stable Isotopic Composition of Mixture and End Members

Plot of stable isotopic (^{18}O vs. ^{2}H) plot of water samples collected in August and November 2003 is given in Fig.11. On this plot, karstic ground water end member is represented by a stream water sample close to sea level. This sample with EC= 300 μS/cm is assumed to be representative of groundwater discharge into the sea. The seawater samples have enriched stable isotopic signatures as expected from the evaporated seawater of Eastern Mediterranean. All other samples comprising of mixtures of sea and freshwaters at varying ratios are distributed between these end members. August and November samples seem to follow two distinct routes probably because of the isotopic enrichment in freshwater end member. Stable isotopic composition of Alpine karstic groundwater discharges is known to show a temporal variation due to their fast recharge/discharge kinetics. It sounds like the freshwater end member in November samples is more isotopically enriched compared to August.

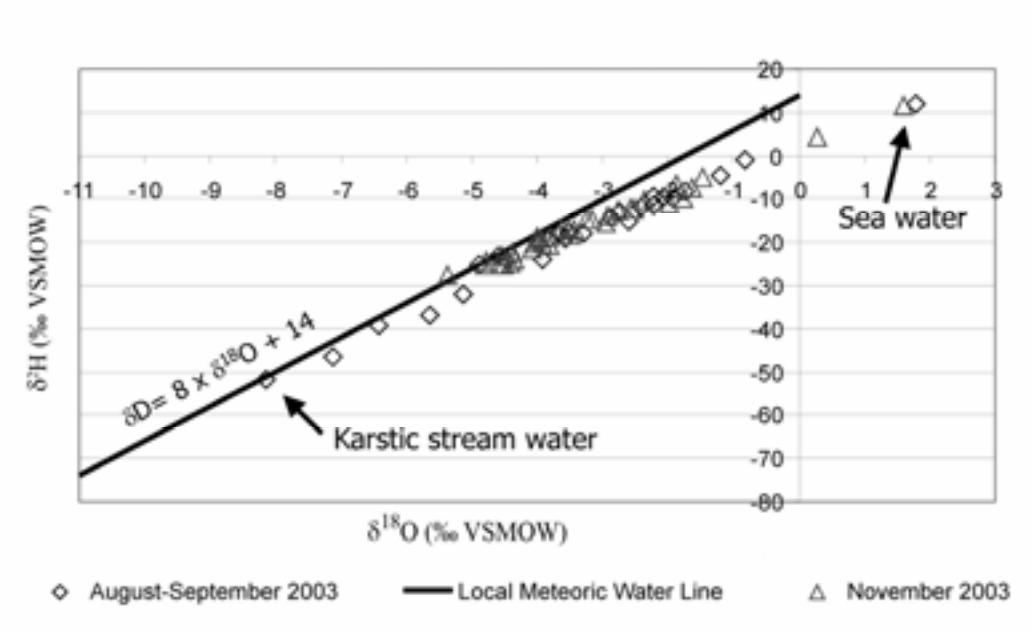

FIG.11. Stable isotopic ($\delta^{18}O/\delta^{2}H$) data plot of water samples collected in August and November 2003.

9. Freshwater Contribution Rate

Freshwater contribution rates in water samples have been determined based on EC values. EC was assumed conservative and any ion source and sink due to freshwater–seawater mixing was assumed negligible. Freshwater EC was assumed to be 300 μS/cm both in August and November when respective seawater ECs were assumed to be 46,000 and 50,000 μS/cm, respectively. Variation of EC-based freshwater contribution rate of water samples is shown in Fig. 12 together with respective ^{18}O compositions. In August samples, freshwater contribution rate varies between 25 % and 60 % while in November slightly higher values are observed. The variation of the ^{18}O composition of samples is strongly correlated with freshwater contribution rates. This suggests that EC behaves conservatively in the mixing process.

10. Temporal Variation of Freshwater Contribution Rate

Figure 13 shows temporal variation of EC-based freshwater contribution rates in August and November at a number of sites that were sampled in both periods. In general, in most of the sites the freshwater contribution rate varies within ±10 % between August and November. It is not clear whether the observed change is due to changes in flow dynamics or not. Uncertainties in EC

measurements and difficulties in collecting water samples exactly the same spot at a site do not allow firm conclusions.

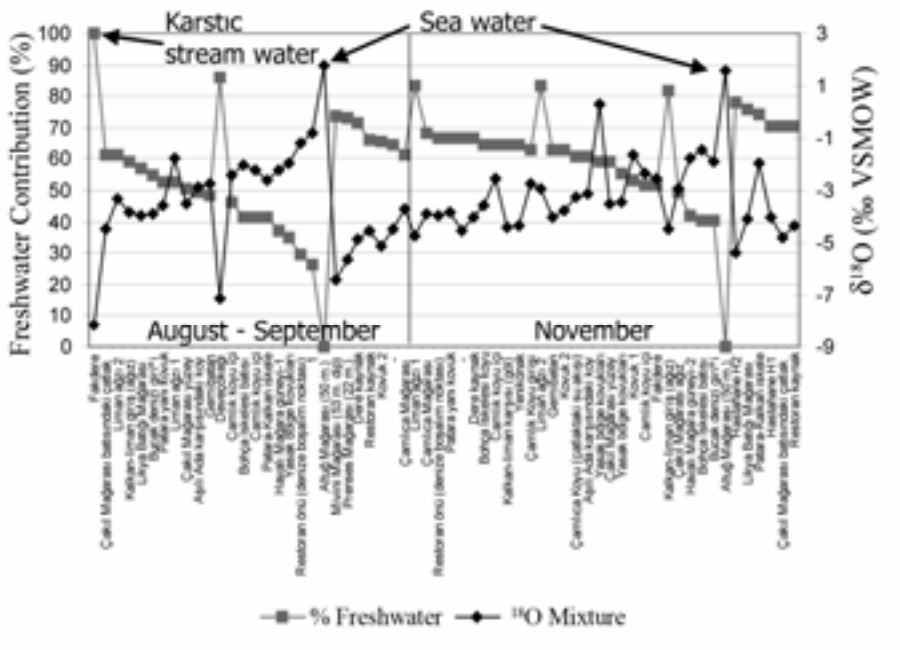

FIG.12. Comparison of freshwater contribution rate with $\delta^{18}O$ composition of samples.

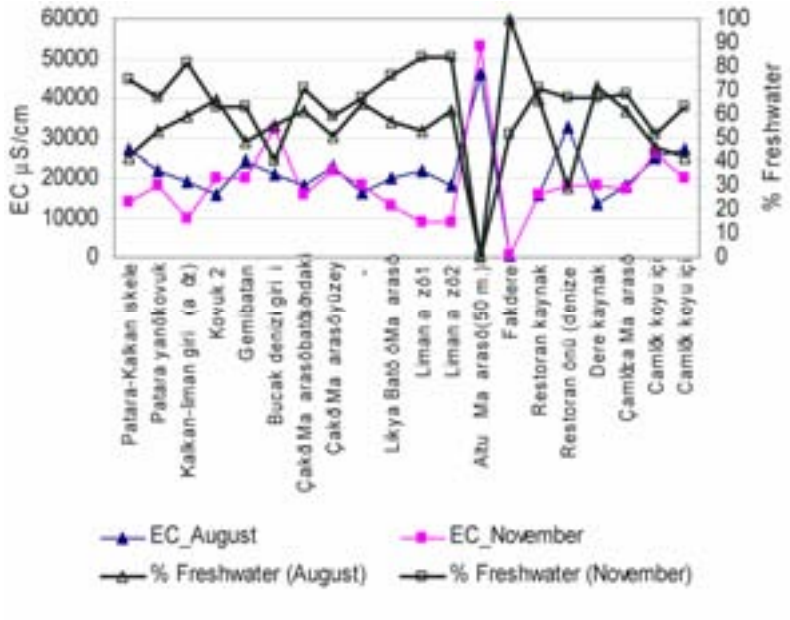

FIG.13. Temporal variation of freshwater contribution rates.

11. Isotopic Composition of Freshwater End Member

Figure 14 a and b show stable isotopic composition of freshwater end members in August and November 2003 samples, respectively. End member isotopic compositions have been determined by using the EC-based freshwater contribution rates and stable isotopic compositions of seawater and samples. Comparison of stable isotopic composition of freshwater end members in both periods reveals that August SGD is isotopically more depleted than November SGD. For example, $\delta^{18}O$ values of August SGD are clustered around –7 to –9 ‰ while in November SGD more depleted values between –8 ‰ and –6 ‰ is observed. This may be due to the contribution of isotopically depleted

early autumn rainfall contribution. In karstic baseflow, the contribution of recent precipitation in outflow decreases towards the end of dry period (i.e. late summer). When the morphology of the recharge area is considered, it appears that short residence time contribution in outflow should comprise mostly of low-elevation rainfall recharge. Because the low elevation rainfall is more enriched compared to long residence time, high altitude recharge, more enriched isotopic composition of freshwater end members of November is most probably due to local rainfall effect.

Moreover, some of the freshwater end members in both periods exhibit evaporative enrichment of rainfall or of seepage water. When the high infiltration velocity of karst aquifer is taken into account, isotopic enrichment during rainfall event seems more plausible. Because, evaporative enrichment in rainfall is more effective at low altitudes, such waters may be attributed to recharge that occurs close to sea level. Increasing number of evaporated samples in November also support this postulate.

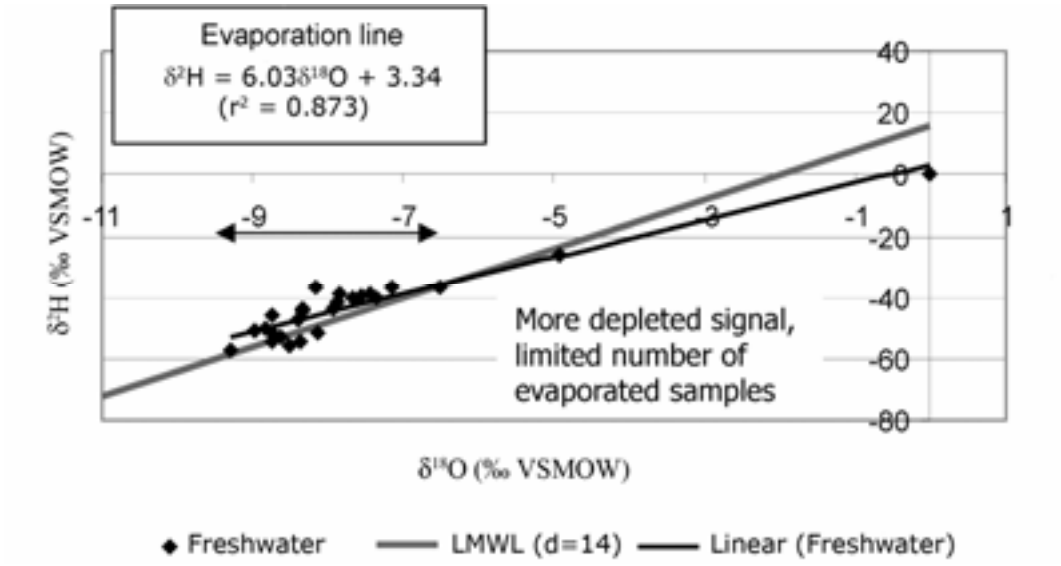

FIG.14a. Stable isotope composition of freshwater end member in August 2003 samples

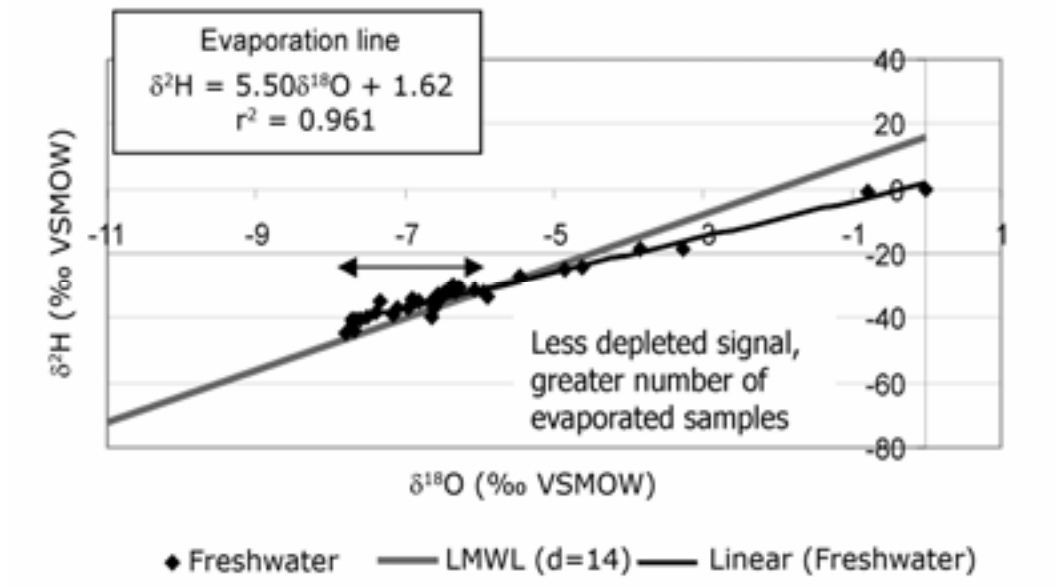

FIG.14b. Stable isotope composition of freshwater end member in November 2003 samples.

12. Tritium as Groundwater Residence Time Indicator

Tritium content is a good indicator of the residence time of groundwater. Tritium contents of SGDs in the study area have been determined for a number of samples. Tritium contents of seawater and freshwater end members in 2003 were determined as ca. 1 TU and 4.5 TU. Two major factors that control tritium content of SGDs are the seawater fraction and the residence time of initial groundwater. Figure 15 suggests that both old and young groundwaters mixed with seawater form SGD. For many of the initial groundwaters, tritium content varies around 1 to 2 TU. Thus, a qualitative groundwater mean residence time of several decades may be attributed to these waters.

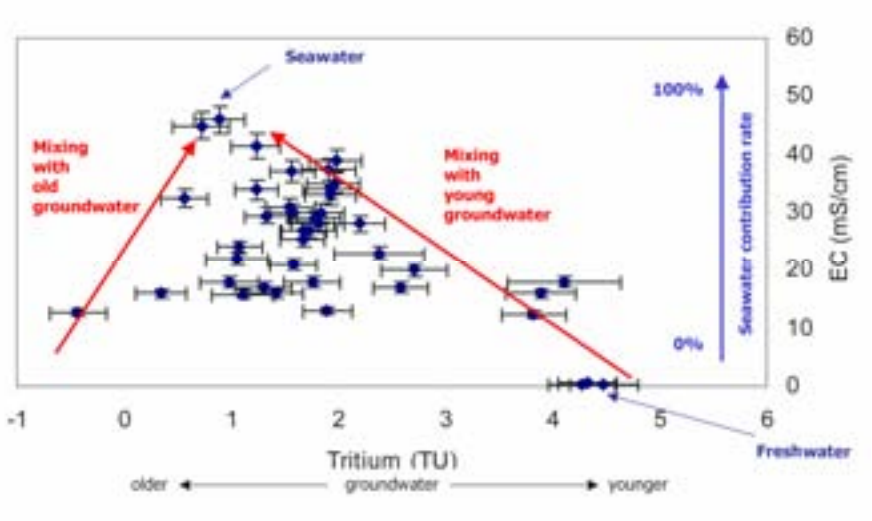

FIG.15. Tritium versus EC plot of selected SGDs.

13. Oxygen-18 as Groundwater Residence Time Indicator

For the study area, seawater and typical fresh groundwater have oxygen-18 values of 2‰ and –8‰. Accordingly, many of the SGDs have oxygen-18 values that are linearly distributed between these end members (Fig.16). However, a limited number of SGDs indicate slightly enriched value for the oxygen-18 of initial groundwater end member. Considering the dependence of oxygen-18 signal on gas–liquid phase equilibrium, enriched oxygen-18 values may be attributed to recharge at low altitude and/or warm season precipitation.

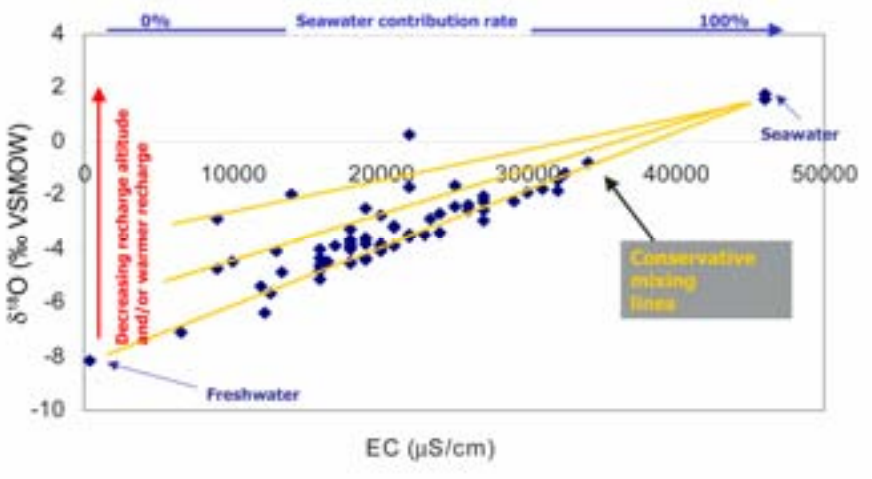

FIG.16. Oxygen-18 versus EC plot of selected SGDs.

14. Spatio–temporal Variation of Seawater Contribution

Since the seawater contribution rate was determined to be temporally variable in many of the SGD sites investigated (see Fig.13), a more elaborate investigation of this process is essential. For this purpose, 'Star-Oddi' data loggers (www.star-oddi.com) were placed in Altug and Mivini caves at points 28 m and 21 m below sea level, respectively. The loggers were set to collect EC and water temperature data every 15 minutes for the period 14 November 2004 and 28 August 2005. The data collected by loggers were compared to relative sea level data recorded at hourly intervals at the Antalya Mareograph Station (located 180 km to the northeast of study area). Similar comparisons were also made for rainfall, air pressure, wind velocity and direction recorded at Kas meteorological station located at coastline in the middle of the study area. Because no apparent relationship between EC, temperature and wind velocity direction were found, the pertinent data is presented in this report.

Long term temporal variation of EC and seawater temperature in Altug and Mivini caves suggests clearly that seawater mixing dynamics in these caves differ remarkably (Fig.17). In both submarine caves, EC and temperature varies linearly though, this relationship is more pronounced in Altug cave (Fig.18). EC and temperature variation in Altug cave follows a declining pattern between November and late April and then starts to rise towards August. In the Mivini cave, both parameters exhibit a wavy pattern that becomes stronger after late April.

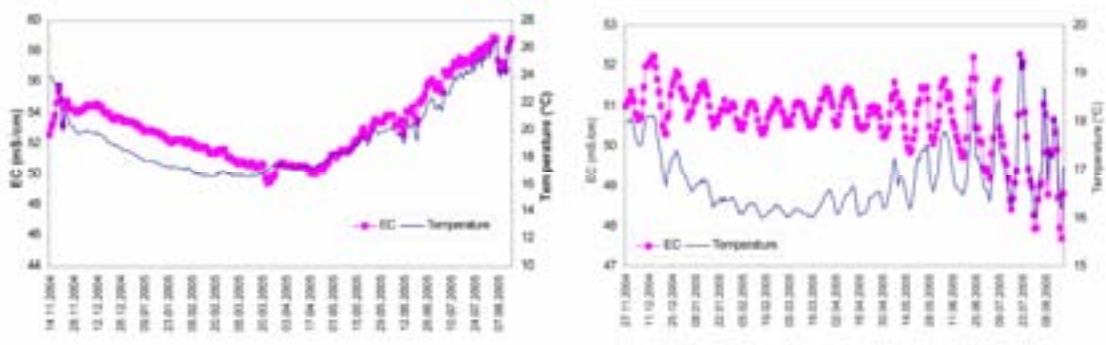

FIG.17. Temporal variation of EC and temperature in selected SGD sites (left: Altug cave, right: Mivini cave).

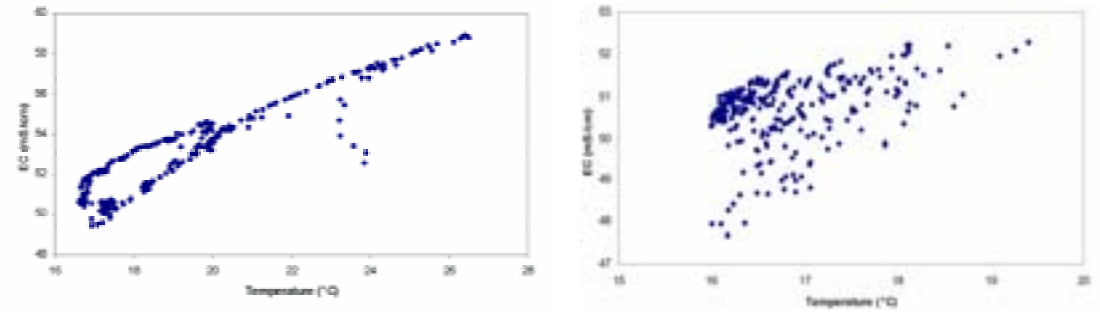

FIG.18. Covariation of EC and temperature in selected SGD sites (left: Altug cave, right: Mivini cave).

Relative sea level is a potential factor that may affect the seawater contribution rate to the SGDs. The relative sea level and associated air pressure data observed at Antalya mareograph station seems to be inversely related (Fig.19). Almost always rising sea level corresponds to decreasing air pressure in the area. However, it also appears that 66.5 per cent of the variation in relative sea level can be explained by air pressure changes (Fig.20).The rest of the variation seems to be associated with moon tide effect.

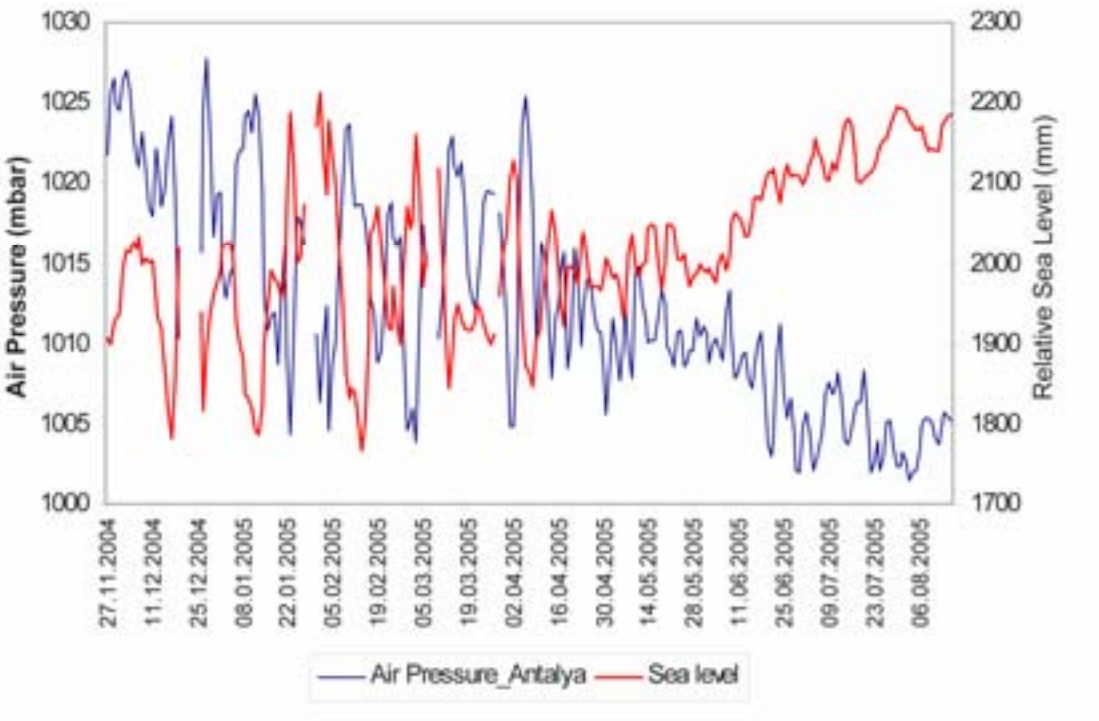

FIG.19. Temporal variation of air pressure and relative sea level at Antalya mareograph station.

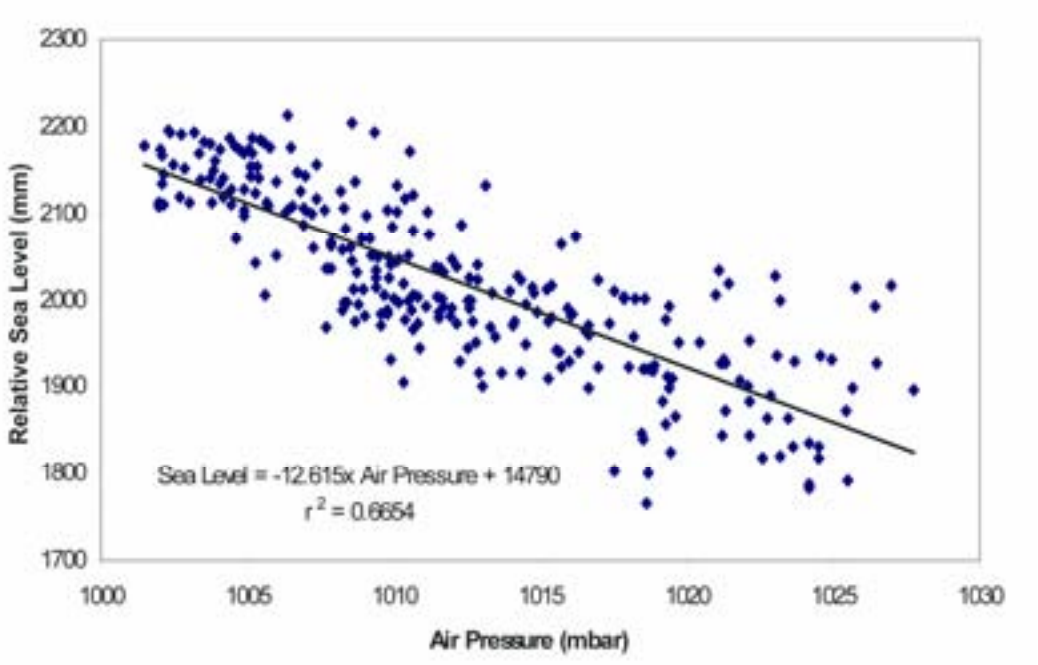

FIG.20. Relationship between air pressure and relative sea level at Antalya mareograph station.

A comparison of temporal EC variation in Altug cave with that of air pressure at Kas station reveals no apparent relationship though, a weak influence may be inferred for Mivini cave (Fig.21). Temporal EC variations in these SGDs are also compared to relative sea level data observed at Antalya mareograph station. Even if this station is located far from the study area, apparent relationship between sea level and air pressure and the similarity of air pressure observed in Antalya and Kas stations allows comparison of both data sets. The relationships between EC and relative sea level series in either cave are different. EC series in Altug cave show no apparent relation to variations in

sea level. However, a weak correspondence between these series may be inferred for Mivini cave (Fig.22).

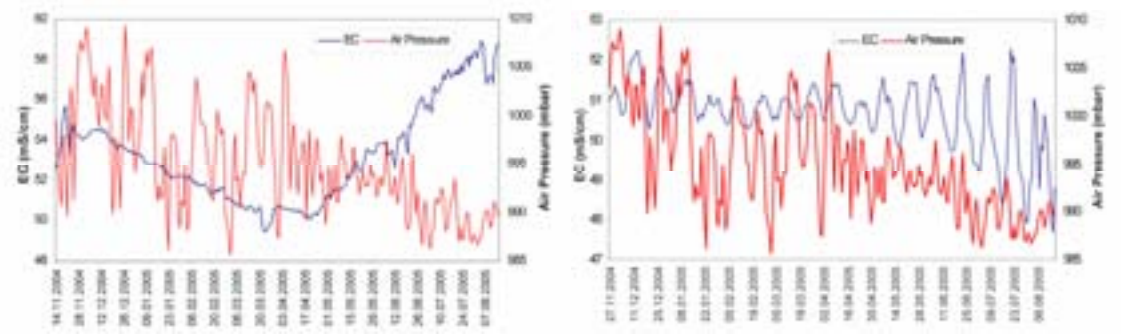

FIG.21. Temporal variation of air pressure and EC in selected SGD sites (left: Altug cave, right: Mivini cave).

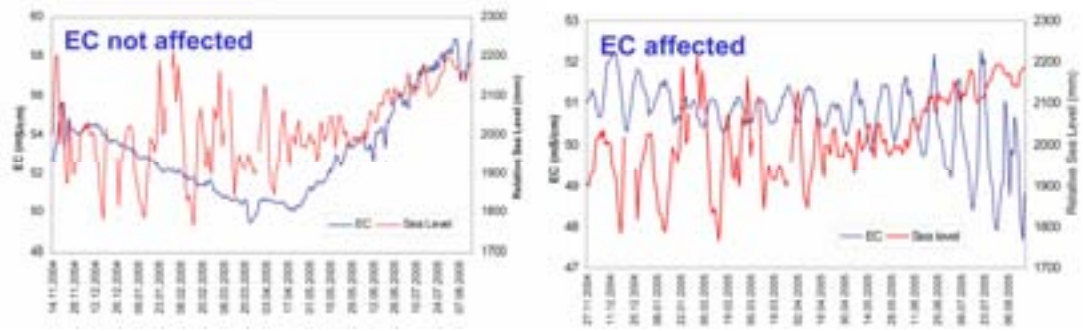

FIG.22. Temporal variation of relative sea level and EC in selected SGD sites (left: Altug cave, right: Mivini cave).

The relationship between rainfall events and EC observed in both caves also differ remarkably between these SGDs (Fig.23). Steady decline of EC in Altug cave seems to be related to rainfall events while, in Mivini cave, such a relationship is not clearly defined. This situation is may be related to the different types of freshwater recharge mechanisms existing in these caves. Temporal variation of EC in Altug and Mivini caves implies the existence (or dominance) of diffuse and conduit type karstic recharge systems, respectively.

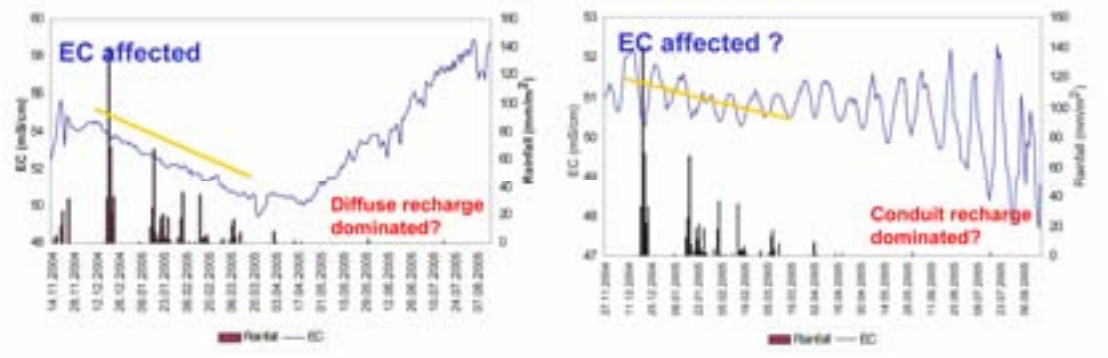

FIG.23. Temporal variation of rainfall and EC in selected SGD sites (left: Altug cave, right: Mivini cave).

We define the moon tide as the sea level rise that occurs due to increasing gravitation attraction of moon. This attraction becomes more severe during the “new moon” and “full moon” periods (spring tides). Figure 24 shows that moon tides are apparently related to elevated EC in Mivini cave whereas

no clear relationship exists in Altug cave. The difference between the EC response of these caves and the moon tide seems to be related to the different types of karstic feed systems. Diffuse and conduit feed systems are more and less resistant to changes in head gradient such as, sea level rise. Therefore, the apparent EC variations in Mivini cave could be related to rapid invasion of seawater into these conduits in this SGD while, in Altug cave, intrusion of seawater into diffuse flow system can not be achieved due to insufficient head gradient imposed by sea level rise.

An overall evaluation of above observations indicates the presence of spatio–temporally complicated flow dynamics in karstic SGDs. The information obtained from temporal logger data is remarkable in view of understanding the behavior of different SGDs. Isotopic data to be collected in line with temporal physico–chemical observations will certainly be of great value in future research attempts.

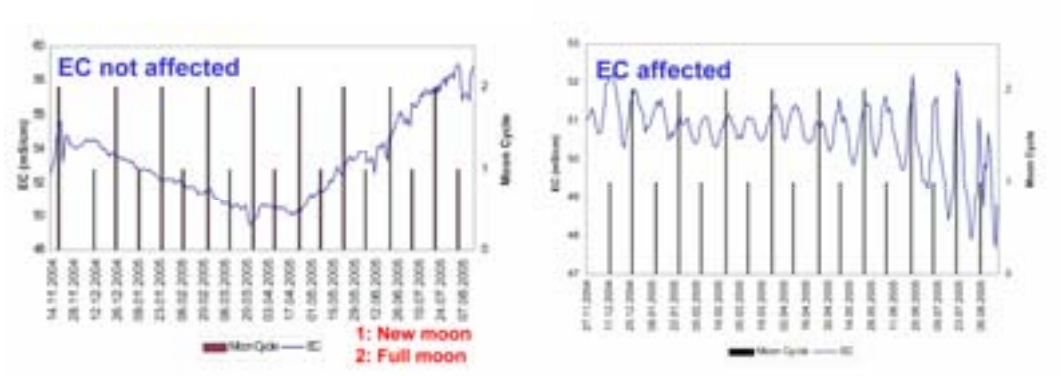

FIG.24. Temporal variation of moon tide and EC in selected SGD sites (left: Altug cave, right: Mivini cave).

15. Conclusions and Suggestions

Major conclusions of this study are summarized below.

- Majority of karstic SGDs are point-wise outflows rather than really homogenous discharges. Determination of the exact location of karstic SGDs requires considerable effort. Although, satellite (thermal and infrared) and lineament (geological ground truth) data are helpful in detecting karstic SGD spot, search dives are inevitable. Many of the SGDs discovered in this study were found by means of systematic search dives. The discovered karstic SGD spots of this study are limited to sportive diving depth (30 m below sea level). Searching deeper SGDs requires use of ROVs (remotely operated vehicles).
- Stable isotopic (^{18}O and ^{2}H) data is quite useful in determining the rate of seawater contribution in karstic SGDs. Though, electrical conductivity (EC) alone can also be used for this purpose, stable isotopes provide additional information on the initial fresh groundwater end member. Timing and altitude of recharging precipitation can easily be determined from stable isotope data.
- In a similar manner, tritium is probably the unique and reliable source of residence time information for the fresh groundwater end member.
- Due to relatively high hydraulic conductivity of karstic systems, hydrodynamics of karstic SGDs are spatio–temporally variable. The seawater contribution rate to an individual karstic SGD may show remarkable fluctuation even within a day. Use of temporally high resolution dataloggers is strongly advised in studying the dynamics of karstic SGDs. Development of automatic sampling devices that are triggered by datalogger signals would help producing invaluable physico–chemical and isotopic data which can help better understanding of karstic SGDs.
- In this study, karstic SGDs are found to respond in different ways to external forcings. Depending on the nature of karstic network that feed an individual SGD, the physico–chemical and isotopic

composition of outflow may or may not be affected by a given external forcing such as, sea tide, moon tide and a rainfall event.

ACKNOWLEDGEMENTS

Authors gratefully acknowledge the extensive contribution of members of Underwater Research Society–Cave Diving Group (SAD–MADAG) to the field studies. Dive explorations have been supported financially by TUBITAK under grant number 103Y025.

RADON AS A TRACER OF SUBMARINE GROUNDWATER DISCHARGE

W.C. Burnett

Department of Oceanography
Florida State University
Tallahassee
United States of America

Abstract. Submarine groundwater discharge (SGD) of groundwater into the coastal zone has received increased attention in the last few years as it is now recognized that this process represents an important pathway for material transport. Assessing these material fluxes is difficult, as there is no simple means to gauge the water flux. To meet this challenge, we have explored the use of a continuous radon monitor to measure radon concentrations in coastal zone waters over time periods from hours to days. Changes in the radon inventories over time can be converted to fluxes after one makes allowances for tidal effects, losses to the atmosphere, and mixing with offshore waters. If one assumes that advective flow of radon-enriched groundwater (pore waters) represent the main input of ^{222}Rn in the coastal zone, the calculated radon fluxes may be converted to water fluxes by dividing by the estimated or measured ^{222}Rn pore water activity. We have also used short-lived radium isotopes (^{223}Ra and ^{224}Ra) to assess mixing between near-shore and offshore waters in the manner pioneered by Moore. During an experiment in the coastal Gulf of Mexico, we showed that the mixing loss derived from the ^{223}Ra gradient agreed very favorably to the estimated range based on the calculated radon fluxes. This allowed an independent constraint on the mixing loss of radon – an important parameter in the mass balance approach. Groundwater discharge was also estimated independently by the radium isotopic approach and was within a factor of two of that determined by the continuous radon measurements and an automated seepage meter deployed at the same site.

1. Introduction

Although not as obvious as river discharge, continental groundwaters also discharge directly into the sea. In spite of the fact that submarine springs and seeps have been known for many years (e.g., written accounts exist from at least the Roman period), these features have traditionally been perceived as hydrologic 'curiosities' rather than objects for serious scientific investigation [1]. However, this perception is changing. Within the last two decades recognition has emerged that, at least in some cases, submarine groundwater discharge (SGD) may be both volumetrically and chemically important [2]. Although SGD may not play a significant role in the global water balance, there are reasons to believe that the geochemical cycles of some major and minor elements may be strongly influenced either by the direct discharge of fresh groundwater into the sea or by chemical reactions that occur during the recirculation of seawater through a coastal aquifer system [3,4]. In addition, it is now recognized that groundwater discharge may be an important pathway for diffuse pollution to the coastal zone where coastal aquifers have become contaminated by septic systems or other pollution sources [5].

SGD is not simple to evaluate, as it tends to be patchy, both spatially and temporally. Water balance approaches can be used but these tend to give only average long term results and are not very precise as the magnitude of SGD is often about the same as the uncertainty in the water balance parameters. Perhaps one of the most promising approaches for regional-scale assessments of SGD is the use of geochemical tracers. The coastal water column tends to integrate natural tracers coming into the system via groundwater pathways. Thus, smaller-scale variations, which would not be of interest for regional studies, are smoothed out. The small-scale variability found in many coastal systems has been one of the serious drawbacks concerning the use of seepage meters, a device that provides direct measurements of SGD [6,7].

We present here our approach for evaluating nearshore SGD via continuous ^{222}Rn measurements. We also compare these results using a completely independent assessment via short- and long-lived

radium isotopes as described by Moore [8]. An automatic seepage meter, similar to the type described by Taniguchi & Fukuo [9] was also deployed in the field area for a further comparison.

2. Tracing Groundwater Using ^{222}Rn

2.1. Radon as an SGD tracer

Although interest in groundwater–surface water interaction has increased dramatically in the last few years, there is actually very little documentation available. One of the principal reasons that information is so limited is because groundwater discharge is so difficult to measure. Traditional hydrogeological or water balance estimates may be off by several orders of magnitude, largely because of difficulties in constraining hydrologic conductivities. One potential means of evaluating groundwater pathways and fluxes into the coastal zone more accurately is through the use of natural tracers. We have been investigating this approach for several years and demonstrated that ^{222}Rn is an excellent tracer [10–12]. The very large enrichment of ^{222}Rn concentration in groundwaters over surface waters (typically 1000-fold or greater), its unreactive nature, and short half-life ($t_{1/2}$ = 3.83 d) make ^{222}Rn an excellent tracer to identify areas of significant groundwater discharge.

2.2. Measurement approach

In spite of the fact that we have made significant progress in our ability to find and measure groundwater seepage areas using a radon monitoring approach, we are hampered in making regional-scale and long term temporal assessments by the time consuming logistical requirements of collecting and analyzing samples in the conventional manner. Historically, measurements of radon concentrations in the water column have been accomplished by standard oceanographic sampling and analysis techniques (radon emanation) for measurement of ^{222}Rn taking the special care required for trace gas sampling [13,14]. Alternatively, more automated systems may be applied in order to increase the sampling resolution and efficiency of the process. We demonstrated recently that a "continuous" radon monitor could provide reasonably high resolution data on the radon concentration of coastal seawater at one location over time [15].

The automated radon system (Fig.1) analyses ^{222}Rn from a constant stream of water (driven by a submersible pump) passing through an air–water exchanger that distributes radon from a running flow of water to a closed air loop. The air stream is fed to a commercial radon-in-air monitor that determines the concentration of ^{222}Rn by collection and measurement of the α–emitting daughters, ^{214}Po and ^{218}Po. Since the distribution of radon at equilibrium between the air and water phases is governed by well known temperature dependence, the radon concentration in the water is easily calculated.

We are using a RAD–7 (Durridge Co., Inc.) for the radon-in-air monitor because it is portable, durable, very sensitive, and operates in a continuous mode. The RAD–7 uses a high electric field with a silicon semiconductor detector at ground potential to attract the positively charged polonium daughters, $^{218}Po^{+}$ ($t_{1/2}$ = 3.10 min; alpha energy = 6.00 MeV) and $^{214}Po^{+}$ ($t_{1/2}$ = 164 μs; 7.67 MeV) that are then counted as a measure of the radon concentration in air. Energy discrimination allows one to select either or both the ^{218}Po or ^{214}Po windows for ^{222}Rn assessment. For faster analyses, the ^{218}Po is preferred, as it will reach radioactive equilibrium with ^{222}Rn in only about 15 minutes. The ^{214}Po lags behind because of the intermediate beta–emitting daughters, ^{214}Pb ($t_{1/2}$ = 27 min) and ^{214}Bi ($t_{1/2}$ = 19.9 min) resulting in an equilibration time of approximately 3 hours.

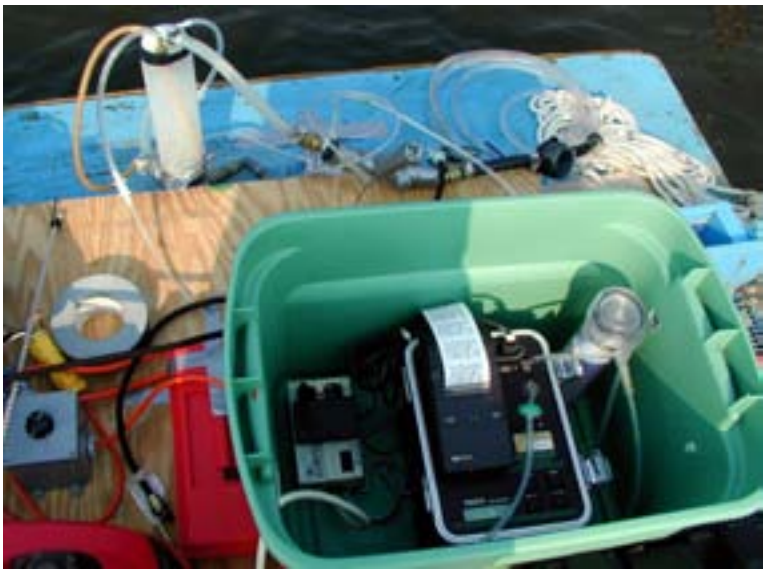

FIG.1. Photo of the water exchanger – RAD–7 continuous monitoring system.

The water–air exchanger is simply a plastic cylinder that has water pumped from the desired water depth entering continuously via an aspirator and a stream of air that is recirculated through a bed of desiccant and then to the RAD–7 for ^{222}Rn measurements. After some time, the radon concentration in the air reaches equilibrium with the radon in the water, the ratio at equilibrium being determined by the water temperature:

$$a' = 0.105+0.405e^{-0.0502T} \quad (1)$$

where a' is the concentration ratio of water to air (about 1:4 at room temperature), and T is the temperature of the water in °C.

The response time of the system depends on the half-life of the ^{218}Po, the volume of the air loop, the speed of transfer of radon from the water to the air (which depends on the efficiency of the aeration, and the speed of the pump), the flow rate of the recirculating air, the volume of water in the exchanger, and the flow rate of water to the exchanger [16]. The half-life of ^{218}Po, 3.1 min, dictates an ultimate theoretical limit, for the 95% response time, of about 15 min, assuming everything else was instantaneous. Since there is about four times more radon in the air phase than the aqueous phase at equilibrium, at least four times more water must flow through the system to deliver all the radon that is required. Again, that is assuming everything is working at maximum efficiency, which is unlikely. In practice, we find that the shortest time necessary for complete equilibration is about 30 – 40 minutes. Once the equilibrium concentration has been obtained, the length of time necessary to collect sufficient information (counts) for a precise measurement depends upon the radon content in the water. In several tests with our system, we find that integration times of about 1 – 2 hours are necessary to achieve uncertainties of 5 – 10%.

2.3. Conceptual model and approach for radon tracing

The main principle of using continuous radon measurements to decipher rates of groundwater seepage is that if we can monitor the inventory of ^{222}Rn over time, making allowances for losses due to atmospheric evasion and mixing with lower concentration waters offshore, any changes observed can be converted to fluxes (Fig.2).

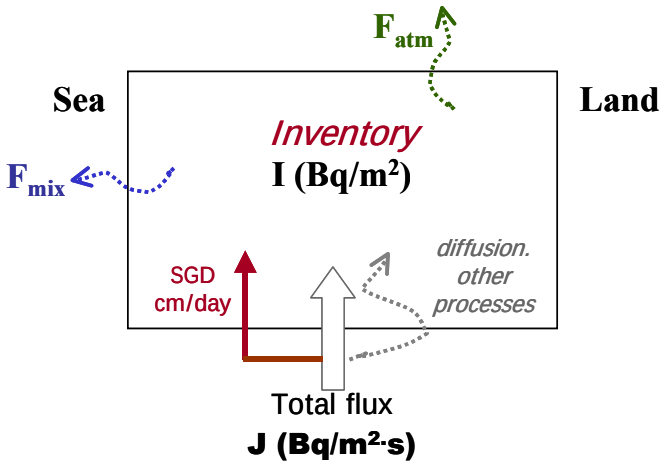

FIG.2. Conceptual model of use of continuous radon measurements for estimating submarine groundwater discharge in a coastal zone. The inventory refers to the total amount of excess ^{222}Rn per unit area. Decay is not considered because the fluxes are evaluated on a very short (1–2 hour) time scale relative to the half-life of ^{222}Rn.

Although changing radon concentrations in coastal waters could be in response to a number of processes (sediment resuspension, long shore currents, etc.), we feel that advective transport of groundwater (pore water) through sediment of Rn–rich solutions is usually the dominate process. Thus, if one can measure or estimate the radon concentration in the advecting fluids, we can easily convert ^{222}Rn fluxes to water fluxes. Our complete procedure for estimating groundwater fluxes from continuous radon measurements in the coastal zone may be summarized by the following steps:

(1) We first perform continuous measurements of ^{222}Rn activities (Bq/m^3) in the coastal water column, water depth, water and air temperatures, wind speed, and atmospheric ^{222}Rn concentrations. All of these measurements may be performed using automated sensors with data logging capabilities.

(2) We then calculate excess (unsupported by ^{226}Ra) ^{222}Rn inventories for each measurement interval, i.e.,

$$I\ (Bq/m^2) = Excess^{222}Rn\ (Bq/m^3) \times \text{water depth (m)} \quad (2)$$

$$Ex^{222}Rn\ (Bq/m^3) = \text{total}\ ^{222}Rn - ^{226}Ra\ (Bq/m^3) \quad (3)$$

(3) $Excess^{222}Rn$ activities in the water column are estimated from spot measurements of ^{226}Ra. While fewer measurements of ^{226}Ra are made, the water column variations tend to be less than those of radon and the activities are typically much less.

The calculated inventories are next normalized to mean tidal height to remove the effect of changing inventory due simply to tidal height variations. This normalization is done for each measurement interval by multiplying the unit change in water depth (m) over the measurement interval times the ^{222}Rn activity offshore (Bq/m^3) during the flood tide and by concentrations in nearshore waters for the ebb tide. The flood tide corrections are negative (since the inventory would be increasing due simply to an increase in water depth) and the ebb tide correction is positive.

(4) We next correct the tide normalized inventories for atmospheric evasion losses during each measurement interval. The total flux across the air–water interface depends on the molecular diffusion produced by the concentration gradient across this interface and turbulent transfer, which is dependent on physical processes, primarily governed by wind speed. We have used

the equations presented by Macintyre et al. [17] and Turner, et al. [18] that relate gas exchange across the sea–air interface to the gradient in the trace gas concentration, temperature, and wind speed. After these calculations, the radon water column inventories have now been corrected for supported ^{222}Rn (^{226}Ra), changes in water level, and atmospheric loss. We call these corrected inventories I^* (Bq/m^2).

(5) 'Net' ^{222}Rn fluxes (F_{net}) are then estimated by evaluating the change in these corrected inventories (Bq/m^2) over each time interval (Δt, generally 1 – 2 h), i.e.,

$$F_{net}(Bq/m^2 \cdot s) = \Delta I^*(Bq/m^2)/\Delta t(s) \quad (4)$$

These fluxes represent the observed fluxes of ^{222}Rn into the coastal water column with all necessary corrections except loss via mixing with lower concentration waters offshore. We thus feel that these net fluxes are minimum values, as we base the estimate on what remains in the system (what we can measure) and higher mixing rates could be compensated for by higher fluxes.

(6) We then estimate minimum mixing losses from inspection of the 'net' fluxes over time. We base these values on the maximum negative fluxes that are invariably present. Since greater mixing losses could be compensated by higher benthic radon fluxes, our estimates must be conservative. The estimated mixing losses are added to the net fluxes in order to derive 'total' Rn fluxes (F_{total}), i.e.,

$$F_{total}(Bq/m^2 \cdot s) = F_{net} + F_{mix}(Bq/m^2 \cdot s) \quad (5)$$

We have not considered diffusion in these flux estimates because the advection term in every coastal system we have investigated has been dominant (factors of about 20–100 times greater than estimated diffusion). If one were working in an environment where diffusion may be more important, an advective–diffusion equation as presented in Cable et al. [11] could be applied.

(7) In order to convert radon flux estimates to water flux, we must measure or estimate the ^{222}Rn concentration of the advecting fluids. In areas where slow seepage through sediment is the dominant process, it is a relatively simple matter to extract pore waters and measure ^{222}Rn and/or perform sediment equilibration measurements [19]. If an area is characterized by inputs of fresh groundwater (from submarine springs, for example), one could measure the groundwater ^{222}Rn activities via collection from monitor wells on shore. Because of processes like tidal pumping, possible non-homogeneous sediment compositions, and the possible influence of different source terms (multiple aquifers, etc.) within a study region, there could be significant variation in the radon concentration term.

(8) Finally, we convert to water fluxes (ω, m/s) by dividing the estimated total ^{222}Rn fluxes (Bq/m^2·s) by the concentration of excess ^{222}Rn ($Ex\ ^{222}Rn_{pw}$, Bq/m^3) in the fluids entering the system, i.e.,

$$\omega(m/s) = \frac{F_{total}}{Ex^{222}Rn_{pw}} \quad (6)$$

We often apply unit conversions to express the groundwater fluxes in cm/day, as these units are convenient – typically in the range of 10–100 cm/day (1.16×10^{-6} – 1.16×10^{-5} m/s).

3. Application – Coastal Gulf of Mexico

3.1. Radon results

We installed the continuous radon monitor into the seawater recirculation system at the Florida State University Marine Laboratory (FSUML) from September 28 to October 3, 2001. This is a site located along an open shoreline within Apalachee Bay, about 60 km south of Tallahassee, Florida. The exchanger, set up inside the laboratory, received a continuous stream of water from the seawater system that has an intake about 300 m offshore in about 1.5 m of water. The residence time of the seawater in this pumping system is approximately two hours. This was taken into account when comparing automated radon data to parameters measured offshore. Previous studies at this site included collection and conventional radon analysis of grab samples of seawater from the same place and time as the continuous monitor with results within the analytical uncertainty of those provided by the continuous monitor [7]. The water depth was continuously monitored at the same location using an ultrasonic depth recorder, so we were able to produce a continuous record of ^{222}Rn inventory as well as concentration over time (Fig.3).

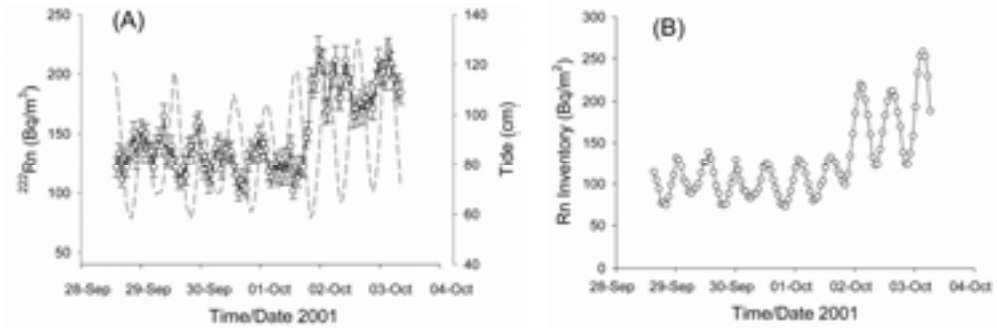

FIG.3. (A) Variation of total ^{222}Rn activities; and (B) excess ^{222}Rn inventories in coastal waters off the FSU Marine Laboratory (FSUML) from 28 September to 3 October 2001.

We also continuously monitored wind speed, air and sea temperatures, and atmospheric radon concentrations over the experimental period. A Taniguchi–style automated seepage meter was deployed within a few metres of the seawater intake. In addition, on one day (2 October) we collected a series of seawater samples (n = 12 at 9 stations) along a transect normal to the shoreline just off FSUML out to a distance of 5 km offshore. These samples were analyzed for ^{222}Rn (radon emanation) and radium isotopes (delayed coincidence counting for ^{223}Ra and ^{224}Ra [20] and gamma spectrometry for ^{226}Ra and ^{228}Ra). This 5-day multitracer experiment is part of a seasonal sampling of this environment that will be reported in more detail elsewhere (Dulaiova, in prep.).

After normalizing to a mean tidal height and correcting for supported radon and estimated atmospheric loss, we calculated the net ^{222}Rn fluxes (Fig.4). These fluxes are clearly not in steady state but fluctuate with an apparent period of approximately 12 hours, most likely a reflection of the mixed, semi-diurnal tides in this region. Apparent negative fluxes also occur with a fairly systematic period, either 24 or 12 hours apart. The dashed line shown in Fig.4 is our estimate (thought to be conservative) of the mixing loss of radon caused by mixing of nearshore (high radon) waters with offshore (low radon) seawater. These estimated mixing losses are added to the 'net' fluxes in order to determine the approximate 'total' radon flux into the coastal zone at the point of sampling.

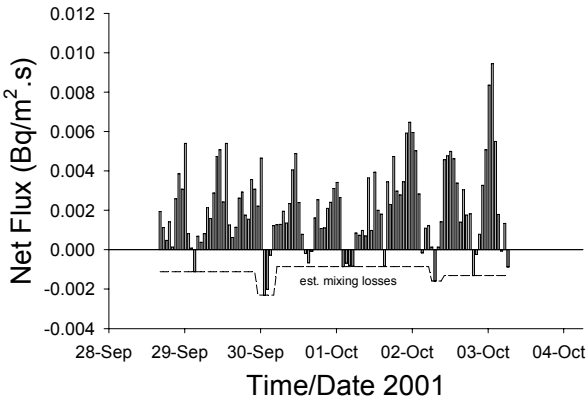

FIG.4. Net radon flux vs. time based on continuous radon measurements at FSUML from 28 September to 3 October 2001.

We have observed this tidal period cyclicity before; both in this region [21] and elsewhere (south of Perth, Australia, for example, we observed a 24-h cycle that corresponded to the diurnal tides in that area). Most likely, groundwater, and associated radon, is responding to: (1) lower hydrostatic pressure at low tides causing increased seepage and thus higher radon fluxes; (2) recirculated seawater is moving through the shallow aquifer and sediments in response to tidal pumping; and/or (3) a combination of both processes. Assuming that the hydraulic gradient is more or less constant during the time scale of our experiment, a decrease in hydrostatic pressure with a lower tide could result in increased seepage (and thus higher radon). Although there are some exceptions in this experiment, most of the peaks in radon concentration occur at the lowest tides (Fig.3a). Tidal pumping and wave set up are known to result in the infiltration of seawater on the high tide with draining on the low tide [22,23]. Since draining typically is slower than filling a coastal aquifer, the waters emerging may well have had a residence time quite a bit longer than the tidal cycle. This would also explain how the recirculated seawater, initially low in radon and short-lived radium isotopes, builds up higher concentrations that are detected by our measurements.

We estimated the relevant ^{222}Rn concentration within the interstitial fluids (2170± 830 Bq/m^3) by performing sediment equilibration experiments from sediments collected in the area (n = 6) in the manner described by Corbett et al. [19]. These measurements are performed in the laboratory by reacting water and sediment for a period long enough that the ^{222}Rn in the fluid reaches a steady state concentration. Dividing the total estimated radon fluxes (Bq/m^2·s) by the presumed ^{222}Rn activity of the advecting fluids (2170 Bq/m^3) for each time interval (1 hour in this experiment) results in estimated water fluxes over this 5-day period (Fig.5).

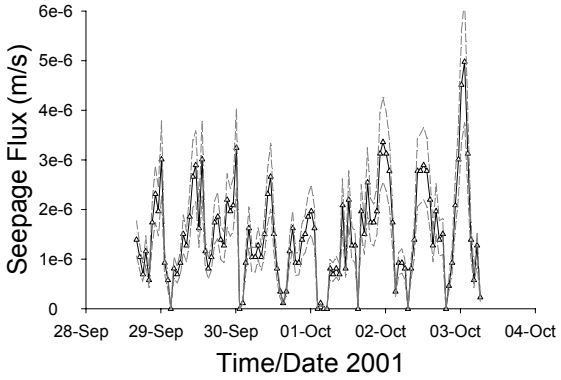

FIG.5. Estimated seepage rates over the experimental period based on the radon model and using a pore water radon concentration of 2170 Bq/m^3. The dashed gray lines above and below the SGD estimates (open triangles) represent ±25% uncertainties.

Our estimated specific discharges ranged from 0 – 5.0×10^{-6} m/s (0 – 43 cm/day; average = 13±9 cm/day; n = 111). The data again displays the 12–hour periodicity reflecting the radon flux pattern. The zero fluxes are a consequence of our choice of using the maximum negative fluxes as our estimate of mixing losses. Adding these values to the net fluxes produces an apparent interval with essentially zero radon flux and thus no water flux. More realistically, these mixing losses are underestimated and there are probably some, perhaps low, seepage rates all the time.

Using daily (24 h) integrated estimated seepage rates from these calculations and assuming this rate is characteristic of the groundwater fluxes for a 200-m band, we estimate the discharge per unit length of shoreline at 2.3 – 3.4×10^{-4} $m^3/m\cdot s$ (20 – 29 $m^3/m\cdot day$). The width of the dominant seepage in this area has been determined in previous studies [21,24]. Although the specific seepage rates are not uniform but tend to decrease more-or-less exponentially as one goes further from shore, our assumption of constant rates is reasonable in this case as the rates are based on radon measurements in the water column that should integrate these small-scale variations.

3.2. Radium isotope results

We collected a line of samples at 9 stations (3 duplicate samples, so n = 12) extending from just offshore out to approximately 5 km offshore and then measured the activities of both the short-lived (^{223}Ra and ^{224}Ra) and long-lived (^{226}Ra and ^{228}Ra) isotopes of radium. Because radium is found at very low concentrations in most natural waters, large volume samples (0.02 to 0.20 m^3) were processed through 'Mn–fibre' cartridges to concentrate the radium [25]. The isotopic measurements of ^{223}Ra and ^{224}Ra were made within 24 hours after collection using delayed coincidence counters and the ^{228}Ra and ^{226}Ra measurements were made at a later date via gamma-ray spectrometry.

The distribution of the short-lived radium species will depend on two processes, decay and mixing. Since the decay rates are known precisely (^{223}Ra and ^{224}Ra have half-lives of 11 and 3.5 days, respectively), the mixing rates can be estimated based on the slope of the Ln activity versus distance plot (Fig.6a).

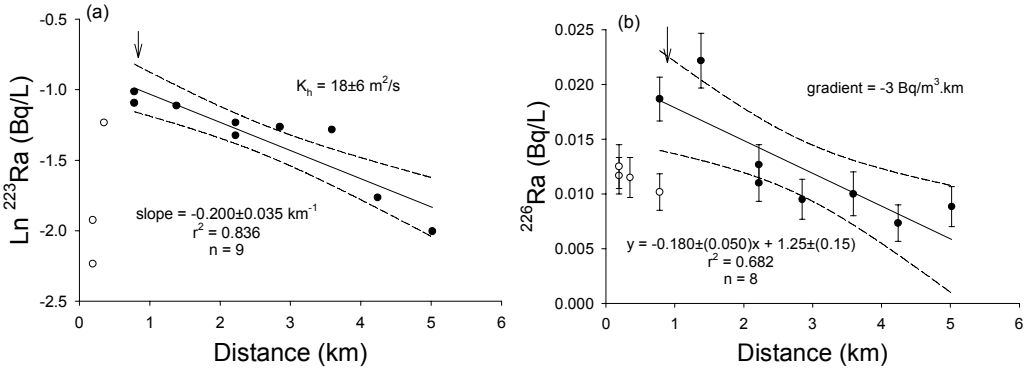

FIG.6. (A). Variation of Ln ^{223}Ra versus distance offshore from the FSU Marine Laboratory, October 2, 2001. The mixing coefficient (K_h) is calculated from the slope of the regression line (filled circles). It is assumed that most of the radium enters near the maximum in the ^{223}Ra (station T-3; ~800 m offshore), perhaps from a submarine spring (approximate location shown by arrow), and mixes with lower concentration waters offshore. (B) ^{226}Ra vs. distance along the same transect as 'A'. The gradient is calculated from the maximum concentration extending offshore (closed data points). The arrow indicates the approximate position of a submarine spring.

We observed a maximum in ^{223}Ra at one of our stations, about 800 m offshore, that may be related to a submarine spring known to occur in that vicinity. Using the methodology of Moore [8], a regression of all data points from the maximum in ^{223}Ra seaward (n = 9) provides an estimated

mixing coefficient of 18±6 m^2/sec. Multiplying the gradient in the measured ^{226}Ra concentration over the same distance (–3 Bq/m^3·km; Fig.6b) by this mixing term provides the offshore flux of the groundwater tracer ^{226}Ra (0.12 Bq/m·s) for a cross section 1 m wide and 2.2 m deep (the average depth of the stations along the transect). Since ^{226}Ra is long-lived (half-life = 1600 years), mixing is the only process that effects its distribution. Assuming that this flux is steady state and balanced by the inflow of groundwater with a known ^{226}Ra concentration, one can easily convert the radium flux to a SGD flux.

While we appear to have fairly good estimates of the offshore mixing and radium flux, the concentration of ^{226}Ra in the groundwater coming into the system is less clear. The data suggest the presence of a submarine spring that is adding radium, and perhaps radon, to the system. The distribution of ^{222}Rn offshore does not show a clear maximum at the point where all the radium isotopes do but is highest inshore (where seepage is likely the highest). Thus while the spring would be expected to be adding radon to the system as well as radium, it may not have a substantially different concentration of ^{222}Rn than waters seeping through the sediments near the shore. Thus, we appear to have a mixed source of radium at this site, seepage through permeable sediments and from the small submarine spring in the area.

Similar measurements were performed about 1 km east of this study in August 2000 [21]. In that study, we observed no indications of spring inputs but there was clearly substantial seepage. Moore estimated SGD in that case using a ^{226}Ra concentration of 15 Bq/m^3 that was based on a measurement of water collected from a fast-flowing seepage meter at that study site. While that was a completely reasonable assumption in that case, the incoming water in the October 2001 experiment (at a nearby but different location) must have a higher concentration for these measurements, as some of the water column measurements exceed 17 Bq/m^3. We examined samples collected and analyzed for ^{226}Ra in shallow piezometers at this site in order to estimate a reasonable concentration for the groundwater. Unfortunately, the range in ^{226}Ra varies tremendously. Using data from Christoff [26], we see a range from 10 to 1453 Bq/m^3 (n = 19 samples in 14 different piezometers) with an average of 387 Bq/m^3. Since this average is skewed by a few very high values, we have elected to use the median concentration, 235 Bq/m^3 as an estimated ^{226}Ra activity in shallow groundwater at this site. Using this value, we calculate that the water flux into this area was about 5.0×10^{-4} m^3/m·s, i.e., a flow of approximately 43 m^3 of groundwater into the sea per unit metre of shoreline per day.

3.3. Comparison of SGD estimates

One of the benefits in applying both the continuous radon and radium isotope approaches to the same system is that we can use the mixing coefficient derived from the short-lived radium to make an independent estimate of the radon loss due to mixing. We have considered that term to be a weak link in the radon SGD assessment. We estimated the total radon flux offshore by multiplying the gradient in the ^{222}Rn concentration along the inshore-to-offshore transect (–9.4 Bq/m^3·km) by the mixing coefficient derived from the ^{223}Ra gradient (18 m^2/s) and the average depth along the transect (2.2 m). This total ^{222}Rn flux per unit width of shore (0.36 Bq/m·s) is also the flux coming from a cross section 1 m wide and 2.2 m deep. Converting this value to a per unit seabed flux for an assumed 200 m wide seepage area results in a unit flux of 1.8×10^{-3} Bq/m^2·s. This compares very favorably to our variable mixing fluxes, assigned by inspection of the 'net' benthic ^{222}Rn fluxes (Fig.4) that ranged from 8.3×10^{-4} – 2.3×10^{-3} Bq/m^2·s with an average of 1.1×10^{-3} Bq/m^2·s. If we had instead used a fixed mixing loss of 1.8×10^{-3} Bq/m^2·s for the entire period of our observations, the average calculated seepage flux would only increase by about 20%.

A comparison of these estimates, both for the August 2000 study as well as the one presented here for October 2001 is given in Table 1.

TABLE 1. ESTIMATES OF WATER FLUX PER UNIT WIDTH OF SHORELINE NEAR FSUML DURING AUGUST, 2000 AND OCTOBER, 2001. THE AUGUST EXPERIMENT WAS PERFORMED ABOUT 1 km EAST OF THE ONE IN OCTOBER. THE MIXING COEFFICIENTS BASED ON ^{223}Ra ARE ALSO SHOWN.

Approach	August 2000 $\times 10^{-4}$ m^3/m·s	October 2001 $\times 10^{-4}$ m^3/m·s
Continuous Radon	2.9 – 4.2	2.3 – 3.4
Radium Isotopes	2.6*	5.0
(Mixing coefficient)	(2.6 m^2/s)	(18 m^2/s)
Automatic seepage meter	3.0**	1.4 – 2.3

*August 2000 measurements by W. Moore, reported in Burnett et al. [21]
**Measurements in August 2000 by M. Taniguchi, reported in Burnett et al. [21]

All three approaches, continuous radon, radium isotopes, and automated seepage meters, produced comparable results in the August 2000 study. In October 2001, the radon measurements indicated similar, but slightly higher rates of flow ($(2.3 – 3.4)\times10^{-4}$ m^3/m·s or 20 – 29 m^3/m·day) than those calculated from the automated seepage meter ($(1.4 – 2.3)\times10^{-4}$ m^3/m·s or 12 – 20 m^3/m·day). Both the radon and seepage meter measurements indicated that the flow was not actually steady state but displayed systematic variations related to the semi-diurnal tides in the area. The estimate based on radium isotopes (5.0×10^{-4} m^3/m·s or 43 m^3/m·day) indicates a flow about a factor of two greater. Because of the apparently mixed sources of radium isotopes into this area, and the wide range in possible ^{226}Ra values in the discharging fluids, there is clearly a fairly high degree of uncertainty concerning this estimate. The August 2000 study, located nearby but at a site apparently not influenced by springs, showed better agreement.

It should be pointed out that all the approaches used in this study measure total flow, i.e., seepage meters and the geochemical tracers applied here do not distinguish between flow driven by terrestrial processes (hydraulic gradient) and recirculated seawater driven by oceanic forcing (tidal pumping, wave set up, etc.). Since there could be many management scenarios where it would be useful to differentiate the source of flow, efforts should be made to quantify the terrestrial versus marine based flows. Coupling isotopic techniques for assessing groundwater flow through the seabed with high precision conductivity measurements should allow one to differentiate between fresh groundwater and recirculated seawater. Other approaches and perhaps tracers will be necessary if the terrestrial groundwater is not fresh.

ACKNOWLEDGMENTS

The author wishes to acknowledge the support from the International Atomic Energy Agency (IAEA) through their Cooperative Research Project (CRP) entitled Nuclear and Isotopic Techniques for the Characterization of Submarine Groundwater Discharge (SGD) in Coastal Zones. I also thank the additional support received from the Intergovernmental Oceanographic Commission (IOC) and the International Hydrologic Program (IHP) of the UNESCO.

REFERENCES

[1] KOHOUT, F.A., Submarine springs: A neglected phenomenon of coastal hydrology, Hydrology, **26** (1966) 391–413.
[2] JOHANNES, R.E., The ecological significance of the submarine discharge of groundwater, Mar. Ecol. Pro. Ser. **3** (1980) 365–373.

[3] ZEKTZER, I.S., IVANOV, V.A., MESKHETELI, A.V., The problem of direct groundwater discharge to the seas, J. Hydrol. **20** (1973) 1–36.
[4] MOORE, W.S., The subterranean estuary: A reaction zone of groundwater and sea water, Mar. Chem. **65** (1999) 1–24.
[5] BUDDEMEIER, R.W., Groundwater flux to the ocean: definitions, data, applications, uncertainties, In: Buddemeier, R.W. (ed), Groundwater Discharge in the Coastal Zone Proceedings of an International Symposium, LOICZ IGBP LOICZ/R&S/96-8, iv+179pp, LOICZ, Texel, The Netherlands (1996) 16–21.
[6] LEE, D.R., A device for measuring seepage flux in lake and estuaries, Limnol. Oceanogr. **22** (1977) 140–147.
[7] BURNETT, W.C., TANIGUCHI, M., OBERDORFER, J., Measurement and significance of the direct discharge of groundwater into the coastal zone, J. Sea Res. **46** 2 (2001) 109–116.
[8] MOORE, W.S., Determining coastal mixing rates using radium isotopes, Cont. Shelf Res. **20** (2000) 1995–2007.
[9] TANIGUCHI, M., FUKUO, Y., Continuous measurements of groundwater seepage using an automatic seepage meter, Ground Water **31** (1993) 675–679.
[10] BURNETT, W.C., CABLE, J.E., CORBETT, D.R., CHANTON, J.P., Tracing groundwater flow into surface waters using natural ^{222}Rn, In: Buddemeier, R.W. (ed), Groundwater Discharge in the Coastal Zone, Proceedings of an Int. Symp., LOICZ IGBP. LOICZ/R&S/96–8, iv+179pp, LOICZ, Texel, The Netherlands (1996) 22–28.
[11] CABLE, J.E., BURNETT, W.C., CHANTON, J.P., WEATHERLY, G.L., Estimating groundwater discharge into the northeastern Gulf of Mexico using radon-222, Earth Planet. Sci. Lett. **144** (1996) 591–604.
[12] CORBETT, D.R., BURNETT, W.C., CABLE P.H., Tracing of groundwater input into Par Pond, Savannah River Site by Rn-222, J. Hydrol. **203** (1997) 209–227.
[13] BROECKER, W.S., An application of natural radon to problems in oceanic circulation, In: Proc. Symp. Diffusion in the Oceans and Freshwaters, Lamont Geological Observatory, New York (1965) 116–145.
[14] MATHIEU, G., BISCAYNE, P., LUPTON, R., HAMMOND, D., System for measurements of ^{222}Rn at low levels in natural waters, Health Phys. **55** (1988) 989–992.
[15] BURNETT, W.C., KIM, G., LANE-SMITH, D., A continuous radon monitor for assessment of radon in coastal ocean waters, J. Radioanal. Nucl. Chem. **249** (2001)167–172.
[16] LANE-SMITH, D., SHEFSKY, S., Proceedings of the American Association of Radon Scientists and Technologists, Las Vegas, Nevada, November 7–10 (1999).
[17] MACINTYRE, S., WANNINKHOF, R., CHANTON, J.P., Trace gas exchange across the air–sea interface in freshwater and coastal marine environments, In: P.A. Matson and R.C. Harriss (eds.) Biogenic Trace Gases: Measuring Emissions from Soil and Water, Blackwell Science Ltd. (1995) 52–97.
[18] TURNER, S.M., MALIN, G., NIGHTINGALE, P.D., LISS, P.S., Seasonal variation of dimethyl sulphide in the North Sea and an assessment of fluxes to the atmosphere, Mar. Chem. **54** (1996) 245–262.
[19] CORBETT, D.R., BURNETT, W.C., CABLE, P.H., CLARK, S.B., A multiple approach to the determination of radon fluxes from sediments, J. Radioanal. Nucl. Chem. **236** (1998) 247–252.
[20] MOORE, W.S., ARNOLD, R., Measurement of ^{223}Ra and ^{224}Ra in coastal waters using a delayed coincidence counter, J. Geophys. Res. **101** (1996) 1321–1329.
[21] BURNETT, W.C., CHANTON, J., CHRISTOFF, J., KONTAR, E., KRUPA, S., LAMBERT,M., MOORE, W.S., O'ROURKE, D., PAULSEN, R., SMITH, C., SMITH, L., TANIGUCHI, M., Assessing methodologies for measuring groundwater discharge to the ocean, EOS **83** (2002) 117–123.
[22] NIELSEN, P., Tidal dynamics in the water table in a beach, Water Resour. Res. **26** (1990) 2127–2134.
[23] LI, L., BARRY, D.A., STAGNITTI, F., PARLANGE J.-Y., Submarine groundwater discharge and associate chemical input to a coastal sea, Water Resour. Res. **35** (1999) 3253–3259.

[24] CABLE, J.E., BURNETT, W.C., CHANTON, J.P., Magnitudes and variations of groundwater seepage into shallow waters of the Gulf of Mexico, Biogeochemistry **38** (1997) 189–205.
[25] MOORE, W.S., Sampling Ra-228 in the deep ocean, Deep Sea Res. **23** (1976) 647–651.
[26] CHRISTOFF, J.L., Quantifying groundwater seepage into a shallow near-shore coastal zone by two techniques, M.S. Thesis, Florida State University (2001) 120p.

ISOTOPE TECHNIQUES FOR ASSESSMENT OF SUBMARINE GROUNDWATER DISCHARGE IN UBATUBA COASTAL AREAS, BRAZIL

J. de Oliveira

Instituto de Pesquisas Energéticas e Nucleares
Centro de Metrologia das Radiações,
Laboratório de Radiometria Ambiental
São Paulo, Brazil

Abstract. We describe here an application of excess ^{222}Rn to estimate submarine groundwater discharge in a series of small embayments of Ubatuba, São Paulo State, Brazil. Excess ^{222}Rn inventories obtained in 24 vertical profiles established from March 2003 to July 2005 varied from $(0.35\pm0.02) \times 10^3$ to $(19\pm5) \times 10^3$ dpm/m^2. The highest inventories of excess ^{222}Rn were observed both in Flamengo and Fortaleza embayments, during summer campaigns (rainy season). The estimated total fluxes required to support inventories measured varied from $(0.06\pm0.01) \times 10^3$ to $(3.4\pm0.9) \times 10^3$ dpm/m^2·d. Considering these results, the submarine groundwater discharge advective rates necessary to balance the sub-pycnocline fluxes calculated in Ubatuba embayments ranged from 0.1×10^{-1} to 1.9 cm/d. Taking into account all fluxes obtained, the percentual variability was 89% (seasonal variation in 3 years period, n = 24 measurements). Although, if we consider each year of study separately, the respective percentual variability estimated are 72% in 2003 (n = 10 measurements), 127% in 2004 (n = 6 measurements) and 97% in 2005 (n = 8 measurements). This work also reports an application of short-lived radium isotopes, ^{223}Ra and ^{224}Ra, to assess residence time and mixing processes of Ubatuba inner shelf waters. This study found that samples collected in June 2000 followed the expected exponential decrease with distance offshore. We assign a dispersion coefficient of 28–39 m^2/s for this study. During January 2002 and November 2003, there was not a consistent decrease of activity with distance offshore. This is likely due to the ruggedness of the coastline where many bays and small islands interrupt simple mixing patterns. To estimate exchange rates during 2002 and 2003, we have used a model based on the decrease in the ^{224}Ra/^{223}Ra activity ratio (AR) with time for samples isolated from fresh inputs of Ra. This model yielded residence times of 1 – 2 weeks for samples collected within 20 km of the coast. We used this residence time to calculate the flux of ^{228}Ra to the study area necessary to maintain the enrichment relative to ocean water. This enrichment is a factor of ten greater than the flux of ^{228}Ra expected from submarine groundwater discharge (SGD) occurring within 50 m of shore.

1. Introduction and Significance

Submarine groundwater discharge (SGD), which includes fresh groundwater and recycled seawater, has been recognized as a widespread phenomenon that can provide important chemical elements to coastal zones, representing an important material flux pathway from land to sea in some areas [1]. It may influence the geochemical cycles of some major and minor elements either by the direct discharge of fresh groundwater into the sea or by chemical reactions that occur during the recirculation of seawater through a coastal aquifer system [2]. Over the past few years, it has been also recognized that groundwater discharge may be a pathway for diffuse pollution to coastal marine systems, where coastal aquifers become impacted by domestic effluents (septic systems and other releases) or other sources of pollution [3,4]. The groundwater flow through coastal marine sediments may be both volumetrically and chemically important [2]. Estimates of global SGD vary widely; some estimates are as high as 10% of the river flow, while most are considerably lower. The SGD fluxes also change with time, due to natural, seasonal and anthropogenic variations in the source functions, such as sea level, tides, rain, permeability, porosity of the bottom sediments or dredging activities.

Natural radionuclides from ^{238}U and ^{232}Th decay series have been applied to trace and to quantify groundwater inputs to the ocean [5–11]. Geochemical tracers, like ^{222}Rn and ^{226}Ra, are advantageous for regional-scale assessments of SGD, because their signals represent values integrated through the water column that removes small-scale variations. These radionuclides are usually enriched in groundwater compared to seawater, can be measured at very low concentrations and are conservative.

This research project has as its main purpose, the application of ^{222}Rn and natural Ra isotopes to trace SGD and evaluate mixing processes into the marine environmental studies performed in a series of small embayments of Ubatuba, São Paulo State. The Ubatuba coastal area is known to be oligo–mesotrophic, because the primary production is limited by the lack of inorganic compounds of nitrogen and phosphorous [12]. The region has been reported to receive nutrient inputs by atmospheric contribution mainly in nitrogenous compounds and in minor degree by terrestrial contribution which limit the local primary production. However, from time to time, intrusions of nutrient and oxygen–rich South Atlantic Central Water (SACW) from the open ocean thermocline may reach the shelf edge, and may further be transferred by coastal upwelling, that is driven by northeasterly winds, providing a third source of nutrients for primary production. However, as a cultural symptom of demographic expansion, waste disposal, domestic and industrial releases, infiltration of septic plumes through the coastline and uncontrolled management of the watersheds, have been affecting these coastal environments, causing eutrophication. For all those reasons, the application of ^{222}Rn and natural Ra isotopes tracer techniques are critical for the assessment of SGD inputs and the future management of groundwater–borne nutrients.

Since 2000, two studies have been carried out in a series of small embayments of Ubatuba, São Paulo State, Brazil. The study site is characterized by fractured granite cliffs descending into the Atlantic Ocean. There is only a thin veneer of coarse–grained sediment that makes up beaches within the numerous bays along the coast.

The November 2003 study was part of a collaborative multinational program designed to investigate submarine groundwater discharge using different techniques tested in different hydrogeologic settings. This intercomparison was sponsored by the Scientific Committee on Oceanic Research (SCOR), the Land–Ocean Interactions in the Coastal Zone (LOICZ), the International Atomic Energy Agency (IAEA), and UNESCO's Intergovernmental Oceanographic Commission (IOC) and International Hydrological Programme (IHP). The primary objective of this last program was an improved understanding of scientific and technical aspects that will enable SGD measurements to be addressed with a higher degree of confidence, including the development and implementation of nuclear and isotopic techniques to assess submarine groundwater discharges. Local benefits of this program extended into the fields of hydrology and coastal oceanography, improving the information already available in São Paulo coastal area.

The development of this project offered an opportunity to better understand groundwater–seawater interactions in the study area, seasonal variations of SGD, the input of pollutants from septic systems and other sources, and allowed a regional assessment of subsurface fluid flow.

2. Geological Setting

This research was carried out in a series of small embayments near Ubatuba, São Paulo State, Brazil. All samples studied here were taken in the selected area between latitudes 23°26'S – 23°46'S and longitudes 45°02'W – 45°11'W, in order to estimate coastal mixing rates and groundwater discharge fluxes (Fig.1).

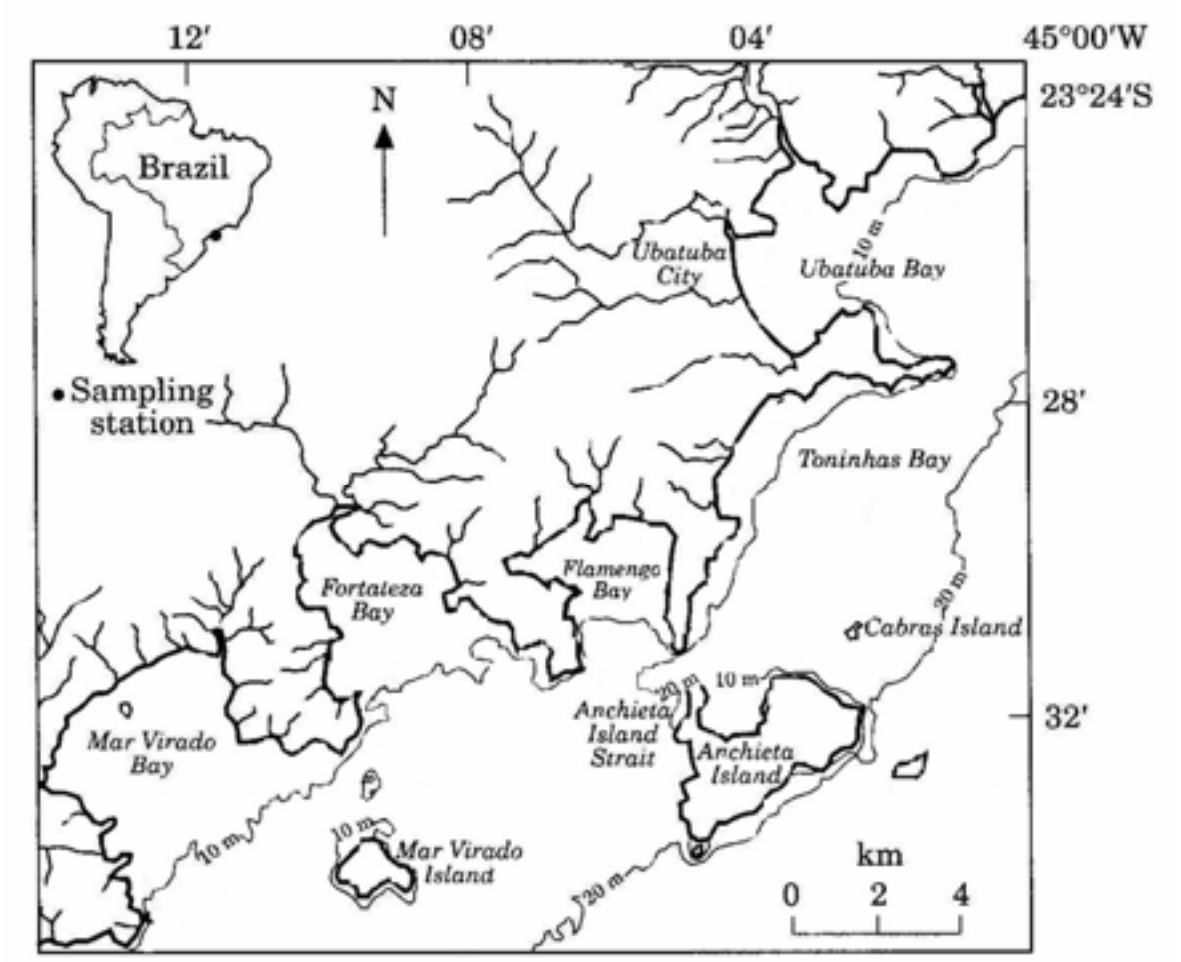

FIG.1. Location of the four embayments studied at Ubatuba coastal area: Flamengo Bay, Fortaleza Bay, Mar Virado Bay and Ubatuba Bay. Ubatuba County is located around 270 km north from São Paulo city, southeast Brazil.

The study area comprises the northernmost part of São Paulo Bight, southeastern Brazil, and is considered a tropical coastal area. The main geologic/geomorphologic feature in the Ubatuba region is the presence of pre-Cambrian granites and migmatites of a mountain chain locally called Serra do Mar (altitudes up to 1,000 metres), which reaches the shore in almost all of the study area and limits the extension of the drainage systems and of Quaternary coastal plains. Wave action is the most effective hydrodynamic phenomenon responsible for the bottom sedimentary processes in the coastal area as well as in the adjacent inner continental shelf [13]. The terrestrial input of sediments is strongly dependent on the rainfall regime, leading to a higher contribution of sediments during summer season. During the summer (November through February), the advance of the South Atlantic Central Water (SACW) over the coast leads to the displacement of the Coastal Water (CW), rich in continental suspended materials, and to the transportation of these sediments to the outer portions of the continental shelf. During winter (May through August), the retreat of the SACW and the decreasing rain restrict the input of sediments from the continental areas. The mean annual rainfall is roughly 1,800 mm, the maximum rainfall rates being observed in February. Sea level varies from 0.5 to 1.5 m, the highest values occurring in months August and September due to greater volume of warm waters of the Brazil Current [14].

In the study area the coastal aquifer system can be classified as a fractured rock aquifer, covered by Pleistocene and Holocene sediments. The discharge pattern of this kind of aquifer is spatially heterogeneous, with preferential flow paths along rock fractures.

In a preliminary study carried out to determine the equivalent concentrations of primordial radionuclides in sediments of the continental shelf off São Paulo, it was found that the content of ^{40}K varied from 0.7% to 2.2%, U from 0.2 ppm to 2.5 ppm and Th from 0.2 ppm to 15 ppm. The $^{234}U/\ ^{238}U$ activity ratio varied from 0.6 to 1.7 [15].

3. Materials and Methods

3.1. Estimating the groundwater discharge using ^{222}Rn as a natural tracer

A potential means of determining groundwater pathways and flux rates into the coastal zone is the application of ^{222}Rn as a natural tracer. The ^{222}Rn levels often found in groundwater are 2 – 4 orders of magnitude higher than those radon levels observed in seawater. Besides that, ^{222}Rn is a natural short-lived radioisotope ($t_{1/2}$ = 3.83 days) and is chemically inert. The radon tracing method is an excellent qualitative tool for identifying areas of spring or seepage inputs in most coastal environments. It can also be a good quantitative tool in shallow marine environments characterized by large amounts of SGD under certain conditions. The approach is particularly sensitive for inner shelf environments when a strong pycnocline is present, as this greatly inhibits radon loss to the atmosphere.

The source of ^{222}Rn in groundwater is from continuous decay of its parent, ^{226}Ra ($t_{1/2}$ = 1620 years), which is present both in the solid and solution phase of an aquifer. ^{226}Ra is part of the ^{238}U decay series, and consequently, is well distributed in sediments and rocks. Some rock types concentrate more ^{226}Ra than others, so the amount of ^{222}Rn produced will be partially based on the distribution of its parent. As ^{226}Ra on or near the surface of mineral grains decays, ^{222}Rn diffuses or is injected into the rock pore waters by recoil processes and becomes part of the solution phase of the aquifer. Concentrations of ^{222}Rn increase as water flows through the aquifer until an equilibrium level (production = decay) is reached which is almost always in great excess of secular equilibrium with its parent isotope, ^{226}Ra. After removal from the aquifer, the primary loss of radon occurs due to decay.

Basically, an assessment of SGD via radon tracing involves 4 steps: (1) measurement of the water column inventory of ^{222}Rn; (2) an accounting of any ^{222}Rn inputs and outputs to the study area by other processes; (3) a calculation of the total input flux of ^{222}Rn to balance the measured inventories (together with any estimated losses); and (4) a calculation, using estimated fluid concentrations for ^{222}Rn and an advection–diffusion model, of the advective transport required to account for the estimated total input flux. A schematic radon mass balance for a coastal environment is shown in Fig.2.

Measurement of the radon concentrations in the water column may be accomplished by standard oceanographic sampling and analysis techniques for measurement of ^{222}Rn taking the special care required for trace gas sampling [16,17]. An analysis of ^{226}Ra, the parent nuclide of ^{222}Rn, is recommended in order to correct for the 'supported' activity of ^{222}Rn, i.e., the amount due to in-growth from the ^{226}Ra dissolved in the water column. Once the concentrations have been determined, ideally as a complete profile through the water column, the inventory is calculated by integrating the excess radon concentrations over water depth.

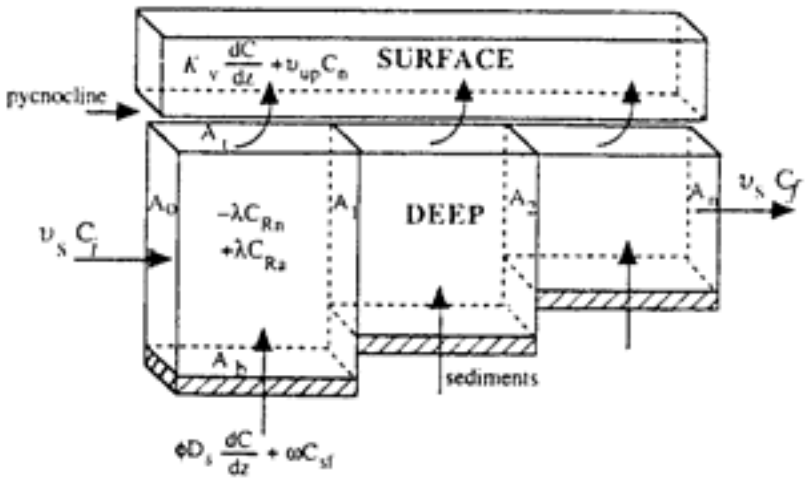

FIG.2. An incremental mass balance of ^{222}Rn in the sub-pycnocline water column was applied using this box model, which allows the sub-pycnocline water column to change with distance up the continental shelf. Sources and sinks considered for ^{222}Rn were (1) total advective–diffusive benthic input processes (ωC_{sf}; ϕD_s (dC/dz)); (2) horizontal transport ($\upsilon_s C_i$; $\upsilon_s C_\beta$); (3) radon production and decay ($\pm \lambda C$); and (4) loss across the pycnocline (K_v (dC/dz) + $\upsilon_{up} C_n$).

Since radon occurs virtually everywhere in the environment, an accounting of the input and loss terms for the area studied is an important part of this approach. Additional inputs include in-growth from the ^{226}Ra dissolved in the water column, and any benthic inputs from diffusion or via physical mixing (bioturbation, sediment resuspension). An important loss term, at least in a shallow water environment, is loss to the atmosphere. Water mass movement can, of course, transport radon–rich or radon–depleted waters into an area of interest. For the purposes of this discussion, it is assumed that horizontal gradients are small and a one dimensional approach is used to calculate inputs and outputs.

The total flux of radon required to support the inventory measured in the system can be estimated by the following equation:

$$J = \frac{I}{(1 - e^{-\lambda t} / \lambda)} \tag{1}$$

where J = the total flux of ^{222}Rn (dpm·m^{-2}·d^{-1}); I = inventory (dpm·m^{-2}), and λ = the decay constant of ^{222}Rn (0.181 d^{-1}). At high values of t (several half-lives of ^{222}Rn), this equation reduces to the inventory divided by 5.5 day mean life [I/(1/λ)] or simply the inventory multiplied by the decay constant, Iλ. This calculation thus assumes a steady-state situation on a time scale of weeks. This condition has been observed in coastal environments in Florida [6]. The main loss from the measured ^{222}Rn inventory will typically be that due to atmospheric evasion.

With this estimate of the required total benthic flux of radon, calculations can be made of the advective component required by using an advection–diffusion equation:

$$\frac{dC}{dt} = K_z \frac{\partial^2 C}{\partial z^2} + \omega \frac{\partial C}{\partial z} + P + \lambda C \tag{2}$$

where C is the radon concentration (activity) in the sediments; z is the depth positive downwards, Kz is the vertical diffusivity; $\partial^2 C/\partial z^2$ and $\partial C/\partial z$ are the ^{222}Rn concentration gradients across the sediment–water interface for diffusion and advection, respectively; ω is the vertical advective velocity; P is the production of ^{222}Rn in pore fluids which is due to recoil after production by ^{226}Ra decay in mineral grains (P = λCeq, where Ceq is the activity of ^{222}Rn in equilibrium with wet sediment determined experimentally, dpm·m^{-3} wet sediment); and λC is radioactive decay of ^{222}Rn. In this situation, K_z is

set equivalent to Ds, the effective wet sediment diffusion coefficient which is corrected for temperature and sediment tortuosity. Advection, ω, and radioactive decay, λ, represent losses from the sediments and are thus defined as negative terms. The solution to eq.2 may be represented by the following:

$$C = \frac{(Co - Ceq)(e^{\frac{z}{2z^*}}) \sinh(\frac{A(zeq - z)}{2z^*})}{\sinh(\frac{Azeq}{2z^*})} \quad (3)$$

where *Co* is the radon activity (dpm·m^{-3}) in the overlying water, at the sediment–water interface, multiplied by sediment porosity to obtain a value corresponding to ^{222}Rn in wet sediment (dpm·m^{-3}); *zeq* is a depth in the sediments much deeper than the depth where *Ceq* initially occurs; *z** is a one-dimensional mixing parameter described by Ds/ω; and A = $[1+4z^* (\lambda/\omega)]^{0.5}$, which includes radioactive decay and advection [6]. When advection of the fluids through sediments is considered, information regarding the radon concentration associated with the subsurface fluids is necessary to estimate accurately the fluid flux across the sediment–water interface. Thus, the estimate of the extent of the water flux through sediments into the overlying water depends critically upon the evaluation of the ^{222}Rn activity in these fluids. If SGD is thought to occur mainly via slow seepage through sediments, a process typically measured at rates on the order of cm·d^{-1}, than a reasonable estimate of the fluid radon concentration may be made from the sediment equilibration approach or from pore water measurements. If more rapid entry points to the sea floor, such as submarine springs, are present than expected radon activities in the discharging fluids would more likely to be similar to those measured in groundwater from the coastal aquifer.

3.2. Radium isotope disequilibrium to delineate coastal mixing rates and submarine groundwater discharge

In the natural radioactive series, there are four radium isotopes: ^{226}Ra ($t_{1/2}$ = 1620 years); ^{228}Ra ($t_{1/2}$ = 5.75 years); ^{223}Ra ($t_{1/2}$ = 11.3 days); ^{224}Ra ($t_{1/2}$ = 3.66 days). Each isotope is produced from the decay of a thorium parent: ^{230}Th ($t_{1/2}$ = 7.54×0^4 years); ^{232}Th ($t_{1/2}$ = 1.40×10^{10} years); ^{227Th} ($t_{1/2}$ = 18.7 days); ^{228}Th ($t_{1/2}$ = 1.91 years), respectively.

Because thorium remains tightly bound to particles while radium daughters are mobilized into the marine environment, sediments provide a continuous source of Ra isotopes to seawater, at rates set by their respective decay constants. Measurements of the Th isotope activities in the sediments and the distribution coefficient of Ra between the sediments and water provide a means of quantifying the potential input of each isotope to the ocean.

Two short-lived radium isotopes ^{223}Ra and ^{224}Ra can be used as tracers to measure the rate of exchange of coastal waters [9]. Shore–perpendicular profiles of ^{223}Ra and ^{224}Ra in surface waters along the coast may be modeled to yield eddy diffusion coefficients. Coupling the exchange rate with offshore concentration gradients, the offshore fluxes of dissolved materials are estimated. For systems in steady state, the offshore fluxes must be balanced by new inputs from rivers, groundwater, sewers or other sources. Also, it was observed that barium and ^{226}Ra contents can be powerful indicators of groundwater input in marine systems, since they have high relative concentrations in the fluids and low reactivity in the coastal ocean. An estimate of the ^{226}Ra offshore flux is made applying the eddy diffusion coefficients to the ^{226}Ra offshore gradient. Complementary data of ^{226}Ra in subsurface fluids provides a mean of calculate the fluid flux necessary to support the ^{226}Ra concentrations found in the marine environment.

Moore [9] used the distribution of the short-lived Ra isotopes to estimate exchange rates in the coastal ocean. The change in concentration or activity (A) with time (t) as a function of distance offshore (x)

for a radioactive tracer with decay constant (λ) may be expressed as a balance of advection, dispersion, and decay, as follows:

$$\frac{dA}{dt} = K_h \frac{\partial^2 A}{\partial x^2} - \omega \frac{\partial A}{\partial x} - \lambda A \tag{4}$$

If net advection can be neglected, this reduces to:

$$\frac{dA}{dt} = K_h \frac{\partial^2 A}{\partial x^2} - \lambda A \tag{5}$$

where K_h is the dispersion coefficient.

The criterion for setting ω = 0 is based on the offshore distribution of conservative tracers such as ^{226}Ra and ^{228}Ra. These long-lived isotopes decay little during the residence time of coastal waters. A constant offshore concentration gradient of these tracers provides evidence that dispersion dominates offshore or onshore advection [9]. In the case where ω = 0, the boundary conditions of eq.5 are as follows:

$$A = A_i \; at \; x = 0$$
$$A \to 0 \; as \; x \to \infty$$

If K_h is constant and the system is steady state,

$$A_x = A_0 \exp\left[-x\sqrt{\frac{\lambda}{K_h}}\right] \tag{6}$$

where, A_x = activity at distance x from coast, A_0 = activity at distance 0 from coast, and λ = decay constant.

A plot of ln ^{223}Ra or ln ^{224}Ra as function of distance from the coast may be used to estimate K_h if the exchange is dominated by dispersion rather than advection and if the system is steady state:

$$\ln A_x = \ln A_0 - x\sqrt{\frac{\lambda}{K_h}} \tag{7}$$

In this case the slope,

$$m = \sqrt{\frac{\lambda}{K_h}} \tag{8}$$

An alternate way to use the short-lived Ra isotopes is to utilize the ^{224}Ra/^{223}Ra AR to estimate the ages of shelf waters [18]. This method is based on the assumptions that the ^{224}Ra/^{223}Ra AR is initialized to a constant value near shore and only changes by decay as the water is isolated from the radium source. The ^{224}Ra/^{223}Ra AR decreases with an apparent half life of 5.4 days, as follows:

$$\left(\frac{^{224}Ra}{^{223}Ra}\right)_{measured} = \left(\frac{^{224}Ra}{^{223}Ra}\right)_{initial} \frac{e^{-\lambda_{224}t}}{e^{-\lambda_{223}t}}$$

3.3. Experimental

3.3.1. Application of the ^{222}Rn approach to estimate SGD in Ubatuba coastal waters

We describe here an application of excess ^{222}Rn to estimate SGD in a series of small embayments of Ubatuba, São Paulo State, Brazil.

Seawater samples were collected at several stations of Ubatuba embayments in top-to-bottom vertical profiles. Temperature and salinity profiles were obtained at the same stations using a 2.00" Micro CTD, from Falmouth Scientific Inc. In each station, seawater samples were collected at 1 – 2 m depth

intervals using a peristaltic pump to purge the sampling tubes and then drawn into 4 L evacuated glass bottles. Seawater was purged for 5 minutes from the hose at each depth prior to filling the sampling bottles, and they were immediately sealed to prevent radon losses. ^{222}Rn was extracted and counted using a modified emanation technique described by Cable *et al.* [5]. Once extracted, the radon gas was collected in a liquid nitrogen cold trap and transferred from the trap to an alpha scintillation cell. After radon stripping and transfer into alpha scintillation cells, samples were stored for 3 hours to allow ^{222}Rn daughters, ^{218}Po and ^{214}Po to equilibrate and counting was performed using a portable radon monitor RDA–200, Scintrex [19]. After the initial radon analysis, the samples were sealed and stored for at least five days for ^{222}Rn ingrowth and then flushed again in order to determine the ^{226}Ra activity. Excess radon was determined as the difference between the total ^{222}Rn in samples and the supported ^{222}Rn, assumed to be equal to the ^{226}Ra activity. These values were decay corrected back to the time of sampling in order to assess the *in situ* excess radon concentrations. Once the concentrations have been determined, ideally as a complete profile through the water column, the inventory was calculated by integrating the excess radon concentrations over water depth intervals. Bottom sediment grab samples were also obtained at each site in order to assess potential diffusive fluxes of ^{222}Rn from sediments.

3.3.2. Use of Ra isotopes in Ubatuba to study coastal dynamics and groundwater input

Activity concentrations of ^{223}Ra, ^{224}Ra, ^{226}Ra and ^{228}Ra have been also measured in seawater, surface and groundwater samples collected in Ubatuba coastal area. All the samples studied were collected during tree sampling cruises performed in June 2000 (winter), January 2002 (summer) and November 2003 (summer), respectively.

Large volume seawater samples (196 L) were pumped from 5 m below the surface into plastic drums on the R/V Velliger II. The sample volume was recorded and the seawater was percolated through a column of manganese coated acrylic fiber (<1 L/min) to quantitatively remove radium from seawater [8]. Samples for salinity and nutrients were also collected in each station.

Additional samples were obtained from a set of monitoring wells and from seepage meters installed in Flamengo Bay in 2003. These samples were processed in the same manner as the surface samples.

The samples collected in June 2000 were sent by express mail to the University of South Carolina at Columbia, SC, for measurement. Samples from January 2002 and November 2003 were measured at the University of São Paulo Marine Laboratory in Ubatuba. Each Mn fiber sample was partially dried with a stream of air and was placed in a closed–loop air circulation system as described by Moore and Arnold [20]. Helium was circulated over the Mn fiber to sweep the ^{219}Rn and ^{220}Rn generated by ^{223}Ra and ^{224}Ra decay through a 1L scintillation cell where alpha particles from the decay of Rn and daughters were recorded by a photomultiplier tube (PMT) attached to the scintillation cell. Signals from the PMT were routed to a delayed–coincidence system. The delayed–coincidence system utilizes the difference in decay constants of the short-lived Po daughters of ^{219}Rn and ^{220}Rn to identify alpha particles derived from ^{219}Rn or ^{220}Rn decay and hence to determine activities of ^{223}Ra and ^{224}Ra on the Mn fiber. The expected error of the short-lived Ra measurements is 10%.

After the ^{223}Ra and ^{224}Ra measurements were complete, the Mn fiber samples were aged for 2–6 weeks to allow initial excess ^{224}Ra to equilibrate with ^{228}Th adsorbed to the Mn fiber. The samples were measured again to determine ^{228}Th and thus to correct for supported ^{224}Ra.

Later, the Mn fibers were leached with HCl in a Soxhlet extraction apparatus to quantitatively remove the long-lived Ra isotopes. The Ra was coprecipitated with $BaSO_4$. The precipitant was aged for 2 weeks to allow ^{222}Rn and its daughters to equilibrate with ^{226}Ra. The ^{226}Ra and ^{228}Ra were measured by gamma spectrometry of a $Ba(Ra)SO_4$ precipitate in a WeGe well germanium detector, after 21 days from the precipitation. The detector is a 78 cm^3 coaxial intrinsic germanium crystal with a 1 cm diameter and 4 cm deep well produced by Princeton Gamma Tech. The ^{226}Ra activities were determined by taking the mean activity of three separate photo peaks of its daughter nuclides: ^{214}Pb at

295.2 keV and 351.9 keV, and ^{214}Bi at 609.3 keV. The ^{228}Ra content of the samples was determined from the 911 keV and 968 keV gamma ray peaks of ^{228}Ac. Both measurements were performed at the Radioisotope Geochemical Laboratory of the University of South Carolina. The expected error of the long-lived Ra measurements is 7%.

4. Results and Discussion

4.1. Application of the ^{222}Rn approach to estimate SGD in Ubatuba embayments and its seasonal variations

The potential diffusive fluxes of ^{222}Rn from sediments are presented in Table 1.

TABLE 1. ACTIVITY OF ^{222}Rn IN EQUILIBRIUM WITH WET SEDIMENT DETERMINED EXPERIMENTALLY, (dpm·m^{-3} WET SEDIMENT) (Ceq), AND RADON ACTIVITY IN THE OVERLYING WATER (dpm·m^{-3}), AT THE SEDIMENT–WATER INTERFACE, MULTIPLIED BY THE SEDIMENT POROSITY TO OBTAIN A VALUE CORRESPONDING TO THE ^{222}Rn IN WET SEDIMENT (dpm·m^{-3}) (Co), MEASURED IN THE UBATUBA EMBAYMENTS SEDIMENT. ACTIVITY OF ^{222}Rn IN PORE WATER (dpm·m^{-3}) (Apw).

Sediment sample	Ceq (dpm·m^{-3})	Porosity	Co (dpm·m^{-3})	Apw (dpm·m^{-3})
Flamengo Bay	1.8×10^5	0.51	1.9×10^4	3.6×10^5
Fortaleza Bay	8.5×10^4	0.49	7.8×10^3	1.7×10^5
Mar Virado Bay	1.3×10^5	0.57	3.0×10^3	2.3×10^5
Ubatuba Bay	1.5×10^5	0.62	8.5×10^3	2.4×10^5
Ubatuba Marine Lab	9.9×10^4	0.41	8.5×10^3	2.4×10^5

Considering the results obtained in the vertical profiles established, the excess ^{222}Rn inventories were estimated for the embayments studied. These data are shown in Table 2, together with the total fluxes required to support the measured inventories, estimated using eq.2 and groundwater advective velocity rates necessary to balance the total fluxes, assessed using eq.3.

During the period of this investigation, the excess ^{222}Rn inventories varied from $(0.35\pm0.02) \times 10^3$ to $(19\pm5) \times 10^3$ dpm/m^2. The highest ^{222}Rn in excess inventories were observed both in Flamengo and Fortaleza embayments (Table 2). The respective fluxes of excess ^{222}Rn in the water column ranged from $(0.06\pm0.0) \times 10^3$ a $(3.4\pm0.9) \times 10^3$ dpm/m^2.

The groundwater advective velocity rates necessary to balance the fluxes of excess ^{222}Rn bellow the pycnocline by advection calculated for Ubatuba embayments varied from 0.1×10^{-1} to 1.9 cm·day^{-1}. However, it is important to notice that the corresponding advective velocity rate of groundwater obtained for Fortaleza Bay was slightly higher than to that one observed at Flamengo Bay, since this parameter is function of the bottom sediment porosity. To evaluate the order of magnitude of these fluxes, the results obtained in this work were compared to values reported for other authors in Florida. The SGD values found in Ubatuba embayments are three orders of magnitude lower than those estimated in a study carried out in the northeastern Gulf of Mexico, covering an area of 620 km^2 [5]. Increased silicate concentrations also were found in Flamengo Bay and Fortaleza Bay bottom waters. Other authors have reported a strong correlation between increased silicate levels, Ba^{2+}, ^{226}Ra and groundwater discharge [10, 21].

The highest inventories of excess ^{222}Rn were observed late in the summer season (March), which corresponds exactly to the month of highest pluviometry (about 350 mm). The annual pluviometric rates at Ubatuba region varies from 1,500 to 2,000 mm. August is the only month presenting pluviometry lower than 100 mm.

Taking into account all SGD fluxes obtained (from March 2003 to July 2005), the percentual variability was 89% (seasonal variation in 3 years period, n = 24 measurements). Although, if we consider each year of study separately, the respective percentual variabilities estimated are 72% in 2003 (n = 10 measurements), 127% in 2004 (n = 6 measurements) and 97% in 2005 (n = 8 measurements).

TABLE 2. EXCESS ^{222}Rn INVENTORIES, TOTAL FLUXES REQUIRED TO SUPPORT INVENTORIES MEASURED AND GROUNDWATER ADVECTIVE RATES NECESSARY TO BALANCE THE SUB-PYCNOCLINE FLUXES ESTIMATED IN UBATUBA EMBAYMENTS (2003/2005).

Vertical Profile depth (m)	**I^{222}Rn excess (dpm·m^{-2})**	**Flux ^{222}Rn excess (dpm·m^{-2}·d^{-1})**	**SGD (ω) (cm·d^{-1})**
March 2003			
Mar Virado Bay (8 m)	$(5.2 \pm 1.9) \times 10^3$	$(0.9 \pm 0.3) \times 10^3$	0.4
Fortaleza Bay (8 m)	$(13 \pm 3) \times 10^3$	$(2.4 \pm 0.5) \times 10^3$	1.3
Sete Fontes (Flamengo Bay) (8 m)	$(19 \pm 5) \times 10^3$	$(3.4 \pm 0.9) \times 10^3$	1.9
Refúgio do Corsário (Fortaleza Bay) (8 m)	$(3.3 \pm 1.1) \times 10^3$	$(0.6 \pm 0.2) \times 10^3$	0.6×10^{-1}
Domingas Dias (Flamengo Bay) (6 m)	$(7.4 \pm 1.8) \times 10^3$	$(1.3 \pm 0.3) \times 10^3$	0.7
Flamengo Bay Center (8 m)	$(5.7 \pm 2.1) \times 10^3$	$(1.0 \pm 0.4) \times 10^3$	0.4
Praia Grande (Anchieta Island) (8 m)	$(5.3 \pm 1.8) \times 10^3$	$(1.0 \pm 0.3) \times 10^3$	0.4
November 2003			
Flamengo Bay			
FB1 (5 m)	$(6.1 \pm 1.6) \times 10^3$	$(1.1 \pm 0.3) \times 10^3$	0.5
FB2 (8 m)	$(13 \pm 4) \times 10^3$	$(2.3 \pm 0.7) \times 10^3$	1.3
FB3 (11 m)	$(12 \pm 4) \times 10^3$	$(2.2 \pm 0.7) \times 10^3$	1.2
May 2004			
Flamengo Bay			
FL (9 m)	$(12 \pm 4) \times 10^3$	$(2.2 \pm 0.7) \times 10^3$	1.2
August 2004			
Fortaleza Bay Center (8 m)	$(3.7 \pm 0.3) \times 10^3$	$(0.7 \pm 0.1) \times 10^3$	0.7
Perequê – Mirim (Flamengo Bay) (5 m)	$(2.7 \pm 0.2) \times 10^3$	$(0.4 \pm 0.0) \times 10^3$	0.2
Perequê–Mirim left side (Flamengo Bay) (2.7 m)	$(1.2 \pm 0.1) \times 10^3$	$(0.2 \pm 0.0) \times 10^3$	0.3×10^{-1}
Perequê – Mirim right side (Flamengo Bay) (3.2 m)	(0.35±0.02) × 103	(0.06 ± 0.0) × 103	0.1 × 10–1
Flamengo Bay Center (8 m)	(3.9 ± 0.2) × 103	(0.6 ± 0.0) × 103	0.1

Table 2 contd.

Vertical Profile depth (m)	$I^{222}Rn$ excess ($dpm \cdot m^{-2}$)	Flux ^{222}Rn excess ($dpm \cdot m^{-2} \cdot d^{-1}$)	SGD (ω) ($cm \cdot d^{-1}$)
March 2005			
Fortaleza Bay Center (9 m)	$(8.3 \pm 0.6) \times 10^3$	$(1.5 \pm 0.1) \times 10^3$	1.9
Flamengo Bay Center (8.2 m)	$(3.4 \pm 0.2) \times 10^3$	$(0.6 \pm 0.0) \times 10^3$	0.8×10^{-1}
Perequê–Mirim left side (Flamengo Bay) (2.4 m)	$(5.4 \pm 0.4) \times 10^3$	$(1.0 \pm 0.1) \times 10^3$	0.4
Perequê – Mirim right side (Flamengo Bay) (2.4 m)	$(4.5 \pm 0.3) \times 10^3$	$(0.8 \pm 0.1) \times 10^3$	0.3
July 2005			
Fortaleza Bay – A1 (2.4 m)	$(4.1 \pm 0.3) \times 10^3$	$(0.7 \pm 0.1) \times 10^3$	0.8
Fortaleza Bay – A2 (12 m)	$(6.0 \pm 0.4) \times 10^3$	$(1.1 \pm 0.1) \times 10^3$	1.3
Flamengo Bay Center (8.2 m)	$(2.6 \pm 0.2) \times 10^3$	$(0.5 \pm 0.0) \times 10^3$	0.2
Perequê – Mirim (4 m)	$(3.3 \pm 0.2) \times 10^3$	$(0.6 \pm 0.0) \times 10^3$	0.3

4.2. Determination of residence time and mixing processes of the Ubatuba inner shelf waters using natural Ra isotopes

Three sampling campaigns were organized to assess the temporal and spatial distribution of the tracers. The sample locations are shown on Fig.3. In June 2000, we collected one transect from Fortaleza Bay to 19 km offshore. In January 2002, we sampled Mar Virado, Fortaleza, and Flamengo Bays, ran one transect north of Vitoria Island, and a second transect off Ubatuba Bay. We also sampled some monitoring wells in Flamengo Bay. In November 2003, we ran one transect out of Flamengo Bay and a second transect extending to Vitoria Island. We again sampled the Flamengo Bay wells and also measured samples obtained from seepage meters in Flamengo Bay. The results are given in Table 3 (surface water samples) and Table 4 (wells and seepage meters).

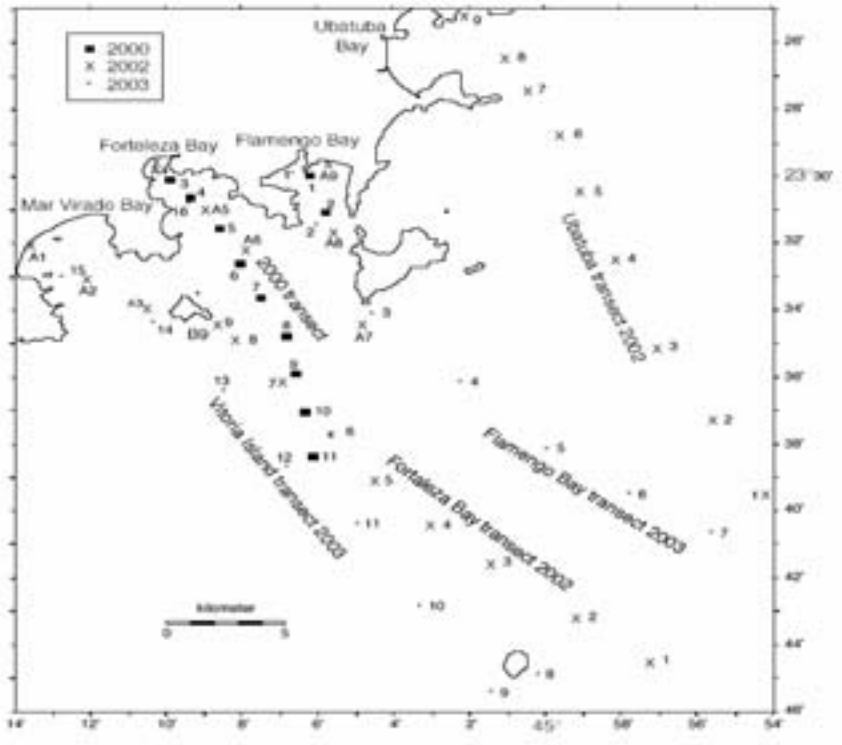

FIG.3. Map of the study area showing cruises conducted in 2000 (squares), 2002 (X) and 2003 (*). The offshore transects are labeled. The labels for samples collected in various bays in 2002 have an A prefix.

TABLE 3. Ra ACTIVITIES (dpm/100L) IN SURFACE WATERS. THE AGES (DAYS) ARE BASED ON ASSUMED INITIAL $^{224}Ra/^{223}Ra$ ACTIVITY RATIO OF 21 (FROM SEEPAGE METERS).

Sample	Location	Date	S (‰)	D (km)	^{226}Ra	^{228}Ra	ex^{224}Ra	^{223}Ra	224/223 AR	Age
2000 Transect										
UB–1	Flamengo Bay	19–Jun–00	35.696	1.0			28.03	2.23	12.6	3.9
UB–2	Flamengo Bay	19–Jun–00	35.881	3.0			20.52	1.75	11.7	4.5
UB–3	Fortaleza Bay	19–Jun–00	35.699	0.9			29.74	2.53	11.8	4.5
UB–4	Fortaleza Bay	19–Jun–00	35.198	3.0			42.82	2.70	15.9	2.2
UB–5	transect	19–Jun–00	35.932	5.1			13.75	1.20	11.5	4.7
UB–6	transect	19–Jun–00	35.965	7.2			8.77	1.12	7.8	7.6
UB–7	transect	19–Jun–00	35.977	9.3			5.98	0.60	10.0	5.7
UB–8	transect	19–Jun–00	35.998	11.5			3.69	0.43	8.6	6.9
UB–9	transect	19–Jun–00	36.001	14.1			1.50	0.43	3.5	13.8
UB–10	transect	19–Jun–00	36.034	16.4			0.84	0.15	5.6	10.2
UB–11	transect	19–Jun–00	36.061	18.6			3.29	0.20	16.5	
Nearshore 2002										
A–1	Mar Virado Bay	23–Jan–02	34.80	1	9.91	24.52	38.53	2.56	15.0	2.6
A–2	Mar Virado Bay	23–Jan–02	35.14	4	9.72	12.66	2.52	0.35	7.2	8.3
A–3		23–Jan–02	34.95	7	9.04	15.47	7.82	0.75	10.4	5.4
A–4	Fortaleza Bay	23–Jan–02	34.22	1	9.96	22.22	27.06	1.62	16.7	1.8
A–5	Fortaleza Bay	23–Jan–02	35.11	4	8.96	14.80	8.07	1.02	7.9	7.5
A–6		23–Jan–02	34.89	7	10.03	18.43	7.06	0.52	13.6	3.4
A–7		23–Jan–02	35.16	13	8.49	10.02	1.06	0.41	2.6	16.1
A–8	Flamengo Bay	23–Jan–02	34.82	6	10.01	18.77	8.46	0.94	9.0	6.5
A–9	Flamengo Bay	23–Jan–02		1	9.79	23.54	31.81	2.48	12.8	3.8
Fortaleza Bay Transect 2002										
B–1	transect	22–Jan–02	35.34	30.6	9.20	9.55	1.97	0.45	4.4	12.1
B–2	transect	22–Jan–02	35.39	27.9	8.82	7.95	1.69	0.16	10.5	5.3
B–3	transect	22–Jan–02	35.35	23.5	7.16	6.54	0.65	0.10	6.3	9.3
B–4	transect	22–Jan–02	34.92	20.4	7.83	7.38	3.08	0.35	8.8	6.7
B–5	transect	22–Jan–02	35.05	17.4	9.79	14.65	4.96	0.79	6.2	9.3
B–6	transect	22–Jan–02	35.00	14.4	10.05	16.05	6.93	0.56	12.3	4.1
B–7	transect	22–Jan–02	35.03	11.5	9.45	18.27	7.10	0.69	10.3	5.5
B–8	transect	22–Jan–02	35.03	9.3	8.43	15.32	6.82	0.85	8.0	7.4
B–9	transect	22–Jan–02	35.02	8.4	10.39	17.11	7.98	0.87	9.2	6.4

Table 3 contd.

Sample	Location	Date	S (‰)	D (km)	^{226}Ra	^{228}Ra	ex^{224}Ra	^{223}Ra	224/223 AR	Age
Ubatuba Bay Transect 2002										
J–1	transect	25–Jan–02	35.73	30	9.05	9.57	1.51	0.33	4.6	11.6
J–2	transect	25–Jan–02	35.55	25	9.49	14.12	3.74	0.58	6.5	9.0
J–3	transect	25–Jan–02	35.37	20	8.93	16.28	6.51	0.64	10.2	5.6
J–4	transect	25–Jan–02	35.53	15	9.47	17.89	8.59	1.16	7.4	8.0
J–5	transect	25–Jan–02	35.65	11	9.55	13.25	7.04	0.79	9.0	6.6
J–6	transect	25–Jan–02	35.58	8	8.88	14.13	5.41	0.67	8.1	7.3
J–7	transect	25–Jan–02	35.34	5	11.22	6.54	6.55	0.98	6.7	8.8
J–8	transect	25–Jan–02	35.67	3	8.88	15.35	6.80	0.61	11.2	4.8
J–9	Ubatuba Bay	25–Jan–02	35.75	1	9.36	18.15	21.83	0.95	23.0	–0.7
Flamengo Bay Transect 2003										
1	Flamengo Bay	18–Nov–03	34.3	0.3	9.73	19.98	21.39	1.61	13.31	3.5
2	transect	18–Nov–03	34.0	0.7	8.10	16.28	10.85	0.92	11.80	4.4
3	transect	18–Nov–03	34.0	0.8	9.57	17.06	10.87	0.82	13.21	3.6
4	transect	18–Nov–03	34.7	5.5	7.84	13.62	2.16	0.46	4.66	11.6
5	transect	18–Nov–03	34.7	10.3	8.31	12.76	1.15	0.32	3.58	13.6
6	transect	18–Nov–03	34.6	14.5	7.65	12.41	1.42	0.40	3.55	13.7
7	transect	18–Nov–03	34.6	18.5	7.11	12.30	1.09	0.34	3.24	14.4
7A	transect	19–Nov–03	34.9	18.5	8.03	14.42	1.38	0.40	3.47	13.8
Vitoria Island Transect 2003										
8	transect	19–Nov–03	34.5	23.0	8.56	11.99	0.32	0.16	2.02	18.0
9	transect	19–Nov–03	34.6		8.35	12.68	0.57	0.20	2.84	15.4
10	transect	19–Nov–03	34.7	17.0	8.17	13.40	1.43	0.28	5.12	10.9
11	transect	19–Nov–03	34.4	12.2	8.01	15.69	4.68	0.70	6.68	8.8
12	transect	19–Nov–03	34.5	8.8	8.96	13.77	1.07	0.31	3.48	13.8
13	transect	19–Nov–03	34.5	4.0	8.30	14.68	1.76	0.39	4.54	11.8
14	transect	19–Nov–03	34.1	0.5	8.45	18.94	16.27	1.33	12.23	4.2
15	Mar Virado Bay	19–Nov–03	34.0	1.5	8.87	18.18	15.88	1.47	10.78	5.1
16	Fortaleza Bay	19–Nov–03	33.6	1.2	8.30	19.94	15.15	1.33	11.43	4.7

S = salinity in ‰; D = distance offshore (km)

TABLE 4. Ra ACTIVITIES (dpm/100L) IN ESTUARY, SEEPAGE, AND GROUNDWATER.

Sample	Location	Date	Salinity (‰)	^{226}Ra	^{228}Ra	ex^{224}Ra	^{223}Ra	224/223 AR
UB-GW	hillside seep	20–Jun–00	0.0			80.8	3.3	24.3
P–1	Ubatuba city well	24–Jan–02	0.8	25.1	37.2	38.4	0.9	41.3
P–2	Ubatuba city well	24–Jan–02	0.1	13.7	93.9	104	3.5	29.7
P–3	Ubatuba city well	24–Jan–02	0.1	11.3	22.6	24.1	2.2	11.1
P–4	Ubatuba city well	24–Jan–02	0.1	11.0	47.4	50.8		
PM–01	Lab well PM–01	24–Jan–02		102	91.2	78.0		
PM–06	Lab well PM–06	24–Jan–02		28.7	124	187		
PM–03	Lab well PM–03	24–Jan–02	25.5	14.5	873	1056	55.9	18.9
PM–08	Lab well PM–08 (3B)	25–Jan–02	26.0	71.5	2141	2284	122	18.7
PM–04	Lab well PM–04 (2A)	25–Jan–02	26.7	163	1440	4524		
PM–05	Lab well PM–05 (3A)	25–Jan–02		163	1440	2161		
PM–09	Lab well PM–09	25–Jan–02		62.1	1207	2330	28.4	82.0
	Rio Escuro estuary	26–Jan–02	30.6	13.8	44.7	57	2.8	20.4
17	seep meters	19–Nov–03	26.4	19.1	402	1221	65	18.8
18	Lab well PM–07 (2B)	20–Nov–03	31.0	135	2377	2718	133	20.4
19	Lab well PM–08 (3B)	20–Nov–03	32.8	76.0	1116	978	32	30.6
20	Lab well PM–04 (2A)	20–Nov–03	32.9	159	2862	2939	100	29.3
21	Lab well PM–05 (3A)	20–Nov–03	33.1	207	1321	2374	60	39.6
22	seep meters	20–Nov–03	26.6	26	435	1716	75	22.9

4.2.1. June 2000

Both ln^{223}Ra and ln^{224}Ra exhibited a strong relationship with distance offshore on this transect (r^2 for ^{223}Ra = 0.949 and for ^{224}Ra = 0.961, with the exception of the most distant point, UB–11) (Fig.4). The slope of ln^{223}Ra indicated a dispersion coefficient of 2.4 km^2/day (28 m^2/s). The ln^{224}Ra data yielded a K_h of 3.4 km^2/d (39 m^2/s).

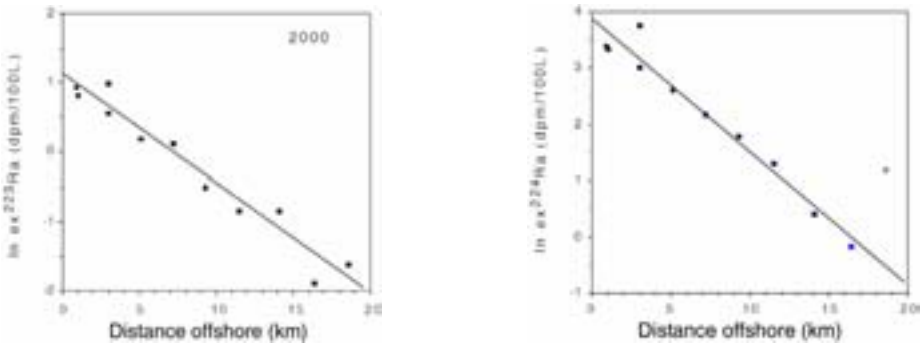

FIG.4. The ln Ra activity as a function of distance offshore for samples collected in 2000. The best-fit line for ^{223}Ra (r^2 = 0.949) yields K_h = 28 $m^2 \cdot s^{-1}$. The best-fit line for ^{224}Ra (r^2 = 0.961) yields K_h = 39 $m^2 \cdot s^{-1}$.

4.2.2. January 2002

For samples collected within the three bays, the offshore distributions of both isotopes were similar to the June 2000 plots (Fig.5). The plot of ln ^{223}Ra vs. distance yielded a dispersion coefficient of 2.7 km^2/sec ($r^2 = 0.86$). The ln^{224}Ra vs. distance plot yielded 2.1 km^2/sec ($r^2 = 0.95$). In both plots, one low Ra sample (A–2) from 4 km was excluded.

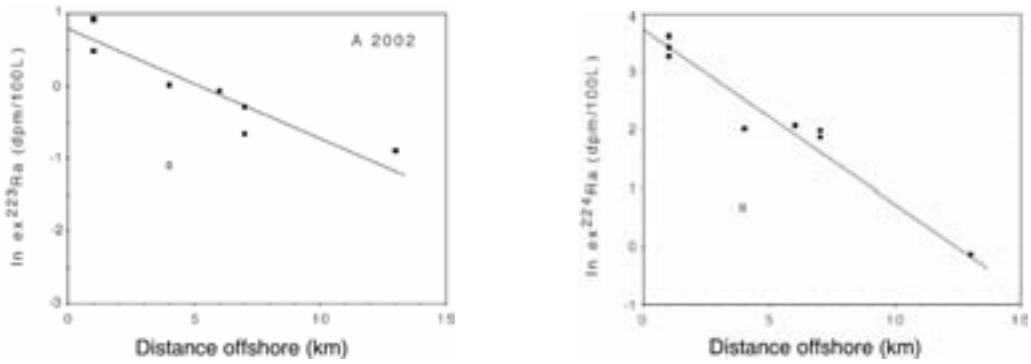

FIG.5. The ln Ra activity as a function of distance offshore for samples collected within 13 km offshore in 2002. The best-fit line for ^{223}Ra ($r^2 = 0.862$) yields $K_h = 24\ m^2 \cdot s^{-1}$. The best-fit line for ^{224}Ra ($r^2 = 0.950$) yields $K_h = 31\ m^2 \cdot s^{-1}$.

The ln Ra activity as a function of distance offshore plots for samples collected on the Fortelaza Bay transect are shown in Fig.6(a). The ^{223}Ra data are reasonably correlated within 20 km of shore, but the correlation breaks down for samples collected between 20 and 30 km. The ln Ra activity as a function of distance offshore for samples collected on the Ubatuba Bay transect is shown in Fig.6(b). Samples collected within Ubatuba Bay and just shoreward of the bay have activities considerably lower than those of samples collected from the bays to the south. Additionally, there is no consistent trend of decreasing activity with distance offshore for these samples. Because of these problems, we are reluctant to assign a K_h to these transects.

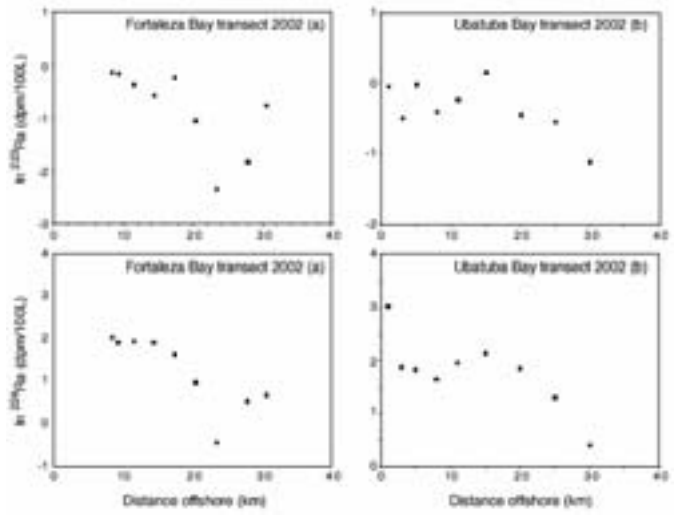

FIG.6. (a) The ln Ra activity as a function of distance offshore for samples collected on Fortaleza Bay transect in 2002. The ^{223}Ra data are reasonably correlated within 20 km of shore, but the correlation breaks down for samples collected between 20 and 30 km. (b) The ln Ra activity as a function of distance offshore for samples collected on the Ubatuba Bay transect in 2002. Samples collected within Ubatuba Bay and just shoreward of the bay have activities considerably lower than those of samples collected from bays lying to the south. Additionally, there is no consistent trend of decreasing activity with distance offshore for these samples.

4.2.3. November 2003

The ln Ra activity as a function of distance offshore plots for samples collected on the Vitoria Island transect are shown in Fig.7(a). There is no consistent trend of decreasing activity with distance offshore for these samples. The ln Ra activity as a function of distance offshore plots for samples collected on the Flamengo Bay transect are shown in Fig.7(b). Samples collected beyond 5 km do not show a decreasing trend of activity with distance. Because of these problems, we are reluctant to assign a K_h to these transects.

The solution to eq.4 depends on several conditions. The system must be steady state, dispersion must be constant throughout the study area, and there can be no addition of Ra beyond the point taken for the initial activity. The transect collected in 2000 appears to obey these conditions as there is an excellent correlation between ln Ra and distance offshore and there is reasonable agreement between the values derived for dispersion from the two isotopes. But this is not the case for the offshore data collected in 2002 and 2003. In 2003 there was no consistent trend of decreasing activity with distance offshore. In 2002 the samples collected within 20 km of shore showed the expected decrease of activity with distance, but the correlation broke down for samples collected between 20 and 30 km. The samples from Ubatuba Bay were significantly lower in activity than the samples collected in the more southern bays. SGD studies in Ubatuba Bay in 2001 indicated lower fluxes compared with the other bays [19], but the differences were not enough to explain the differences measured in 2002. This leads us to conclude that during the 2002 and 2003 sampling campaigns, one or more of the conditions necessary for the use of eq.4 were not met. Therefore we must seek alternative ways to estimate exchange times.

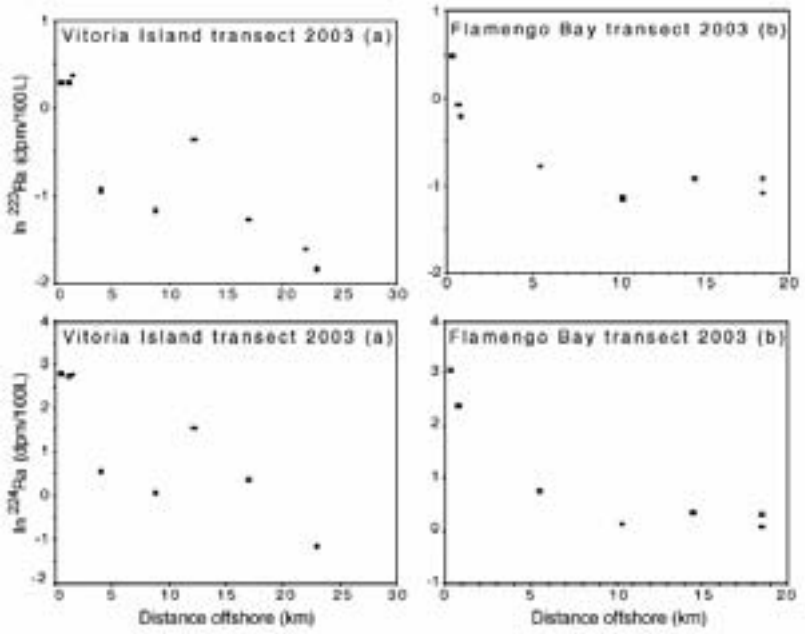

FIG.7.(a) The ln Ra activity as a function of distance offshore for samples collected on the Vitoria Island transect in 2003. There is no consistent trend of decreasing activity with distance offshore for these samples. (b) The ln Ra activity as a function of distance offshore.

The $^{224}Ra/^{223}Ra$ age model does not depend on steady state conditions or constant mixing patterns. We used samples collected from seepage meters in Flamingo Bay in 2003 to initialize the age model. These samples had a $^{224}Ra/^{223}Ra$ AR = 21. Because the natural $^{238}U/^{235}U$ AR = 21.7 and the natural abundance $^{232}Th/^{238}U$ AR ~1, the supported $^{224}Ra/^{223}Ra$ AR = 21.7, close to the value measured in the seepage water.

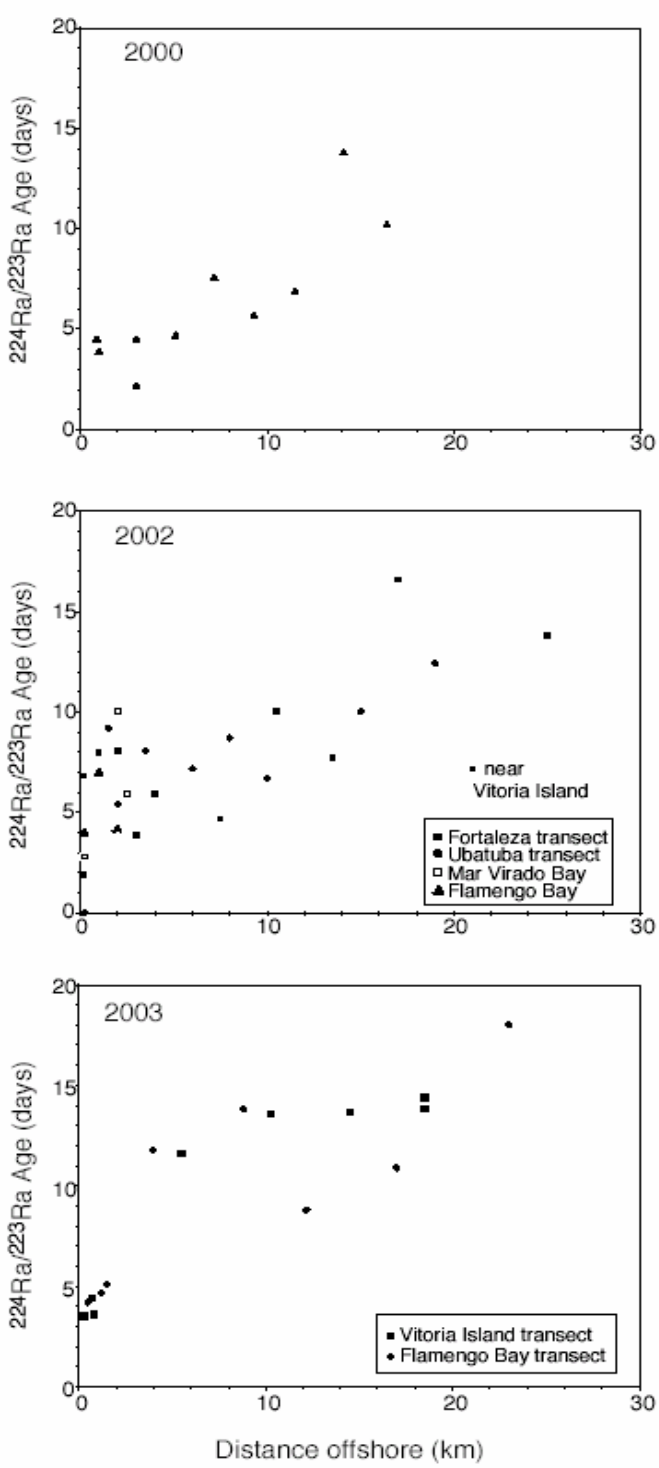

FIG.8. Age vs. distance offshore for all samples. Samples collected in the bays have ages in the range 2 to 10 days relative to the water collected in the seepage meter. Farther offshore there is a trend of increasing age with distance. Most samples from 10 to 25 km offshore have ages in the range of 7 to 15 days.

The calculated age vs. distance offshore for all samples is shown in Fig.8. Samples collected in the bays have ages in the range of 2 to 10 days relative to the water collected in the seepage meter. Further offshore there is a trend of increasing age with distance. Most samples from 10 to 25 km offshore have ages in the range 7 to 15 days. The one exception to this was a sample collected near Vitoria Island in 2003.

The primary objective for the study using short-lived Ra was to provide an estimate of rates of exchange between the coastal waters and the open ocean to use in models of SGD. Tracer concentrations in coastal waters depend on the flux of SGD, the concentration of the tracer in the SGD, and how quickly the signal is lost by exchange with the open ocean. We can use measurements of a long-lived Ra isotope, ^{228}Ra (half life = 5.7 years), to illustrate how this works. The average ^{228}Ra activity in the coastal water to 25 km offshore in 2003 was 15.5±2.72 dpm/100L (Table 3). The ocean end member (12.15±0.22 dpm/100L) can be estimated from the most distant samples from shore, 7 and 8 (Table 3). Thus, the enrichment of ^{228}Ra in the coastal water is 3.36±2.73 dpm/100L. The known volume that exhibits this enrichment is 14km along shore × 25 km offshore × 10 m depth, or 3.5×10^{9} m^3. The total ^{228}Ra enrichment is $1.2\pm1.0 \times 10^{11}$ dpm. If the residence time is taken as 10 days, the average flux of ^{228}Ra is $1.2\pm1.0 \times 10^{10}$ dpm·d^{-1}.

Nearshore SGD fluxes were estimated from seepage meters [22] and ^{222}Rn [23]. These studies concluded that the average nearshore SGD flux was 13±6 $cm^3 \cdot cm^{-2} \cdot d^{-1}$. The total shoreline length of the 14 km long study area is ~40 km due to the rugged nature of the coastline. If the nearshore SGD flux occurs between this shoreline and 50 m offshore [22, 24], the total nearshore SGD flux is $2.7\pm1.2 \times 10^5$ $m^3 \cdot d^{-1}$. We can translate this nearshore SGD flux into a ^{228}Ra flux using the activities of ^{228}Ra measured in water emerging from seepage meters. Two samples of this water had ^{228}Ra activity = 415 dpm/100L (Table 4). If the ^{228}Ra enrichment is caused by the SGD flux of water with this composition, the nearshore SGD ^{228}Ra flux must be $1.1\pm0.5 \times 10^9$ dpm·d^{-1}. Using a 10-day residence time, this nearshore SGD flux can support an excess ^{228}Ra inventory in the 3.5×10^9 m^3 study area of $1.1\pm0.5 \times 10^{10}$ dpm. In spite of the large uncertainty associated with each estimate, it is clear that the estimated nearshore seepage cannot support the measured excess ^{228}Ra in the coastal water. The seepage estimate is only 10% of the measured ^{228}Ra enrichment, implying that offshore SGD is ten times more important than the nearshore flux.

5. Conclusions

The direct discharge of groundwater into near-shore marine environment may have significant environmental consequences because groundwater in many areas has become contaminated with a variety of substances like nutrients (mainly from septic systems), heavy metals, radionuclides and organic compounds. As almost all coastal zones are subjected to flow of groundwater either as submarine springs or disseminated seepage, coastal areas are likely to experience environmental degradation. Transport of nutrients to coastal waters may trigger algae blooms, including harmful algae blooms, having negative impacts on the economy of coastal zones.

Measurements of SGD along the South American coast and over fractured aquifers are especially rare. A reconnaissance of submarine groundwater discharge using ^{222}Rn as a natural tracer disclosed a substantial inflow of groundwater, which includes both fresh and saline pore water [19]. Preliminary measurements carried out at Ubatuba coastal area showed fluxes of groundwater in Flamengo Bay to average 4.3 cm^3 of pore water per square centimeter of the sea floor per day (or, in short, 4.3 cm·d^{-1}). Direct measurements of SGD were also made using vented benthic chambers [19]. Measured fluxes were approximately 21 cm·day^{-1}. The disparity between these estimates may be explained by the spatial and seasonal variabilities of SGD documented in that previous study.

In order to evaluate seasonal variations, several vertical profiles were established in Ubatuba embayments (from March 2003 to July 2005). The results obtained showed highest excess ^{222}Rn inventories occurring late in the summer season (March), which corresponds exactly to the month of highest pluviometry (about 350 mm) and consequently, highest discharge. It seems to indicate that the main control on temporal variations in groundwater flow in Ubatuba embayments is precipitation, since recharge was governed largely by this phenomenon.

Once both tidal and seasonal oscillations can induce changes in the fluxes of SGD through coastal aquifers, large data sets are frequently necessary to accurately predict temporal variations in groundwater discharge.

During the period of this investigation, the percentual variability on SGD fluxes estimated using ^{222}Rn as a tracer was 89%, taking into account all fluxes determined (seasonal variation in 3 years period, and n = 24 measurements). Although, if we consider each year of study separately, the respective percentual variabilities estimated are 72% in 2003 (n = 10 measurements), 127% in 2004 (n = 6 measurements) and 97% in 2005 (n = 8 measurements).

Concerning to the application of natural Ra isotopes in Ubatuba, although the $^{224}Ra/^{223}Ra$ age method does not yield tightly defined ages, it provides an estimate of 1 to 2 weeks for the residence time of water within 25 km of shore. It also illustrates that the ages do not follow a single trend with distance offshore. This is likely due to the ruggedness of the coastline, where many bays and small islands interrupt simple mixing patterns. As water circulates through these bays, small-scale eddies may develop and propagate onto the shelf. Changes in wind direction must also have a strong effect on the eddy formation and the circulation. The likelihood of achieving steady state on a time scale of days to weeks is small. Thus it is not surprising that the advection–diffusion model yields inconsistent results. We used the residence times of the coastal water and the enrichment of ^{228}Ra relative to the ocean to estimate the flux of ^{228}Ra necessary to maintain this enrichment. Our results indicate that the nearshore (0 to 50 m) SGD flux could support only 10% of the measured ^{228}Ra enrichment. This implies that there is considerable offshore SGD.

ACKNOWLEDGEMENTS

The authors of this report are grateful for the collaboration received from W.S. Moore (University of South Carolina) and W.C. Burnett (Florida State University) during all those years of study. Without their cooperation, these experiments could not have been conducted. We also acknowledge support received from the International Atomic Energy Agency (IAEA), which financed these activities through their coordinated research project (CRP) entitled Nuclear and Isotopic Techniques for the Characterization of Submarine Groundwater Discharge (SGD) in Coastal Zones, in special to Pavel P. Povinec (Marine Environment Laboratory) and Kshitij M. Kulkarni (Isotope Hydrology Section). We wish to thank the personnel at the marine laboratory of the University of São Paulo, and other investigators who were very helpful during the sampling campaigns. P. da Costa, A. Elísio, K. Almeida e Keila Cristina Pinheiro assisted in the field work and laboratory. Financial support was provided by International Atomic Energy Agency Research Contract 12151, and by Fundação de Amparo à Pesquisa no Estado de São Paulo – FAPESP, project n° 2002/08154–9. Logistical support was provided by Instituto de Pesquisas Energéticas e Nucleares – IPEN and Instituto Oceanográfico da Universidade de São Paulo – IOUSP.

REFERENCES

[1] JOHANNES, R.E., The ecological significance of the submarine discharge of groundwater, Mar. Ecol. Pro. Ser. **3** (1980) 365–373.

[2] BURNETT, W.C., KIM, G., LANE–SMITH, D., A continuous radon monitor for assessment of radon in coastal ocean waters, J. Radioanal. Nucl. Chem. **249** (2001) 167–172.

[3] BUDDEMEIER, R.W., Groundwater flux to the ocean: definitions, data, applications, uncertainties, In: Buddemeier, R.W. (ed), Groundwater Discharge in the Coastal Zone, Proc. Int. Symp. LOICZ IGBP LOICZ/R&S/96–8, iv+179pp, LOICZ, Texel, The Netherlands (1996) 16–21.

[4] RUTKOWSKI, C.M., BURNETT, W.C., IVERSON, R.L., CHANTON, J.P., The effect of groundwater seepage on nutrient delivery and seagrass distribution in the northeastern Gulf of Mexico, Estuaries **22** (1999) 1033–1040.
[5] CABLE, J.E., BURNETT, W.C., CHANTON, J.P., WEATHERLY, G.L., Estimating groundwater discharge into the northeastern Gulf of Mexico using radon-222, Earth Planet. Sci. Lett. **144** (1996) 591–604.
[6] CORBETT, D.R., CHANTON, J., BURNETT, W.C., DILLON, K., RUTKOWSKI, C., FOURQUREAN, J., Patterns of groundwater discharge into Florida Bay, Limnol.Oceanogr. **44** (1999) 1045–1055.
[7] CORBETT, D.R., KUMP, L., DILLON, K., BURNETT, W., CHANTON, J., Fate of wastewater-borne nutrients in the subsurface of the Florida Keys, USA. Mar. Chem. **69** (2000) 99–115.
[8] MOORE, W.S., Large groundwater inputs to coastal waters revealed by ^{226}Ra enrichments, Nature **380** (1996) 612–614.
[9] MOORE, W.S., Application of ^{226}Ra, ^{228}Ra, ^{223}Ra, and ^{224}Ra in coastal waters to assessing coastal mixing rates and groundwater discharge to oceans, Earth Planet. Sci. Lett. **107** 4 (1998) 343–349.
[10] MOORE, W.S., The subterranean estuary: A reaction zone of groundwater and seawater, Mar. Chem. **65** (1999) 111–125.
[11] RAMA, MOORE, W.S., Using the radium quartet for evaluating groundwater input and water exchange in salt marshes, Geochim. Cosmochim. Acta **60** (1996) 4645–4652.
[12] BRAGA, E.S., MULLER, T.J., Observation of regeneration of nitrate, phosphate and silicate during upwelling off Ubatuba, Brazil, 23°S, Cont. Shelf Res. **18** (1998) 915–922.
[13] MAHIQUES, M.M., Sedimentary dynamics of the bays off Ubatuba, State of São Paulo, Boletim do Instituto Oceanográfico, São Paulo **43** 2 (1995) 111–122.
[14] MESQUITA, A.R., Marés, circulação e nível do mar na Costa Sudeste do Brasil, Relatório Fundespa, São Paulo (1997).
[15] PEREIRA, E.B., HAMZA, V.M., FURTADO, V.V., ADAMS, J.A.S., U, Th and K content, heat production and thermal conductivity of São Paulo, Brazil, continental shelf sediments: a reconnaissance work, Chem. Geol. **58** (1986) 217–226.
[16] BROECKER, W.S., An application of natural radon to problems in oceanic circulation, In: Proc. Symp. Diffusion in the Oceans and Freshwaters, Lamont Geological Observatory, New York (1965) 116–145.
[17] MATHIEU, G.G., LUPTON, R.A., HAMMOND, D.E., System for measurement of ^{222}Rn at low levels in natural waters, Health Phys. **55** 6 (1988) 989–992.
[18] MOORE, W.S., Ages of continental shelf waters determined from ^{223}Ra and ^{224}Ra, J. Geophys. Res. **105** (2000) 22117–22122.
[19] OLIVEIRA, J., FARIAS, L.A., MAZZILLI, B.P., BURNETT, W.C., CHRISTOFF, J., BRAGA, E.S., FURTADO, V.V., Reconnaissance of submarine groundwater discharge at Ubatuba coast – Brazil, using ^{222}Rn as a natural tracer, J. Environ. Radioact. **69** (2003) 37–52.
[20] MOORE, W.S., ARNOLD, R., Measurement of ^{223}Ra and ^{224}Ra in coastal waters using a delayed coincidence counter, J. Geophys. Res. **101** (1996) 1321–1329.
[21] MOORE, W.S., SHAW, T.J., Chemical signals from submarine fluid advection onto continental shelf, J. Geophys. Res. **103** (1998) 21543–21552.
[22] BOKUNIEWICZ, H., TANIGUCHI, M., ISHITOBI, T., CHARETTE, M., ALLEN, M., KONTAR, E.A., Direct measures of submarine groundwater discharge (SGD) over a fracture rock aquifer in Ubatuba Brazil, Estuar. Coast. Shelf Sci. (2007) in press.
[23] BURNETT, W.C., PETERSON, R., MOORE, W.S., OLIVEIRA, J., Radon and radium isotopes as tracers of submarine groundwater discharge – Results from the Ubatuba, Brazil SGD assessment intercomparison, Estuar. Coast. Shelf Sci. (2007) in press.
[24] STIEGLITZ, T., TANIGUCHI, M., NEYLON, S., Spatial heterogeneity of submarine groundwater discharge, Ubatuba, Brazil, Estuar. Coast. Shelf Sci. (2007) in press.

DEVELOPMENT OF OPERATIONAL SYSTEM FOR MONITORING AND STUDYING GROUNDWATER DISCHARGE AND SEAWATER INTRUSION IN COASTAL ZONES

E.A. Kontar

Experimental Methods Laboratory (EML SIO)
P.P. Shirshov Institute of Oceanology
Russian Academy of Sciences, Moscow
Russian Federation

Abstract. One of the important challenges facing coastal zone managers today is how to identify, measure and monitor coastal submarine groundwater discharge (SGD) and seawater intrusion (SWI) and how to evaluate its influence on cumulative impacts of coastal land use decisions over distance and time. Several geochemical and geophysical techniques can help to solve the problem and provide direct or indirect monitoring of saltwater in coastal aquifers. We report here the results of a three dimensional (3D) geoelectrical survey carried out near the harbour in Donnalucata along the southeastern coast of Sicily. A geoelectrical survey and geo-mapping of the spatial distribution of the saltwater–freshwater interface in the coastal zone was conducted during the IAEA–SGD experiment in Sicily (IAEA SGD CRP 2001–2006). The Transient Electromagnetic Method (TEM) allows a subsurface sounding up to 300 m deep. This study shows the presence of two layers with various types of salt mineralization of subsurface waters in the coastal zone of Donnalucata. Geoelectrical data were taken for two subsurface layers with different types of subsurface water: resistivity = 5.37 Ω·m and with mineralization of the groundwater between 2000 – 2500 mg/L (basic water–saturated horizon from 5 to 15 m deep), and a second zone (depths from 50 to 70 m deep) with resistivity = 3.32 Ω·m and mineralization of groundwater between 4500 – 5000 mg/L. Analysis of the geoelectrical data has shown that there is a zone of maximum discharge located in the channel between two piers of the harbour. This maximum discharge reflects the existence of a known specific local karstic groundwater phenomena off the coastal zone of Donnalucata, which was confirmed with the method presented here. The geoelectromagnetic data confirmed the observations made by seepage meters and *in situ* measurements of ^{222}Rn concentration and salinity, which showed at some places high seepage rates of recirculated seawater. Although overuse and contamination of groundwater are not uncommon throughout Sicily the proximity of coastal aquifers to saltwater creates unique issues with respect to groundwater sustainability in coastal region of Donnalucata. These issues are primarily those of possible SW into freshwater aquifers and changes in the amount and quality of fresh groundwater discharging to coastal saltwater ecosystems. The work has been carried out in the framework of the IAEA's coordinated research project on 'Nuclear and Isotopic Techniques for the Characterization of Submarine Groundwater Discharge in Coastal Zones'.

1. Introduction

One of the important challenges facing coastal zone managers today is how to identify, measure and monitor groundwater discharge and seawater intrusion and how to evaluate its influence on cumulative impacts of coastal land use decisions over distance and time [1–4]. Understanding the multivariable dimensions of groundwater management in coastal zones can be improved through the application of innovative information technologies (the application of neural networks to data analysis, optimization, pattern recognition, image identification, etc.) and by using new generations of non-invasive techniques for groundwater exploration [5–7], which can be successfully combined with nuclear and isotopic techniques [4] and will help to understand the results obtained using these techniques [1, 2].

This report is a result of research conducted by a team of Russian scientists (E.A. Kontar, L.I. Lobkvsky, I.A. Garagash, I.Ya. Rakitin, Yu.R. Ozorovich and F.A. Babkin). According to our opinion, further development of electromagnetic sounding as a geophysical method [8–11] in combination with nuclear and isotopic techniques for investigation of SGD [4] is a useful subject for this type of research, because this method can provide clear understanding of the fluctuation of the interface between freshwater and groundwater in the coastal zone over temporal and spatial dimensions.

We proposed a principally new operative monitoring system, the MARSES TEM system, which has certain abilities and advantages that are defined by its multifunctional methodological application that

can be used as an operative system for water search tasks (groundwater table), definition of waste levels, and monitoring changes in subsurface horizons, etc. Also this system can be applied to solve long term tasks for monitoring natural subsurface ecosystems, subsurface horizons, soil salinity levels, salinity gradients, and groundwater levels. All of these parameters can be used to track seasonal and climatic changes in selected coastal areas. The distinctive difference in our proposed coastal monitoring system is measurement of soil humidity along the coast at all depths down to the groundwater level. It is not possible to detect these subsurface horizon humidity parameters by any other monitoring means, such as observation wells or ground digs, etc.

The goal of our contribution aims at obtaining a fundamental understanding of the physical and chemical processes taking place at the dynamic of subsurface freshwater/seawater interface by carrying out detailed studies on a small scale, at one or two sites in a coastal area. This should provide a conceptual framework for understanding the effects of these processes on a larger scale and over longer periods of time. A fundamental understanding of the processes involved is presently not available. Insight into the controlling processes and the development and testing of a coupled variable density flow, multi-species transport, and reaction code will increase the possibilities for sustainable management of coastal aquifers.

At the current moment there is a standalone portable non-invasive subsurface research instrument available. The instrument is based on TEM measurement technology. It is capable of measuring the resistivity of subsurface slices up to 100 – 150 m and works with a stock IBM compatible portable computer using a serial interface. Brief technical details of the instrument are as follows:

- weight: 1.5 kg; size (mm): 103×27×310
- working temperature: –20ºC to +65ºC
- power consumption: more that 50 measurements at maximum depth.

During 2002 we conducted two successful field tests of the MARSES TEM system: in Sicily, Italy and on Long Island, USA. In this report we will discuss the results obtained during the experiment in Sicily.

2. Research Background

In the course of cooperation within the framework of Russian space research missions devoted to the exploration of Mars, soil slice conditions were found to be similar to Earth's arid and semi-arid lands, and compact, light and reliable instruments known as the MARSES TEM were developed for subsurface sounding and mapping applications. More specifically, these instruments relate to methods for mapping, tracking, and monitoring: groundwater, groundwater channels, groundwater structures, subsurface pollution plumes, mapping interconnected fracture or porous zones, leaks in earthen dams, leaks in drain fields, monitoring changes in subsurface water flow, changes in ion concentration in the groundwater, monitoring *in situ* leaching of solutions, movements of heap leaching solutions, changes in subsurface redox or reaction fronts, underground chemical reactions, subterranean bio-reactions, or other subsurface water and related geological structures. Our recent research work has been devoted to the development of the newest technologies for monitoring subsurface processes in coastal zones and has revealed significant comparative advantages. The major advantages are:

(1) Flexible software development technology gives an opportunity to adapt this monitoring system to solve different tasks: monitoring of groundwater discharge, identification of saltwater intrusion and groundwater level, etc.

(2) At the present time the geophysical equipment and instrumentation market does not have similar systems for non-invasive exploration of subsurface ecosystems. The system we present has been developed on the basis of space mission technologies and stringent requirements in its hardware and software.

(3) A distinctive feature of this flexible architecture (that closely correlates to sustainable development) gives an opportunity to build a system by using unified instrumentation and special software for resolving particular monitoring tasks.

(4) These advantages in system monitoring make possible the development of integrated monitoring systems for different urban, dry land, arid and semiarid coastal zone lands.

(5) Usage and maintenance simplicity in the automatic mode and the possibility of exchanging working modules along service procedures provides an opportunity to apply this system in any region with no need to develop a service and maintenance station network. The estimated rate of guaranteed constant work is up to 5 years.

(6) A high degree of accuracy for reconstructed teal thermodynamic, as well as physical and geological parameters acquired during measurements of geoelectric slices makes the MARSES TEM system one of the most competitive and innovative for further development and use for monitoring and studying groundwater discharge and seawater intrusion in coastal zones.

3. Modernization and Testing of the MARSES TEM System

3.1. Theory

The physical and mathematical bases of TEM are described fully and sufficiently in the literature (for example, F. Kamenetsky (in Russian) 'Electromagnetic geophysical researches' Moscow, GEOS, 1997). Here we shall state only the basic aspects of the theory having direct relation to the technology of soundings with TEM–FAST 48.

One of the few models of media, for which the formulas, simple and accessible to the analysis of TEM signals are received, is the model of the homogeneous half-space. For understanding and estimation of opportunities with the TEM we shall consider asymptotic estimation of signals for late and early stages. The late stages of transient $t = t/(\mu R^2/\rho) >> 1$ for one-turn, round antennas R and r, lying above the homogeneous half-space with resistivity ρ and magnetic permeability of vacuum μ, are described by the formula:

$$E(t)/I = 0.05*(\pi^{1/2}\mu^{5/2})/\rho^{3/2}(r^2R^2)\, t^{-5/2} \qquad (1)$$

The registered signal is proportional to conductivity $\sigma^{3/2} = 1/\rho^{3/2}$ and to product R^2r^2. Thus, in TEM the amplitude of signals at late stages is rather sensitive to changes of conductivity of the section in comparison, for example, with methods of direct current. Besides, the signals E(t)/I at $t/(\mu R^2/\rho) >> 1$ do not depend on a site of receiving loop r<R. The formula (eq.1) is true as well at a height h above the surface of the half-space of antennas. At late stages of transience, the signal, registered in the receiving antenna, is caused by currents induced in the current's ring inside section with effective radius R_{eff} and 'attitude' depth $H_{eff} \sim R_{eff}$. $R_{eff} = (t\rho/\mu)^{1/2}$, some times exceeding the radius of the transmitting loop $R_{eff} >> R$ (Fig.1).

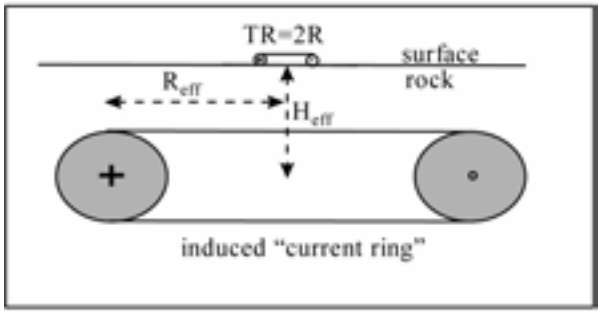

FIG.1. Electromagnetic subsurface sounding.

The vertical magnetic field created by this contour is practically homogeneous within the limits of its area at $h<R_{eff}$, therefore registered signals proportional to derivative of magnetic field over time, do not depend on the site of their receiving. This property of late stages TEM determines the high depth of researches in a combination with good resolution of the method ($E \sim\sigma^{3/2}$). Early stages of transient $t_0<<1$ for the coincident antennas R = r do not depend on the resistivity of media:

$$E(t)/I = \mu R/(2t) \quad (2)$$

At early stages ($t_0<<1$) for small receiving antennas $r/R <<1$ the signals are proportional to specific resistivity of media ρ and do not depend on time t:

$$E(t)/I = 3\pi\rho\ (r^2/R^3) \quad (3)$$

3.2. Monitoring

The MARSES TEM sounding instruments are based on time domain electromagnetic sounding technology. MARSES TEM is portable, reliable geoelectrical sounding instruments made to satisfy small space requirements for simple and intuitive usage.

The depth of subsurface sounding is from 300 – 500 m using TEM technology. Areas of application are of groundwater, prospecting deposits, hydrogeological research, geological surveys, required before construction of buildings, ecological research, archeological and subterranean objects search, monitoring of high risk industrial and engineering objects, research and testing of rock samples.

The structure of this monitoring system organization is outlined in Fig.2. A number of MARSES instruments should be placed in the coastal zone of ecological hazard to provide measurements in the areas of interest. Using a radio system it will be possible to transmit data to headquarters, where the data will be processed and stored for future use and reference. Using modelling and visual presentation software it will be possible to make the information visual through graphs, charts, time variation and other easy to understand formats of the monitored area.

The significant advantage of this system in comparison to known ecological hazard monitoring systems is its cost effectiveness. It does not require expensive satellite monitoring of the coastal zone or employment of satellites in data transfer. Another advantage is its compact and ready-to-use nature that allows rapid measurements at any required area. Moreover, the cost of this device is less than competitors'.

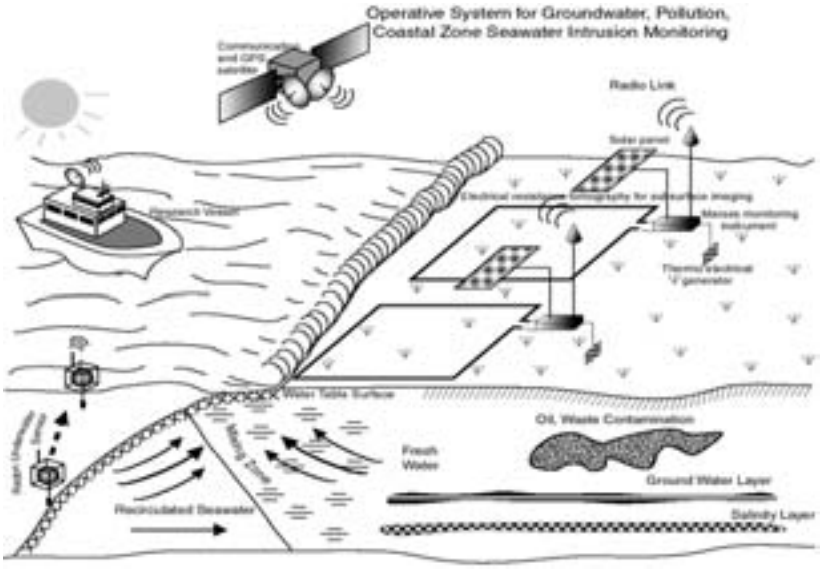

FIG.2. The coastal zone subsurface monitoring system organization structure.

In contrast to many competitors' instruments with similar areas of application, MARSES TEM has exceptional advantages among small depth sounding devices. Because the MARSES TEM hardware was developed to be employed in space research missions it possesses a unique portability and is dramatically low in weight. It fits inside a suitcase, with antenna, supporting notebook, batteries and all. Usage of a PC notebook for data processing makes it easier to view the results, process them, prepare reports and send them to headquarters. MARSES TEM supplies reliable data in areas with high EM distortions (about 1V and higher), such as in industrial zones and on urban streets. Sounding parameters can be easily adjusted from the PC.

At the present moment there is no mobile operative monitoring system based on non-invasive technology and methodology. Thus development of these innovative monitoring systems has high potential and broad perspectives for application.

As this system was developed within the framework of space research missions, it possesses unique methodological and technological features and advantages in comparison to other monitoring systems based on different principles and methods.

4. Preliminary Results of Tests

During the first year of the contract we conducted two field tests of the MARSES TEM system: in Sicily, Italy (March 2002) and on Long Island, USA (May 2002). A distinctive feature of the experiments with sounding of the subsurface horizons was the realization of simultaneous measurements of the geoelectrical sections at two points 70 m apart for the various cycles of a tidal wave over a period of several days. These measurements for the first time have revealed spatial and time variability of the saltwater/freshwater interface, and indicate the effect of complex transformation of the salt and fresh water interface in a coastal zone. The preliminary analysis of the time variation of the geoelectrical section shows high correlation with the daily tide and nonlinear transformation of the boundary of the saltwater/freshwater interface in the process of its spreading offshore.

5. Geophysical Survey of the Saltwater – Freshwater Interface and Sea Spring Zone in the Marina di Ragusa Area, Sicily, Italy

5.1. Hydrogeology of the Marina Di Ragusa beach study area

The Marina di Ragusa beach study area (Fig.3) is located in the south portion of Sicily Island. The study of the geological characteristics of the territory has allowed us to identify the aquifer that supplies the emptying into the sea along this stretch is Sicilian coastline exactly. It is a carbonatic aquifer in which karstic phenomena have taken on a determining function in conditioning underground water circulation that locally assumes artesian characteristics. A second alluvial aquifer has also been pointed out that is partly supplied through lateral contact and through artesianism by deep aquifer.

The links between tectonics first morphology and underground circulation are then evident. The supply of the main deep aquifer occurs on the Hyblaean relief. The frequent presence in the carbonatic series, made up of outcrops of marly or argillaceous–marly interbeds, determines impermeable levels and clears the frequent presence of contact springs in the basins in the area. The calculations carried out allowed us to assess the entity of the effective infiltration in the territory's different areas according to the nature of the terrain and the climatic conditions and the entity of the river waterbed interchanges which have revealed themselves to be determining in quantifying the supply volume of the aquifers.

5.2. Measurements of the spatial distribution geoelectrical sections of the saltwater/freshwater interface

The geophysical survey area (Figs 3 and 4) was situated along Mole I (axis Y) and the coastal line (axis X) : Pier Well #1, #2, #3 were in an internal area of sounding antennas (sounding antennas were

in the form of square ordinary wire – 60×60×60×60 m, the length of one side of square is 60 m). Along an axis Y the mole, which actually has divided two zones of measurement, is located. Along an axis X the coastal line is located. Geophysical measurements were carried out in a zone between a Mole I, a coastal line and road which closed the study area from the city's building in the north side.

FIG.3. Photo of survey area on Marina Di Ragusa, Donnalucata, Sicily.

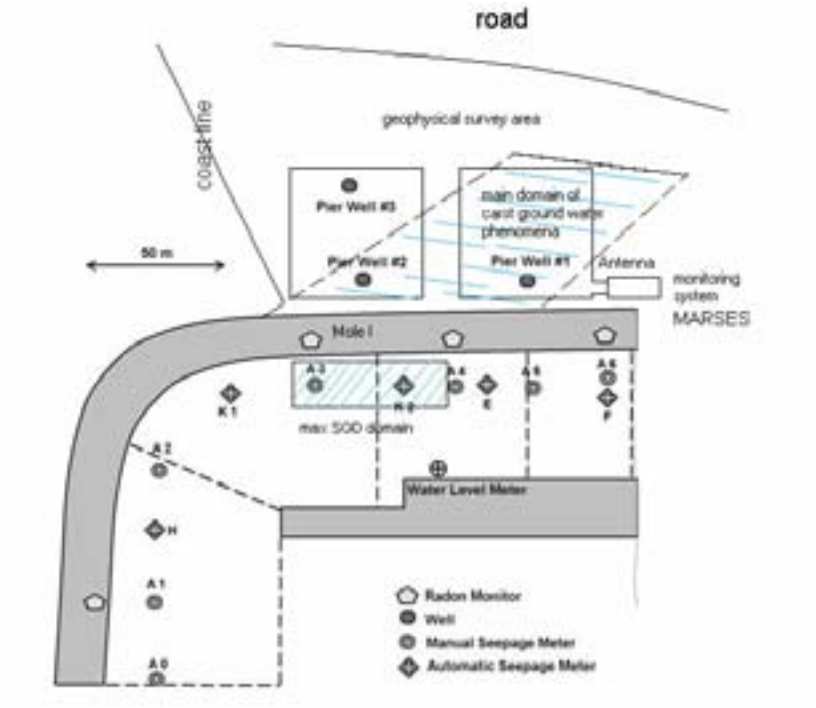

FIG.4. Geophysical survey area and locations of manual and automated seepage meters.

A distinctive feature of the experiment with sounding of the subsurface horizons on Sicily Island was the realization of measurements of the geoelectrical sections for three dimensional (3D) geological section study area.

The analysis of the 3D structure of the geoelectrical data (Figs 5 to 8) shows the presence of two horizons with various mineralizations of subsurface waters. The first horizon begins with a depth approximately 1–5 m, with the basic water–sated horizon from 5 up to 15 m with mineralization of subsurface water in order to 2000 – 2500 mg/L. The given zone can be considered as a typical saltwater interface zone.

The second horizon at depths from 50 up to 70 m represents a typical karstic horizon with a mineralization of subsurface waters in order to 4000 – 5000 mg/L distinct from the first horizon – the top horizon of survey area. The given horizon is a typical source for sea springs phenomena. The presence of the sea springs were shown as well in measurements in a coastal zone with the use of isotopic techniques.

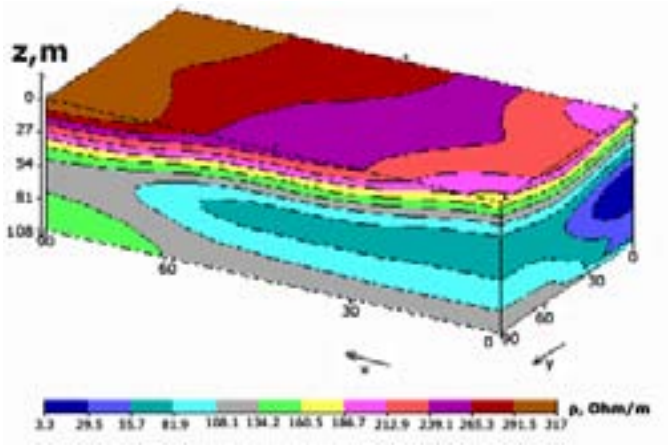

FIG.5. This 3D geoelectrical image shows all geoelectrical structures of the study area. The mole is parallel along an axis Y, the coastal line is along an axis X. The blue horizon is the main stream subsurface flow as karstic phenomena.

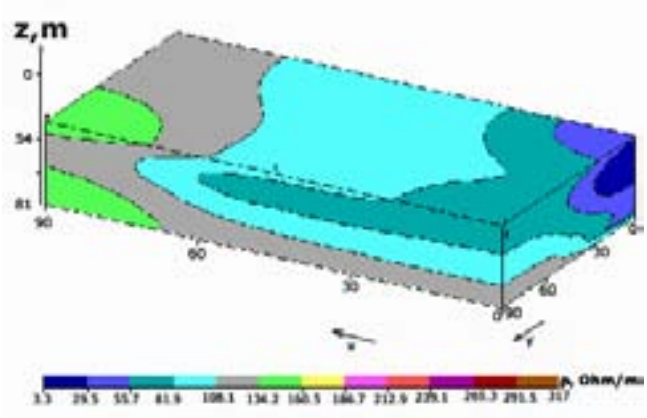

FIG.6. The same 3D image of geoelectrical section without upper part this study area.

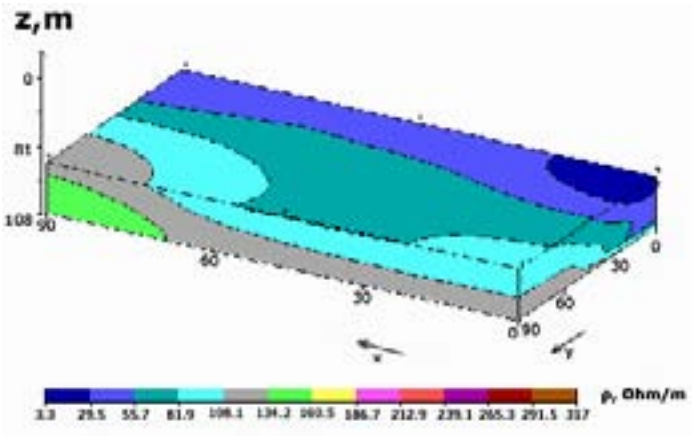

FIG.7. The 3D image of geoelectrical section of the lower part subsurface study area.

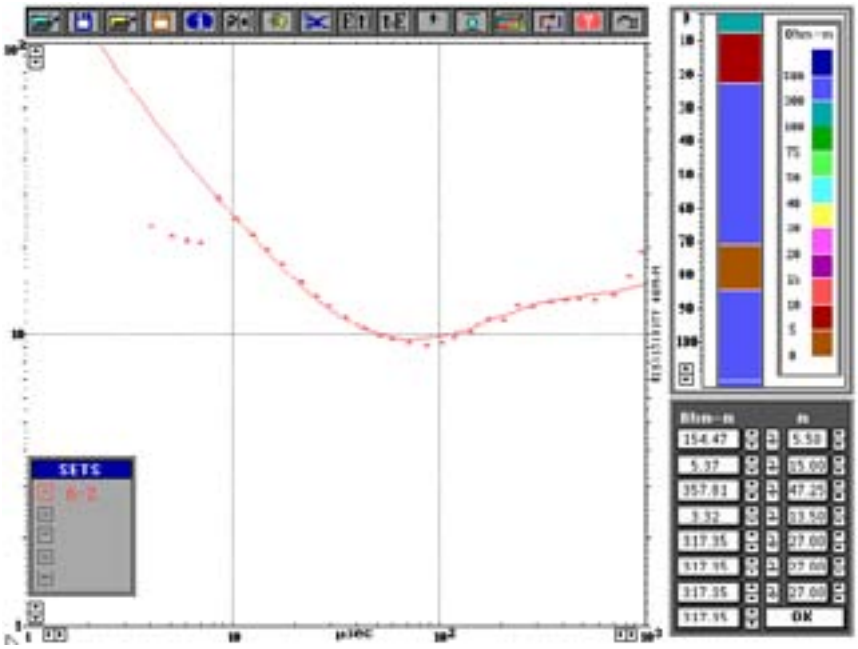

FIG.8. In this figure is shown the example of real sounding curve – geoelectrical section of one of study field point. On the right side of this picture is the result of inversion solution this curve and transform to formation resistivity of different subsurface layers. In this picture the geoelectrical data have been given with two subsurface zones with different subsurface water: resistivity = 5.37 Ω·m and with mineralization in groundwater in order of 2000–2500 mg/L (basic water saturated horizon from 5 up to 15 m depth), and second zone (depths from 50 up to 70 m) with resistivity = 3.32 Ω·m and mineralization in groundwater in the order of 4500–5000 mg/L.

5.3. Relations between formation resistivity and specific conductance

An example of inversion solution transferred from geophysical data to physical parameters has been done by Fitterman. [7,8] for a study area in Florida and on the base model development and laboratory measurements sand probes from the study area in Marina Di Ragusa, Sicily, 2002. Archie's law relates the electrical resistivity of water saturated rocks (ρ_f) to the resistivity of the contained pore water (ρ_o) through the formation factor $F = \rho_f / \rho_o$. The formation factor accounts for the influence of porosity on the electrical resistivity. If the formation factor can be estimated from borehole measurements, then formation resistivity values obtained from interpretation of surface and laboratory geophysical measurements of the sample soils can be used to estimate the specific conductance (SC) of the pore fluid and mineral geological formation. If, in addition, the relationship between specific conductance and chloride concentration is known, then the chloride concentration of the formation can be estimated from the geophysical data. Laboratory measurement of water samples provides a means of determining this latter relationship (Fig.9).

To estimate the formation factor, induction logs were measured in a total of 23 existing and specially drilled boreholes in the study area. This provided very detailed resistivity–depth information. The formation resistivity was averaged over the screened interval of the wells (typically 10 ft). The wells were then pumped and a water sample collected after sufficient time for the well bore to be purged. The specific conductance of the sample was measured. For shallow wells the conductivity was directly measured in the well.

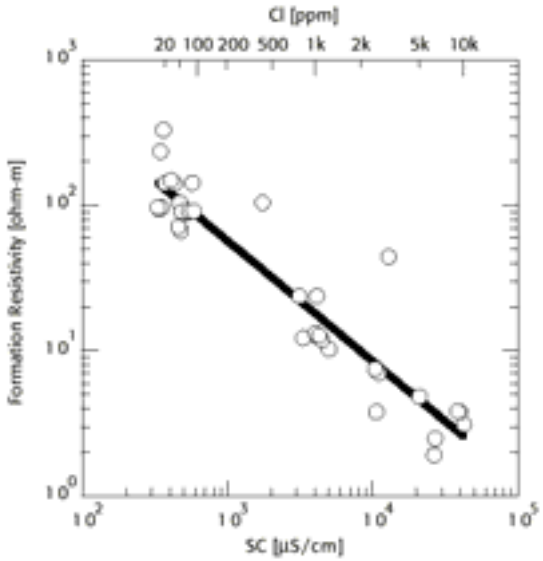

FIG.9. Relationship between formation resistivity, pore water conductivity and chloride content based on induction logs and water sample measurements. Relationship valid for the surficial aquifer in the study [6].

The data for all of the measured wells is shown in Fig.9. Both the formation resistivity and SC span over two sets of measurements gives a good range of values for developing a correlation. Due to the inherent scatter in the data, the pore water conductivity is estimated from the formation resistivity with an uncertainty of a factor of 2–3. While this uncertainty is much larger than expected for conductivity probe or laboratory measured values, it is adequate for use in regional scale aquifer studies where the value of SC would be interpolated between wells that are 10 or more km apart. Some of this uncertainty stems from the fact that the wells are from a wide range of depths with some of the deeper wells being below the study aquifer. Thus there are some differences in the geologic units, though all wells were screened in porous zones, which were good water producers.

From induction logs, which measure formation resistivity and measurements of water conductivity, both in the borehole and from samples pumped from the wells, the following relationship was established:

$$SC = 81200\rho_f^{-1.062} \quad (4)$$

where SC is the specific conductance in µS/cm and ρ_f is the formation resistivity in Ω·m. This relationship (Fig.9) can be used to convert interpreted layer resistivity to SC of the saturating pore fluid.

Often chloride ion concentration is of interest to hydrogeologic modelers. To convert specific conductance to chloride ion concentration we use a relationship established for surface waters shown in Fig.9. The specific conductivity increases nonlinearly with chloride concentration for chloride levels below 650 ppm. At higher chloride concentrations, the relationship becomes linear. Using the local data for SC–Cl relation and equation (1.4), the ρ_f– Cl graph in Fig.10 was generated.

The chloride ion concentrations of fresh and saline groundwaters are usually quite different resulting in large differences in formation resistivity for fresh and saline saturated geologic materials. The graph shown in Fig.10 provides a way of estimating chloride levels from inverted TEM data, however, it must be stressed that this relationship is based upon an assumption that ground water in the area has the same SC–Cl relationship as surface water. This is a reasonable assumption as the source of Cl is most likely from seawater for both ground and surface water. Because of its statistical nature there is

some uncertainty in eq.(4), and consequently in the formation–resistivity–chloride relationship. Nonetheless, this relationship is useful provided its limitations are understood.

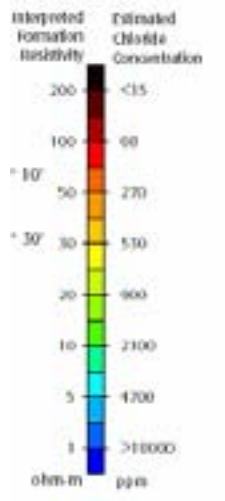

FIG.10. Empirical relationship between formation resistivity and chloride concentration of pore water on the basis of [7, 8] interpretation results.

Using the above results for the comparative analysis of the data and techniques on the basis of modeling development and laboratory measurements of soil probes the following dependencies which enable connection of the data on geophysical sounding directly with salinity and porosity subsurface horizons were received in a model relationship (Figs. 11, 12).

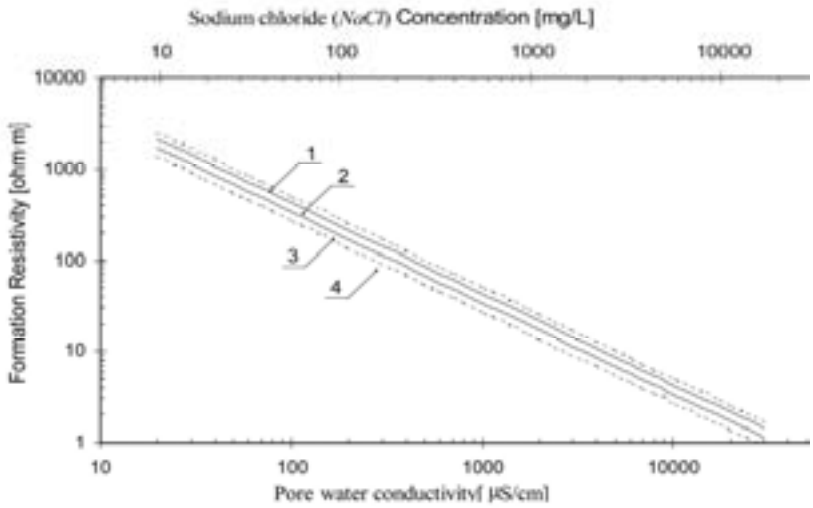

FIG.11. Model relationship between formation resistivity [Ω·m], pore water conductivity [μS/cm], and sodium chloride content [mg/L] in pore water for fractionary (0.25 < d < 0.5 mm), full water saturated sands based on laboratory resistivity measurements sand probes from study area (Marina Di Ragusa study area) in frequency range 0.3 – 10 MHz for different pore coefficient K: 1 - $K_П$ = 30%; 2 - $K_П$ = 35%; 3 - $K_П$ = 42.5%; 4 - $K_П$ = 50%.

More detailed description and comparative analysis of the given model development and laboratory measurements for interpretation results of geophysical sounding will be submitted in the second part of the given work.

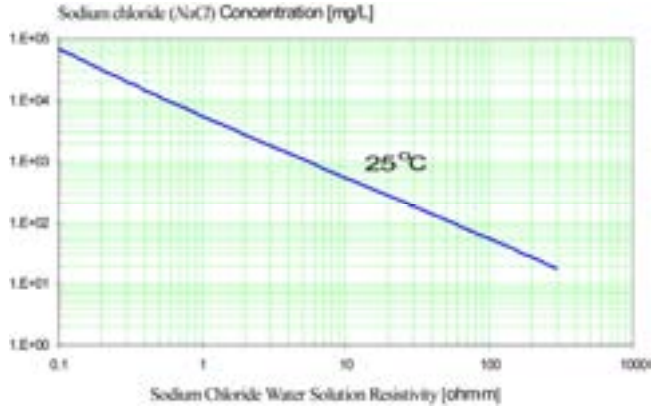

FIG.12. Relationship between pore water resistivity (Ω·m) and chloride content (mg/L) on the base model performance and laboratory measurements of sand probe from study area in Marina Di Ragusa.

5.4. Laboratory geophysical measurements

Laboratory geophysical measurements refer to the empirical characterization of physical rock properties such as porosity and permeability and their relationship to other physical rock properties that are directly measured on the field sites. As a rule, this measurement was provided on the special laboratory device with detecting resistivity of the sample soil from study area with dependence from frequency in the range from several kHz up to 1 MHz.

6. Techniques and Method of Measurements

Measurements were carried out by a method of a variation of interelectrode distances at two frequencies of electromagnetic field – 300 kHz and 1 MHz measurement condenser with varied of interelectrode distance for definition resistivity and dielectric constant in the frequency range of 30 kHz to 500 MHz (Fig. 13).

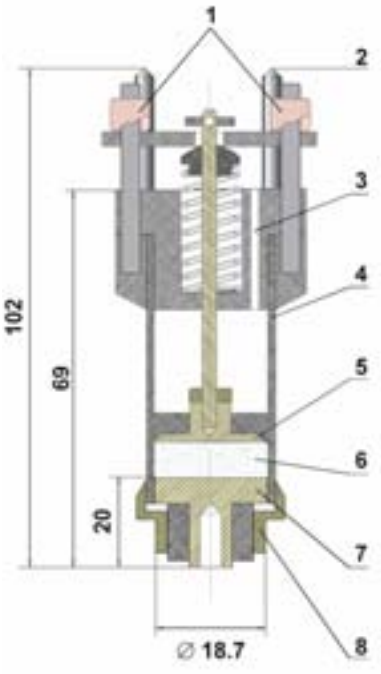

1. Press nuts
2. Support for installation of a micrometer
3. Aperture for selection of a superfluous liquid
4. The glass cylinder
5. Mobile electrode
6. Measurement sample of soil
7. Non-mobile electrode
8. Protective electrode.

FIG.13. Measurement condenser with varied of interelectrode distance for definition resistivity and dielectric constant in the frequency range 30 KHz – 500 MHz.

7. Results of Laboratory Measurements and Calibrations

Results of laboratory measurements for dielectric permittivity and formation resistivity for sand probes from study area in Marina Di Ragusa are introduced in Figs. 14 and 15.

Sample # 2a (Fig. 14) is a selected sample of sand with initial volumetric humidity (31.4%), which is appropriate to the place where this sample was collected.

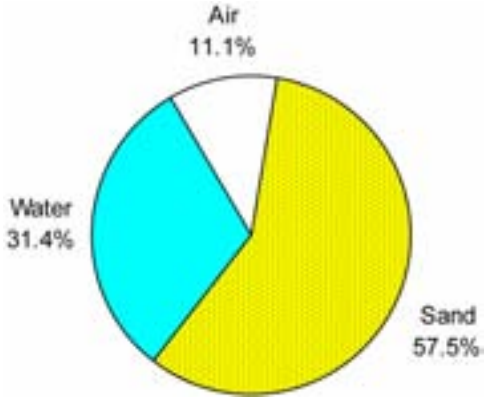

Table: Sample #2a.		
Factor of porosity, %	42.5	±0.4
Volumetric humidity, %	31.4	±0.3
Weight humidity, %	20.6	±0.3
Dielectric permittivity, rel.units. Frequency 1 MHz	19.3	±0.5
Formation resistivity, ohm·m. Frequency 1 MHz	47.2	±0.5
Dielectric permittivity, rel.units. Frequency 300 kHz	19.7	±1.7
Formation resistivity, ohm·m. Frequency 300 kHz	47.2	±0.6

FIG.14. System composition for sample 2a.

Sample #2b (Fig.15) is the selected sample of sand with volumetric humidity (38.8 %), which is appropriate to conditions of full water-pore content.

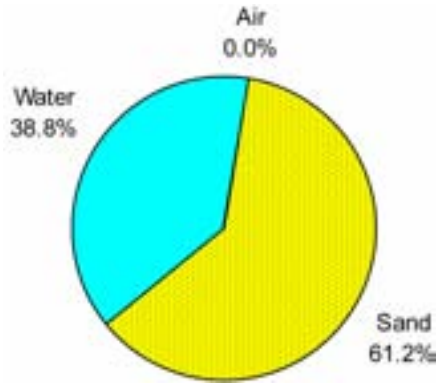

Table 2: Sample #2b.		
Factor of porosity, %	38.8	±0.2
Volumetric humidity, %	38.8	±0.2
Weight humidity, %	23.9	±0.1
Dielectric permittivity, rel.units. Frequency 1 MHz	24.2	±0.7
Formation resistivity, ohm·m. Frequency 1 MHz	36.9	±0.5
Dielectric permittivity, rel.units. Frequency 300 kHz	26.3	±5.3
Formation resistivity, ohm·m. Frequency 300 kHz	37.1	±0.7

FIG.15. System composition for sample 2b.

From the above modeling representation and laboratory measurements dependences presented on Figs.14 and 15, the estimated data on salinity and porosity of the given horizons on the basis of measured formation resistivity were obtained. This given complex of model representation and laboratory measurements of samples of soil combined with field measurements formation resistivity allows construction of the estimated dependence formation resistivity from the chloride component and porosity of soil for subsurface horizons in the sounding area.

8. Comparative Study and Estimation of Total Groundwater Discharge

Analysis of the geophysical data shows the reason for the increase of maximum discharge in the domain of measurements A3–A4, revealed according to the results obtained by all methods and different tools used in the offshore zone in the channel between the two piers (see Fig.4). This maximum discharge reflects the specific geological structure in the display of karstic groundwater phenomena. Thus geophysical exploration has allowed observation of the source and structure of this phenomenon and has enabled an estimation of the total discharge in the offshore zone, and the degree of salinity of the given horizon. As a result of the construction of ‘Mole I’ the zone of superficial

groundwater was changed, i.e. the mole has blocked a superficial drain. It can be seen as an example of the infringement of balance in a natural ecosystem and its change due to the construction of the mole. From the given laboratory measurements and tests of sand probes in zones Well 2 and Well 3 the values of resistivity ~47 Ω·m were received. We may determine the value of the salinity and conductivity of the pore water in this test probe of sand, which approximately equals to salinity ~500 mg/L and to the conductivity of the pore water ~1000 μS/cm (the typical aquifer water conductivity at the top of the survey area is 450, 500, 600 μS/cm).

This data is very close to the measured conductivity of pore water (~17, 22, 6 mS/cm) and salinity (~0.03 g/mL) in this zone as obtained by the MEL–IAEA group. Consequently in future comparative experiments it is necessary to specify the processes of reception of these data and the technique of their measurement.

From the SGD measurements obtained by seepage meters (see the report of M. Taniguchi) the SGD data obtained ranges from 5.5 to 19.3 L/min·m in the study area (with the average of 12.1 L/min·m).

The maximum discharge of groundwater and SGD measured by seepage meters was in the area of measurement points A3–A4. Also this area coincides with the subsurface zone of maximum groundwater discharge reflected by data from our geophysical measurements.

The summary of estimations of the groundwater discharge area is preliminary S = 60 m × 15 m and the estimated total groundwater discharge in this area is 12000 – 16000 L/min·m^2.

9. Conclusions

Further development of electromagnetic sounding as a geophysical method in combination with nuclear and isotopic techniques for investigation of SGD is a useful subject for this type of research, because this method can provide clear understanding of the fluctuation of the interface between freshwater and groundwater in the coastal zone over time and spatial dimensions. Potential directions for field geophysical methods include the development of improved interpretation techniques, particularly for three-dimensional interpretation and integration with other data sets and the development of survey techniques for high-resolution measurements of geoelectrical slices of small study areas using simultaneous measurements with four sounding loops for spatial and temporal surveys in 3D geoelectrical section.

Additional methodical measurements are necessary for the reception of complex geoelectrical data study area with physical and chemical parameters of subsurface horizon in the field sites, which include:

- Chloride content based on water sample measurements at the field sites.
- Measurements of resistivity in the upper level of the sounding area and the conductivity directly on induction logs measured in the well.
- Laboratory measurements of resistivity of soil samples from the sounding area.

After implementation of all the requirements stated above we have an opportunity to construct closed measures in saltwater interface, which will allow connection between data of isotope and geophysical measurements *in situ*. This method will allow for the expansion of information on spatial and temporal variations in the saltwater interface, its structural and geological properties, which are not possible to obtain in a different way. At the present time there is no method for adequate and direct measurement of porosity, salinity and resistivity of soil on subsurface horizons *in situ*. For this reason these given methodical and experimental tasks for the exploration of the saltwater interface using different field instrumentations represents an important direction for future research for comparative studies in SGD and saltwater interaction, and vadose zone flow processes, pollution determination and monitoring of the coastal zone.

ACKNOWLEDGEMENTS

The authors would like to thank Pavel P. Povinec, Jean Comanducci and B. Oregioni (IAEA Marine Environment Laboratory, Monaco) for operative support during the expedition in Sicily. We are grateful to Pradeep K. Aggarwal and Kshitij M. Kulkarni (Isotope Hydrology Section of the IAEA) for the tremendous cooperation and their very useful critical comments, which helped us to improve the report.

REFERENCES

[1] KONTAR, E.A., OZOROVICH, Y.R., SALOKHIDDINOV A., AZHIGALIYEV Y.B., Study of Groundwater–Seawater Interactions in the Aral Sea Basin, Proc. Int. Conf. Low-lying Coastal Areas – Hydrology and Integrated Coastal Zone Management, 9–12 September 2002, Bremerhaven, Germany (2002) 225–230.

[2] BURNETT, W.C., CHANTON, J., CHRISTOFF, J., KONTAR, E.A., KRUPA, S., LAMBERT, M., MOORE, W., O'ROURKE, D., PAULSEN, R., SMITH, C., SMITH, L., TANIGUCHI, M., Assessing Methodologies for Measuring Groundwater Discharge to the Ocean, EOS **83** (2002) 117–123.

[3] KONTAR, E.A., Submarine Monitors and Tracer Methods for Investigations of Groundwater Discharge into the Coastal Zone, Proc. 34th Int. Liege Colloquium on Ocean Dynamics, Liege, (2002) 30.

[4] KONTAR, E.A., BURNETT, W.C., POVINEC, P.P., Submarine Groundwater Discharge and Its Influence on Hydrological Trends in the Mediterranean Sea, Proc. CIESM Workshop: Tracking long term hydrological change in the Mediterranean Sea, Monaco (2002) 109–114.

[5] STEWART, D.C., ANDERSON, W.L., GROVER T.P., LABSON V.F., Shallow subsurface mapping by electromagnetic sounding in the 300 kHz to 30 MHz range: model studies and prototype system assessment, Geophysics (1994) 1201–1210.

[6] OLHOEFT, G.R., Electrical properties from 10 – 10^9 Hz – physics and chemistry, 2nd Int. Sym. Physics and Chemistry of Porous Media, Schlumberger Doll (986).

[7] FITTERMAN, D., DESZCZ–PAN, M., STODDARD, C.E., Results of Time–Domain Electromagnetic Soundings in Everglades National Park, Florida, US Geological Survey Fact Sheet OFR (1999) 99–426.

[8] FITTERMAN, D., Geophysical mapping of the freshwater/saltwater interface in Everglades National Park, Florida, US Geological Survey Fact Sheet FS–173–96 91996).

[9] OZOROVICH, Y.R., LINKIN V.M., SMYTHE W., Mars Electromagnetic Sounding Experiment – MARSES, Proc. LPI Conf., Houston (1999).

[10] OZOROVICH, Y.R., et al., Geomonitoring shallow depth structure and groundwater by MARSES TEM instrument, Proc. SEG Conf., Houston (1999).

[11] OZOROVICH, Y.R., et al., Operational system for groundwater, salt/water intrusion and pollution determination and monitoring, Proc. Conf. New Paradigms for the Prediction of Subsurface Condition – Euro Conference on the Characterisation of the Shallow Subsurface: Infrastructure and Assessment, Spa, Belgium (2001).

RADIUM ISOTOPES AS TRACERS OF COASTAL MIXING AND SUBMARINE GROUNDWATER DISCHARGE

W.S. Moore

Department of Geological Sciences,
University of South Carolina,
Columbia, South Carolina, United States of America

Abstract. This report details the use of four naturally occurring isotopes of radium in investigations of submarine groundwater discharge (SGD) and other applications in coastal oceanography and hydrology. The focus is an evaluation of estuarine and coastal ocean exchange rates and an estimation of SGD and associated fluxes to coastal waters. In many cases radium isotopes can be used to separate SGD fluxes into those coming from surficial and from deeper aquifers.

1. Introduction

Within the decay series of uranium and thorium are four radium isotopes (Fig.1). All derive from decay of thorium parents, which are tightly bound to particles. Due to a reduction in the adsorption coefficient of radium with increasing salinity [1], radium daughters are mobilized in the marine environment. Sediments thus provide a continuous source of Ra isotopes to marine waters at rates set by the decay constants of the Ra daughters. Measurements of the Th isotope activities in the sediments and the distribution coefficient of radium between the sediments and water provide a means of quantifying the potential input of each Ra isotope to the water. With half-lives ranging from 3.66 days (^{224}Ra) to 11.4 days (^{223}Ra) to 5.7 years (^{228}Ra) to 1600 years (^{226}Ra), this quartet of isotopes can provide powerful constraints on processes occurring in estuaries, salt marshes, and the coastal ocean.

Salty groundwater contacts more sediment surfaces than do surface waters, therefore groundwaters usually have high activities of Ra. As salty groundwater flushes through the sediments, Ra is transferred to the coastal ocean. Once lost from the sediments, the Ra isotopes regenerate at different rates. The long lived ^{226}Ra requires 1600 years to regenerate 50% of its activity, but ^{228}Ra regenerates 50% of its activity in 5.7 years. Because the sediments retain Th but not Ra, they serve as a constant source of Ra to marine waters. Surficial coastal aquifers that are continuously flushed with salt water have low activities of ^{226}Ra. Deeper aquifers that are flushed less efficiently often have higher ^{226}Ra.

The discovery of high activities of ^{226}Ra in the coastal ocean that could not be explained by input from rivers or sediments coupled with measured high ^{226}Ra in salty coastal wells led to the hypothesis that submarine groundwater discharge (SGD) was responsible for the elevated activities [2]. Earlier, similar reasoning had been used to deduce a large SGD flux to the Swanatee River [3]. The excess ^{226}Ra in a salt marsh was also explained by SGD [4]. Since then excess ^{226}Ra has been a diagnostic tracer of SGD in the coastal ocean [5–19].

The two short lived Ra isotopes, ^{223}Ra and ^{224}Ra, provide additional evidence of groundwater input. Rama and Moore [4] used the four Ra isotopes to determine that groundwater input to the North Inlet salt marsh occurred where tidal creeks were cut into deeper aquifers rather than through muddy surficial sediments. The short-lived isotopes may also provide a means of estimating the residence time of estuarine and coastal waters [18, 20–21]. The residence time is important because it provides the time scale available for components to accumulate in the water column.

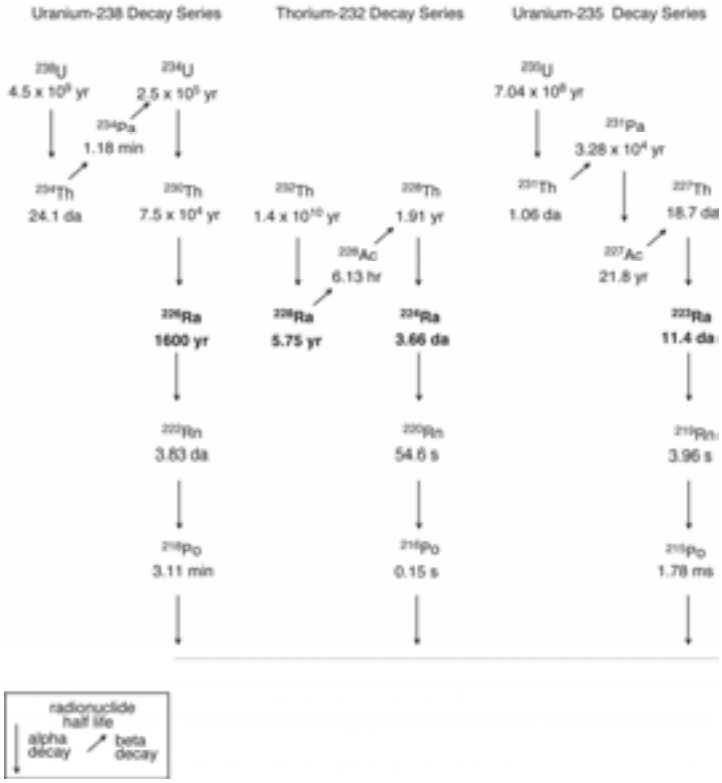

FIG.1. Isotopes of the uranium and thorium decay series.

2. Measurements of Radium Isotopes

Ra isotope measurements are made by filtering 20 – 400 L of surface water or 1 – 20 L groundwater into plastic buckets. The sample volume is recorded and the water is pumped through a column of manganese coated acrylic fiber (Mn fiber) to quantitatively remove Ra [22]. Each Mn fiber sample is partially dried with a stream of air and placed in closed loop air circulation system described by Moore and Arnold [23]. Helium is circulated over the Mn fiber to sweep the ^{219}Rn and ^{220}Rn generated by ^{223}Ra and ^{224}Ra decay through a 1 L scintillation cell where alpha particles from the decay of Rn and daughters are recorded by a photomultiplier tube (PMT) attached to the scintillation cell. Signals from the PMT are routed to a delayed coincidence system pioneered by Giffin et al. [24] and adapted for Ra measurements by Moore and Arnold [23]. The delayed coincidence system utilizes the difference in decay constants of the short-lived Po daughters of ^{219}Rn and ^{220}Rn to identify alpha particles derived from ^{219}Rn or ^{220}Rn decay and hence to determine activities of ^{223}Ra and ^{224}Ra on the Mn fiber. The expected error of the short-lived Ra measurements is 10%. Because counts are only recorded in coincidence, the background of this system is extremely low.

After the ^{223}Ra and ^{224}Ra measurements are complete, the Mn fiber samples are aged for 2 – 6 weeks to allow initial excess ^{224}Ra to equilibrate with ^{228}Th adsorbed to the Mn fiber. The samples are measured again to determine ^{228}Th and thus to correct for supported ^{224}Ra.

After these measurements are completed, the Mn fibers are leached with HCl in a Soxhlet extraction apparatus to quantitatively remove the long lived Ra isotopes. The Ra is coprecipitated with $BaSO_4$. The precipitant is aged for 2 weeks to allow ^{222}Rn and its daughters to equilibrate with ^{226}Ra. Alternately the Mn fiber can be ashed or compressed into a standard geometry and measured directly after the ingrowth period. The samples are measured in a gamma ray spectrometer to assess the activities of ^{226}Ra and ^{228}Ra [25]. The expected error of the long-lived Ra measurements is 7%.

Standards are used to calibrate the efficiency of the counters. For ^{224}Ra the standard is prepared by adsorbing ^{232}Th in equilibrium with its daughters onto a column of Mn–fiber. For ^{223}Ra the standard is

^{227}Ac in equilibrium with its daughters. These standards are prepared with activities similar to that of samples. They are treated just as the samples described above in the delayed coincidence system. For ^{226}Ra a standard solution having an activity about 10 – 100 times the sample activity is precipitated with $BaSO_4$ as described above. For ^{228}Ra the standard is a solution of ^{232}Th with daughters in equilibrium. This is treated the same way as the ^{226}Ra standard.

3. Interpretation of Radium Isotope Data

3.1. Separating sources of SGD

Moore [13] used the ^{228}Ra/^{226}Ra AR to distinguish groundwater derived from the upper Floridan Aquifer (UFA) vs the surficial aquifer (SA) in samples collected on the Gulf coast of Florida near the FSU Marine Lab (30°N). He found that most surface water samples fell along a mixing line having a ^{228}Ra/^{226}Ra AR = 2.5, indicating a surficial aquifer source (Fig.2). However, some offshore samples fell off this trend and toward a sample from an artesian well in the UFA. Springs in the area were also influenced by the UFA source. Moore [13] used a 3 end member mixing model to assess the relative amounts of water from the open Gulf, the offshore UFA, and the nearshore SA in the surface water samples. A result of the model was the presence of a significant and variable UFA component in the surface water.

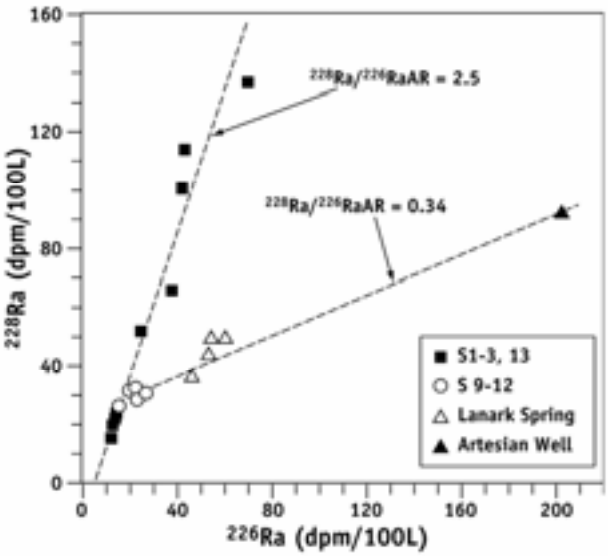

FIG.2. Samples collected near the FSU Marine Lab [13] show large radium enrichments. Nearshore surface water samples (shown as squares) fall on a trend having a ^{228}Ra/^{226}Ra mixing ratio = 2.5. Most samples collected offshore (also shown as squares) fall on the same trend. Some samples collected offshore (circles) have lower salinity and fall below the trend for the other offshore samples. These lower salinity samples fall near a mixing line that includes samples collected near a submarine spring (open triangles) and an onshore artesian well from the Florida aquifer (triangles). The mixing ratio for these samples is 0.34. These data illustrate the use of the long-lived Ra isotopes for differentiating signals derived from the surficial and the Floridan aquifers.

The following equations are used to establish the 3 end member mixing model.

$$f_o + f_{ns} + f_{os} = 1.00 \quad (1)$$

$$^{226}Ra_o f_o + {}^{226}Ra_{ns} f_{ns} + {}^{226}Ra_{os} f_{os} = {}^{226}Ra_m \quad (2)$$

$$^{228}Ra_o f_o + {}^{228}Ra_{ns} f_{ns} + {}^{228}Ra_{os} f_{os} = {}^{228}Ra_m \quad (3)$$

where,

f is the fraction of ocean (o), nearshore SGD (ns), or offshore SGD (os) end member,

Ra_o is ^{226}Ra or ^{228}Ra activity in the ocean end member,

Ra_{ns} is ^{226}Ra or ^{228}Ra activity in the nearshore SGD end member,

Ra_{os} is ^{226}Ra or ^{228}Ra activity in the offshore SGD end member,

Ra_m is measured ^{226}Ra or ^{228}Ra activity in the sample.

These equations may be solved for the fractions of each end member.

$$f_{NS} = \frac{\left(\frac{^{228}Ra_M - {}^{228}Ra_O}{^{228}Ra_{OS} - {}^{228}Ra_O}\right) - \left(\frac{S_M - S_O}{S_{OS} - S_O}\right)}{\left(\frac{^{228}Ra_{NS} - {}^{228}Ra_O}{^{228}Ra_{OS} - {}^{228}Ra_O}\right) - \left(\frac{S_{NS} - S_O}{S_{OS} - S_O}\right)} \tag{4}$$

$$f_{OS} = \frac{S_M - S_O - f_{NS}(S_{NS} - S_O)}{S_{OS} - S_O} \tag{5}$$

$$f_O = 1.00 - f_{NS} - f_{OS} \tag{6}$$

A similar result was obtained from samples collected on the southern coast of Sicily [19]. Springs from a limestone aquifer discharging on the beach and just offshore had much lower $^{228}Ra/^{226}Ra$ AR than did shallow wells on the beach. Samples collected in the nearshore zone as well as samples collected in seepage bags fell between the isotopic composition of these sources. Again the 3–end member model was able to resolve these sources.

3.2. Evaluating coastal ocean exchange times and SGD fluxes

To evaluate the balance of radium in the coastal ocean, the exchange rate or residence time of the water must be known. Moore [20] used the short-lived Ra isotopes to estimate exchange rates. The model used was a one-dimensional advection–dispersion model. The change in concentration or activity (A) with time (t) as a function of distance offshore (x) for a radioactive tracer with decay constant (λ) may be expressed as a balance of advection, dispersion, and decay

$$\frac{dA}{dt} = K_h \frac{\partial^2 A}{\partial x^2} - \omega \frac{\partial A}{\partial x} - \lambda A \tag{7}$$

If net advection can be neglected, this reduces to

$$\frac{dA}{dt} = K_h \frac{\partial^2 A}{\partial x^2} - \lambda A \tag{8}$$

where K_h is the dispersion coefficient. In this case the boundary conditions are

$$A = A_i \; at \; x = 0$$
$$A \to 0 \; as \; x \to \infty$$

If K_h is constant and the system is steady state,

$$A_x = A_0 \exp\left[-x\sqrt{\frac{\lambda}{K_h}}\right] \tag{9}$$

where,

A_x = activity at distance x from coast

A_0 = activity at distance 0 from coast

λ = decay constant

A plot of ln ^{223}Ra or ln ^{224}Ra as function of distance from the coast may be used to estimate K_h if the exchange is dominated by dispersion rather than advection and if the system is steady state.

$$\ln A_x = \ln A_0 - x\sqrt{\frac{\lambda}{K_h}} \tag{10}$$

In this case the slope m is,

$$m = \sqrt{\frac{\lambda}{K_h}} \tag{11}$$

The long-lived Ra isotopes are used to assess the relative roles of advection and dispersion. Decay of ^{226}Ra and ^{228}Ra may be neglected over the time scale of shelf water exchange. Figure 3 is a plot of the distance-averaged activity of ^{226}Ra and ^{228}Ra as a function of distance offshore for repeated occupations of offshore transects in the South Atlantic Bight reported by Moore [20].

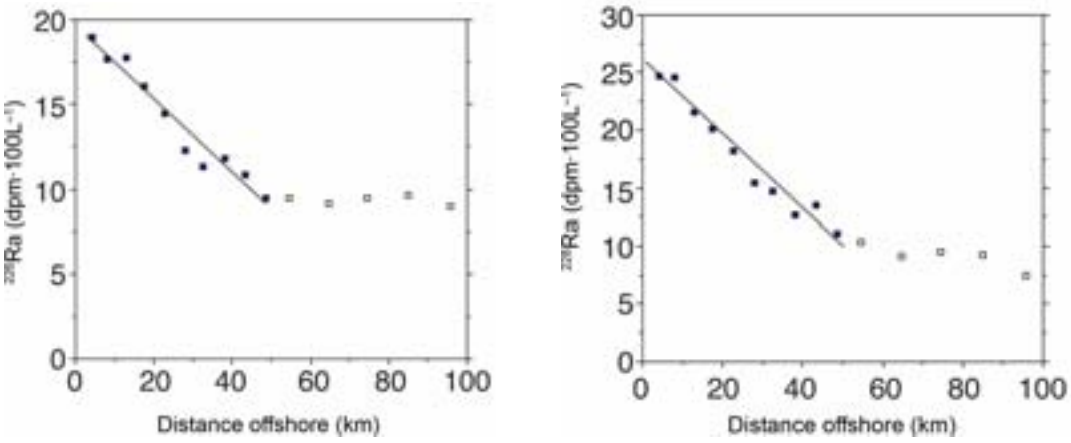

FIG.3. The distance-averaged distribution of the long-lived Ra isotopes across the continental shelf of South Carolina [20].

For ^{226}Ra the data within 50 km of the coast fit a line with a slope of –0.219 dpm·100L^{-1}·km^{-1} having R^2 = 0.951; for ^{228}Ra the slope is –0.319 dpm·100L^{-1}·km^{-1} with R^2 = 0.959. These excellent linear correlations are strong evidence that the distributions within 50 km of the coast are controlled by dispersion with negligible net advection.

There is clearly a break in slope at 50 km offshore for both isotopes. Two processes could cause this change. Advection of water from the southwest could interrupt the profile. Such advection is consistent with the wind pattern during this cruise [26] and the flow of the Gulf Stream. The break in slope could also be produced by more rapid mixing of water in the 50 – 100 km region or to a large eddy transporting Ra from another area. Because of these possibilities the mixing can only be determined for the inner 50 km.

During the same cruise activities of ^{223}Ra and ^{224}Ra were measured. These results were distance averaged for repeated transects as described above. Figure 4 shows the activities of the ln transforms of ^{223}Ra and ^{224}Ra as a function of distance from shore. For ln ^{223}Ra the distribution within 50 km of shore has a slope of –0.0439 dpm·100L^{-1}·km^{-1} with R^2 = 0.973. The distribution of ln^{224}Ra over the same interval has a slope of –0.0724 dpm·100L^{-1}·km^{-1} with R^2 = 0.986. Using equation 10 and its

assumptions, the value of K_h derived from ^{223}Ra is 31.5 km^2·d^{-1} (360 m^2·s^{-1}); for ^{224}Ra equation 10 yields K_h = 36.2 km^2·d^{-1} (420 m^2·s^{-1}). The differences in these estimates may be due in part to differences in the time and space scales of dispersion. The longer lived ^{223}Ra looks at a larger scale than ^{224}Ra. However, it is encouraging that in this experiment the estimates from the two short lived isotopes are very similar.

We may use the estimates derived here to calculate the flux of ^{226}Ra and ^{228}Ra from the coast to the ocean as described by Moore [20]. The flux of a conservative tracer can be estimated from the product of the offshore concentration gradient and K_h. The ^{226}Ra gradient is –0.219 dpm·100L^{-1}·km^{-1} or –2.19 × 10^9 dpm·km^{-3}·km^{-1}. For K_h = 34 km^2·d^{-1} (the average of the two estimates), the offshore ^{226}Ra flux is 7.5 × 10^{10} dpm·km^{-2}·d^{-1}. This Ra is transported offshore in the 10 m deep surface layer; therefore, the offshore flux is 7.5 × 10^8 dpm·km^{-1}·d^{-1}. The total flux for the 80 km coastline from Charleston, SC, to Winyah Bay, SC, is 6 × 10^{10} dpm·d^{-1}. If this flux can be scaled to the 320 km coastline of the entire study area, the flux would be 2.4 × 10^{11} dpm·d^{-1}. The ^{228}Ra data indicate an offshore flux of this isotope for the entire study area of 3.5 × 10^{11} dpm·d^{-1}. Based on the ^{226}Ra data used here and an assumed 30 day residence time for waters of the inner shelf, Moore [2] estimated that the ^{226}Ra flux from this coastline was 2.1 × 10^{11} dpm·d^{-1}.

To use the flux of the long-lived Ra isotopes to estimate SGD, we must know the Ra activity in the source water that supplies the SGD. Salty groundwater along this coast has a ^{226}Ra activity in the range 2 – 10 dpm/L with most values in the range 4 – 8 dpm/L. If we take 6 dpm/L as the average, the SGD flux may be calculated by dividing the ^{226}Ra flux by the average ^{226}Ra in the groundwater. This yields a flux of 3.5 × 10^{10} L/day or 400 m^3/sec.

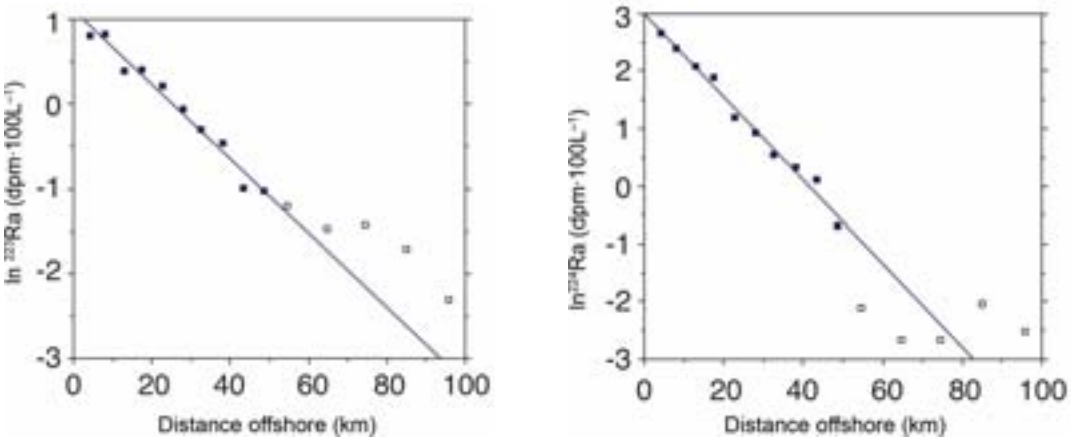

FIG.4. The distance-averaged distribution of the ln transform of the short-lived Ra isotopes across the continental shelf of South Carolina [20].

3.3. Evaluating fluxes of other components

If we know the composition of other components in the SGD, estimating their fluxes once the SGD flux is known, is trivial. However, in making the SGD flux based on ^{226}Ra we had to take the average ^{226}Ra that had been measured in coastal wells. Another approach is to look for relationships between Ra and other components in the groundwater. If such relationships are found, the component/Ra ratio in the groundwater can be multiplied by the Ra flux to yield the component flux. Such an approach was used by Moore et al. [11] to estimate nitrogen and phosphorus fluxes to coastal waters. They found strong relationships between total dissolved nitrogen (TDN) and ^{226}Ra and total dissolved phosphorus (TDP) and ^{226}Ra and used these relationships to determine TDN and TDP fluxes. Figure 5 shows the relationships measured in monitoring wells off the South Carolina coast.

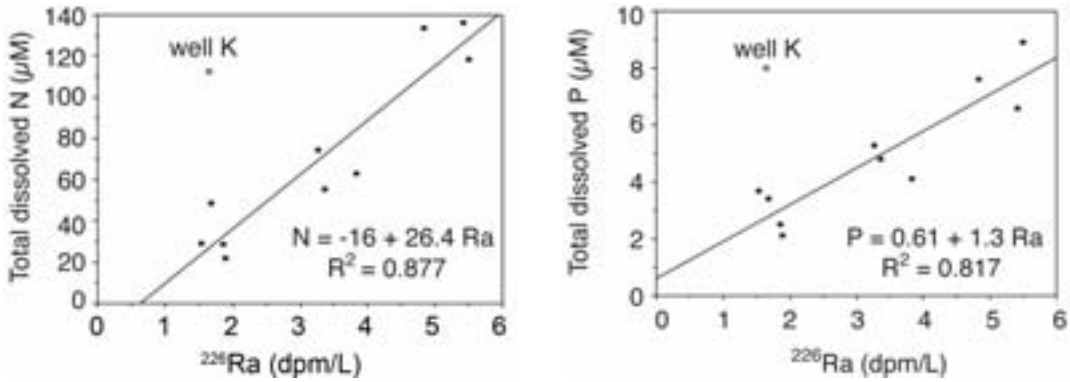

FIG.5. The concentrations of total dissolved nitrogen and phosphorus display strong correlations with ^{226}Ra in samples from monitoring wells (excluding K) off the South Carolina coast [11].

Assuming that the water supplying excess ^{226}Ra to the coastal ocean is similar to these well waters, we use the nutrient–Ra correlation to estimate the nutrient flux (Fig.5). For example the total dissolved phosphate (TDP) to ^{226}Ra ratio is 0.93 $\mu M \cdot dpm^{-1}$. To support a ^{226}Ra flux of 1.5×10^{11} $dpm \cdot d^{-1}$, the accompanying TDP flux is 1.4×10^{5} $moles \cdot d^{-1}$. The total dissolved nitrogen (TDN)/^{226}Ra ratio is 26.4 $\mu M \cdot dpm^{-1}$; thus the TDN flux would be 4.0×10^{6} $moles \cdot d^{-1}$.

3.4. Evaluating estuary residence times

Moore [21] developed a model to estimate the ages of water masses in the coastal ocean. This model assumed that radium was only added to the water near the shoreline; after the water left the coast and lost contact with the bottom, radium additions ceased. This model is not applicable to estuaries and salt marshes where radium additions from sediments and groundwater are continuous. To use radium isotopes to estimate ages in these systems, Moore et al. [18] used a different approach. A similar approach was developed by Hwang et al. [17].

Assume the system under study is in steady state, that is radium additions are balanced by losses. Additions include radium fluxes from sediment, river, and groundwater; losses are due to mixing and, in the case of ^{223}Ra and ^{224}Ra, radioactive decay. Write an equation for the ^{224}Ra balance:

$$F\ ^{224}Ra = I\ ^{224}Ra\ (\lambda_{224} + 1/\tau) \quad (12)$$

where F ^{224}Ra is the total flux of ^{224}Ra to the system, I ^{224}Ra is the inventory of ^{224}Ra in the system, λ_{224} is the decay constant for ^{224}Ra, and τ is the apparent age of water in the system. We can write a similar equation for ^{228}Ra; but, because the half-life is 5.7 years, the effect of decay can be ignored.

$$F\ ^{228}Ra = I\ ^{228}Ra\ (1/\tau) \quad (13)$$

Now divide eq.12 by eq.13.

$$F\ (^{224}Ra/^{228}Ra) = I\ ^{224}Ra\ (\lambda_{224} + 1/\tau)/\ I\ ^{228}Ra\ (1/\tau) \quad (14)$$

This equation can be rearranged and solved for τ:

$$\tau = [F(^{224}Ra/^{228}Ra) - I(^{224}Ra/^{228}Ra)]/I(^{224}Ra/^{228}Ra)\lambda_{224} \quad (15)$$

In this case F ($^{224}Ra/^{228}Ra$) is the ($^{224}Ra/^{228}Ra$) activity ratio (AR) of the flux into the system, I ($^{224}Ra/^{228}Ra$) is the ($^{224}Ra/^{228}Ra$) AR in the system, and λ_{224} is the decay constant of ^{224}Ra (0.19 day^{-1}). Here we use the $^{224}Ra/^{228}Ra$ AR because the time scale is appropriate to the ^{224}Ra half-life. In cases where ages are expected to be on the order of weeks, a similar equation based on ^{223}Ra (λ = 0.0608 day^{-1}) would be more appropriate.

This model is quite sensitive to the value selected for the $^{224}Ra/^{228}Ra$ AR of water entering the system. This can be determined by finding areas of discharge via infrared imaging or other techniques and measuring shallow groundwaters at these sites. Another approach is to collect as much data as possible from shallow permeable sediments and plot ^{224}Ra vs ^{228}Ra to determine the average activity ratio.

4. Summary

There are good reasons why radium is closely linked to SGD studies. Because radium is highly enriched in salty coastal groundwater relative to the ocean, small inputs of SGD can be recognized as a strong radium signal. In many cases this signal can be separated into different SGD components using the two long-lived Ra isotopes. The short-lived Ra isotopes are useful in evaluating the residence time or mixing rate of estuaries and coastal waters. Such estimates coupled with distributions of the long-lived Ra isotopes enables a direct estimate of radium fluxes. At steady state these fluxes must be balanced by fresh inputs of Ra to the system. If other sources of Ra can be evaluated, the Ra flux that must be sustained by SGD can be evaluated. By measuring the Ra content of water in the coastal aquifers, the amount of SGD necessary to supply the Ra is determined. SGD fluxes of other components are determined by measuring their concentrations in the coastal aquifer or by determining relationships between the component and Ra and multiplying the component/Ra ratio by the Ra flux.

REFERENCES

[1] LI, Y.-H., MATHIEU, G., BISCAYE, P., SIMPSON, H.J., The flux of 226-Ra from estuarine and continental shelf sediments, Earth Planet. Sci. Lett. **37** (1977) 237–241.

[2] MOORE, W.S., Large groundwater inputs to coastal waters revealed by ^{226}Ra enrichments, Nature **380** (1996) 612–614.

[3] BURNETT, W.C., COWART, J.B., DEETAE, S., Radium in the Suwannee River and estuary: spring and river input to the Gulf of Mexico, Biogeochemistry **10** (1990) 237–255.

[4] RAMA, MOORE, W.S., Using the radium quartet for evaluating groundwater input and water exchange in salt marshes, Geochim. Cosmochim. Acta **60** (1996) 4645–4652.

[5] MOORE, W.S., The effects of groundwater input at the mouth of the Ganges–Brahmaputra Rivers on barium and radium fluxes to the Bay of Bengal, Earth Planet. Sci. Lett. **150** (1997) 141–150.

[6] MOORE, W.S., SHAW, T.J., Chemical signals from submarine fluid advection onto the continental shelf, J. Geophys. Res. **103** (1998) 21543–21552.

[7] MOORE, W.S., The subterranean estuary: a reaction zone of ground water and sea water, Mar. Chem. **65** (1999) 111–126.

[8] KREST, J.M., MOORE, W.S., GARDNER, L.R., Marsh nutrient export supplied by groundwater discharge: evidence from radium measurements, Glob. Biogeochem. Cycles **14** (2000) 167–176.

[9] CHARETTE, M.A., BUESSELER, K.O., ANDREWS, J.E., Utility of radium isotopes for evaluating the input and transport of groundwater-derived nitrogen to a Cape Cod estuary, Limnol. Oceanogr. **46** (2001) 465–470.

[10] KELLY, R.P., MORAN, S.B., Seasonal changes in groundwater input to a well-mixed estuary estimated using radium isotopes and implications for coastal nutrient budgets, Limnol. Oceanogr. **47** (2002) 1796–1807.

[11] MOORE, W.S., KREST, J., TAYLOR, G., ROGGENSTEIN, E., JOYE, S., LEE, R., Thermal evidence of water exchange through a coastal aquifer: Implications for nutrient fluxes, Geophys. Res. Lett. **29** (2002) doi: 10.1029/2002GL014923.

[12] CROTWELL, A.M., MOORE,W.S., Nutrient and Radium Fluxes from Submarine Groundwater Discharge to Port Royal Sound, South Carolina, Aquat. Geochem. **9** (2003) 191–208.

[13] MOORE, W.S., Sources and fluxes of submarine groundwater discharge delineated by radium isotopes, Biogeochemistry **66** (2003) 75–93.

[14] KIM, G., LEE, K.-K., PARK, K.-S., HWANG, D.-W., YANG, H.-S., Large submarine groundwater discharge (SGD) from a volcanic island, Geophys. Res. Lett. **30** (2003) doi:10.1029/2003GL018378.

[15] KREST, J.M., HARVEY, J.W., Using natural distributions of short-lived radium isotopes to quantify groundwater discharge and recharge, Limnol. Oceanogr. **48** (2003) 290–298.
[16] MOORE, W.S., WILSON, A.M., Advective flow through the upper continental shelf driven by storms, buoyancy, and submarine groundwater discharge, Earth Planet.Sci. Lett. **235** (2005) 564–576.
[17] HWANG D.W., KIM, G., LEE, Y.-W., YANG, H.-S., Estimating submarine inputs of groundwater and nutrients to a coastal bay using radium isotopes, Mar. Chem. **96** (2005) 61–71.
[18] MOORE, W.S., BLANTON, J.O., JOYE, S., Estimates of Flushing Times, Submarine Groundwater Discharge, and Nutrient Fluxes to Okatee River, South Carolina, J. Geophys. Res. (2006) in press.
[19] MOORE, W.S., Radium Isotopes as Tracers of Submarine Groundwater Discharge in Sicily, Cont. Shelf Res. **26** (2006) 852–861.
[20] MOORE, W.S., Determining coastal mixing rates using radium isotopes, Cont. Shelf. Res. **20** (2000) 1993–2007.
[21] MOORE, W.S., Ages of continental shelf waters determined from ^{223}Ra and ^{224}Ra, J. Geophys. Res. **105** (2000) 22117–22122.
[22] MOORE, W.S., Sampling Radium-228 in the Deep Ocean, Deep Sea Res. **23** (1976) 647–651.
[23] MOORE, W.S., ARNOLD, R., Measurement of ^{223}Ra and ^{224}Ra in coastal waters using a delayed coincidence counter, J. Geophys. Res. **101** (1996) 1321–1329.
[24] GIFFIN, C., KAUFMAN, A., BROECKER, W.S., Delayed coincidence counter for the assay of actinon and thoron, J. Geophys. Res. **68** (1963) 1749–1757.
[25] MOORE, W.S., Radium Isotope Measurements Using Germanium Detectors, Nucl. Inst. Methods **223** (1984) 407–411.
[26] MOORE, W.S., KJERFVE, B., TODD, J.F., Identification of rain–freshened plumes in the coastal ocean using Ra isotopes and Si, J. Geophys. Res. **103** (1998) 7709–7717.

MODELLING METHOD FOR SGD PHENOMENON AND SGD MEASUREMENTS IN THE GULF OF TRIESTE

PART A: MODELLING METHOD FOR SIMULATION OF SGD PHENOMENON

R. Rajar

Faculty of Civil and Geodetic Engineering
University of Ljubljana, Slovenia

Abstract. A new methodology to determine the location and strength of SGD is proposed where the salinity distribution in the water body is simulated by a 3D numerical model. Measurement of the salinity field (or any other parameter, typical for SDG source) is needed in the region of the SGD. The applied model PCFLOW3D is a 3D, nonlinear baroclinic numerical model which was originally developed to simulate the hydrodynamic circulation and transport–dispersion of different contaminants such as mercury or radionuclides. It has been completed with the possibility of simulation of transport–dispersion of any parameter arriving with the SGD source from the bottom (e.g. salinity, nutrients, radon). The basic idea is to assume a location and strength of the SGD, simulate the parameter distribution, and compare it with the measured distribution. The final information on SGD is obtained by the trial and error procedure. Possible application of the modelling method was proven with comparison to the SGD measurements in Sicily.

1. Proposed Methodology of Numerical Simulation of SGD Phenomenon

Numerical modelling is an additional methodology for determination of location and strength of SDG sources in coastal zones [1]. The modelling of *groundwater* seepage is mostly used. Differently, the proposed method applies numerical modelling of salinity concentration *in the water body*, usually in a coastal bay.

Each of the known experimental methods for evaluation of SGD has some shortcomings: they are either complex, expensive, or need special equipment and/or trained personnel. On the other hand it is relatively simple to measure the field of concentration of some parameters, especially salinity. The proposed method of application of a three–dimensional numerical model is based on the fact that *only the concentration distribution of salinity needs to be measured to determine location and strength of a SGD.* Measured concentration of some other parameters, which show typical gradients in the vicinity of SDGs, as e.g., temperature, radon, or isotope tracers, can also be used to this purpose.

Inflow of fresh (or less saline) water from SGD causes distinctive changes in the salinity concentrations in the vicinity of the SGD inflow. As the density of less saline water is smaller than the original water density in the region, upwelling velocities occur normally. Due to the law of conservation of mass this causes a circulation in a wider region around SGD, which depends on the strength of the SGD inflow discharge, topography of the region and on several other factors, affecting the velocity field, as wind and tide.

A three–dimensional numerical model can simulate the concentrations and distributions of the investigated parameters, together with the velocity field in the vicinity of SGD. During simulations the equation of mass conservation of salinity must be fulfilled, as also the dynamic equilibrium of the flow. It is possible, therefore, to locate and estimate strength of a SGD source using numerical modelling by applying an inverse methodology: we assume a location and strength of SGD source(s), and then we simulate the velocity and salinity distribution in the region by the model and compare the results with the measured distribution. With the trial–and–error methodology we find out the real location and strength of the SGD source(s).

2. Description of PCFLOW3D Model

The applied model PCFLOW3D is a 3D, nonlinear and baroclinic numerical model. The continuity equation and the equation for the surface boundary condition are applied additionally. The numerical solution is based on the implicit finite volume numerical method of Patankar. The hybrid (combination of central and upwind) numerical scheme is applied.

Horizontal turbulent viscosity is calculated by the Smagorinsky principle. The one equation turbulence model of Koutitas has been used to determine the vertical eddy viscosity. The advection–diffusion equation for temperature and salinity are solved coupled with the above–mentioned equations. The equation of state determines the density, which is taken into account in the momentum equations in the next time step.

The PCFLOW3D model includes three modules (Fig.1): the basic *hydrodynamic module*, where the velocity field is determined; *sediment transport module* and *transport–dispersion module*, which simulates dispersion of different pollutants. The model has been described in Čermelj et al. [2]. Specifically the model has been developed to simulate toxic mercury compounds [3, 4]. The model has been used for solving several practical cases of pollutant transport, as e.g. radioactive pollutants in the Japan Sea [5], outflow of sediment and plutonium from the Mururoa lagoon after French nuclear experiments [6] or dispersion of agricultural pollution in the lagoons of the NW Mexico [7].

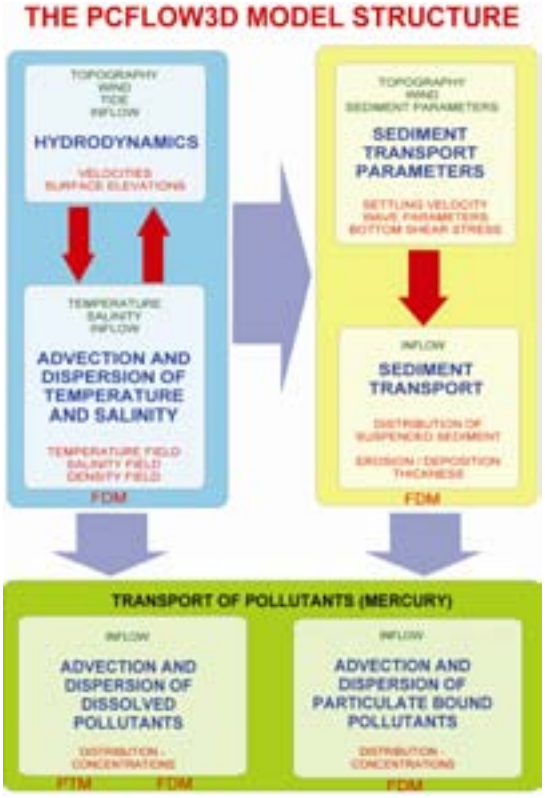

FIG.1. Scheme of the PCFLOW3D model structure.

For the purpose of simulation of SGD phenomena, several improvements of the model have been included. In 2004 the model has been completed with the possibility of simulation of the phenomena, caused by SGD sources with smaller salinity from the bottom of the water body. As the salinity gradients are often very small, the model must be accurate enough to simulate their influence on the flow. For the purpose of SGD simulations, the turbulence model of Koutitas was not accurate enough, and the Mellor–Yamada turbulence model has been included. The influence of stratification on the eddy viscosity and diffusivity is directly taken into account in this method. Also the hybrid numerical scheme has been replaced by more accurate, second order QUICK scheme.

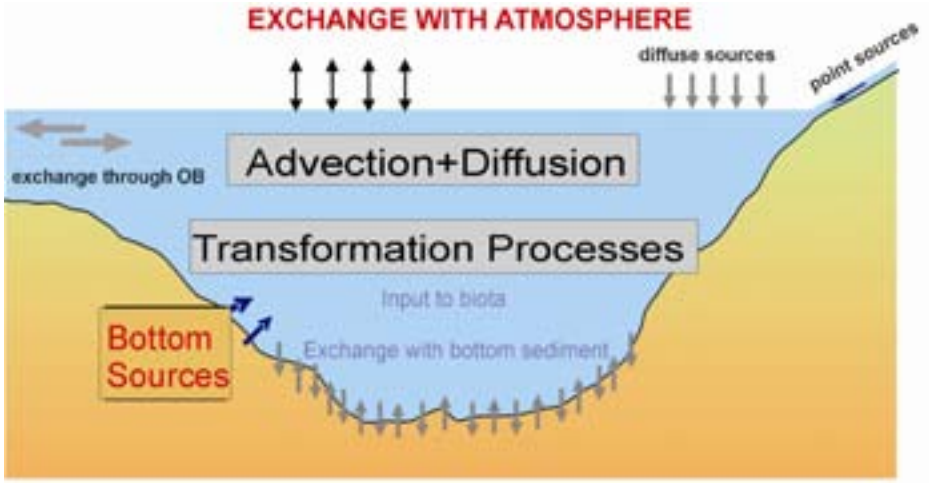

FIG.2. Scheme of the transport–dispersion module for any contaminant, where SGD sources of fresh or less saline water from the bottom are included.

3. Demonstration Case: Simulation of SGD in a Coastal Bay

For the first verification of the method, we have simulated a flow in a bay of simplified (rectangular) form. Fig.3 shows the basic dimensions and parameters. The bay is 300 m long, its depth is 10 m at the open boundary and it decreases linearly towards the coast, where the depth is 5 m. At the open boundary, tidal water level oscillation is applied, with the amplitude of ± 0.5 m, and period of 12.4 h. Wind speed of 12 m/s is applied, its direction from the open boundary towards the coast. The SGD source is located 93 m from the inside coast. For more clear demonstration of the phenomenon, the source is allocated on a bottom area over the whole width of the bay, the length of the SGD area is 3.0 m (Fig.3). The flow and dispersion are thus transformed to 2D phenomena. The SGD source velocity is 0.01 m/s, and its salinity is 30, the basic salinity in the bay being 36.

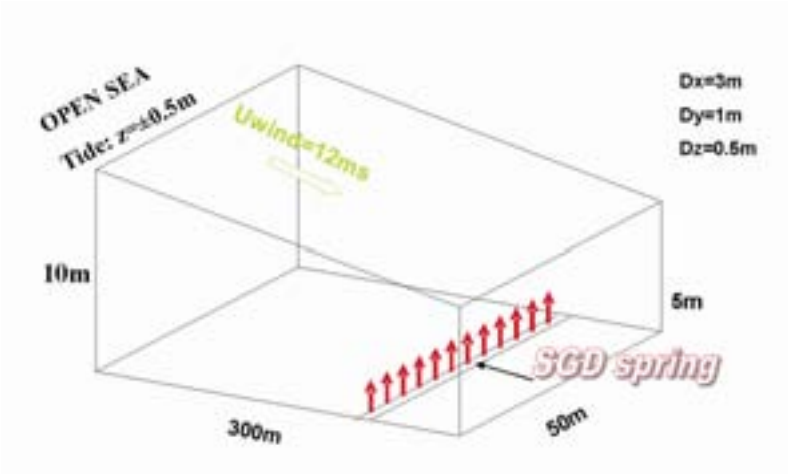

FIG.3: Simplified domain (Bay A) for testing the PCFLOW3D model simulations of SGD.

As the wind forcing prevails over the tidal influence, the flow is mainly circulating, the surface wind shear stress forcing the velocities in the surface layers towards the coast, while there is a weaker counterflow out of the bay at the bottom.

Figure 4 shows the salinity distribution in the vertical cross section at two times after the SGD outflow.

For this demo case there was no possibility of verification of the results, only the capabilities of the PCFLOW3D model are demonstrated.

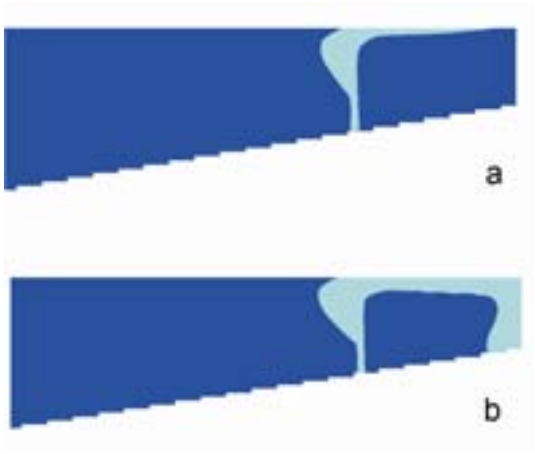

FIG.4. Salinity distribution in the vertical section of Bay A, simulation by PCFLOW3D model. (a) T = 2h 00 min;(b) T = 2h 15 min.

4. Case Study: Sicily

In March 2002, the IAEA team carried out measurements of SGD discharges in the Donnalucata boat basin in Sicily (Figs. 5 and 6). It was possible to use the measured parameters for rough verification of the proposed modeling method for detection of SGD.

Timing of the simulations is March 22, 2002, at 11h. The following input data were used:

The basin (Fig.6) is approximately 175 m long and max. 48 m wide, numerical grid being Dx = 2.00 m and Dy = 2.089 m. The depth is max. 2.5 m, decreasing in the eastern part. The measurements have shown [8] that the SGD sources are non–uniformly distributed over the whole bottom of the boat basin. Measurements of SGD inflow discharge was carried out at some locations, marked with small circles in Fig.6. For the purpose of numerical simulations measured inflow velocity was assumed to be constant in each region A to E (Fig.6), with the values of: 2, 2; 35.7; 2.8; 2.0; and 15.1 cm/day [8]. Hydrodynamic circulation in the computational region was simulated at first, it is presented in Fig.5. Wind from WSW, with the velocity of 6 m/s was taken into account. Tidal elevation changes were below 10 cm and were not taken into account in this case. Then salinity was simulated, with the initial value of 38.2, the salinity of the inflow SGD sources assumed to be 1‰.

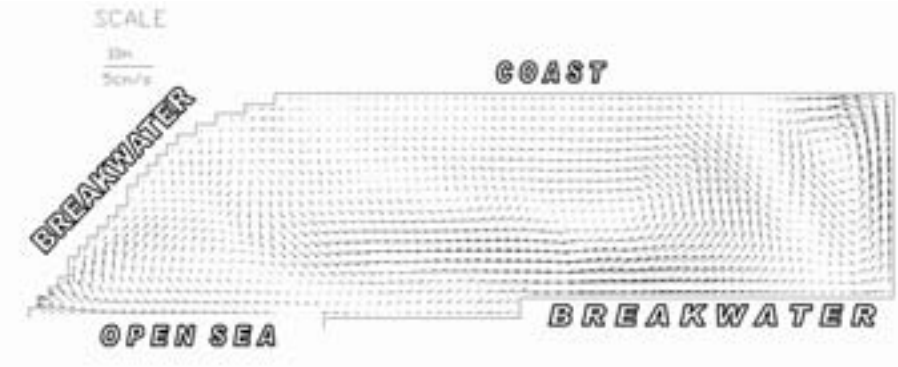

FIG.5. Depth averaged velocities in the boat basin on March 22, 2002 at 11h: results of simulation by PCFLOW3D model.

As in this case the location and strength of SGD were known, we simulated the hydrodynamic and salinity fields for the described input data. Figure 6 represents a comparison of the measured and simulated salinity distribution.

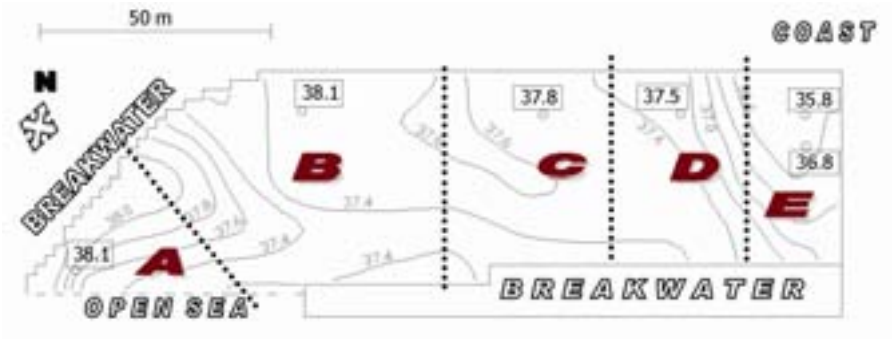

FIG.6. The region of SGD measurements in the Donnalucata boat basin (Sicily): comparison of salinity distribution simulated by PCFLOW3D model (isolines) with measured salinity (numbers in rectangles) on 22 March 2002 at 11h.

The agreement can be considered satisfactory, although not very good. There are several reasons for discrepancies: (1) The inflow of the SGD was measured at some discrete points only, the input data for the simulations were approximate; (2) Salinity was measured at the marked locations (numbers in rectangles, Fig.6) for a very short time, mostly for some minutes only, while the phenomenon is unsteady; (3) Influence of tide, which was not simulated, at least partly influences the phenomenon; (4) Not all the parameters, affecting the hydrodynamic and salinity distribution phenomena were known, as e.g. exact initial salinity and temperature distribution along the depth, or conditions at the open boundary.

5. Possible Application of the Modelling Method

When applying the method, we must be aware, that first of all, the whole hydrodynamic velocity field in the vicinity of the SGD must be simulated, and then the transport/dispersion of salinity (or other typical parameter). For this purpose the following parameters *must* be known or measured:

(1) salinity (or other parameter) distribution in the region, measured in a relatively dense grid of locations, also over the depth; as the gradients of velocity and salinity caused by the SGDs are usually very small, the measurements of salinity must be accurate enough.

(2) precise topography of the region

(3) data on all the forcing factors, as wind velocity and direction, tidal data, inflow of rivers.

(4) initial conditions, as salinity and temperature distribution in the region at the initial time of the simulation

(5) boundary conditions, especially at the open boundaries

(6) precipitation (if important)

Fortunately, most of the above mentioned parameters usually have to be measured for other purposes.

As other methods, also this one can be most efficiently applied in specific conditions, i.e. whenever the initial and boundary conditions are well defined, and when the forcing factors (wind, tide) cause a distinctive hydrodynamic circulation. When the SGD are located in a relatively closed bay, the water exchange is very slow, the salinity is very much mixed, its gradients are extremely small and the model simulations become difficult and unreliable. However, in most coastal areas wind effect is usually important, and besides tidal residual flow causes enough water exchange, that the flow and transport–dispersion of the typical parameter can be simulated reliably.

6. Conclusions

The model simulation results confirmed the possibility of successful application of the proposed modelling method in most SGD studies. In some cases, if the salinity distribution is measured accurately enough, and basic data on hydrodynamic forcing factors are known, the modelling method by itself can give good information on the location and discharge of the SGD source(s).

The main disadvantage of the method is the fact, that several other input data for the model simulations should be measured, i.e. all the parameters that influence the hydrodynamics and salinity concentration in the region. Also, the method can become unreliable in the cases of very small circulation velocities.

For final verifiation of the method, detailed measurements of salinity and additional parameters should be available from a SGD measuring campaign.

REFERENCES

[1] OBERDORFER, J.A., Hydrogeological modelling of submarine groundwater discharge: comparison to other quantitative methods, Biogeochemistry **66** (2003) 159–169.

[2] RAJAR, R., ČETINA, M., Hydrodynamic and Water Quality Modelling: An experience, Ecol. Model. **101** (1997) 195–207.

[3] RAJAR, R., ŽAGAR, D., ŠIRCA, A., HORVAT, M., Three–dimensional modelling of mercury cycling in the Gulf of Trieste, Sci. Total Environ. **260** (2000) 109–123.

[4] RAJAR, R., ŽAGAR, D., ČETINA, M., AKAGI, H., YANO, S., TOMIYASU, T., HORVAT, M., Application of three–dimensional mercury cycling model to coastal seas, Ecol. Model. **171** (2004) 139–155.

[5] ČETINA, M., RAJAR, R., POVINEC, P., Modelling of Circulation and Dispersion of Radioactive Pollutants in the Japan Sea, Oceanol. Acta **23** 7 (2000) 819–836.

[6] RAJAR. R, ŽAGAR, D., Transport of Sediments and Radionuclides from Mururoa Lagoon into the Ocean, In: The Radiological Situation at the Atolls of Mururoa and Fangataufa, Chapter 3.2, Technical Report by International Advisory Committee (1998) 29–38.

[7] RAJAR, R., ČETINA, M., GONZALES–FARIAS, F., PINTAR, M., Modelling of pollutant dispersion in Mexican coastal Lagoons, V: LI, Guifen (ed). XXIX IAHR Congress Proceedings, Theme D: Hydraulics of Rivers, Water Works and Machinery, September 16–21, Beijing, China. 21st century: the new era for hydraulic research and its applications: proceedings. Theme B, Environmental hydraulics and eco–hydraulics. Beijing: Tsinghua University Press, (2001) 176–181.

[8] TANIGUCHI, M., Seepage measurements in Sicilian waters – preliminary results from the 2002 expedition (2003).

MODELLING METHOD FOR SGD PHENOMENON AND SGD MEASUREMENTS IN THE GULF OF TRIESTE

PART B: GEOCHEMICAL CHARACTERIZATION OF THE SUBMARINE SPRING OFF IZOLA (GULF OF TRIESTE, N ADRIATIC SEA)

J. Faganeli[1], N. Ogrinc[2], L. M. Walter[3], J. Žumer[4]

[1]Marine Biological Station, National Institute of Biology
Piran, Slovenia
[2]Department of Environmental Sciences, J. Stefan Institute
Ljubljana, Slovenia
[3]Department of Geological Sciences, University of Michigan
Ann Arbor, USA
[4]Diving Center, Port of Koper
Koper, Slovenia

Abstract. First results of the geochemical research performed in a submarine spring near Izola are presented. It was found that the spring discharge of nutrients to the southern part of the Gulf is of less importance relative to the other freshwater discharges, representing <4% of the total freshwater nutrient input.

1. Introduction

Submarine groundwater springs are widespread coastal phenomena which occur wherever hydrogeological gradients enable lateral and upward groundwater transport [1]. Karstic coastlines [2, 3], modern and paleoriver channels [4], geopressured aquifires [5, 6], geothermal aquifers [7], mountainous shorelines with large tidal amplitudes and lagoons with heightened evaporation [8] are most important locales for submarine groundwater discharges. A submarine spring derived from meteoric and seawater mixing within an aquifier can be considered a subterranean estuary because it displays many of the key chemical features of surface estuary [9]. In subterranean estuaries, geochemical reactions between the mixed waters and host aquifer materials can enhance sediment/water geochemical exchange and significantly affect the coastal water mass balance of nutrients and other reactive constituents [10 and references therein].

The aim of the present study is to determine the complete geochemical composition of a submarine spring located 0.8 km offshore of Izola (Gulf of Trieste, northern Adriatic Sea, see Figs. 1 and 2) to identify the source(s) of spring water and to determine via comparison with conservative tracers (e.g. Cl, Mg) the significance of geochemical reactions occurring at the mixing zone.

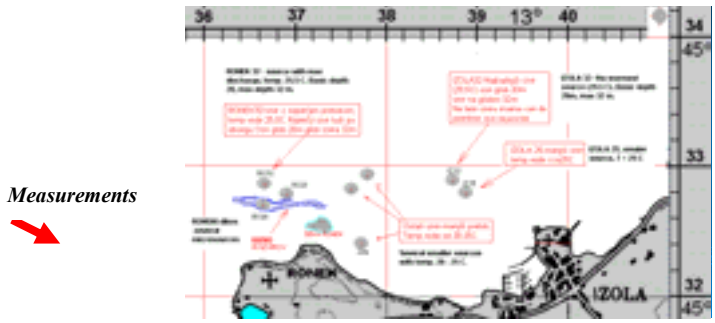

FIG.1. Location of the region of several SGDs along the Slovenian coast, near Izola (Gulf of Trieste, Northern Adriatic). Described measurements are from spring RO 32.

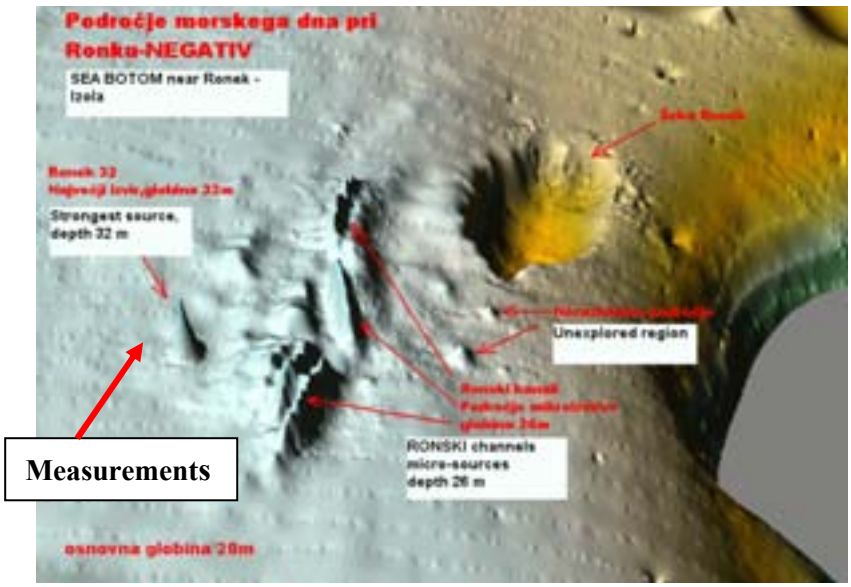

FIG.2. 3D presentation of the SGD region near Izola (presented as negative).

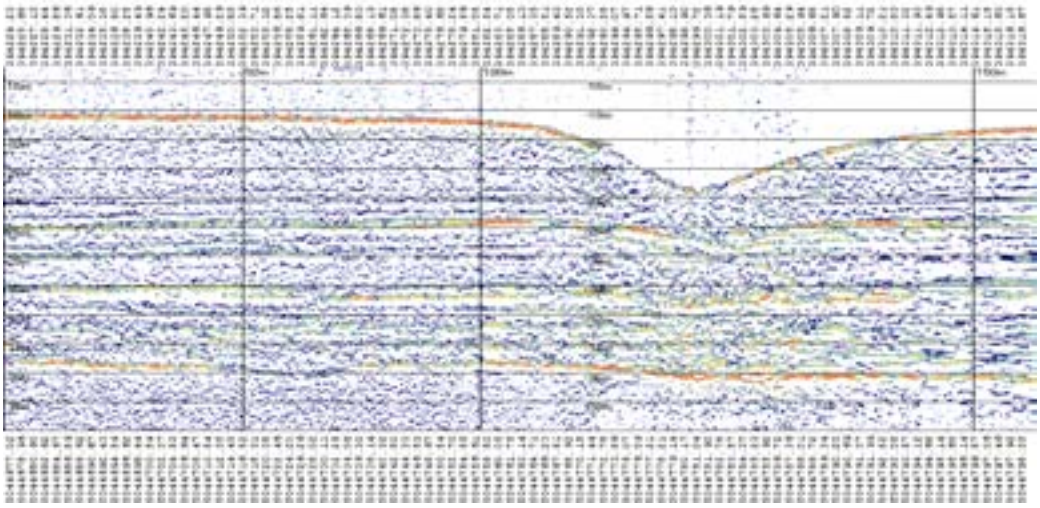

FIG.3. Parametric acoustic profile of Izola submarine spring (Courtesy of Harphasea Koper, Slovenia).

2. Materials and Methods

Samples – Water samples were collected in November 2003 at the Izola submarine spring (45° 32.911'N, 13° 38.752'W). To obtain the most pristine sample of the spring water, SCUBA divers inserted a polyethylene tube (6 mm i.d.) into the well and samples were collected by syringe. Water samples were filtered through 0.45 μm Millipore HA membrane filters in a N_2–filled glove bag under N_2 pressure of 0.4 MPa. In spring water pH, total alkalinity (TA), dissolved inorganic carbon (DIC), ^{13}C composition of DIC ($\delta^{13}C_{DIC}$), sulphide, and N and P nutrients were analyzed immediately. Water samples for cation determinations were acidified using ultrapure HNO_3.

Analyses – The pH of spring waters was measured using a UniFET microelectrode. TA was determined by Gran titration. Ammonia, phosphate and sulphide were analyzed colorimetrically and Cl^- titrimetrically [11]. Analyses of the following elements (Ca, Mg, Na, K, Sr, Ba, B, Mn, Fe, Zn, Si, Li and Al) were performed by ICP–OES. The concentrations of DIC were determined on a UIC Coulometrics CO_2 Coulometer. The precisions, based on replicate analyses, were ±0.01 for pH, ±1% for TA, and ±2% for DIC and metals, and ±5% for nutrients, chloride and sulphide, respectively. The stable isotopic composition of DIC was determined with the modified method of extraction [12]. The

isotope ratios of extracted CO_2 was then determined directly from the headspace by Isotope Ratio Mass Spectrometer – IRMS (Europa Scientific 20–20) with preparation module for trace gas samples ANCA–TG equipped with a Gilson autosampler. The results are reported using conventional delta (δ notation relative to PDB in permil (‰)). Overall analytical error was ±0.2‰. All measuring data are collected in Table 1.

TABLE 1. CHEMICAL COMPOSITION OF THE IZOLA SPRING WATER, 'AVERAGE' SEAWATER AND KARST GROUNDWATER FORM SW SLOVENIA [13]

Solutes/L	Izola spring	Seawater	Groundwater
Na (mM)	73.7	468.03	0.21
Mg (mM)	3.14	53.08	0.19
K (mM)	1.96	10.21	0.02
Ca (mM)	8.12	10.25	2.23
Sr (mM)	0.11	0.09	0.003
B (mM)	0.12	0.27	–
Si (mM)	0.67	0.007	0.15
Al (μM)	0.33	0.02	0.11
Ba (μM)	0.487	0.073	0.385
Mn (μM)	0.404	0.004	0.013
Fe (μM)	0.351	0.036	0.08
Zn (μM)	0.05	0.002	0.04
Li (μM)	26.3	26.1	72.5
DIC (mM)	4.03	2.33	4.33
$\delta^{13}C_{DIC}$ (‰)	–3.5	–0.9	–12.0
NH_4^+ (mM)	0.06	0.001	–
TDN (mM)	0.08	0.02	–
PO_4^{3-} (μM)	1.4	0.1	–
TDP (μM)	1.5	0.15	–
pH	7.09	8.15	7.70
Salinity (‰)	5	35	

3. Results and Discussion

The solute composition of Izola spring water was compared to typical groundwater from SW Slovenia and to the composition of the average seawater (Table 1). The salinity of submarine spring water was 5‰ consistent with dilution in ambient seawater by advection and mixing. The reducing submarine spring water is evidenced by the presence of sulphide (0.22 mM). The spring water is rich in Ca–DIC. The concentrations of Na, K, Mg and Sr are much higher in spring water compared to the groundwater and, except for Ca, about 10–fold lower than in seawater. The calcite saturation index indicates that calcite dissolution is thermodynamically favored in the spring water. The enrichment of DIC in the Izola spring relative to the seawater can be explained by oxidation of organic matter within the spring which could be also seen in the lower $\delta^{13}C_{DIC}$ value. Additionally, the realised of CO_2 can also promote calcite dissolution in the spring.

Therefore, mixing of seawater supersaturated with respect to calcite with fresh groundwater saturated with respect to calcite results in the solution where calcite dissolution occurs. This mechanism can be explained by non–linear dependence of activity coefficient on ionic strength and by the nonlinear dependence of calcite solubility on pCO_2 [9,14].

Selected elements (Fe, Mn and Ba) suggest some interesting deviations from seawater values as well. Mn and Fe concentrations were up to 10 to 100 times higher than in the average seawater and groundwater. The behavior of these two redox couples conforms to a predictable oxidation state transformation in the reducing groundwater from more particles reactive to more soluble +2 states. Ba was also enriched in spring water relative to seawater probably due to biologically mediated precipitation of barite ($BaSO_4$) in seawater. Concentration of Al and Zn in spring water were close to onshore groundwater and higher than the average seawater. Nutrient data from the submarine spring water show that N is mostly (75%) and P almost totally present as NH_4^+ and PO_4^{3-}, respectively, which could also be the consequence of organic matter degradation present in the spring. Concentration level of Si was, on the other hand, very similar to pore waters concentrations [15], and B very similar to seawater concentrations. On the other hand, the seawater concentrations of nutrients were an order of magnitude lower than the spring water concentrations.

These results suggest that meteoric waters discharged off Izola are geochemically similar to karst groundwater, characteristic of those in SW Slovenia, mixed with about 15% of the seawater based on the comparison with conservative tracers (e.g. Cl, Mg). Hence, the onshore flow regime appears to extend onto the Gulf of Trieste. The concentrations of major solutes in the spring water are similar to those found in the study of [10] of the submarine spring off Crescent Beach in Florida. As is the case in Izola, the source aquifer for the spring water is not a single geological formation, but a more diffuse and complicated karst–influenced mixing regime. Considering the spring discharges in the Gulf of Trieste of 1 m^3/min it seems that the flux of metals and nutrients to the southern part of the Gulf of Trieste is of lesser importance compared to other fresh water discharges [16] representing <0.2% and <4%, respectively, of the freshwater input.

ACKNOWLEDGEMENT

This research was financially supported by IAEA under Research Contract No. 12156.

REFERENCES

[1] JOHANNES, R.E., THE ECOLOGICAL SIGNIFICANCE OF THE SUBMARINE DISCHARGE OF GROUND WATER, MAR. ECOL. PRO. SER. 3 (1980) 365–373.

[2] BACK, W., HANSHAW, B.B., PYLER, T.E., PLUMMER, L.N., WEIEDE, A.E., Geochemical significance of ground water discharge in Caleta Xel Ha, Quintana Roo, Mexico. Water Res. **15** (1979) 1521–1535.

[3] PAULL, C.K., SPEISS, F., CURRY, J., TWICHELL, D., Origin of Florida canyon and the role of spring sapping on the formation of submarine box canyons, Geol.Soc. Am. Bull. **102** (1990) 502–515.

[4] CHAPELLE, F.H., The Hidden sea, Geoscience Press, Tucson, AZ (1997) 238p.

[5] MANHEIM, F.T., Evidence for submarine discharge of water on the Atlantic continental slope of southern United States, and suggestions for further search, Trans. N.Y. Acad. Sci. **29** (1967) 839–853.

[6] KOHOUT, F.A., WALKER, E.H., BOTHNER, M.H., HATHAWAY, J.C.M., Fresh ground water found deep beneath Nantucket Island, Massachusetts, J. Res. U.S. Geol. Surv. **4** (1976) 511–515.

[7] KOHOUT, F.A., Ground water flow and the geothermal regime of the Floridian Plateau, Trans. Gulf Coast Assoc. Geol. Soc. **17** (1967) 339–354.

[8] SIMMS, B.S., Dolomitization by ground water flow systems in carbonate platforms, Trans. Gulf Coast Assoc. Geol. Soc. **34** (1984) 411–420.
[9] MOORE, W.S., The subterranean estuary: a reaction zone of ground water and sea water, Mar. Chem. **65** (1999) 111–125.
[10] SWARZENSKI, P.W., REICH, C.D., SPECHER, R.M., KINDINGER, J.L., MOORE, W.S., Using multiple geochemical tracers to characterize the hydrogeology of the submarine spring off Crescent Beach, Florida, Chem. Geol. **179** (2001) 187–202.
[11] GRASSHOFF, P.N., EHRHARDT, M., KREMLING, K., Methods of Seawater Analysis, Verlag Chemie, Weiheim (1983).
[12] CAPASSO, G., FAVARA, R., GRASSA, F., INGUAGGIATO, S., LONGO, M., Automated techniques for preparation and measuring stable carbon isotope of total dissolved inorganic carbon in water samples ($\delta^{13}C_{DIC}$), 7th International Conference on Gas Geochemistry, Freiberg, Germany, 22–26 September 2003, Programme & Abstract Book (2003) 38p.
[13] KUKAR, N., Geochemical mapping of Slovenia using spring waters (Geokemično kartiranje Slovenije z vodo izvirov), Graduation Thesis, University of Ljubljana (1998) 104p.
[14] PLUMMER, L.N., Mixing of sea water with calcium carbonate groundwater, Geol. Soc. Am. Mem. **42** (1975) 219–236.
[15] ČERMELJ, B., BERTUZZI, A., FAGANELI, J., Modelling of pore water nutrient distribution and benthic fluxes in shallow coastal waters (Gulf of Trieste, northern Adriastic), Wat. Air Soil Pollut. **99** (1997) 435–444.
[16] TURK, V., POTOČNIK, B., Pollution hot spots and sensitive areas along the Slovenian coast, Ann. Ser. Hist. Nat. **11** (2001) 239–252.

SUBMARINE GROUNDWATER DISCHARGE EXPERIMENTS IN INDIA

B.L.K. Somayajulu*

Planetary and Geosciences Division
Physical Research Laboratory
Ahmedabad, India

Abstract. Salinity, DO, nitrate, phosphate and silicate along with Ra isotopes (^{228}Ra and ^{226}Ra) have been measured at selected sites along the east and west coast of India in order to identify potential sites for the submarine groundwater (SGD). The result of the preliminary study does not provide unequivocal evidence for SGD due to dominant influence of local pollution on the chemical parameters. The long term seasonal measurements are essential to document SGD influence.

1. Introduction

Interest in SGD has increased tremendously during the past about one decade. Quite a few coastal regions in the world have been identified and intercomparison exercises have been conducted [1, 2]. The results of these exercises indicate that SGD does take place and more quantification is needed to identify regions with large discharges.

India has a long coast line of ~7500 km and should have potential SGD sites both on the east and west coasts (Fig. 1). The east coast of India borders the Bay of Bengal into which six large rivers drain from India and the seventh one is River Irrawaddy from Myanmar (formerly Burma), annually discharge in excess of 1015 L of water containing ~ 1015 g sediment [3, 4]. Most of this discharge takes place during the summer or Southwest Monsoon season (May–September). The other one known as the North East or Winter Monsoon (October–January) is active only in some parts of the country and does not significantly contribute to the annual rainfall over India. It is also to be noted that whereas the Arabian Sea receives very little rainfall during the year, the average annual rainfall over the Bay of Bengal is ~300 cm [5]. One more important geological feature is the tilt of the Deccan plateau due to which most of the rivers that incept on the western side of peninsular India flow across the country and drain into the Bay of Bengal [6]. It is also realized by remote sensing techniques that buried paleoriver channels do exist [7] which can be conduits for subsurface water flow should high rainfall result. As far as rain on land is concerned, the highest rainfall in peninsular India takes place on the west coast between Mumbai and Trivandrum (Fig.2) due to orography, the highest rainfall is recorded in Mangalore (~400 cm/year). The high rainfall over the ~100 km patch between the west coast and the Western Ghats discharges into the Arabian Sea and it has been shown that the sediments off the Mangalore coast hold records of past rainfall variations [8]. The other interesting region is the coast of Saurashtra, Gujarat in western India (Fig. 1) where there is salinity ingression due to excessive use of coastal groundwaters in the past. The upper parts of the coastal region is covered with a carbonate rock known as miliolite which is pervious to water exchange with the sea [9]. Considering, the above two stations have been chosen for a preliminary study, an account of which is described in the following sections. In addition, salinity monitoring of the coastal waters (up to ~100 m depth), especially between Cauvery and mouth of Krishna has been initiated with the help of the National Institute of Ocean Technology, which will later be extended to other coastal regions of the country. These will help in identifying potential SGD sites. An account of the studies conducted during the first year of the project is given in the following sections.

* *Due to a serious injury, B.L.K. Somayajulu was not able to pursue these studies further.*

2. Sites, Materials and Methods

The two selected sites are: (i) coastal strip between Visakhapatnam and Bhimilipatnam on the east coast and (ii) Veraval town on the Saurashtra on the west coast (Fig. 1).

Salinity, dissolved oxygen and nutrients (nitrate, nitrite, phosphate and silicate) to a precision of better than 5%, along with Ra isotopes, ^{228}Ra and ^{226}Ra (in 100L of water) were measured using standard techniques [10–13]. Oxygen isotopes ($\delta^{18}O$) will be measured in all the future collections.

Salinity survey in the coastal waters between Cauvery and Chennai (formerly Madras) was carried out using CTD probes. (Fig. 4). Surface Chlorophyll indicate productivity distribution along both east and west coasts around the sampling locations were obtained using remote sensing data from the Space Application Centre, Ahmedabad.

FIG. 1. Location of sampling stations on the east and the west coasts of India indicated by open circles.

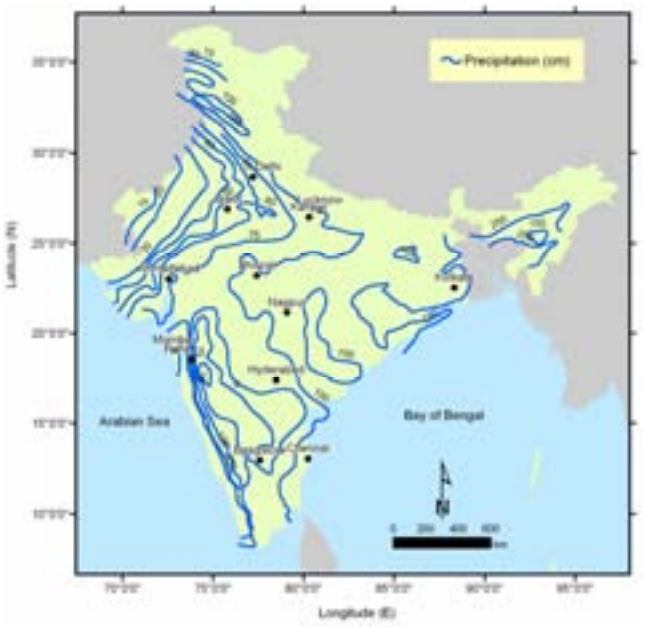

FIG.2. Map of India showing annual rainfall contours.

3. Results and Discussion

The nutrient (nitrate, phosphate and silica) along with salinity, ^{228}Ra, ^{226}Ra and $^{228}Ra/^{226}Ra$ activity ratio, henceforth denoted as [228/226], are given in Table 1.

TABLE 1. SALINITY, NUTRIENTS AND Ra ISOTOPE CONCENTRATIONS IN INDIAN COASTAL REGIONS.

Sample Code	Location	Salinity	Nitrate	Phosphate	Silica	^{228}Ra	^{226}Ra	[228/226]
			----------µM·dm^{-3}----------			-----dpm/100L-----		
East coast, Visakhapatnam (17.6ºN, 83.4ºE)								
VSP 1	RC/NIO TW*							
	Nov 2000	0.27	142	0.68	154	4.4±0.4	2.4±0.2	1.8±0.2
	Jan 2002	0.27	139	0.81	165	2.2±1.5	0.6±0.4	3.9±3.3
	Aug 2002	0.47	86.4	1.89	173	1.5±0.7	1.2±0.3	1.2±0.6
VSP 2	Appugarh TW**							
	Nov 2000	1.22	35.2	0.61	81.8	202±4	6.7±0.2	30.±1
	Jan 2002	1.35	15.8	1.26	50.2	255±9	42.4±1.5	6±0.3
	Aug 2002	1.82	24.3	0.85	58.3	152±7	26.2±1.3	5.8±0.4
VSP 3	Lawsons Bay SW							
	Nov 2000	34.95	21.1	1.23	8.9	42.6±1.9	21.3±0.6	2.0±0.1
	Jan 2002	28.7	30.3	0.63	4.36	69.6±2	13±0.6	5.4±0.3
	Aug 2002	34.0	12	2.07	3.45	29±1.8	11.1±0.7	2.6±0.2
VSP 4	Harbour SW							
	Nov 2000	34.82	26.5	4.27	9.9	55.2±1.7	31.7±0.5	1.7±0.1
	Jan 2002	28.9	35.3	9.72	11.2	36.4±2.1	22.6±0.7	1.6±0.1
	Aug 2002	31.9	145	38.2	24.9	25.6±1.5	27.3±0.8	0.94±0.06
VSP 5	KotaVeedhi TW**							
	Nov 2000	1.49	171	1.86	150	157±4	6.0±0.3	26±1.5
	Jan 2002	0.81	332	2.07	143	119±5	5.3±0.6	21.5±2.6
	Aug 2002	1.01	280	5.94	98.8	101±3	4.4±0.4	22.8±2.1
VSP6	Harbour, Turning Basin							
	Aug 2002	27.5	52.6	51.4	50.2	29.1±1.4	25±0.7	1.2±0.1
VSP7	Bhimili Temple TW**							
	Jan 2002	0.27	329	0.81	118	24.7±2.6	81.5±1.9	0.3±0.03
	Aug 2002	0.74	98.9	1.75	101	27.8±1.4	91.5±1.7	0.3±0.02
VSP8	Bhimili Gollapalem TW**							
	Jan 2002	0.54	103	1.93	150	4.9±0.6	1.1±0.1	4.6±1.9
	Aug 2002	0.74	111	4.68	203	3.8±0.7	1.0±0.3	3.8±0.2
VSP9	Bhimili lighthouse TW**							
	Jan 2002	0.54	407	1.84	44.7	77.8±2.9	20.7±0.8	3.8±0.2
	Aug 2002	0.74	111	4.68	96.7	61.9±2.6	15.7±0.8	3.9±0.3
VSP10	Bhimili SW							
	Jan 2002	27.8	137	0.67	5.42	53.8±0.3	19.4±0.8	2.8±0.1
	Aug 2002	34	11.8	0.54	2.54	26.9±1.4	8.8±0.5	3.1±0.2

Table 1. contd.

Sample Code	Location	Salinity	Nitrate	Phosphate	Silica	^{228}Ra	^{226}Ra	[228/226]
			----------µM·dm^{-3}---------			-----dpm/100L-----		
West Coast, Veraval (20.7ºN, 70.3ºE), January 2001								
S 1	Chorwad SW	34.8	1.02	1.35	13.4	10.7±1.7	8.7±0.7	1.2±0.2
S 2	Jherari GW^{+}	3.8	1.02	1.08	76.9	40.5±2.6	30.5±1.2	1.3±0.1
S 3	Kanik GW^{+}	0.93	93.4	1.8	117	29.2±1.2	26.0±0.5	1.1±0.1
S 4	Maliya GW^{+}	0.47	123	1.39	175	1.0±0.5	1.7±1.0	1.7±1.3
S 5	Loej GW^{+}	8.06	123	0.67	85.6	135±4	135±5	1.0±0.05
S 6	Gadu GW^{+}	1.01	72	0.49	129	9.4±1.7	6.0±0.7	1.6±0.3

SW: Seawater; TW: Tube well; *Depth ~70m, ** <20 m; [228/226]: Activity ratio of ^{228}Ra/^{226}Ra; GW: Groundwater (dugwells), +Average depth 15–30 m; Errors quoted propagated 1σ standard deviation on counting rates.

For the Vishakhapatnam region the data were collected during three periods/seasons, November 2000, January 2002 and August 2002 whereas for Bhimilipatnam (also known as Bhimunipatnam, Fig. 4) only two sets of measurements during Jan and August 2002 exist. Sampling at Veraval was done only in January 2001 (Table 1). The data are discussed separately for Vishakhapatnam – Bhimilipatnam strip and for Veraval. A preliminary account of the study based on one time sampling can be found in [14, 15].

3.1. Vishakhapatnam – Bhimilipatnam

The study area (Fig. 3) is covered with hills of different (~50 – 250 m) elevations and plains, which are 0 to ~20 m above mean sea level. The main rocks in the area belong to the Khondalite group of Archean age. Charnokites and pegmatites also appear in smaller amounts [16, 17]. Red soils are also present in some areas. The average annual rainfall is ~100 cm [5, 18] as most of the rainfall occurs during the southwest monsoon period, a few showers do occur during northeast monsoon period. Unusual rainfall can occur due to depressions forming in the Bay of Bengal. In fact, Bay of Bengal is known to be the seat of cyclones that have tremendous effect on the health and wealth of India.

FIG.3. Vishakhapatnam – Bhimilipatnam coastal strip with sampling locations.

The coastal strip (Fig. 3) has several open dug wells which range in depth from ~2 to 15 m. During the last decade and a half, however, more tube wells have been drilled and fitted with hand pumps, the depth of these are <~20 m. [19] observed that water level in wells has some response with rainfall in the region.

The first sample to be measured for all the parameters was the ~70 m deep tube well in the compound of the Regional Center of the National Institute of Oceanography (VSP–1) is fresh water (s = 0.27–0.47‰) which has high nutrients nitrate (N), phosphate (P) and silicate (S) during all the three periods, 86.4–142, 0.7–1.9, 154–173 μM/L, respectively. It has very low ^{228}Ra (<4 dpm/100L) and barely measurable ^{226}Ra (<2.4 dpm/100L). The second being Appugarh (VSP–2), a small fisherman village which is about 100 m from the water line on the beach and the third is the coastal (Lawson's Bay) seawater (VSP–3) with salinities ranging from 28.7–34.95‰ and has 29.6–69.6 dpm ^{228}Ra and 11.1 to 21.3 dpm ^{226}Ra per 100L. The Nutrients N and S are low whereas P shows small variation between the three samples. It is the low salinity (s = 1.22–1.82‰) VSP–2 that has the highest ^{228}Ra (152–255 dpm/100L) and ^{226}Ra (6.7–42.4 dpm/100L). Such behaviour is expected according to the studies of [14,15,20] which indicate low to mid-salinity regions of the estuaries have Ra isotope maxima due to enhanced leaching of particulate matter. This is most uncontaminated part of the area. Since the VSP–1 is from a deeper tube well compared to the rest (Table 1), two new locations of freshwater wells (having depths similar to the others) have been recently identified and samples collected for processing.

About 2 km south of this location is the entrance to Vishakhapatnam (natural) Harbour (Fig.3) one arm of which receives the city sewage. Sample VSP–6 is collected from the Turning basin in harbour which is close to the sewage channel. It has the highest phosphate of all samples, 51.4 μM/L (Table 1, Fig. 5). VSP–5 and 4 are similar to VSP–2 and 3 as far as salinities are concerned, except that VSP–5 (Kotaveedhi sample) has higher nitrate and phosphate contents (Table 1, Fig. 4) probably due to sewage seepage. Silicate does not seem to be affected by the sewage and it behaves as per expectations Viz. freshwater has the highest concentrations and seawater has the lowest (Fig.4). Unusually high nitrate and phosphate concentrations in some of the samples would have to be attributed to some kind of local pollution. This aspect is being looked into in greater detail.

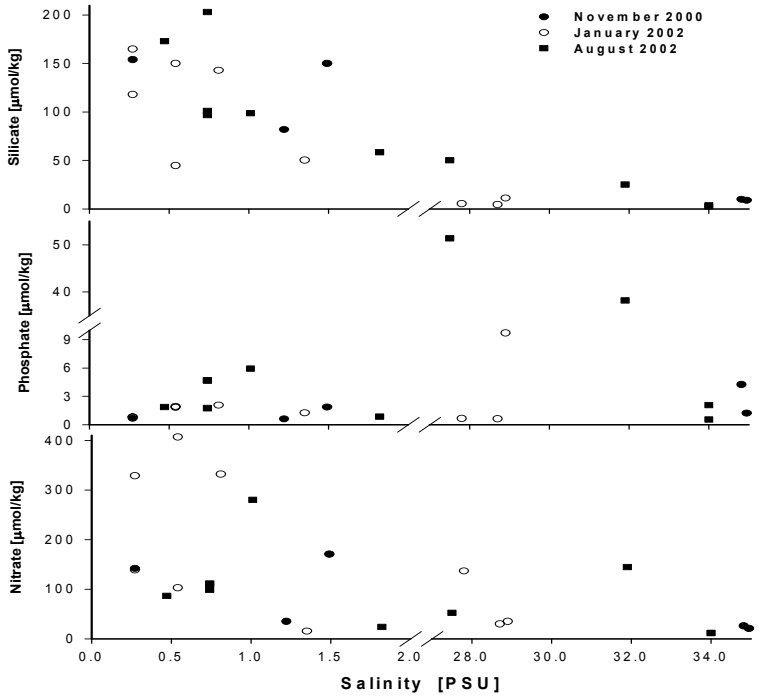

FIG.4. Plot of nutrient data as a function of salinity.

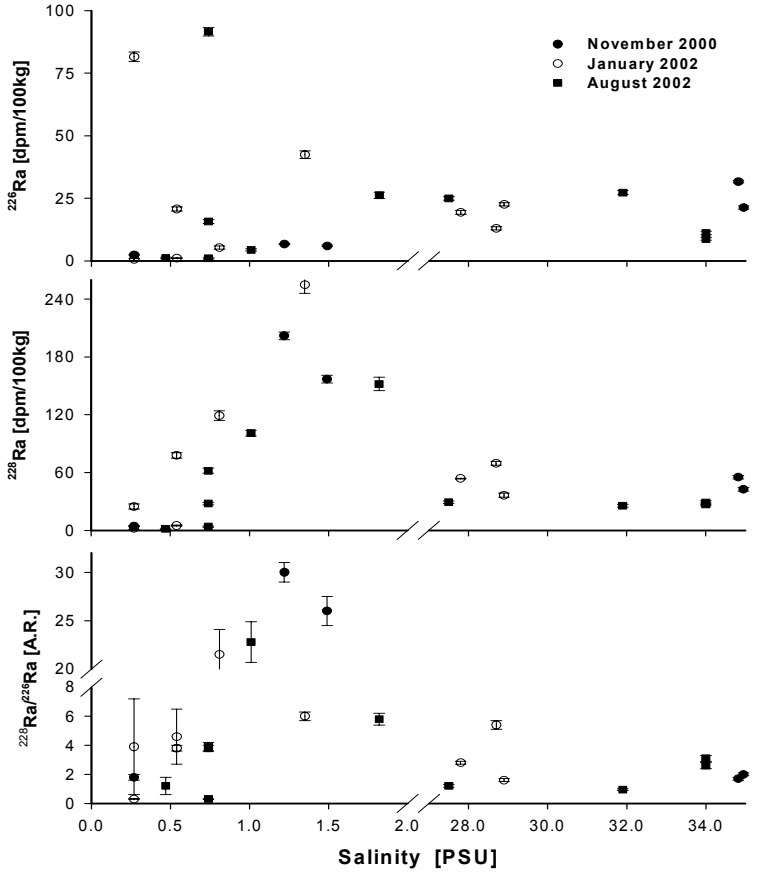

FIG. 5. Plot of ^{226}Ra, ^{228}Ra, $^{228}Ra/^{226}Ra$ as a function of salinity.

The Ra isotope data as a function of salinity in the two or three different periods of collection are shown in Fig. 5. In general the Ra isotopes, both ^{228}Ra and ^{226}Ra behave like in estuaries [20]; low concentrations are seen in fresh waters (s<0.5) and highest in waters of salinities 0.6 – ~2.0 (^{228}Ra ranges from 100–250 dpm/100L (Table 1) and relatively lower in seawater, 25–60 dpm/100L. The only unusually high ^{226}Ra of 81 and 92 dpm/100L occurs in Bhimili Temple TW with s = 0.27 and 0.74, respectively. More seasonal data are needed. There seems to be some effect of pollution on the ^{226}Ra (see data for VSP–4 and 6 (Table 1). More seasonal measurements are planned at some new sites.

3.2. Veraval

Veraval on the Saurashtra (west) coast of India is a region known for high productivity. The surficial rocks of most of coastal Saurashtra consist of miliolites of Late Quaternary [21] overlying on Tertiary carbonates, the basal Rock being Deccan Trap basalt (for details on geology, see [9]). The rain is scanty, <20 cm/a [5]. Due to over use of groundwater, seawater intrusion is reported and today the coastal wells are fairly saline and not fit for drinking. The first data set of $^{228,226}Ra$, nutrients and salinity collected during January 2001, are given in Table 1.The same pattern of variation as a function of salinity is seen. The freshwaters are high in nutrients and low in Ra. The seawater has lower nutrients and higher Ra contents compared with the fresh waters. Groundwaters from s = ~1 to 8 have the highest Ra concentrations and moderate nutrient contents (Table 1). More studies are planned.

4. Coastal Productivity

It is clearly seen from the Landsat imageries that very close to coast there is high as evidenced by Chlorophyll both on the east and west coasts of India which cover the locations under this study. Chlorophyll maximum in the subsurface waters off the study area on the coast (Fig. 6) indicates that

there has to be nutrient supply to account for this. An isotope based horizontal eddy diffusivities are high and can provide rapid nutrient transfer from coast to open sea [13, 22] throughout the year. Since upwelling is not prevalent all through the year and since groundwaters have high nutrient content, far higher than upwelling waters, one has to resort to SGD as a source. This argument assumes that there is no sewage discharge into such areas. More work is needed and this is being planned.

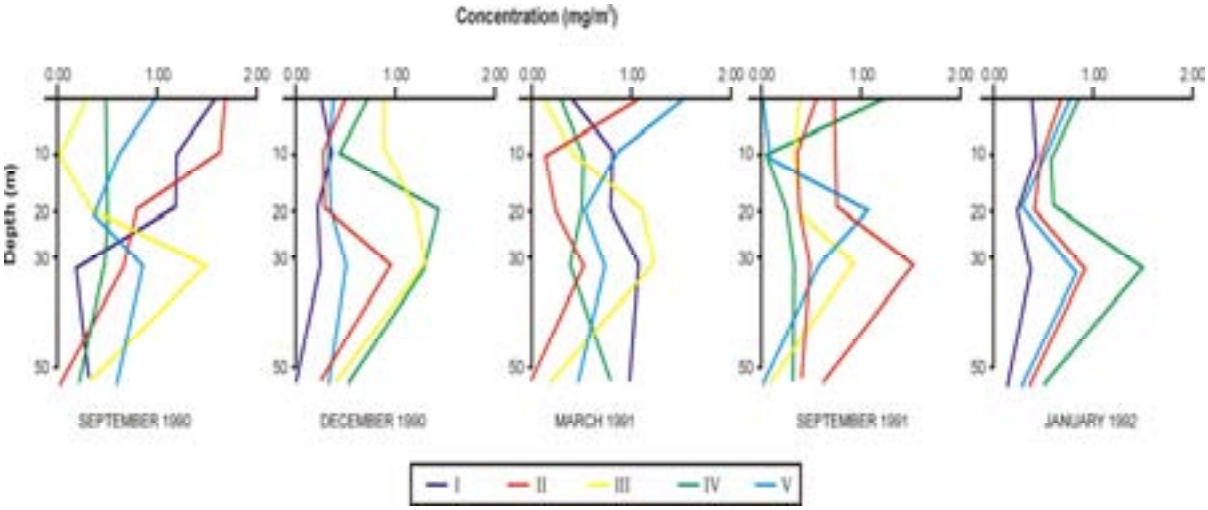

FIG. 6. Chlorophyll concentrations as a function of depth on the east coast near Vishakhapatnam.

ACKNOWLEDGEMENTS

The author wishes to thank V.V. Sarma, RC NIO, Vishakhapatnam, G. Janikiraman, NIOT, Chennai, R.K. Sarangi and S. Naik, Space Applications Centre, Ahmedabad for their valuable collaboration.

REFERENCES

[1] BURNETT, W.C., TURNER, J., LOICZ Group investigates Groundwater Discharge in Australia, LOICZ News Lett., **18** (2001) 1–4.
[2] BURNETT, W.C., KONTAR, E., BUDDEMEIER, R., Magnitude of SGD and its Influence in coastal oceanographic processes, Ann. Rep. SCOR WG 112 (2001).
[3] MILLIMAN, J.D., MEADE, R.H., Worldwide delivery of river sediment to the oceans, J. Geol. **91** (1983) 1–29.
[4] UNESCO, Discharge of selected rivers of the world, vol. II and III, Paris (1971).
[5] PANT, G.B., RUPA KUMAR, K., Climates of South Asia, John Wiley, UK (1997).
[6] RAO, K.L., India's water wealth, Orient Longman, New Delhi, India (1975).
[7] VAIDYANADHAN, R., (ed) Quaternary Deltas of India, Memoir 22, Geol. Soc. India, Bangalore, India (1991) 291p.
[8] SARKAR, A., RAMESH, R., SOMAYAJULU, B.L.K., AGNIHOTRI, R., JULL, A.J.T., BURR, G.S., High resolution Holocene monsoon record from the eastern Arabian Sea, Earth Planet. Sci. Lett. **177** (2000) 209–218.
[9] MERH, S.S., Geology of Gujarat, Geol. Soc. India Pub., Bangalore, (1995) 224p.
[10] STRICKLAND, J.D.H., PARSONS, T.R., A Practical Handbook of seawater Analysis, Bull 167, 2nd Edition, Fish. Bd. Canada, Ottawa, Canada (1972).
[11] MOORE, W.S., Sampling ^{228}Ra in the deep ocean, Deep Sea Res. **23** (1976) 647–651.
[12] MOORE, W.S., Ra isotope measurements using germanium detectors, Nucl. Instrum. Meth. **233** (1984) 407–411.
[13] RENGARAJAN, R., SARIN, M.M., SOMAYAJULU, B.L.K., SUHASINI, R., Mixing in the surface waters of the western Bay of Bengal using ^{228}Ra and ^{226}Ra, J. Mar. Res. **60** (2002) 255–279.

[14] SOMAYAJULU, B.L.K., RENGARAJAN, R., JANI, R.A., Geochemical cycling in Hooghly estuary, India, Mar. Chem. **79** (2002) 171–183.
[15] SOMAYAJULU, B.L.K., SARMA, V.V., NAIR, S., GUPTA, S.K., Preliminary studies concerning SGD in Indian Coastal regions, Revista Brasileira de Pesquisa Desenvolvimento (2002).
[16] SARMA, V.V.J., PRASAD, N.V.B.S.S., PRASAD, P.R., The hydrogeochemistry of groundwaters along the Visakhapatnam – Bhimilipatnam coast with regard to their utility for drinking, domestic and irrigational purposes, J. Assoc. Exp. Geophys. **2** (1982) 37–51.
[17] RAMAM, P.K., MURTY, V.N., Geology of Andhra Pradesh, Geol. Soc. India Pub., Bangalore, India (1997) 245p.
[18] SARMA, V.V.J., PRASAD, N. V. B. S. S. AND PRASAD, P. R., Distribution of rainfall along the coastal strip of Vishakhapatnam – Bhimilipatnam, Andhra Pradesh, Proc. Seminar on Hydrology, Osmania University., Hyderabad, India, (1983b) 45–50.
[19] SARMA, V.V.J., PRASAD, N.V.B.S.S., PRASAD, P.R., A study of water level fluctuations and estimation of recharge and recession along the coastal strip of Visakhapatnam – Bhimilipatnam, J. Assoc. Expl. Geophys. **4** (1983a) 49–65.
[20] ELSINGER, R.J., MOORE, W.S., ^{224}Ra, ^{228}Ra and ^{226}Ra in Winyah Bay and Delaware Bay, Earth Planet. Sci. Lett. **64** (1983) 430–436.
[21] BASKARAN, M., RAJAGOPALAN, G., SOMAYAJULU, B.L.K., Th-230/U-234 and C-14 dating of the Quaternary carbonate deposits of Saurashtra, India, Isot. Geosci. **79** (1989) 65–82.
[22] SOMAYAJULU, B.L.K., SARIN, M.M., RAMESH, R., Denitrification in the Eastern Arabian Sea: Evaluation of the role of continental margins using Ra isotopes, Deep Sea Res. **43** (1996) 111–117.

EVALUATIONS OF SUBMARINE GROUNDWATER DISCHARGE AND SALTWATER – FRESHWATER INTERFACE BY USES OF AUTOMATED SEEPAGE METERS AND RESISTIVITY MEASUREMENTS

M. Taniguchi

Research Institute for Humanity and Nature
Kyoto, Japan

Abstract. Seepage measurements of submarine groundwater discharge (SGD) were carried out in March 2002 in the Donnalucata boat basin in southeastern Sicily. SGD rates measured by manual seepage meters ranged from 5.5 to 19.3 L/min/m (with an average of 12.1 L/min/m), which was 0.6 and 5.9 times the SGD determined in Florida and Perth, respectively. The spatial distribution of SGD was found to be highly variable along ~300 m long coast area. Semi-diurnal SGD variations which anti-correlated with tide were found using newly developed automated seepage meters that can provide continuous SGD data with high resolution. These variations may be attributed to the tidal effect, when a greater hydraulic gradient, observed at low tide, moves groundwater from land to the ocean, and an opposite effect is observed at high tide. Groundwater discharge rates were estimated from borehole groundwater temperature and pore water temperature under the seabed to be 0.92 to 3.6 cm/day in Cockburn Sound, Western Australia. Automated and manual seepage meters measured larger groundwater discharge rates of 13.7 to 16.3 cm/day. This may be caused that observed seepage rates by seepage meters include not only terrestrial fresh groundwater discharge but also recirculated saltwater. On the other hand, the discharge rates estimated from subsurface temperature may consist of only terrestrial fresh groundwater discharge. Measurements of electric resistivity of the seabed and of the electric conductivity of submarine groundwater discharge (SGD) collected in seepage meters have been made in Ubatuba, Brazil. A diurnal variation of SGD conductivity was found under the condition of semi-diurnal tidal changes over a period of four days. SGD comprised a combination of submarine fresh groundwater discharge (SFGD) of terrestrial origin, and of recirculated saline groundwater discharge (RSGD) of marine origin. The maximum of the terrestrially derived fraction SFGD/SGD was found at a distance of 50 m offshore. A lower SFGD/SGD ratio was found closer to shore, where the highest SGD flux was measured. SGD conductivity and ground resistivity displayed a diurnal cyclicity at semi-diurnal tidal water level variations, indicating that tidal water level fluctuations may not be the primary driver of SGD flux at Ubatuba.

1. Introduction

Submarine groundwater discharge (SGD) is increasingly recognized as an important pathway for water and dissolved material from the land to the ocean [1, 2]. SGD consists not only of terrestrial fresh water (submarine fresh groundwater discharge: SFGD), but also of recirculated saline groundwater discharge (RSGD) of marine origin [3]. Salinity or conductivity is an important parameter in governing the 'water quality' of a coastal area. Therefore, we use the term 'quality of SGD' to distinguish between these two types of SGD.

The quality, or nature, of SGD at locations along a shore-perpendicular transect depends on the location (and shape) of the freshwater–saltwater interface along the transect. At the sediment surface landward and seaward from the interface, SGD consists of SFGD and RSGD respectively. Within the interface zone, SGD consists of a combination of the two types, in a ratio that is determined by the balance between hydraulic gradients and density gradients in groundwater and seawater.

Saltwater–freshwater interfaces have been intensively studied in hydrological sciences for many years, chiefly because saltwater intrusion due to excessive groundwater mining is a serious problem for water resources in coastal areas. Badon–Ghyben [4] and Herzberg [5] first studied the phenomenon of seawater intrusion into groundwater aquifers in coastal regions. Subsequently, many numerical simulations and related works attempt to evaluate mechanisms governing this process [6–8].

SGD from aquifers on the land into the ocean and seawater intrusion from the ocean into aquifers on land are complementary processes, functioning in opposite direction of flow as a result of the hydraulic gradient across the coastal freshwater–saltwater interface being directed away from shore, or towards shore respectively. In this report, field measurements on SGD and freshwater–saltwater interface in Sicily (Italy), Perth (Australia), and Ubatuba (Brazil) are described.

2. Study areas

2.1. Sicily, Italy

The first experiment site is located in Sicily, Italy (Fig. 1). Seven manual (Lee–type) seepage meters (A_0, A_1, A_2, A_3, A_4, A_5 and A_6) and five automated (continuous type) seepage meters (H, K1, K2, E and F) were deployed to measure SGD (Fig.1) in the Donnalucata boat basin (the province of Ragusa) at the southeastern coast of Sicily. The geologic setting, meteorological and hydrological conditions were described in detail by Aureli [9].

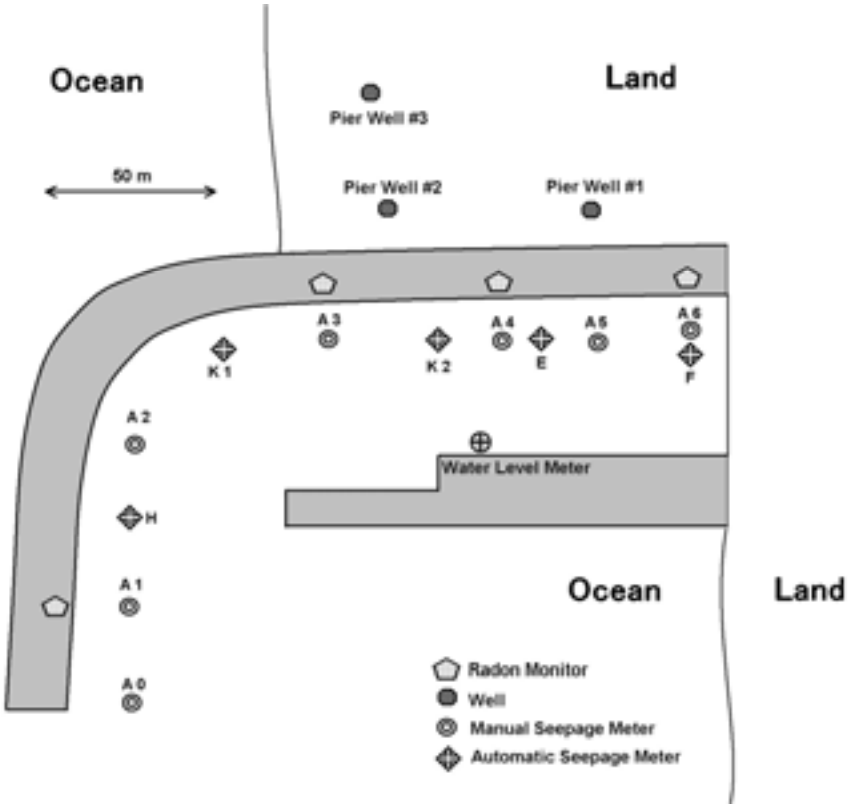

FIG. 1. Location of the study site in Sicily, Italy. The shoreline at low tide, locations of three seepage meters and two transect lines (A and B) are shown.

Measurements using manual and automated seepage meters were carried out from March 19 to 23, 2002. Plastic bags for the manual seepage meters were changed every one to a few hours depending on the volume of the SGD. The bags were pre-filled with 1 L of water to prevent the measurement artefact of the seepage meter. Measurements using manual seepage meters were made from the morning to the evening with help of divers. Continuous measurements of SGD by automated seepage meters were done every 10 min.

Sea water level was also measured continuously near the jetty (Fig. 1) every 3 min [10].

2.2. Perth, Australia

The second experimental site for the study (Fig. 2) was located near to Northern Harbour, approximately 10 km south of Fremantle in Western Australia. Smith and Hick [11] describe the hydrogeology and aquifer water balance for this region of the Swan Coastal Plain. Superficial sediments consisting predominantly of limestone overlain by sand extend to a depth of approximately 30 m below sea level. Beneath this is a relatively impermeable aquitard consisting of Cretaceous sandstone, siltstone and shale. Shallow groundwater is recharged by rainfall infiltration through well-drained sandy soils and un-utilised groundwater drains laterally toward the coast and discharges along the shoreline of Cockburn Sound. All bores considered in this study are installed into the shallow groundwater system within the superficial sediments.

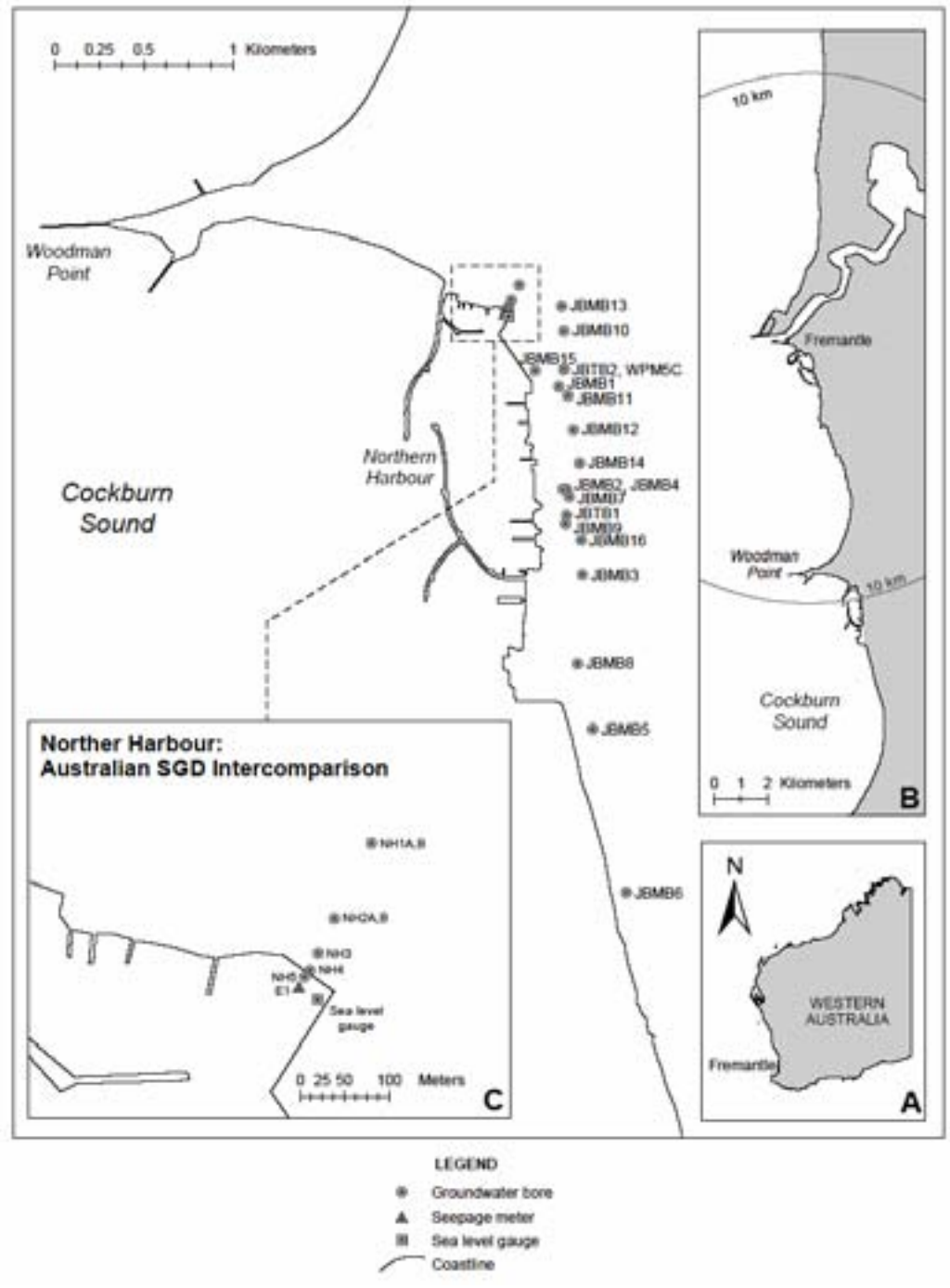

FIG.2. Location of the study site in Perth, Australia.

Temperature measurements in boreholes were collected using a pre-calibrated thermistor thermometer at 50 cm intervals from the water table to the bottom of the boreholes. Electrical conductivity (EC) was measured at the same intervals. These data were collected on two occasions, 29 February 2000 and 28–29 November 2000.

Submarine groundwater discharge at E1 (Fig.2, insert C) was measured using a Lee type manual seepage meter [12] as well as an automated seepage meter every five minutes during the period from 8:00 pm on 28 November 2000 to 10:00 am on 4 December 2000. The automated seepage meter used the principle of heat convection caused by water flow. The basis of the method is measurement of the temperature gradient between the downstream and upstream positions of the flow tube through which SGD is amplified. The meter is described in detail by Taniguchi and Iwakawa [13], and compared with other types of seepage meter by Taniguchi et al. [14].

Submarine pore water temperatures at different depths were measured every five minutes near to the sea level gauge inside of Northern Harbour (Fig.2, insert C) using thermistor thermometers. The measurement depths were 5, 10, 30 and 50 cm below the seabed and data was collected during the period 1:00 pm on 27 November 2000 to 7:00 pm on 6 December 2000.

2.3. Ubatuba, Brazil

The third intergovernmentally sponsored intercomparison of methods to study SGD was carried out in November 2003 at Flamengo Bay near the city of Ubatuba, São Paulo State, Brazil (Fig. 3). The geomorphologic and hydrogeological characteristics of the area are controlled by the presence of fractured crystalline rocks. The granites and migmatites of the mountain chain Serra do Mar with altitudes up to 1,000 m reach the shore of the study area and limit the extension of the drainage systems and of the Quaternary coastal plains [15]. The mean annual rainfall is about 1,800 mm, with maximum rainfall usually occurring in February. Tidal sea level variations range from 0.5 to 1.5 m, the highest values occurring in months August/September due to greater volume of warm waters of the Brazil Current [16]. Despite the small drainage basins between the mountain range and the shore, freshwater discharge is sufficient to reduce the salinity of coastal waters. Three automated continuous-heat-type seepage meters were located at 10 m, 40 m, and 50 m distance offshore from the low tide mark in Flamengo Bay (Fig. 3).

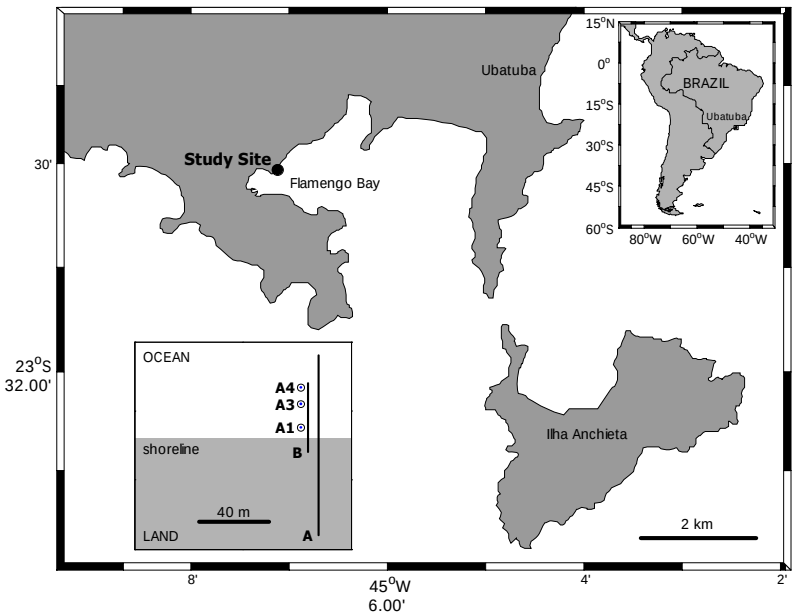

FIG. 3. Location of the study site in Ubatuba, Brazil.

3. Methods

3.1. SGD flux and electric conductivity of SGD

SGD fluxes were measured by uses of automated seepage meters. The measurement of flow in these automated seepage meters is based on the effect of heat convection induced by water flow by measuring the temperature gradient of the water flowing between the downstream and upstream positions in a horizontal flow tube with a diameter of 1.3 cm, which is connected to the chamber. The principle of the automated seepage meter is described in detail by Taniguchi and Iwakawa [13] and Taniguchi et al. [17]. The average depth of the seawater was 0.3 m, 1.2 m, and 1.5 m at the location of seepage meters A1, A3, and A4, respectively. The seepage meter chambers had a diameter of 0.57 m, and water in the chamber is replaced within a day if seepage rate is equal to or larger than 10^{-7} m·s^{-1}.

The electric conductivity of the water within the chambers was measured continuously with conductivity–temperature–depth (CTD) sensors (DIK 603A CTD, Daiki Rika Kogyo Co., Ltd.) deployed in the chambers of the seepage meters.

Tidal (sea) level was recorded every 10 minutes at A1 before noon of 18 November and at A4 after noon of 18 November 2003, using a pressure transducer which was attached to the outside of the chamber of the seepage meter. The groundwater in a well located 20 m inland from the landward end of transect line A was sampled, in order to determine the conductivity of the SFGD end member.

3.2. Subsurface resistivity

Subsurface resistivity investigations have been carried out to reveal the structure of the flow field of the freshwater component of SGD. Such measurements allow for predictions of entry points of fresh SGD. While it is not possible to derive absolute SGD fluxes from such geoelectrical measurements, the relative distribution of SGD can be investigated in great detail, especially where seepage or discharge follows preferential flow paths. The (bulk) resistivity of the seabed and the land surface along two shore-perpendicular transect lines was determined by inverse modelling of remotely sensed resistivity measured on electrodes deployed only on the surface, using the commercial electrode array Sting R1 IP/Swift（AGI）. The 28 electrodes of the array were arranged in a Wenner configuration (equally spaced) with a distance between electrodes of 10 m and 3 m for the transects A and B, respectively. The software RES2DINV ver. 3.50 (Geotomo Software) was used for the resistivity analyses.

4. Results

4.1. SGD and S–F interface in Sicily

Five to seven SGD measurements were obtained by manual seepage meters at every location each day. Figure 4 shows the temporal and spatial variations (along the transect line) variations of SGD obtained by manual seepage meters from 19–23 March 2002. As can be seen, SGD decreases from the coast (location A6) to the location A4, however, maximum SGD rates were found at location A3. SGD decreases then again from location A3 to further offshore. Daily average of SGD obtained by manual seepage meters ranges from 5.5 to 19.3 L/min/m, and the average of SGD for five days was 12.1 L/min/m. The reason why the maximum SGD was found not close to the shoreline but at A3 is not clear. Salinity and ^{222}Rn measurements showed that SGD at this site is represented by recirculated seawater [18].

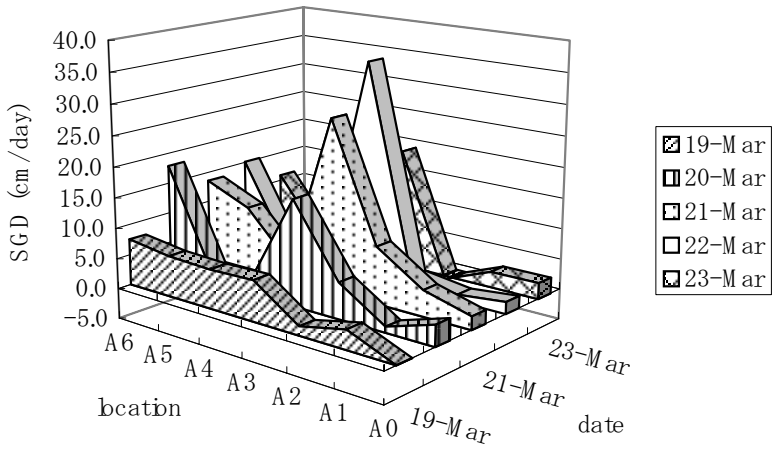

FIG. 4. Temporal and spatial changes on SGD in Sicily, Italy.

According to the calculations of total discharge into a domain of 37 m wide (along shore between two jetties) by 253.5 m long (out to sea), the daily average of SGD from the domain ranges from 214 to 714 L/min (0.20 to 0.71 m^3/min) with the average of 449 L/min (0.45 m^3/min).

4.2. SGD and S–F interface in Perth

Changes in SGD measured by the automated seepage meter at E1 are shown in Fig.5 as well as tidal elevation data observed by the sea level gauge (Fig.2, C). The average of SGD rate during the observation period (from 8:00 pm on 28 November 2000 to 10:00 am on 4 December 2000) was 16.3 cm/day. This compares with SGD measurements made using manual Lee–type seepage meters [19], which at E1 had daily average values of 3.8, 7.9, 14.2, 13.3, 24.2, and 18.8 cm/day for 28, 29, 30 November, 1, 2, 3 December, respectively [12]. The general increase of SGD may be caused by the general decrease in tidal elevation. The total average of SGD measured using the manual seepage meter at E1 was 13.7 cm/day. Figure 5 indicates that diurnal variations of SGD were observed. Taniguchi et al. [17] observed semi-diurnal (half-day) variations of SGD in the Gulf of Mexico, and Taniguchi [3] measured both diurnal and semi-diurnal variations of SGD due to tidal effects in Osaka bay, Japan.

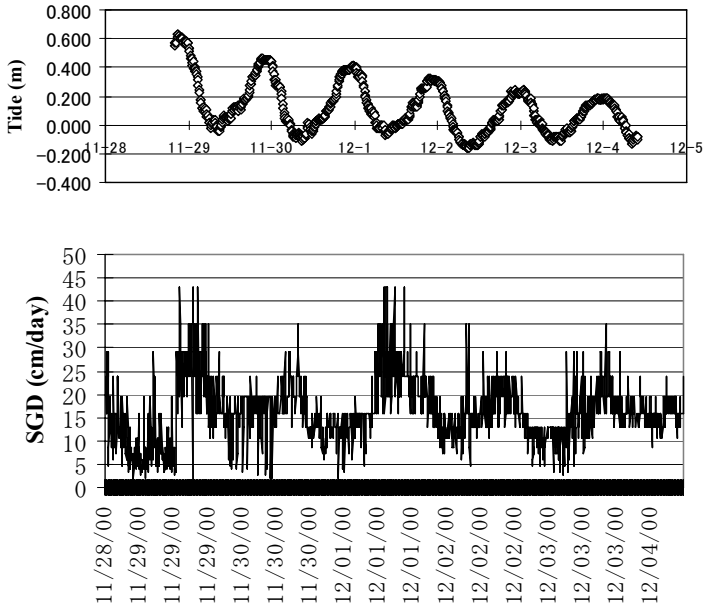

FIG. 5. Temporal changes in tide and SGD at Perth, Australia.

Change in pore water temperature at depths of 5, 10, 30 and 50 cm below the seabed is shown in Fig.6. Diurnal variations in pore water temperature were observed and may have been caused by diurnal variation in air temperature. The depth of seawater near the sea level gauge was less than 1 m during the observation period; diurnal variation of air temperature may have penetrated to the measurement depths with time lags.

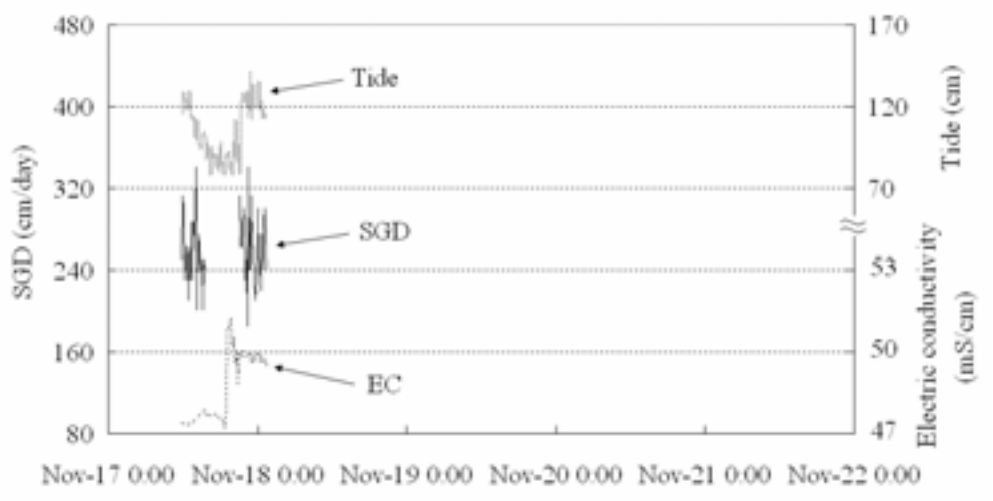

FIG. 6. Temporal changes in tide, SGD rate, and electric conductivity of SGD at A1.

The Krupaseep [20] measured seawater temperatures in the range 21.5 – 23.8 °C during the same period that pore water temperatures were collected. Therefore, shallow pore water temperatures less than 21 °C may indicate groundwater discharge. Also, although the tide and solar heating were both diurnal, they had different phases during the observation period. High tide occurred around midnight and low tide around 9 am – 12 pm in the morning. This could account for the bi-modal temperature response in pore water temperature at the depths of 5 and 10 cm below the seabed.

Subsurface temperature should be treated as 2D or 3D because the groundwater flow system is generally 2D or 3D. However, the groundwater flow near the coast, in particular at seabed, becomes vertical upward [21, 22]. Therefore, we may treat the subsurface temperature as 1D for first order approximation.

4.3. SGD and S –F interface in Ubatuba

Temporal variations in tidal sea level, SGD rate, and conductivity of SGD at A1, A3, and A4 are shown in Figs 6, 7, and 8, respectively. The amplitude of the semi-diurnal tidal variation was about 50 cm. The averaged SGD rates were 260 cm/day (3.01×10^{-5} m/s) at A1, 3.8 cm/day (4.35×10^{-7} m/s) at A3, and 185.6 cm/day (2.15×10^{-5} m/s) at A4. Semi-diurnal variations of SGD were observed at two of the three stations. Temporal variations of SGD rates are discussed in more detail by Bokuniewicz et al. [23].

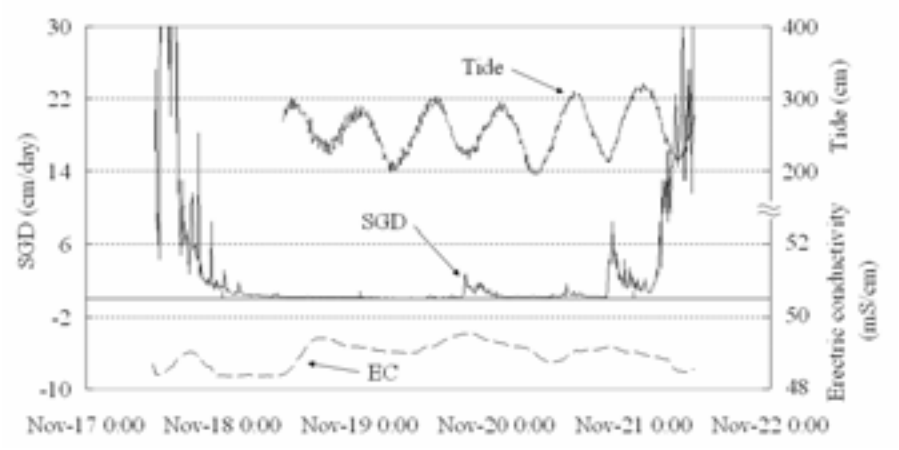

FIG.7. Temporal changes in tide, SGD rate, and electric conductivity of SGD at A3.

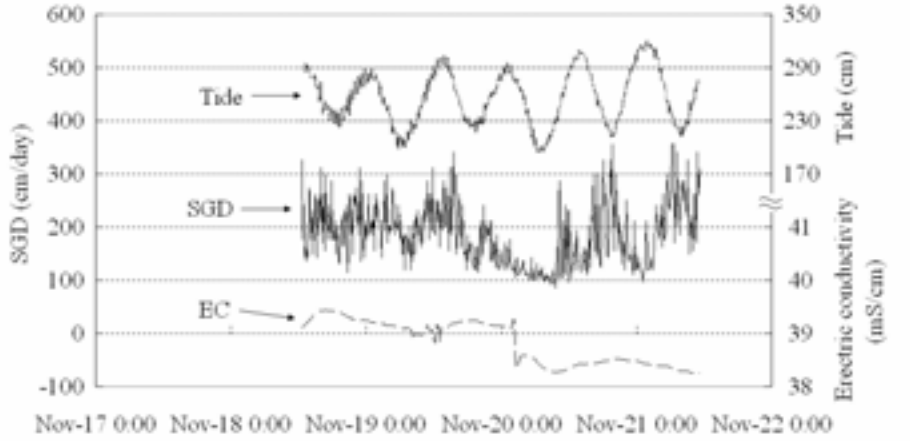

FIG.8. Temporal changes in tide, SGD rate, and electric conductivity of SGD at A4.

The average conductivity at A1, A3, and A4 was 48.7, 48.9 and 40.0 $mS \cdot cm^{-1}$, respectively. The highest conductivity of SGD was found at low–high tides at A3 and A4. As can be seen from Fig.7 and Fig.8, high conductivity was found at high SGD, and diurnal changes of the electric conductivity of SGD were found.

Diurnal variations of electric conductivity of SGD are apparent at sites A3 and A4 (Figs 7 and 8), with ranges of variations of ca. 0.8 $mS \cdot cm^{-1}$ and 0.5 $mS \cdot cm^{-1}$ at A3 and A4 respectively (Figs 7 and 8). The conductivity of ambient seawater and freshwater in the bore was 51.6 $mS \cdot cm^{-1}$ and 0.066 $mS \cdot cm^{-1}$ respectively. The ranges of changes in electric conductivity of SGD were about 0.8 mS/cm at A3 (Fig. 7) and 0.5 mS/cm at A4 (Fig.8). As can be seen from Fig. 7 and Fig. 8, high conductivity was found at high SGD.

The spatial distribution, and its changes with time, of the subsurface resistivity are shown in Fig. 9 and Fig.10 for the long and short transect respectively. Figure 9 shows the transition from rising tide to falling tide, with high tide at 1pm in the centre graph. The darker tone shows fresher water (higher resistivity), and lighter tone shows saltier water (lower resistivity). The arrows show the locations of the shore line and the y-axis shows the elevation. The freshwater–saltwater boundary is almost vertical with the wedge landward at the shallow depth, and moves toward offshore at high tide (1 pm), in consistency with the results of changes in electric conductivity (Figs 7 and 8). In other words, lowest overall ground resistivity (high conductivity) was found at high tide. Temporal variations of the resistivity with a high spatial resolution along the line B are shown in Fig.10.

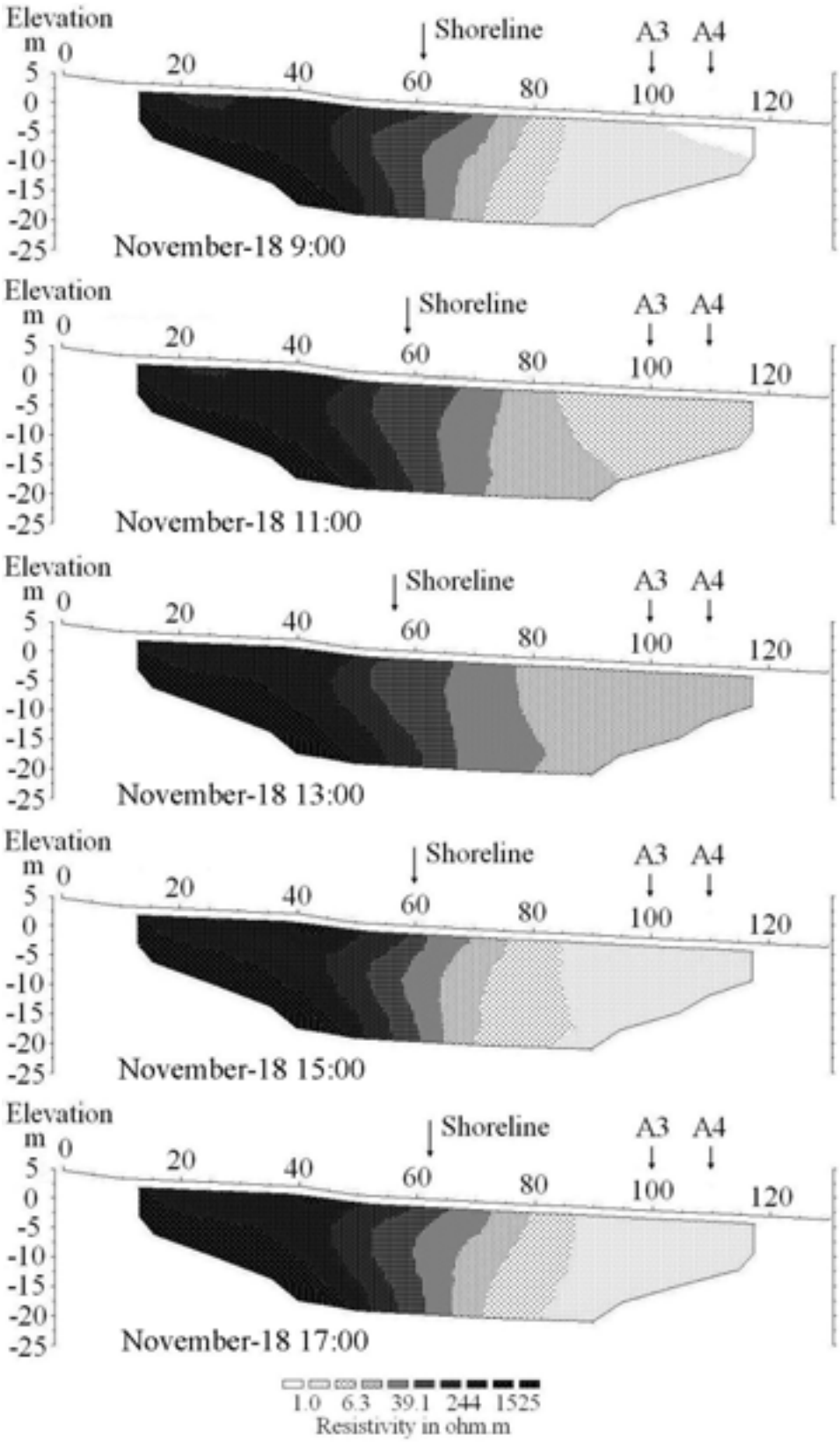

FIG.9. Temporal variation of resistivity of the seabed along the line A with 10 m interval probes at 9 am, 11 am, 1 pm, 3 pm, and 5 pm (from top to bottom) on 18 November 2003. The arrows indicate the location of the shoreline at low tide and the y-axis shows the elevation. The darker colour indicates higher resistivity representing relative freshening of the pore water and lighter colour shows lower resistivity representing saltier pore water.

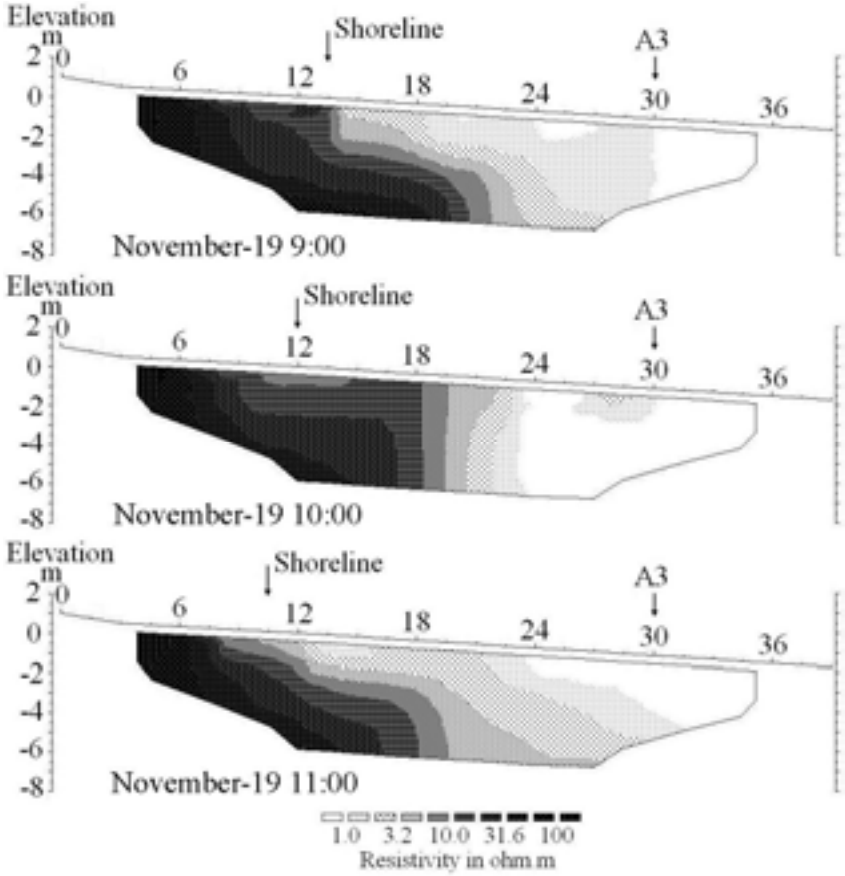

FIG.10. Temporal variation of resistivity of the coastal pore water along the line B with 3 meter interval probes at 9 am, 10 am, and 1 pm (from top to bottom) on 19 November 2003. The arrows indicate the location of the waterline at low tide, and the y-axis shows the elevation. Note the difference in scale compared with Fig.9.

5. Discussion

5.1. Comparison of SGD

SGD assessment intercomparison exercises have been organized in several coastal sites including (1) the northeastern Gulf of Mexico, Florida, United States of America, and (2) Southwest of Perth, Australia. SGD measurements showed that Sicily was 0.589 and 5.9 times of SGD in Florida and Perth, respectively. One of the reasons of this difference may be hydrogeology.

Taniguchi et al. [3] defined that SGD which consists of submarine fresh groundwater discharge (SFGD) and recirculated saline groundwater discharge (RSGD). They also defined RSGD consists of recirculated water due to wave set-up, recirculated water due to tidally-driven oscillation, and recirculated water due to convection (either density or thermal). Therefore the total submarine groundwater discharge (SGD) includes both a terrestrial component of net fresh groundwater and an oceanic component of recirculated seawater. SGD measured by seepage meters consists of both SFGD and RSGD; therefore, it may be better to compare each component of SGD in different places. Then, we may be able to evaluate hydrological effects (mainly SFGD) and oceanographic effects (mainly RSGD) on SGD.

Taniguchi and Iwakawa [13] compared the terrestrial fresh SGD and recirculated saline SGD for the total SGD in Osaka Bay, Japan. They calculated SFGD rate by multiplying the observed hydraulic gradients between sea level and groundwater level, and the estimated hydraulic conductivity under the

assumption of Darcy's Law. They found the ratio of SFGD to SGD ranged from 4% and 29% in Osaka Bay, Japan. Ratios of SFGD to SGD were also estimated in other studies to be 35% using seepage meters and salinity measurements by Gallagher et al. [24], 10% using ^{222}Rn and ^{226}Ra measurements by Hussain et al. [25], and 4% using numerical simulations by Li et al. [26].

Unfortunately, the SGD experiment in Sicilian coastal water was not designed to separate fresh terrestrial SGD and recirculated saline SGD. In order to evaluate both hydrological and oceanographic effects on SGD, further investigation of SGD may be needed by separating SGD into SFGD and RSGD.

5.2. SGD estimations by uses of subsurface temperature

To evaluate the groundwater fluxes from borehole temperature–depth profiles, type curve analyses using heat conduction–convection theory were carried out for NH2A and NH1A (Fig.2a). The best matching of type curves yielded values of $\beta = -2.8$ for NH1A and $\beta = -3.5$ for NH2A. Setting $\kappa = 1.6$ W $℃^{-1}\cdot m^{-1}$ and $c_o\rho_o = 4.18 \times 10^6$ J $℃^{-1}\cdot m^3$, v_z was calculated to be –0.92 cm/day (upward flux) at NH1A and –0.96 cm/day at NH2A. The thermal property values assumed for sand and applied in this analysis were adopted from Taniguchi et al. [27].

According to the continuous measurements of SGD rates by an automated seepage meter and Lee–type manual seepage meters, the average of SGD for each meter during the entire observation period varied in the range 13.7–16.3 cm/day. Groundwater discharge rates estimated from subsurface temperature in NH1A and NH2A were 0.92 and 0.96 cm/day and SGD estimated from pore water temperature was 3.6 cm/day. Therefore, SGD rates measured by seepage meters were larger than those estimated from subsurface temperature. One explanation is that seepage rates measured by seepage meters may include both terrestrial groundwater discharge and recirculated salt water [3]. On the other hand, the discharge rates estimated from subsurface temperature may consist of only terrestrial fresh groundwater discharge. Although subsurface temperature cannot tell whether recirculated seawater is a component of the SGD, however, different temperature between pore water and seepage water [20] may support this argument.

The difference between SGD rates estimated from the pore water temperature at 10 m offshore from the coast and the rates estimated from the temperature–depth profile at 75 m and 160 m inland may be caused by the geographical location of the measurements. According to the SGD analyses by Kohout [28], the area that can effectively convey groundwater flow near the coast is smaller than that the area that can effectively convey groundwater inland. Therefore, the velocities must increase toward the coast. These estimates also represent the vertical component of the groundwater flow. The landward regions experience predominantly horizontal flow. On the other hand, the streamline of the groundwater at the coast are more vertical and it has larger vertical component of the velocity.

5.3. Relative contributions of SFGD and RSGD

In order to separate SGD into its two components submarine fresh groundwater discharge (SFGD) and recirculated saline groundwater discharge (RSGD), analyses of water and material budgets using two end members can be made. Here, water balance and material balance equations at the seabed are described as follows; SGD = SFGD + RSGD, and $C_{SGD} \times SGD = C_{SFGD} \times SFGD + C_{RSGD} \times RSGD$, where C_{SGD}, C_{SFGD}, and C_{RSGD} are conductivity of SGD, SFGD and RSGD, respectively. The fresh terrestrial groundwater at 20 m inland from the end of resistivity cable at a conductivity of C_{SFGD} = 0.066 $mS\cdot cm^{-1}$ and sea water at C_{RSGD} = 51.6 $mS\cdot cm^{-1}$ were used as end members of SFGD and RSGD, respectively. Average SGD conductivity was 48.7, 48.9 and 39.9 $mS\cdot cm^{-1}$ at A1, A3, and A4, respectively, and an average SGD was 260 $cm\cdot day^{-1}$ (3.01×10^{-5} $m\cdot s^{-1}$), 3.8 $cm\cdot day^{-1}$ (4.35×10^{-7} $m\cdot s^{-1}$), and 185.6 $cm\cdot day^{-1}$ (2.15×10^{-5} $m\cdot s^{-1}$) at A1, A3, and A4, respectively. Time series of SFGD and ratio

of SFGD (= SFGD/SGD) were calculated and shown in Fig.11. The average of the relative contribution of SFGD (= SFGD/SGD) were about 5.5%, 5.1%, and 24.8% at A1, A3, and A4, respectively.

5.4. Migration of the saltwater–freshwater interface with time

In general, a landward migration of the saltwater–freshwater interface would be expected to occur at high tide due to an increased hydraulic pressure of the water overlying the marine sediments. However, here the opposite was observed: the interface moved further offshore, despite an increase in tidal water level. This suggests that there are additional driving forces at play, with at least similar-order-of-magnitude effect as water tidal level variation, an interpretation that is supported by the lack of correlation of the conductivity recorded in the seepage meters with tidal record. It is intuitive to assume that rapid, periodic changes in recharge may in part be responsible for the decoupling of conductivity and tide [23,29].

Taniguchi et al. [30] employed similar methods in Siranui, Japan to evaluate the relationship between temporal changes in saltwater–freshwater interface and SGD. They found that the highest SGD occurred just landward of the interface, and that the processes of SGD differ between the offshore and near shore environments. Temporal changes of the ground resistivity at the depth of 2.5 m below the seabed with the distance from shore are shown in Fig.12 together with changes in electric conductivity of SGD at A3 and A4. As can be seen from Fig.12, the maximum resistivity (minimum electric conductivity) was found at 12:00 at 15 m, at 13:00 at 25m and 35m, and at 15:00 at 45m and 55m. The time delay of the maximum resistivity shows the pore water exchange depending on the tidal changes. Although the data is limited to 10 hours observation time, it suggests a diurnal variation of subsurface resistivity, thus indicating that the diurnal conductivity variation observed in the seepage meters is indeed driven by hydraulic forcing, and is not an instrumental artefact.

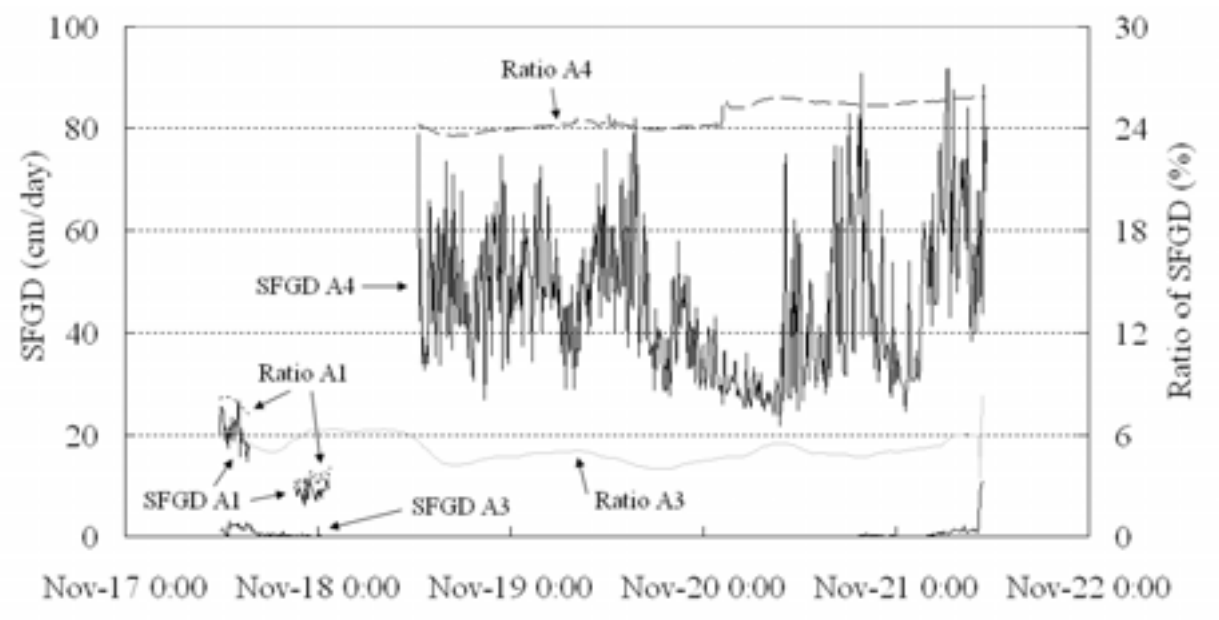

FIG.11. Temporal changes in SFGD rate (A1, A3 and A4) and ratio of SFGD to SGD (Ratio A1, A3, and A4).

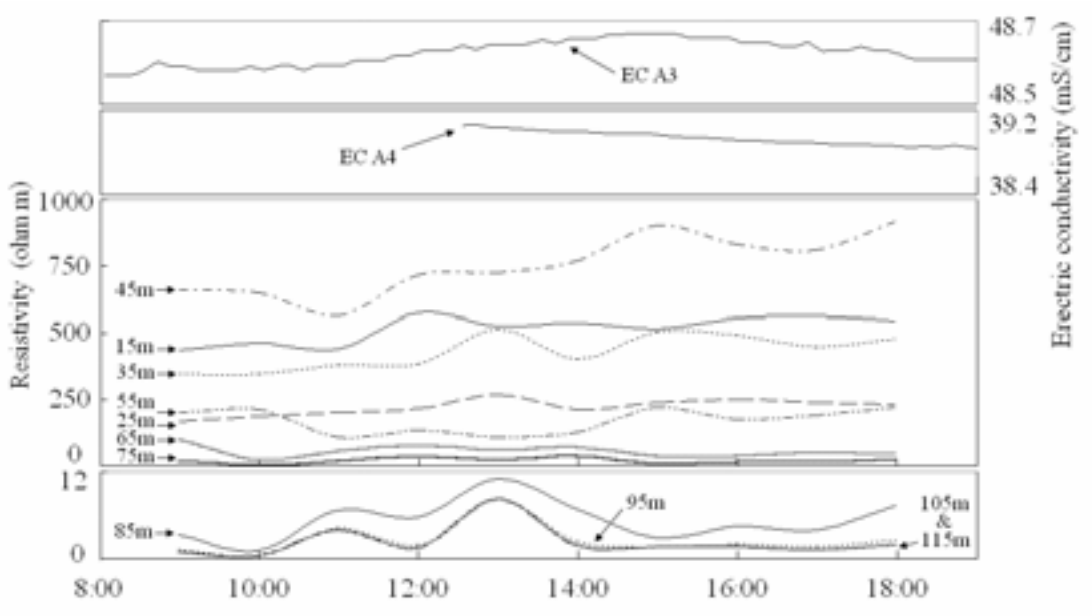

FIG.12. Temporal changes of resistivity of the pore water at the depth of 2.5 m below the sea bed with the distance from the shore line at low tide.

5.5. Relationship of SFGD/SGD ratio and coastal aquifer properties

In areas where a homogenous, unconfined coastal aquifer is connected to the ocean, the SFGD/SGD ratio monotonically decreases with distance from shore, to a maximum distance at which SFGD/SGD = 0 and RSGD/SGD = 1. This distance depends on aquifer properties and relative driving forces caused be hydraulic gradient [31]. Where heterogeneous properties exist, this relationship does not exist, and instead the SFGD/SGD ratio will depend on the location of preferential flowpaths. The presented data suggests that preferential flowpaths exist, that result in a non-monotonical relationship of SFGD/SGD with distance from shore. These observations are consistent with findings of other workers during the international experiments [23,28].

Note that although the comparatively highest SGD flow rate was found at the site nearest to shore (A1), the SFGD/SGD ratio was comparatively low at this site, indicating a comparatively weaker influence of terrestrial groundwater. It is possible that a shallow layer of saltier water in the sediment at A1 was pushed up by an inland hydraulic head, resulting in a higher RSGD/SGD ratio. In summary, we suggest that in spatially complex coastal settings, the spatial distribution of SFGD/SGD ratio collected in seepage meters provides an indication of the degree of spatial heterogeneity of the shallow aquifer system that is connected to the ocean.

6. Conclusions

The conclusions of this study are;

(1) SGD obtained by manual seepage meters ranges from 5.5 to 19.3 (with the average of 12.1) L/min/m in Sicily, Italy.

(2) Semidiurnal variations of SGD due to tidal effects were found by using automated seepage meters which can provide continuous SGD data with high resolution.

(3) Large heterogeneity of the SGD distribution was found in Sicily, Italy.SGD in this study area, Sicily was 0.589 and 5.9 times of SGD in Florida and Perth, respectively.The average of SGD rate, 16.3 cm/day, measured using an automated seepage meter agreed well with the average SGD

rate, 13.7 cm/day, measured using manual (Lee–type) seepage meters at E1, which was located 10 m offshore from the coast, in Perth.

(6) Diurnal variations of SGD due to tidal effects were observed in continuous measurements of SGD made using the automated seepage meter in Perth.

(7) Upward groundwater fluxes were estimated from borehole temperature and pore water temperature using type curve methods to be 0.92 cm/day and 0.96 cm/day at 75 m and 160 m inland from the coast, and 3.6 cm/day at 10 m offshore seabed, respectively in Perth.

(8) The SGD estimated from subsurface temperature may consist of only terrestrial fresh groundwater discharge. However, SGD rates observed by seepage meters may include both fresh groundwater discharge and recirculated saline water. Therefore, the standard seepage meter measurements of SGD might strongly overestimate freshwater flow from terrestrial origin.

(9) Diurnal variation of SGD conductivity was found under the condition of semi-diurnal tidal changes. There was only one peak of the resistivity of the pore water at each location near the coast. This may be caused by the time delay of the mixture of terrestrial fresh water (SFGD) and RSGD may be one of the reasons.

(10) The freshwater–saltwater interface moves toward offshore at high tide, this is consistency to the changes of electric conductivity of SGD.

(11) The maximum of the SFGD/SGD ratio was found at not near shore but offshore. On the other hand, low SFGD/SGD ratio was found at near shore although the highest SGD was obtained there.

(12) The geophysical observations presented here are consistent with SGD being highly variable in space and time in the Ubatuba region, likely as a response to the heterogeneity of the local fractured rock aquifer. We suggest that in spatially complex coastal settings, the spatial and temporal variation of the SFGD/SGD ratio collected in seepage meters provides an indication of the degree of spatial heterogeneity of the shallow aquifer system that is connected to the ocean.

ACKNOWLEDGEMENTS

The author acknowledges support from the International Atomic Energy Agency (IAEA), which financed this activity through their coordinated research project (CRP) entitled Nuclear and Isotopic Techniques for the Characterization of Submarine Groundwater Discharge in Coastal Zones. Lastly, I wish to thank the local organizers of the experiments in Sicily, Perth, and Brazil.

REFERENCES

[1] MOORE, W.S., Large groundwater inputs to coastal waters revealed by ^{226}Ra enrichments, Nature **380** (1996) 612 –614.
[2] BURNETT, W.C., TANIGUCHI, M., OBERDORFER J.A., Measurement and significance of the direct discharge of groundwater into the coastal zone, J. Sea Res. **46** 2 (2001) 109–116.
[3] TANIGUCHI, M., BURNETT, W.C., CABLE,J.E., TURNER, J.V., Investigation of submarine groundwater discharge, Hydrol. Process. **16** (2002) 2115–2129.
[4] BADON–GHYBEN, W., Nota in verband met de voorgenomen putboring nabil Amsterdam' Tijdschr. K. Inst. Ing., The Hague **27** (1888–1889).
[5] HERZBERG, A., Die Wasserversorgung einiger Nordseebader, J. Gasbeleucht. Wasserversorg. **44** (1901) 815 –819, 842 –844.
[6] SEGOL, G., PINDER, G.F., Transient simulation of saltwater intrusion in Southeastern Florida, Water Resour. Res. **12** (1976) 65–70.
[7] FREEZE R.A., CHERRY, J.A., Groundwater, Prentice Hall, Englewood Cliff, (1979) 604p.

[8] HUYAKORN, P.S., ANDERSON, P.F., MERCER, J.W., WHITE, H.O., Saltwater intrusion in aquifers, Development and testing of a three–dimensional finite element model, Water Resour. Res. **23** (1987) 293–312.
[9] AURELI, A., The submarine springs in Sicily. Report of the Instituto di Geologia e Geofisica, Universita di Catania, Sicily (1992) 21p.
[10] BURNETT, W.C., DULAIOVA, H., Radon as a tracer of submarine groundwater discharge into a boat basin in Donnalucata in Sicily. Cont. Shelf Res. **26** (2006).
[11] SMITH, A.J., HICK, W.P., Hydrogeology and aquifer tidal propagation in Cockburn Sound Western Australia, CSIRO Land and Water Technical Report 06/01 (2001).
[12] BURNETT W.C., TURNER J.V., LOICZ group investigates groundwater discharge in Australia, LOICZ Newsletter **18** (2001) 1–4.
[13] TANIGUCHI, M., IWAKAWA, H., Measurements of submarine groundwater discharge rates by a continuous heat–type automated seepage meter in Osaka Bay, Japan, J Groundw. Hydrol. **43** 4 (2001) 271－277.
[14] TANIGUCHI, M., BURNETT, W.C., CABLE, J.E., TURNER, J.V., Assessment methodologies of submarine groundwater discharge, In: Land and Marine Hydrogeology, M. Taniguchi, K. Wang, T. Gamo (eds) Elsevier, Amsterdam (2003) 1–23.
[15] MAHIQUES, M.M., Sedimentary dynamics of the bays off Ubatuba, State of Sao Paulo, Boletim do Instituto Oceanografico, Sao Paulo **43** 2 (1995) 111–122.
[16] MESQUITA A. R., Mares, circulacao e nivel do mar na Coasta Sudeste do Brasil, Relatorio Fundespa, Sao Paulo (1997).
[17] TANIGUCHI, M., BURNETT, W.C., SMITH, C.F., PAULSEN, R.J., O'ROURKE, D., KRUPA, S.L., CHRISTOFF, J.L., Spatial and temporal distributions of submarine groundwater discharge rates obtained from various types of seepage meters at a site in the Northeastern Gulf of Mexico, Biogeochemistry (2003).
[18] POVINEC, P.P., AGGARWAL, P.K., AURELI, A., BURNETT, W.C., KONTAR, E.A., KULKARNI, K.M., MOORE, W.S., RAJAR, R., TANIGUCHI, M., COMANDUCCI, J.-F., CUSIMANO, G., DULAIOVA, H., GATTO, L., GROENING, M., HAUSER, S., LEVY-PALOMO, OREGIONI, B., OZOROVICH, Y.R., PRIVITERA, A.M.G., SCHIAVO, M.A., Characterisation of submarine groundwater discharge offshore south-eastern Sicily, J. Environ. Radioact. **89** (2006) 1–21.
[19] LEE, D.R., A device for measuring seepage flux in lakes and estuaries, Limnol. Oceanogr. **22** (1977) 140–147.
[20] KRUPA, S., Personal communication, (2002).
[21] MCBRIDGE, M.S., PFANNKUCH, H.O., The distribution of seepage within lakebeds, J. Res. USGS **3** (1975) 505 –512.
[22] FUKUO, Y., KAIHOTSU, I., A theoretical analysis of seepage flow of the confined groundwater into the lake bottom with a gentle slope, Water Resour. Res. **24** (1988) 1949–1953.
[23] BOKUNIEWICZ, H., TANIGUCHI, M., ISHITOIBI, I., CHARRETTE, M., ALLEN, M., KONTAR E., Direct measures of submarine groundwater discharge over a fractured rock aquifer in Ubatuba, Brazil, Estuarine Coastal Shelf Sci. (2007)(in press).
[24] GALLAGHER, D.L., DIETRICH, A.M., REAY, W.G., HAYES, M.C., SIMMONS, G.M. Jr., Ground water discharge of agricultural pesticides and nutrients to estuarine surface water, GWMR Winter (1996) 118–129.
[25] HUSSAIN N., CHURCH,T.M., KIM, G., Use of ^{222}Rn and ^{226}Ra to trace groundwater discharge into the Chesapeak Bay, Mar. Chem. **65** (1999) 127–134.
[26] LI, L., BARRY, D.A., STAGNITTI, F., PARLANGE, J.-Y., Submarine groundwater discharge and associated chemical input to a coastal sea, Water Resour. Res. **35** (1999) 3253–3259.
[27] TANIGUCHI, M., SHIMADA, J., TANAKA, T., KAYANE, I., SAKURA, Y., SHIMANO, Y., DAPAAH-SIAKWAN, S., KAWASHIMA, S., Disturbances of temperature–depth profiles due to surface climate–change and subsurface water flow: (1) An effect of linear increase in surface temperature caused by global warming and urbanization in the Tokyo metropolitan area, Japan, Water Resour. Res. **35** (1999) 1507–1517.

[28] KOHOUT, F.A., The flow of fresh water and salt water in the Biscayne aquifer of the Miami area, Florida; in Sea Water in Coastal Aquifers, USGS Water Supply Paper 1613-C (1964) 12–32.
[29] STIEGLITZ, T., TANIGUCHI, M., NEYLON, S**.**, Spatial variability of submarine groundwater discharge in Ubatuba coastal area, Estuar. Coast. Shelf Sci. (2007) (in press).
[30] TANIGUCHI, M., ISHITOBI, T., SHIMADA, J., Dynamics of submarine groundwater discharge and freshwater–seawater interface, J. Geophys. Res. **111** (2006) C01008, doi:10.1029/2005JC002924.
[31] BOKUNIEWICZ, H., Groundwater seepage into Great South Bay, New York, Estuar. Coast. Shelf Sci. **10** (1980) 437–444.

APPENDIX

LIST OF PUBLICATIONS OF THE SCOR/LOICZ, IAEA, UNESCO PROJECTS ON SUBMARINE GROUNDWATER DISCHARGE

General Papers

[1] BURNETT, W.C., Offshore springs and seeps are focus of working group. EOS 80 (1999) 13–15.

[2] CABLE, J.E., BURNETT, W.C., TANIGUCHI, M., OBERDORFER, J., Bibliography for Submarine Groundwater Discharge, Scientific Committee on Oceanic Research (SCOR), Working Group 112 (2000) (http://www.jhu.edu/~scor/WG112.htm)

[3] BURNETT, W.C., BOLKUNIEWICZ, H.J., Are groundwater inputs to the coastal zone important? Proc. Int. Symp. Low-lying Coastal Areas; Hydrology and Integrated Coastal Zone Management, Bremerhaven, Germany (2002) 45–52.

[4] BOKUNIEWICZ, H.J., BUDDEMEIER, R., Maxwell, B., Smith, C., The typological approach to submarine groundwater discharge (SGD), Proc. Int. Symp. Low-lying Coastal Areas; Hydrology and Integrated Coastal Zone Management, Bremerhaven, Germany (2002) 201–205.

[5] DESTOUNI, G., PRIETO, C., Submarine groundwater discharge, climate change and the coastal zone, Proc. Int. Symp. Low-lying Coastal Areas; Hydrology and Integrated Coastal Zone Management, Bremerhaven, Germany (2002) 219–224.

[6] KONTAR, E.A., OZOROVICH, Y.A., SALOKHIDDINOV, A., Study of groundwater–seawater interactions in the Aral Sea Basin, Proc. Int. Symp. Low-lying Coastal Areas; Hydrology and Integrated Coastal Zone Management, Bremerhaven, Germany (2002) 225–230.

[7] TANIGUCHI, M., Temporal variations of submarine groundwater discharge and freshwater/saltwater interaction in the coastal zone, Proc. Int. Symp. Low-lying Coastal Areas; Hydrology and Integrated Coastal Zone Management, Bremerhaven, Germany (2002) 257–262.

[8] BURNETT, W.C., CHANTON, J., CHRISTOFF, J., KONTAR, E., KRUPA, S., LAMBERT, M., MOORE, W., O'ROURKE, D., PAULSEN, R., SMITH, C., SMITH, L., TANIGUCHI, M., Assessing methodologies for measuring groundwater discharge to the ocean, EOS 83 (2002) 117–123.

[9] PRIETO, C., DESTOUNI, G., Quantifying tidal effects on submarine groundwater discharge, IUGG Conference, Sapporo, Japan (2003).

[10] TANIGUCHI, M., BURNETT, W.C., CABLE, J.E., TURNER, J.V., Assessment Methodologies for Submarine Groundwater Discharge, In: Land and Marine Hydrogeology (Eds: M. Taniguchi, K. Wang, T. Gamo), Elsevier Publications, Oxford (2003) 208p.

[11] BURNETT, W.C., CHANTON, J.P., KONTAR, E., Submarine Groundwater Discharge, Biogeochemistry **66** (2003) 202p.

[12] DESTOUNI G., C. PRIETO, 2003. On the possibility for generic modeling of submarine groundwater discharge, Biogeochemistry **66** (2003) 171–186.

[13] DESTOUNI, G., JARSJÖ, J., Groundwater discharge into the Aral Sea, 35th International Liège Colloquium on Ocean Dynamics: 'Dying and Dead Seas', Liège (2003).

[14] ANONYMOUS, Submarine Groundwater Discharge: Management Implications, Measurements, and Effects, IHP-VI, Series on Groundwater No. 5, IOC Manuals and Guides No. 44 (2004) 35p.

[15] BURNETT, W.C., Measurement and potential importance of submarine groundwater discharge, In: Isotopes in Environmental Studies–Aquatic Forum 2004, Proc. Int. Conf., Monaco, International Atomic Energy Agency, Vienna (2006) 195.

[16] AURELI, A., FIDELIBUS, D., PRIVITERA, A.M.G., ZUPPI, G.M., Salt water intrusion in the aquifers south oriental coastal zones of Sicily, In: Isotopes in Environmental Studies–Aquatic Forum 2004, Proc. Int. Conf., Monaco, International Atomic Energy Agency, Vienna (2006) 208–211.

[17] AGGARWAL, P.K., KULKARNI, K.M., POVINEC, P.P., HAN, L.–F., GROENING, M., Environmental isotope investigation of submarine groundwater discharge in Sicily, Italy, In: Isotopes in Environmental Studies–Aquatic Forum 2004, Proc. Int. Conf., Monaco, International Atomic Energy Agency, Vienna (2006) 212–213.

[18] AURELI, A., BARROCU, G., CUSIMANO, G., FIDELIBUS, D., GATTO, L., HAUSER, S., SCHIAVO, M.A., TULIPANO, L., ZUPPI, G.M., Hydrochemistry and isotopic characteristics of the submarine springs of south-eastern Sicily, In: Isotopes in Environmental Studies–Aquatic Forum 2004, Proc. Int. Conf., Monaco, International Atomic Energy Agency, Vienna (2006) 216–218.

[19] BURNETT, W.C., PETERSON, R., DULAIOVA, H., Groundwater inputs via ^{222}Rn and Ra isotopes off Ubatuba, Brazil, In: Isotopes in Environmental Studies–Aquatic Forum 2004, Proc. Int. Conf., Monaco, International Atomic Energy Agency, Vienna (2006) 219—220.

[20] JARSJÖ, J**.**, DESTOUNI, G., Groundwater discharge into the Aral Sea after 1960, J. Mar. Sys. **47** (2004) 109–120.

[21] SHIBUO, Y., JARSJÖ, J., DESTOUNI, G., Modelling seawater–groundwater interactions in the Aral Sea region, Abstract H21B-1019, AGU Fall meeting, San Francisco (2004).

[22] BURNETT, W.C., DULAIOVA, H., STRINGER, C., PETERSON, R., Submarine groundwater discharge: its measurement and influence on the coastal zone, J. Coast. Res. **39** (2006) 35–38.

[23] CABLE, J., MARTIN, J., TANIGUCHI, M., A review of submarine ground water discharge: biogeochemical inputs and leaky coastlines, 22–41, In: Submarine Groundwater, (Eds: I.S. Zekster, R.G. Dzhamalov, L.G. Everett) CRC Press (2006) ISBN: 0849335760, 512p.

[24] CORBETT, R., CABLE, J., MARTIN, J., Direct measurements of submarine ground water discharge using seepage meters, 86–99, In: Submarine Groundwater, (Eds: I.S. Zekster, R.G. Dzhamalov, L.G. Everett) CRC Press (2006) ISBN: 0849335760, 512p.

[25] SHIBUO, Y., JARSJÖ, J., DESTOUNI, G., Modeling groundwater–seawater interactions in the Aral Sea region, In: Groundwater and Saline Intrusion (Eds: Araguás, L., Custodio, E., Manzano, M.), Insitututo Geologico y Minero de España, Serie: Hidrogeología y Aguas Subterráneas No 15 Madrid (2005) 163–171.

[26] PRIETO, C., Groundwater–seawater interactions: Seawater intrusion, submarine groundwater discharge and temporal variability and randomness effects, PhD Thesis in Water Resources Engineering, KTH Architecture and the Built Environment, TRITA–LWR PhD thesis, the Royal Institute of Technology, Stockholm (2005).

[27] PRIETO, C., DESTOUNI, G., Quantifying hydrological and tidal influences on groundwater discharges to coastal waters, Water Resour. Res. **41** W12427 doi:10.1029/2004WR003920 (2005).

[28] SHIBUO, Y., JARSJÖ, J., DESTOUNI, G., Bathymetry–topography effects on saltwater–fresh groundwater interactions around the shrinking Aral Sea, Water Resour. Res. **42** W11410 doi:10.1029/2005WR004207 (2006).

[29] JARSJÖ, J., ALEKSEEVA, I., SCHRUM, C., DESTOUNI, G., Simulation of groundwater–seawater interactions in the Aral Sea basin by a coupled water balance model, International Association of Hydrological Sciences (IAHS) Red Book Series (2005) in press.

[30] MOORE, W.S., The role of submarine groundwater discharge in coastal biogeochemistry, J. Geochem. Explor. **88** 1 (2006) 389–393.

[31] BURNETT, W.C., AGGARWAL, P.K., H. BOKUNIEWICZ, H., CABLE, J.E., CHARETTE, M.A., KONTAR, E., KRUPA, S., KULKARNI, K.M., LOVELESS, A., MOORE, W.S., OBERDORFER, J.A., DE OLIVEIRA, J., OZYURT, N., POVINEC, P., PRIVITERA, A.M.G., RAJAR, R., RamEssur, R.T., J. SCHOLTEN, J., STIEGLITZ, T., TANIGUCHI,M., TURNER, J.V., Quantifying submarine groundwater discharge in the coastal zone via multiple methods, Sci. Total Environ. **367** (2006) 498–543.

[32] SHIBUO, Y., JARSJÖ, J., DESTOUNI, G., Bathymetry–topography effects on saltwater–fresh groundwater interactions around the shrinking Aral Sea, Water Resour. Res. **42** (2006) W11410, doi:10.1029/2005WR004207.

[33] JARSJÖ, J., ALEKSEEVA, I., SCHRUM, C., DESTOUNI, G., Simulation of groundwater–seawater interactions in the Aral Sea basin by a coupled water balance model, In: From Uncertainty to Decision Making, ModelCare 2005 (Eds: M.F.P. Bierkens, K. Kovar, J.C. Gehrels), International Association of Hydrological Sciences (IAHS) Red Book Series, Paper no. IAHS 304-30-145 (2006).

Western Australia Experiment (2000)

[34] BURNETT, W.C., TURNER, J.V., LOICZ group investigates groundwater discharge in Australia. LOICZ Newsletter **18** (2001) 1–4.

[35] TANIGUCHI, M., J. TURNER, J.V., SMITH, A.J., Evaluations of groundwater discharge rates from subsurface temperature in Cockburn Sound, Western Australia, Biogeochemistry **66** (2003) 111–124.

[36] SMITH, A.J., NIELD, S.P., Groundwater discharge from the surficial aquifer into Cockburn Sound Western Australia: Estimation by inshore water balance. Biogeochemistry 66 (2003) 125–144.

Donnalucata, Sicily Experiment (2001)

[37] POVINEC, P.P., AGGARWAL, P.K., AURELI, A., BURNETT, W.C., KONTAR, E.A., KULKARNI, K.M., MOORE, W.S., RAJAR, R., TANIGUCHI, M., COMANDUCCI, J.-F., CUSIMANO, G., DULAIOVA, H., GATTO, L., GROENING, M., HAUSER, S., LEVY-PALOMO, I., OREGIONI, B., OZOROVICH, Y.R., PRIVITERA, A.M.G., SCHIAVO, M.A., Characterization of submarine groundwater discharge offshore south-eastern Sicily, J. Environ. Radioact. **89** (2006) 81–101.

Continental Shelf Research, vol. 26, 2006

[38] SCHIAVO, M.A., HAUSER, S., CUSIMANO, G., GATTO, L., Geochemical characterization of groundwater and submarine discharge in the south-eastern Sicily, 826–834.

[39] TANIGUCHI, M., BURNETT, W.C., DULAIOVA, H., Kontar, E.A., POVINEC, P.P., MOORE, W.S., Submarine groundwater discharge measured by seepage meters in Sicilian coastal waters, 835–842.

[40] KONTAR E.A., OZOROVICH, Y.R., Geo-electromagnetic survey of the fresh/salt water interface in the coastal southeastern Sicily, 843–851.

[41] MOORE, W.S., Radium isotopes as tracers of submarine groundwater discharge in Sicily, 852–861.

[42] BURNETT, W.C., DULAIOVA, H., RADON as a tracer of submarine groundwater discharge into a boat basin in Donnalucata, Sicily, 862–873.

[43] POVINEC, P.P., COMANDUCCI, J.-F., I. LEVY–PALOMO, I., OREGIONI, B., Monitoring of submarine groundwater discharge along the Donnalucata coast in the south-eastern Sicily using underwater gamma-ray spectrometry, 874–884.

Shelter Island, New York Experiment (2001)

[44] SHOLKOVITZ, E.R., HERBOLD, C., CHARETTE, M.A., An automated dye-dilution based seepage meter for the time-series measurement of submarine groundwater discharge, Limnol. Oceanogr. Methods **1** (2003) 17–29.

[45] RAPAGLIA, J.P., Distribution of Submarine Groundwater Discharge at Coastlines, M.S. thesis, Marine Sciences Research Center, Stony Brook University (2003) 83p.

[46] DULAIOVA, H., BURNETT, W.C., CHANTON, J.P., MOORE, W.S., Bokuniewicz, H.J., CHARETTE, M.A., SHOLKOVITZ, E., Assessment of groundwater discharges into West Neck Bay, New York, via natural tracers, Cont. Shelf Res. **26** (2006) 1971–1983.

Ubatuba, Brazil Experiment (2003)

[47] BOKUNIEWICZ, H.J., KONTAR, E., RODRIGUES, M., KLEIN, D.A., Submarine Groundwater Discharge (SGD) patterns through a fractured rock aquifer: a case study in the Ubatuba coastal area, Brazil Revista de la Asociacion Argentina de Sedimentologia **11** (2004) 9–16.

[48] De OLIVEIRA, J., ELÍSIO, A.C.R., TEIXEIRA, W.E., PERES, A.C., BURNETT, W.C., POVINEC, P.P., SOMAYAJULU, B.L.K., BRAGA, E.S., Isotope techniques for assessment of submarine groundwater discharge and coastal dynamics in Ubatuba coastal areas, Brazil, J. Coast. Res. **39** (2006) 1084–1086.

[49] De OLIVEIRA, J., CHARETTE, M., ALLEN, M., De SANTIS BRAGA, E., VERONESE FURTADO, V., Coastal water exchange rate studies at the southeastern Brazilian margin, using Ra isotopes as tracers. In: Radionuclides in the Environment (Eds: P.P. Povinec, J.A. Sanchez–Cabeza), Elsevier, Amsterdam (2006) 345–359.

[50] POVINEC, P.P., LEVY–PALOMO, I., COMANDUCCI, J.–F., De OLIVEIRA, J., OREGIONI, B., Privitera, A.M.G., Submarine groundwater discharge investigations in Sicilian and Brazilian coastal waters using an underwater gamma-ray spectrometer, In: Radionuclides in the Environment (Eds: P.P. Povinec, J.A. Sanchez–Cabeza), Elsevier, Amsterdam (2006) 373–381.

[51] POVINEC, P.P., BOKUNIEWICZ, H., BURNETT, W.C., CABLE, J., CHARETTE, M., MOORE, W.S., OBERDORFER, J.A., De OLIVEIRA, J., PETERSON, R.N., STIEGLITZ, T., TANIGUCHI, M., Isotope tracing of submarine groundwater discharge offshore Ubatuba, Brazil: Results of the IAEA–UNESCO SGD project, J. Environ. Radioact. (2007) submitted.

Estuarine, Coastal and Shelf Science, vol. 76, 2008

[52] OBERDORFER, J.A., CHARETTE, M., ALLEN, M., MARTIN, J.B., CABLE, J.E., Hydrogeology and Geochemistry of near-shore submarine groundwater discharge at Flamengo Bay, Ubatuba, Brazil, 457–465.

[53] BOKUNIEWICZ, H., TANIGUCHI, M., ISHITOIBI, T., CHARRETTE, M., ALLEN, M., KONTAR, E.A., Direct measures of submarine groundwater discharge over a fractured rock aquifer in Ubatuba, Brazil, 466–472.

[54] CABLE, J.E., MARTIN, J.B., In situ evaluation of nearshore marine and fresh pore water transport in Flamengo Bay, Brazil, 473–483.

[55] TANIGUCHI, M., STIEGLITZ, T., ISHITOBI, T., Temporal variability of water quality of submarine groundwater discharge in Ubatuba, Brazil, 484–492.

[56] STIEGLITZ, T., TANIGUCHI, M., NEYLON, S., Spatial Variability of Submarine Groundwater Discharge, Ubatuba, Brazil, 493–500.

[57] BURNETT, W.C., PETERSON, R., MOORE, W.S., De OLIVEIRA, J., Radon and radium isotopes as tracers of submarine groundwater discharge – results from the Ubatuba, Brazil SGD assessment intercomparison, 501–511.

[58] MOORE, W.S., DE OLIVEIRA, J., Determination of residence time and mixing processes of the Ubatuba, Brazil, inner shelf waters using natural Ra isotopes, 512–521.

[59] POVINEC, P.P., De OLIVEIRA, J., BRAGA, E.S., COMANDUCCI, J.–F., GASTAUD, J., GROENING, M., MORGENSTERN, U., TOP, Z., Isotopic, trace element and nutrient characterization of coastal waters from Ubatuba inner shelf area, south-eastern Brazil, 522–542.

LIST OF PARTICIPANTS

Aureli, A.

Department of Water Resources Management
University of Palermo
Via S. Paolo 66
95123 Catania,
Italy
Tel.: 0039 095 7311 763
Fax.: 039 095 7318027
E-mail: Prof-Aureli@iol.it

Bayari, S.C.

Department of Geological Engineering
Hacettepe University
06800 Ankara
Turkey
Tel.: 0090 312 297 77 40
Fax.: 0090 312 297 77 80
E-mail: serdar@hacettepe.edu.tr

Burnett, W.C

Department of Oceanography
Florida State University
Tallahassee
FL 32306-4320
United States of America
Tel.: 850-644-6703
Fax.: 850-644-2581
E-mail: wburnett@mailer.fsu.edu

De Oliveira, J.

Departamento de Radioprotecao (IPEN/CNEN)
Av. Lineu Prestes, 2242, Cidade Universitaria
Caixa Postal 11049
05508-000 São Paulo
Brazil
Tel.: 5511-3816- 9293
Fax.: 55 11 3816 9118
E-mail: joliveir@ipen.br

Kontar, E.A.

P.P. Shirshov Institute of Oceanology
Russian Academy of Sciences
36 Nakhimovskiy Prospekt
Moscow 117218
Russian Federation
Tel.: 7-095-129-2181
E-mail: kontar@cityline.ru

Moore, W.S.
Department of Geological Sciences
University of South Carolina
700 Sumter Street
Columbia, SC29208
United States of America
Tel.: 1(803)777-2262
Fax.: 1(803) 777-6610
E-mail: moore@geol.sc.edu

Rajar, R.
Faculty of Civil and Geodetic Engineering
University of Ljubljana
Hajdrihova 28
1000 Ljubljana
Slovenia
Tel.: 386 1 7234654
Fax.: 386 1 2519 897
E-mail: rrajar@fgg.uni-lj.si

Somayajulu, B.L.K.
Oceanography & Climate Studies Area
Earth Sciences Division
Physical Research Laboratory
Navrangpura, Ahmedabad 380 009
India
Tel.: 91-(0)79-646 2129
Fax.: 91-(0)79-630 1502
E-mail: soma@prl.ernet.in

Taniguchi, M.
Research Institute for Humanity and Nature (RIHN)
457-4, Motoyama, Kamigamo, Kita-ku
Kyoto, 603-8047
Japan
Tel: 81-75-707-2255
Fax:81-75-707-2506
E-mail: makoto@chikyu.ac.jp